



Università degli Studi di Ferrara

DOTTORATO DI RICERCA IN

Scienze della Terra

CICLO XXVII

COORDINATORE Prof. Massimo Coltorti

**Sediment transport and morphodynamics of mixed  
beaches: case studies of two Mediterranean sites**

Settore Scientifico Disciplinare GEO/04

**Dottorando**

Dott. Grottoli Edoardo

**Tutore**

Prof. Ciavola Paolo

Anni 2012/2014

# *Table of contents*

<b>1. INTRODUCTION .....</b>	<b>5</b>
<b>1.1 Motivation .....</b>	<b>6</b>
<b>1.2 State of the arts on mixed beaches.....</b>	<b>7</b>
1.2.1 - Classifications and reviews .....	7
1.2.2 - Sediment transport .....	14
1.2.3 - Influence of sediment characteristics on transport.....	15
<b>2. STUDY AREAS .....</b>	<b>17</b>
<b>2.1 - Portonovo beach.....</b>	<b>18</b>
<b>2.2 - Marina di Pisa beach .....</b>	<b>21</b>
<b>3. MATERIALS AND METHODS.....</b>	<b>24</b>
<b>3.1 - Radio tracers: RFID technology .....</b>	<b>25</b>
<b>3.2 - Experiment set up .....</b>	<b>27</b>
3.2.1 - Portonovo experiments.....	28
3.2.2 - Marina di Pisa experiment.....	34
<b>3.3 - Surface samplings and grain size analyses .....</b>	<b>36</b>
<b>3.4 - Topographic surveys .....</b>	<b>38</b>
<b>3.5 - Volume variation estimation .....</b>	<b>40</b>
<b>3.6 - Shoreline variation estimation.....</b>	<b>40</b>
<b>3.7 - Storm events identification.....</b>	<b>41</b>
<b>3.8 - Analysis of tracer characteristics.....</b>	<b>41</b>
3.8.1 - Statistical analysis .....	41
3.9.2 - Threshold of tracer motion .....	43

<b>4. PEBBLE TRANSPORT: DISPLACEMENTS ON THE SHORT AND LONG TERM</b>	<b>44</b>
4.1 - Portonovo beach	45
4.1.1 - Short term tracer recovery	45
4.1.2 - Long term tracer recovery	51
4.2 - Marina di Pisa beach	55
4.2.1 - Short term tracer recovery	55
4.3 - Discussion	59
<b>5. PEBBLE TRANSPORT IN THE SHORT TERM: INFLUENCE OF SIZE AND SHAPE OF PARTICLES (PORTONOVO BEACH)</b>	<b>69</b>
5.1 - The role of size	70
5.1.1 - Displacement and recovery of pebbles based on their size	70
5.1.2 - Statistical analyses	72
5.1.3 - Threshold of tracer motion	74
5.2 - The role of shape	75
5.2.1 - Displacement and recovery of pebbles based on their shape	75
5.2.2 - Statistical analyses	77
5.3 - The combinational role of size and shape	79
5.3.1 - Displacement of pebbles based on the combinational effect of size and shape	79
5.4 - Statistical analyses	81
5.5 - Discussion	83
<b>6. BEACH EVOLUTION (PORTONOVO BEACH)</b>	<b>89</b>
6.1 - Topographic variation	90
6.2 - Shoreline variation	108
6.3 - Volumetric variation	121
6.4 - Discussion	122
<b>7. SURFACE SEDIMENT VARIABILITY (PORTONOVO BEACH)</b>	<b>127</b>
7.1 - One-year variability	128

<b>7.2 - Analysis of sediment parameters: dispersion maps.....</b>	<b>130</b>
7.2.1 - Mean diameter ( $M_z$ ) variability.....	130
7.2.2 - Sorting ( $\sigma_1$ ) variability.....	130
7.2.3 - Skewness ( $S_k$ ) variability .....	131
<b>7.3 - Discussion .....</b>	<b>135</b>
<b>8. CONSIDERATIONS ON FILL MATERIAL CHARACTERISTICS FOR NOURISHMENT PURPOSES .....</b>	<b>141</b>
<b>8.1 - Italian and worldwide overview on gravel nourishment projects.....</b>	<b>142</b>
<b>8.2 - Which fill material? .....</b>	<b>143</b>
8.2.1 - Recommendations on fill material for the case studies. ....	147
<b>9. CONCLUSIONS.....</b>	<b>150</b>
<b>REFERENCES.....</b>	<b>154</b>
<b>LIST OF FIGURES.....</b>	<b>169</b>
<b>LIST OF TABLES.....</b>	<b>178</b>
<b>APPENDIX A.....</b>	<b>181</b>
<b>APPENDIX B.....</b>	<b>183</b>
<b>APPENDIX C.....</b>	<b>186</b>
<b>ACKNOWLEDGEMENTS.....</b>	<b>198</b>

# ***1. Introduction***

## 1.1 Motivation

The main intent of this work is to improve the knowledge on sediment transport of mixed beaches with particular focus on the coarse fraction. Given the lack of information and foremost the actual quality level of in-depth analyses on coarse and mixed beaches, especially in comparison to what is already known about the sandy equivalent, several hypotheses were assumed to be demonstrated from field data acquirement. First of all, the knowledge improvement of pebble transport in microtidal beaches during low-energy conditions and in short periods of time. The investigation was possible by means of radio tracer technique (RFID Radio Frequency Identification). The remarkable asset of the technique is to univocally gather displacement information for each single pebble, allowing to compare direct field measurements with existing models of sediment transport, usually based on indirect measures and in need of statistical treatment to decrease as much as possible an error which is nevertheless irremovable. Pebble transport was investigated during short fair-weather spans of time (6 and 24 h after the tracer injection) and also monitored in the long term (months to 1 year). It is clear that different factors exert control on beach dynamic during severe storm events rather than under low energy conditions. In the latter case it is likewise spontaneous to generate assumptions to be tested, such as if any selective transport of pebbles, based on their size and shape, is possible, or which hydrodynamic factor is the most decisive to destabilize the sediment particle at equilibrium; keeping in mind that the swash zone is certainly the most active part of a mixed beach and several factors affect its dynamic. All the previous purposes had to be supported by a strong substrate of morphodynamics concepts, suited on the basis of constant field data gathering. The classical morphodynamics study approach of beach is to consider here as sustain of the sediment transport findings and useful to observe the actual response of a replenished beach. Nourishment practices are increasingly chosen by local policies to improve beach stability in critical areas, even on mixed beaches, but there is still a relative lack of information regarding the post-replenishment behaviour of these beaches, never forgetting that a knowledge refinement, on which refill material is the best fitting for specific replenished areas, is also needed.

## **1.2 State of the arts on mixed beaches**

### *1.2.1 - Classifications and reviews*

Since mixed and coarse grained beaches have been studied, many authors have basically focused on the field description of morphological features and sediment arrangements. On the basis of these evident characteristics some scientists tried to conceive classification schemes with the justifiable aim to suite them for all cases. Despite a substantial improvement has been around the first decade of this millennium, a classification perfectly suitable for any beach is yet to be established. When the first peak of interest on gravel beaches emerged around 1960s, Bluck (1967) proposed a qualitative model based on field observations of six beaches of South Wales. He described the surface sediment stretching these beaches, distinguishing among four particle cross-shore zones on the basis of their shapes. According to Bluck (1967) two types of gravel beaches are assumed: the Sker type, and the Newton type, on the basis of erosional or accretionary structures created by the wave reworking. Both these two typology has the same particles zones (“landward large disc zone”, “imbricate zone”, “infill zone”, “outer frame”) which basically vary for a different sequential arrangement (Figure 1-1). The two facies types (Sker and Newton) reflect respectively a high and a lower energy environment (Mason and Coates, 2001). As stated by Orford (1975) they are not exclusive of a specific beach, but mostly representative of the ambient energy conditions.

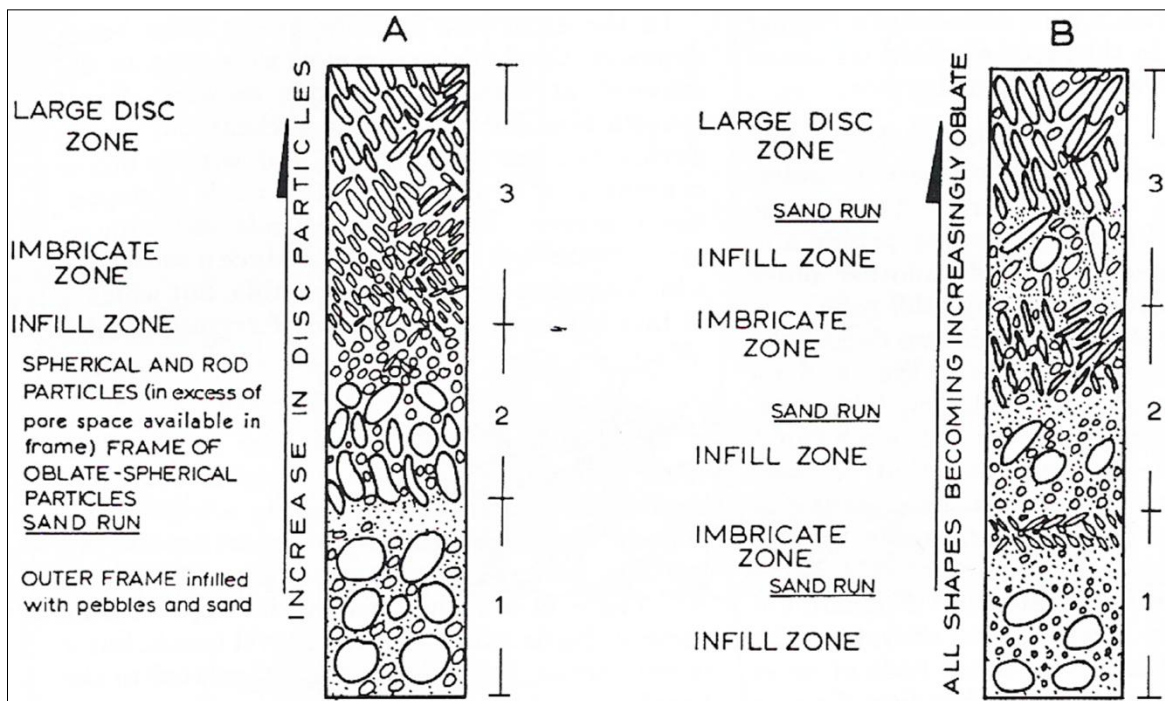


Figure 1-1. A) Construction cycle of a “Sker” type beach and B) a “Newton” type beach (Bluck, 1967).

Bluck (1967) realised a detailed description of the internal structures of a gravel beach, lately improved in his recent work with other case studies (Bluck, 2011), always ascribing a prominent role to the particle shape in the construction phase of a gravel beach. The Bluck’s works took place on beaches affected by an important tidal range that, joined to the wave action, obviously lead to a more complex selection of beach material, as also confirmed by Mason and Coates (2001). A more comprehensive classification of mixed and coarse-grained beaches was ratified by Jennings and Shulmeister (2002). The authors proposed a classification scheme which still represents the only one that is suitable for most of the worldwide coarse grained and mixed beaches. Three different types of beaches are conceived: pure gravel beach, mixed sand and gravel beach (MSG), and composite beach. The pure gravel beach has a completely gravelly profile with minor berms and a strong sediment sorting. The main grain size range from -2 to -6 phi. These characteristics make the profile linear with highly steep beachface ( $\tan \beta$  values between 0.1 and 0.25, and a mean beachface slope of 0.18; Table 1-1; Figure 1-2). Previous researchers described pure gravel beaches, giving information mainly based on field observations. According to Carter and Orford (1993) pure gravel beaches are highly reflective at all stages of the tidal cycle. Surf zone processes are absent and edge wave development control the morphodynamics regime, with associated cusped morphology (Sherman et al., 1993).



Cusps can be either accretionary or erosional in these kinds of beaches (Sunamura and Aoki, 2000). Surging and collapsing waves dominate under all conditions but during storm events (Jennings and Shulmeister, 2002). The mixed sand and gravel beach (MSG) is whereas characterised by a complete intermixing of sandy and gravelly sediments (Kirk, 1980; Jennings and Shulmeister, 2002). Grain size varies from coarse sand to pebble (0.5 to -6 phi). Beach slope varies from 0.04 to 0.12 values and well developed step represents the main break point of the profile slope. Beach cusps are frequent and often well-formed on more than one tier (Jennings and Shulmeister, 2002). During fair-weather periods, swash processes control the hydrodynamic regime; consequently the swash zone is the most dynamic part of the beach relative to sediment transport (Kirk, 1980). Plunging and collapsing waves are typical of these kind of beaches (Figure 1-2), while little is known, according to Jennings and Shulmeister (2002), about their behaviour under severe storms conditions. The composite gravel beach occurs when hydraulic sorting is able to clearly separate the beach profile in two distinct parts: one seaward, sand dominated, with lower gradient ( $\tan \beta = 0.03-0.1$ ); the other landward, gravel dominated, with an higher  $\tan \beta$  value between 0.1 and 0.15 (Jennings and Shulmeister, 2002). Given these characteristics, spilling waves will form with a dissipative surf zone at low tide and a long-shore bar-trough system may develop (Figure 1-2).

Type	Beach site	Tide	Beach slope	Average grain size (φ)	Storm berm grain size (φ)	High-tide grain size (φ)	Swash Grain Size (φ)	Hsig (offshore m)	Average wave period (s)	Iribarren No.	Beach width (m)
PG	9	micro	0.14	-2.39	-2.26	-2.90	-1.82	1.25	9.00	2.27	51.63
PG	10	micro	0.13	-2.49	-2.57	-2.79	-2.01	1.25	9.00	2.12	50.40
PG	15	micro	0.23	-6.13	-6.59	-6.48	-4.63	1.25	9.00	3.79	23.89
PG	16	micro	0.23	-6.03	-6.54	-6.35	-4.39	1.25	9.00	3.79	25.04
PG	25	micro	0.10	-2.99	-3.66	-2.01	-2.82	1.25	9.00	1.58	38.40
PG	11	micro	0.24	-5.21	-5.58	-4.88	-5.08	1.25	9.00	4.00	18.50
PG	12	micro	0.20	-4.20	-2.66	-5.04	-3.99	1.25	9.00	3.26	28.01
MSG	1	micro	0.11	-3.85	-5.22	-1.65	-1.54	1.25	9.00	1.83	32.22
MSG	2	micro	0.11	-4.85	-5.14	-5.47	-2.77	1.25	9.00	1.82	43.41
MSG	13	micro	0.12	-4.41	-1.71	-5.89	-0.11	1.25	9.00	1.85	36.44
MSG	14	micro	0.12	-5.21	-5.83	-5.60	-2.39	1.25	9.00	1.94	31.96
MSG	28	micro	0.08	-4.89	-5.14	-5.47	-3.27	1.25	9.00	1.35	55.94
MSG	3	micro	0.09	-2.88	-4.31	-0.04	-0.33	1.25	9.00	1.48	46.55
MSG	4	micro	0.09	-4.72	-5.36	-5.14	-1.38	1.25	9.00	1.43	48.98
MSG	5	micro	0.08	-3.73	-4.28	-4.29	0.08	1.25	9.00	1.23	63.74
MSG	6	micro	0.08	-3.93	-3.04	-5.18	-0.48	1.25	9.00	1.31	61.15
MSG	7	micro	0.09	-1.65	0.92	-1.10	-2.75	1.25	9.00	1.37	65.75
MSG	8	micro	0.08	-1.75	0.94	-1.09	-2.90	1.25	9.00	1.25	69.66
MSG	17	micro	0.09	-4.84	-5.60	-5.06	-1.85	1.25	9.00	1.40	39.83
MSG	18	micro	0.09	-3.88	-4.81	-3.72	-1.62	1.25	9.00	1.43	50.85
MSG	19	micro	0.04	-3.74	-3.49	-4.82	0.36	1.25	9.00	0.68	68.00
MSG	20	micro	0.07	-3.38	-3.49	-4.21	-0.69	1.25	9.00	1.08	50.95
MSG	21	micro	0.09	-4.05	-4.83	-4.08	-2.15	1.25	9.00	1.41	76.10
MSG	22	micro	0.06	-3.18	-3.68	-3.51	-1.53	1.25	9.00	0.90	98.00
MSG	23	micro	0.07	-4.07	-4.64	-4.55	-1.12	1.25	9.00	1.08	60.00
MSG	24	micro	0.09	-4.25	-4.49	-4.59	-3.40	1.25	9.00	1.39	48.00
MSG	26	micro	0.06	-3.82	1.24	-5.30	-1.35	1.25	9.00	0.97	76.80
MSG	27	micro	0.08	-4.44	-5.10	-4.75	-2.02	1.25	9.00	1.35	49.35
MSG	30	micro	0.08	-4.10	-5.26	-3.63	0.42	1.25	9.00	1.31	32.00
MSG	31	meso	0.08	-4.85	-5.99	-4.44	-0.14	1.25	9.00	1.26	74.00
MSG	42	micro	0.08	-3.74	-4.66	-3.66	-1.09	1.25	9.00	1.32	34.00
COMP	29	micro	0.10	-4.83	-5.63	-5.09	-0.92	1.25	9.00	1.55	11.48
COMP	32	meso	0.07	-5.34	-5.89	-5.79	-2.67	2.00	7.00	0.69	63.20
COMP	33	meso	0.07	-4.56	-4.33	-5.53	-2.09	2.00	7.00	0.69	51.08
COMP	34	meso	0.05	-4.77	-5.53	-4.85	-2.78	2.00	7.00	0.53	63.26
COMP	35	meso	0.13	-5.09	-5.68	-5.25	-3.71	2.00	7.00	1.23	34.00

Table 1-1. Morphological parameters of studied beaches by Jennings and Shulmeister (2002).

The lack of classification scheme was partially camouflaged by some remarkable paper reviews. Kirk (1980) was the first author who tempts to offer a comprehensive scientific point of view of the state of the arts at that time, collecting works of different nature dealing with mixed and gravel beaches. He presented and discussed several aspects and distinctive characteristics relating to processes, sediments and morphology of mixed beaches basing on New Zealand beach study. Kirk's work was essentially the first morphodynamic study of mixed beaches which could include all the crucial features of those environments (i.e. sediment characteristics, wave parameters, profile evolution, sediment transport and sediment variations both along and cross-shore). He also determined an ideal visual scheme of a mixed beach (Figure 1-3), based on field observations of New Zealand beaches that can be generally believed valid elsewhere.

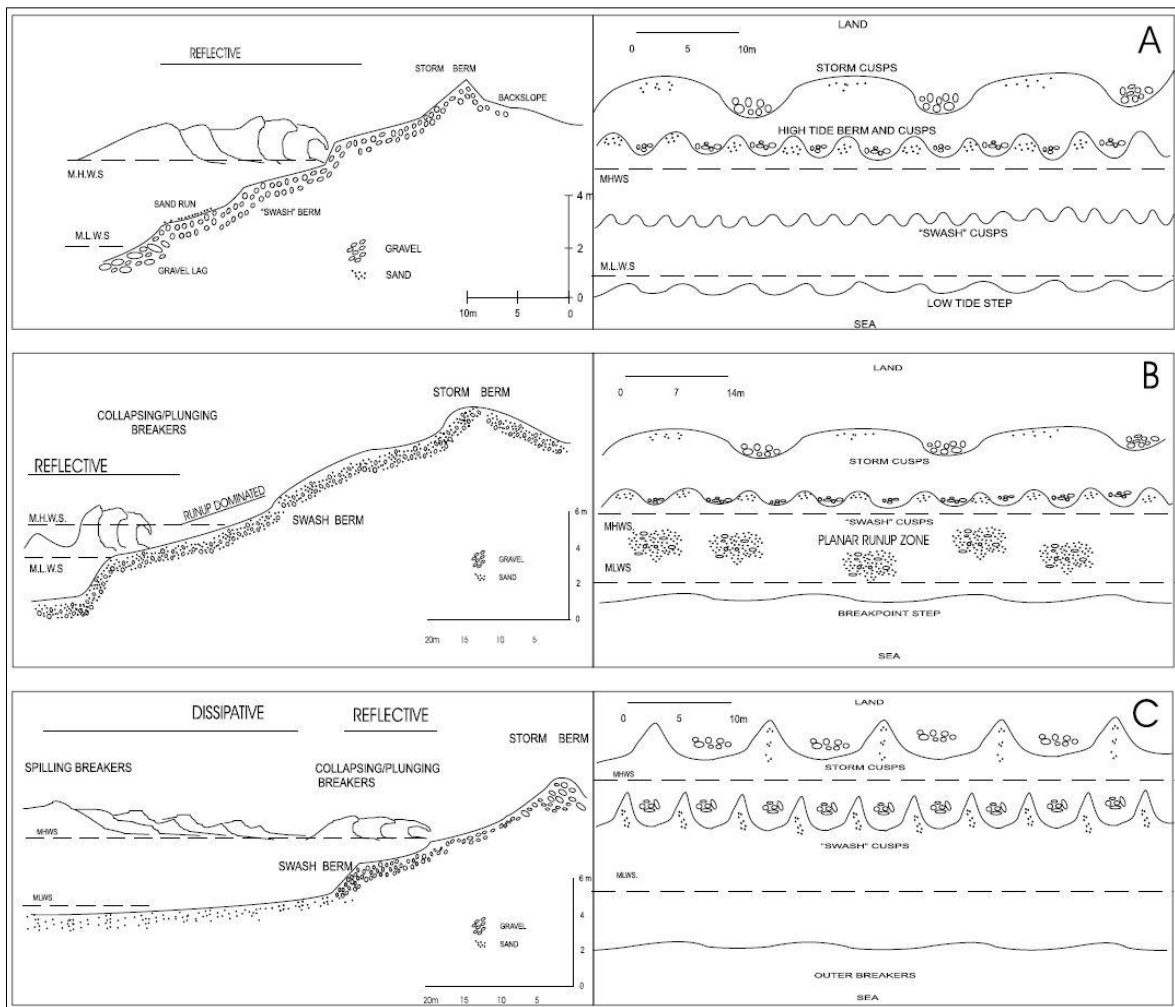


Figure 1-2. Schematic representation of the three types of beaches proposed by Jennings and Shulmeister (2002): A) pure gravel beach, B) mixed sand and gravel beach (MSG), C) composite beach.

According to Kirk (1980), mixed beaches are typically narrow, steep between  $5$  and  $12^\circ$  and broadly convex in profile shape. Four elements are shown in Figure 1-3 and can normally be identified on a mixed beach: a backshore zone landward the highest run up limit of storm swash; a steep foreshore extending from the topmost berm (or cliff base) to the wave break point; a lower foreshore marked by a distinct break point step or low tide terrace; a clear slope change, seaward of the breaker zone, between a steep gravel nearshore and a gently sloping and sandy inner shelf surface. Two decades later, Mason and Coates (2001) resumed the Kirk's work giving a long range review on processes affecting mixed beaches. They distinguished in a first and second order factors influencing sediment transport on these environments.

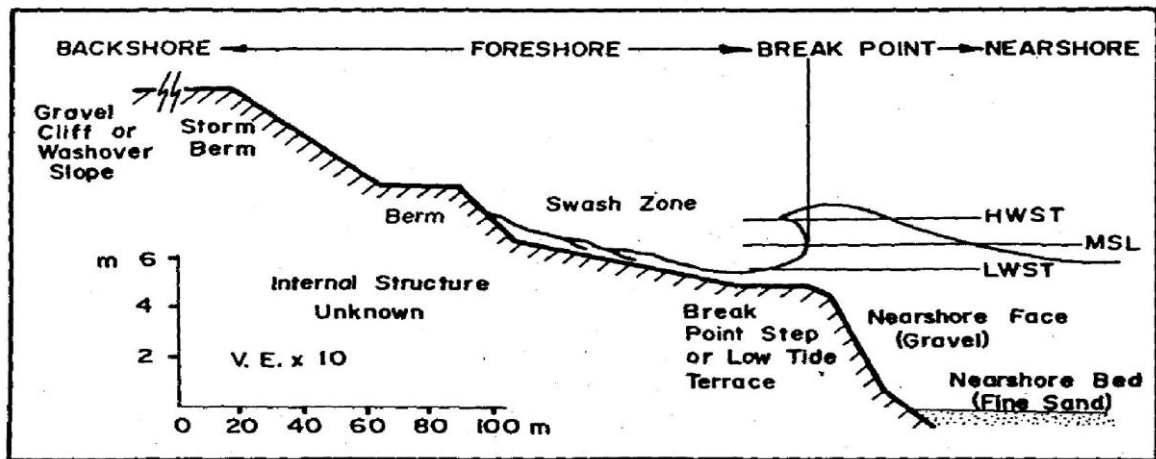


Figure 1-3. Typical morphology and zonation of mixed sand and gravel beach profiles according to Kirk (1980).

Among the first order factors the authors cited several components such as: hydraulic conductivity, groundwater infiltration, wave reflection and threshold of motion. A less crucial role seems to have sediment shape, tidal range, specific gravity, armouring phenomena and chemical processes. If one can agree with what the authors considered more important on controlling beach processes, it must be said that all the secondary factors were, and still are, poorly analysed and inadequately understood. Only few works have been focalised on those “second order” aspects of mixed beach morphodynamics. Mason and Coates gave also a fairly complete archive of the most relevant works of those years based on field experiments (Caldwell and Williams, 1985; Brampton and Motyka, 1987; Hill, 1990; Bujalesky and Gonzalez-Bonorino, 1991; Walker et al., 1991; McKay and Terich, 1992; Nordstrom and Jackson, 1993) or dealing with the development of beach model from laboratory tests (Petrov, 1989; Quick and Dyksterhuis, 1994; Holmes et al., 1996). In the recent years, Buscombe and Masselink (2006) were the last scientists that felt to draft a review paper on mixed and gravel beaches. Their intent was to review all the short-term processes that affect beach foreshore and beachface, highlighting the key aspects for future research. “Morpho-sedimentary-dynamics” (MSD), was the new coined term by Carter and Orford (1993), later deeply discussed and refined by Masselink and Puleo (2006) and by Buscombe and Masselink (2006). The term wants to focus the reciprocal relationship between the morphology evolution, the sediment transport and the hydraulic properties on a mixed or gravel beach. These three aspects should be present in every future research, representing the minimum number of parameters to understand in order to adequately describe the state of a beach. According to the authors, spatial heterogeneity of sediment properties (grain size and shape in particular) is both an

expression and a control on gravel beach morphodynamics. The paper of Buscombe and Masselink (2006) contains a comprehensive review of the most recent works dealing with hydrodynamics factors, sediment transport (sorting and grading of sediments, longshore and cross-shore transport, transport modes) and morphological features (step, cusps, storm beach, foreshore dynamics). The concept of “Morpho-sedimentary-dynamics” (MSD) is shown in Figure 1-4, where the interactions between and within the surf zone and the swash zone morphodynamic system are represented. A morpho-sedimentary-dynamics (MSD) approach treats sediments, and the spatial variation of sediment characteristics, not as a boundary condition but as a fundamental and integral aspect which permeates through morphodynamics, which may act as both an expression and control on gravel beach behaviour (Buscombe and Masselink, 2006).

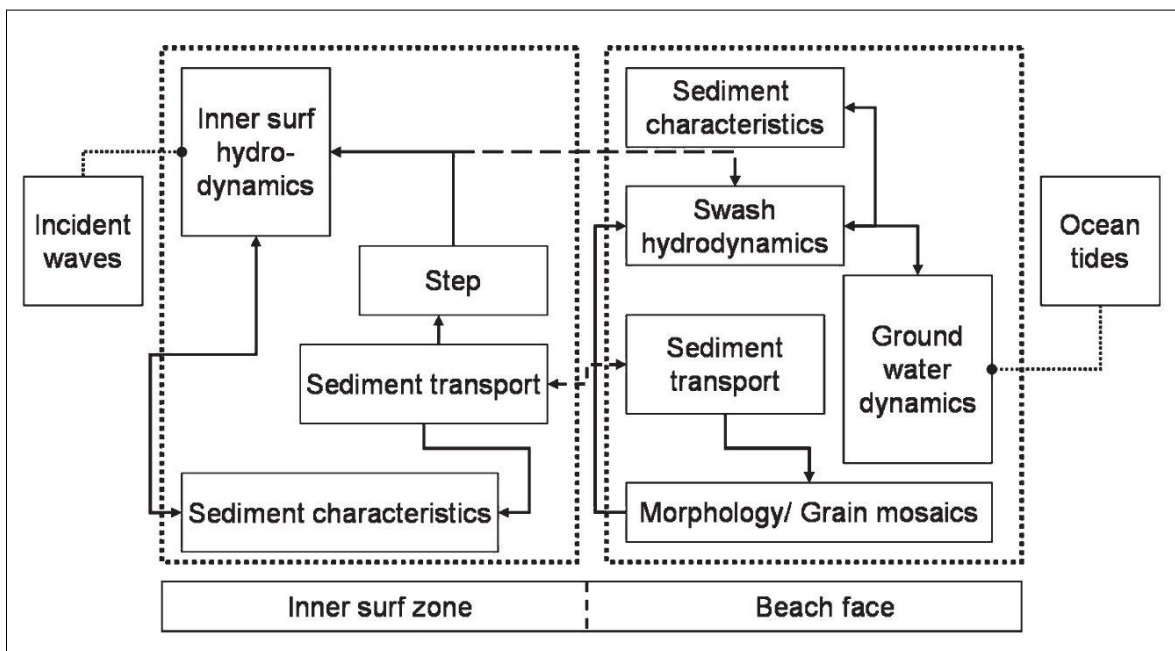


Figure 1-4. Conceptual morpho-sedimentary-dynamics diagram for gravel beachface. This diagram was already drafted by Masselink and Puleo (2006) and later modified by Buscombe and Masselink (2006) in the current form. The diagram illustrates interactions between and within the surf zone and the swash zone morphodynamic system.

As regularly happens when it is attempted to study natural processes, the more it is tried to define precise theoretical classes, the more is easy to find cases in between. Any beach classification or conventional scheme, as far as simple, is not perfectly suitable for each case of study: it is common to recognize distinctive characteristics in theory assumed for specific beach categories also for different ones, or observe beach behaviours which are not strictly fitted in one single typology.

### *1.2.2 - Sediment transport*

Sediment transport along ocean shorelines is a foremost aspect in the morphological evolution of coastal environments, the factors responsible for sediment displacement driving the morphodynamics of a given beach between erosion and accretion in the process of achieving some form of equilibrium. Understanding the principles of beach morphodynamics and following the pathways of sediment movement have been major objectives of beach studies over past decades (e.g., Komar and Inman, 1970; McCave, 1978; Wright et al., 1985; Salomons and Mook, 1987; Ciavola et al., 1997, 1998; White, 1998; Short, 1999; Benavente et al., 2005; Silva et al., 2007; Poizot et al., 2013; Sancho-García et al., 2013). Although more attention has generally been given to sandy beaches, mainly because it is easier to carry out field experiments on sand-sized sediments rather than gravel-sized ones (Buscombe and Masselink 2006), a renewed interest in the investigation of coarse-clastic beaches can be observed in recent years (e.g., Allan et al. 2006; Curtiss et al. 2009; Bertoni et al. 2010; Miller et al. 2011; Curoy 2012). The understanding of sediment transport in coastal environments has in recent years improved mostly because of novel technical solutions that solved many of the logistical problems encountered previously. For instance, the possibility of tracking individual pebbles by means of the RFID (Radio Frequency IDentification) technique provided a major boost toward the unravelling of coarse sediment displacement mechanisms (Allan et al. 2006; Bertoni et al. 2010). In addition, the use of gravel and pebble nourishment as a form of coastal protection has progressively increased because they are more resistant to wave scour than are sandy beaches (Masselink and Hughes 2003). Improving the knowledge of sediment transport in mixed beaches is therefore of particular importance, especially in the swash zone where the magnitude of transportation is likely to be more significant rather than on sand beaches (Van Wellen et al., 1999a; 2000). In the past, most work dealing with coarse sediment transport on beaches was carried out in high-energy environments (e.g., Bluck 1967; Ibbeken and Schleyer 1991; Deguchi et al. 1998; Packham et al. 2001; Buscombe and Masselink 2006; Curoy 2012). A few studies dealing with low-energy coarse-clastic beaches mainly concentrated on their response to episodic storms or the aftermath of high-energy events (e.g., Bertoni et al. 2010, 2012a; Bertoni and Sarti 2011; Ellis and Cappiotti 2013).

### 1.2.3 - Influence of sediment characteristics on transport

Several hydrodynamic factors exert significant control on sediment transport for gravel and mixed sand-gravel beaches, and these factors are still poorly understood. As already cited in the paragraph 1.1, some comprehensive review of these forces was made in the recent past (Kirk, 1980; Mason and Coates, 2001; Buscombe and Masselink, 2006), but finding clear correlations between sediment characteristics and hydrodynamic agents still represents a hard challenge, especially in the swash zone. A conceptual model of sediment transport on a gravel beach was proposed by Carter and Orford (1991): they listed a series of probabilistic opportunities (Figure 1-5) in which an incoming clast may face on the active zone of a gravel beach (within a finite time period), including incorporation, washover or projectile rejection, acceptance, attrition or breakage, abandonment, or gravity-assisted loss offshore.

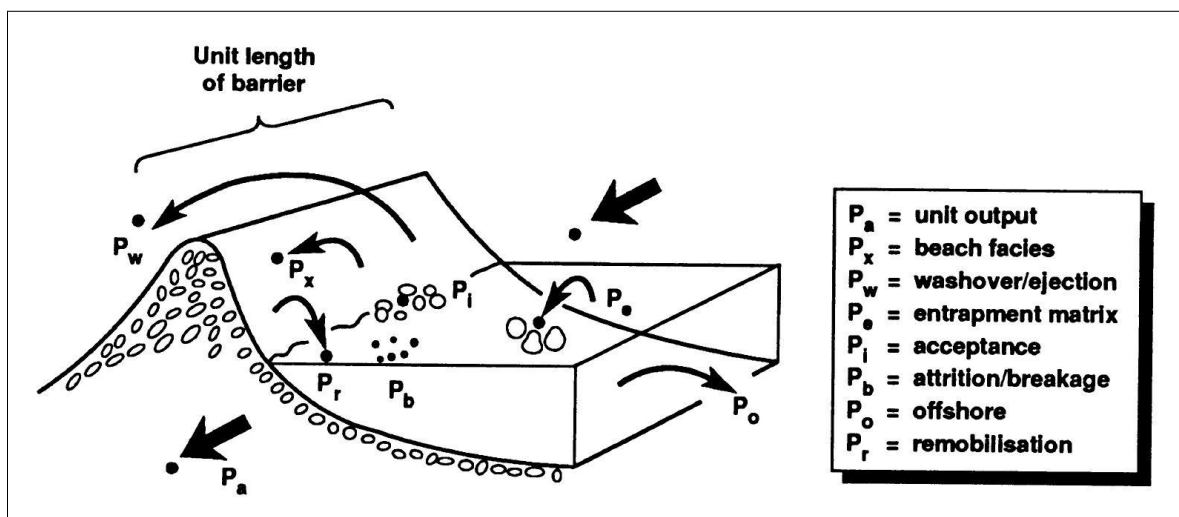


Figure 1-5. Conceptual model of the probabilistic nature of a sediment grain transport on a gravel beach (Carter and Orford, 1993, after Carter and Orford, 1991).

Gravel is not only larger, but usually varies over several orders of magnitude greater than beach sands (Buscombe and Masselink, 2006) and this characteristic creates extremely evident texture variations on coarse clastic beach surfaces, which cyclically raises the interest of researchers. After the early papers which mainly focused on the description of particle characteristics (Wentworth, 1922b, 1923; Zingg, 1935), a first peak of interest on the relationship between hydrodynamics factors and sediment characteristics came through around the 1970s and 1980s (Bluck, 1967; Carr, 1969; McLean and Kirk, 1969; Carr et al., 1970; McLean, 1970; Carr, 1971; Gleason and Hardcastle, 1973; Orford, 1975; Kirk,

1980; Caldwell, 1981; Williams and Caldwell, 1988; Isla, 1993; Isla and Bujalesky, 1993), a further renewed interest in sediment transport based on different coarse particle characteristics formed during the first decade of this millennium (Buscombe and Masselink, 2006; Ciavola and Castiglione, 2009; Bluck, 2011; Bertoni et al., 2012a). Textural mosaics of different clast shapes and sizes are common and different cross-shore size-shape zonation and modes of transport were demonstrated by many authors (Bluck, 1967; Orford, 1975; Williams and Caldwell, 1988; Isla, 1993; Ciavola and Castiglione, 2009; Hayes et al., 2010; Bluck, 2011), although the relative importance of size and shape in sorting is yet to be resolved (Buscombe and Masselink, 2006). Orford (1975) noted that the roles of size and shape cannot be easily separated; using both factors is therefore well-advised to establish the degree of pebble zonation on a beach. Williams and Caldwell (1988) proposed a model wherein the influence of particle size is more important on the sorting of sediments when energy conditions are high, while particle shape predominates when energy conditions are low and cross-shore sediment transport prevails. Because most of the cited papers were undertaken on meso- or macro-tidal beaches, except for Ciavola and Castiglione (2009), whose dataset provided insights on a micro-tidal beach, the aim of this work would theorise further ideas on this type of beach by attempting to discriminate whether shape and size affect pebble displacements in the swash zone differently under low-energy conditions. Furthermore, thanks to the RFID technology that enables the unambiguous identification of pebbles, it is possible to describe the movement of each individual particle according to its characteristics such as shape and size. This tracing technique, according to Van Wellen et al. (2000), is currently best suitable to obtain short-term transport rates on coarse-grained beaches.



## ***2. Study Areas***

## 2.1 - Portonovo beach

Portonovo is a town located on the northern edge of the Conero Headland in the central sector of the Adriatic Sea; the study mixed beach is located on the eastern side of the town (Figure 2-1). The beach is approximately 500 m long and 20 to 50 m wide and is bounded by two boulder armours built between 1940s and 1960s to protect historical buildings (Regione Marche, 2005). The beach is approximately NW-SE oriented. The southern portion of the beach is wider and slightly embayed, whereas the northern part is narrower and straight. In the central zone of the area the backshore is limited by a seawall parallel to the shoreline, while the northern part is limited by a small cliff. The beach was formed by a prehistoric landslide from the north-eastern slope of Conero Headland (Coccioni et al., 1997). Cliff erosion is the only sediment source as there is no river input and the beach sediments consist of marls and limestones. In 2010, a replenishment made of alluvial material, compatible with the original sediment, was carried out by local authorities: pebbles and cobbles (4-100 mm in diameter) of limestone were injected to contain beach erosion. The total amount of infill material deployed on Portonovo beaches between 2006 and 2011 was approximately 18500 m<sup>3</sup>: most of the part was unloaded on the western side of the village (personal communication by officers of the Regione Marche). The exact quantity released in 2010 in the study site is unknown. The beach sediment grain size varies from medium sand to cobble with a prevalent gravel fraction mainly formed by pebbles. The beach looks extremely heterogeneous regarding the surface sediment grain size: sand and scattered gravel accumulations cover the backshore, with barely continuous stripes of different grain size parallel to the shoreline, already noted by many authors in local beaches (Van Straaten, 1965; Pigorini, 1968; Van Straaten, 1970; Brambati et al., 1973; Brambati et al., 1983; Curzi, 1986; Curzi and Tomadin, 1987). In Portonovo stripes of different grain size are mainly given by normal and stormy wave action and visually highlighted by long storm berms. The gravel fraction usually occupies the swash zone, with granules and fine pebbles normally found on the berm and in the swash zone and cobbles and boulders usually found on the step zone. The beachface typically slopes 0.2, whereas the seabed seaward of the step is approximately 0.01, as normally known for the Adriatic seabed. According to the Jennings and Shulmeister (2002) classification, Portonovo is a mixed sand and gravel beach (MSG) where a complete intermixing of sandy and gravelly sediments occurs (Figure 2-2), and results as a reflective beach for the Wright and Short (1984) classification of beaches. In this part of the coast, the littoral drift, influenced by “Levante” (E) and “Scirocco” (SE) winds, is directed northwards (Colantoni

et al., 2003; Regione Marche, 2005), but this has no effect on the beach sediment transport because of its longshore boundaries. The tide regime in the Adriatic Sea is semidiurnal and the average tidal range at spring tide in Ancona area is 0.47 m, with a maximum record of 0.58 m (Colantoni et al., 2003). The typical wave directions recorded by the Ancona offshore wave buoy of ISPRA (ISPRA - Servizio Mareografico “Rete Ondametrica Nazionale”, Bencivenga et. al., 2012) in the period 1999-2006 are from SE (20%) and NE (16%) (Figure 2-3), which correspond to the typical storm directions (“Scirocco” wind from SE and “Bora” wind from NNE) for the Adriatic Sea.

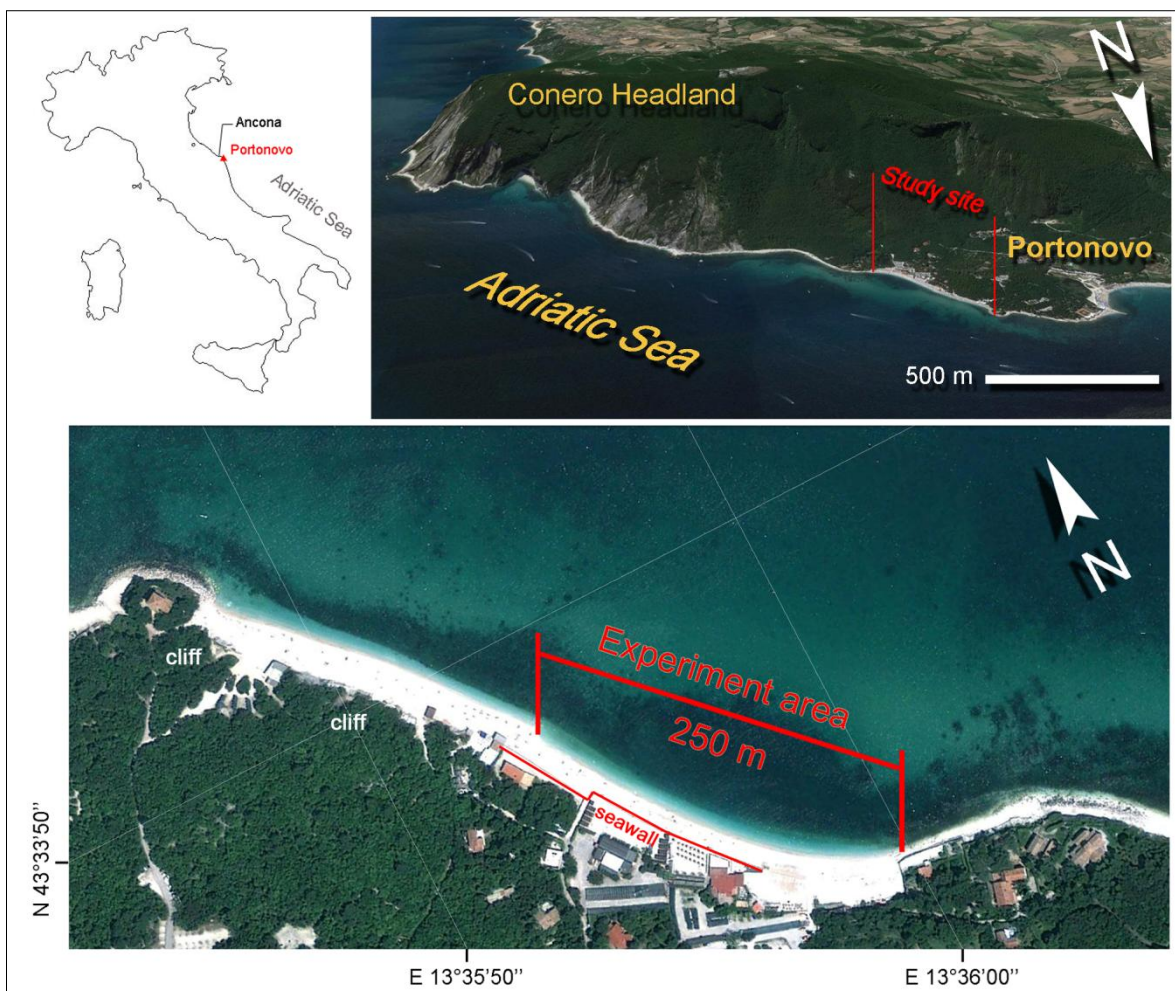


Figure 2-1. Portonovo study area.

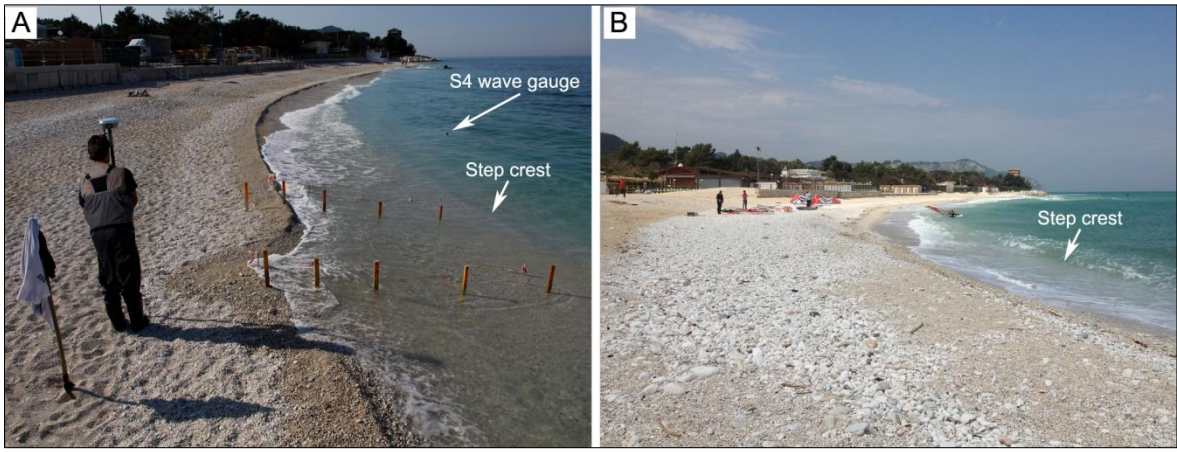


Figure 2-2. Overall view of the beach during the first (A) and the second experiment (B).

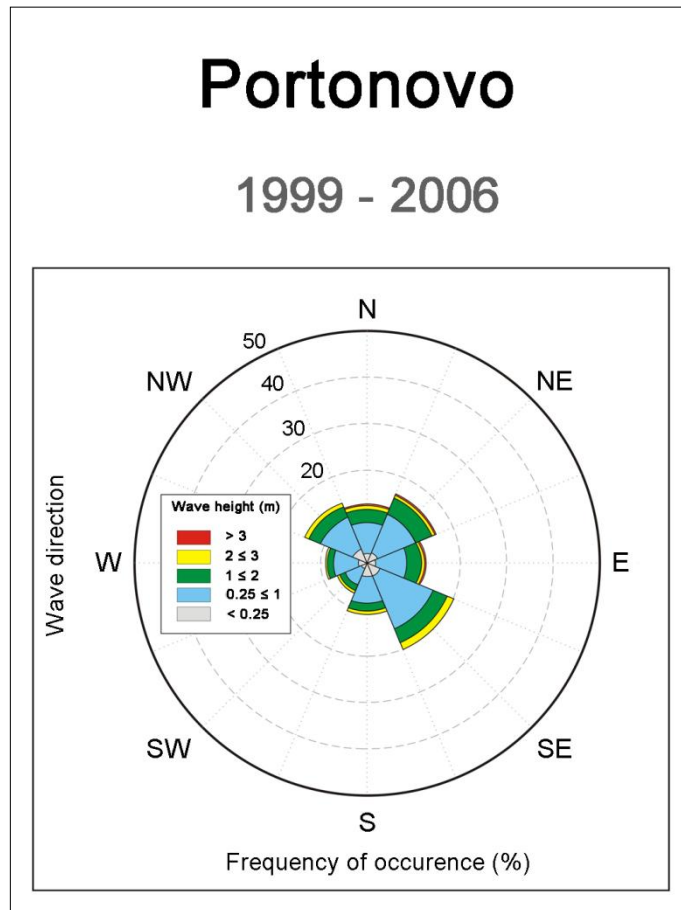


Figure 2-3. Multiyear wave climate for Portonovo (recording period from 1999 to 2006). Wave data recorded by ISPRA buoy of Ancona (ISPRA - Servizio Mareografico “Rete Ondametrica Nazionale”).

## 2.2 - Marina di Pisa beach

The mixed beach chosen on the western side of the Italian coast is located in Marina di Pisa, a small town stretching on the left side of the Arno River, only 11 Km southwest of the city of Pisa (Figure 2-4). The beach is named Barbarossa, is 180 m long and 15-30 m wide and is approximately oriented N-S (Figure 2-4; Figure 2-5). The width variation is due to the presence of some structures that were built on the backshore. Moreover, the beach is bounded on both sides by groins that prevent coarse sediments from leaving the system (Bertoni and Sarti, 2011) and a seawall, made of large boulders, separates the backshore from the littoral promenade (Figure 2-4). Barbarossa is an artificially replenished beach built in 2008 within a large protection scheme conceived by local authorities to prevent the town littoral zone from erosion and boost the local business. The native sandy beach profile was covered by marble pebbles and cobbles 60-100 mm in diameter derived from quarry waste (Figure 2-5). The replenishment pebbles mainly occupy the backshore and the step area, rather the swash zone is normally comprised of finer sediment (medium to coarse pebbles). The step base is still made of pebbles but here occurs the sediment transition to the typical and native grain size which is medium to fine sand (Bertoni et al., 2012a). The beachface has a steep slope of 0.17, whereas the sandy seabed seaward of the step is flat sloping 0.01, which is a typical value for this part of the Ligurian Sea and the rest of the region (Cipriani et al., 2001, Bertoni et al., 2012a).

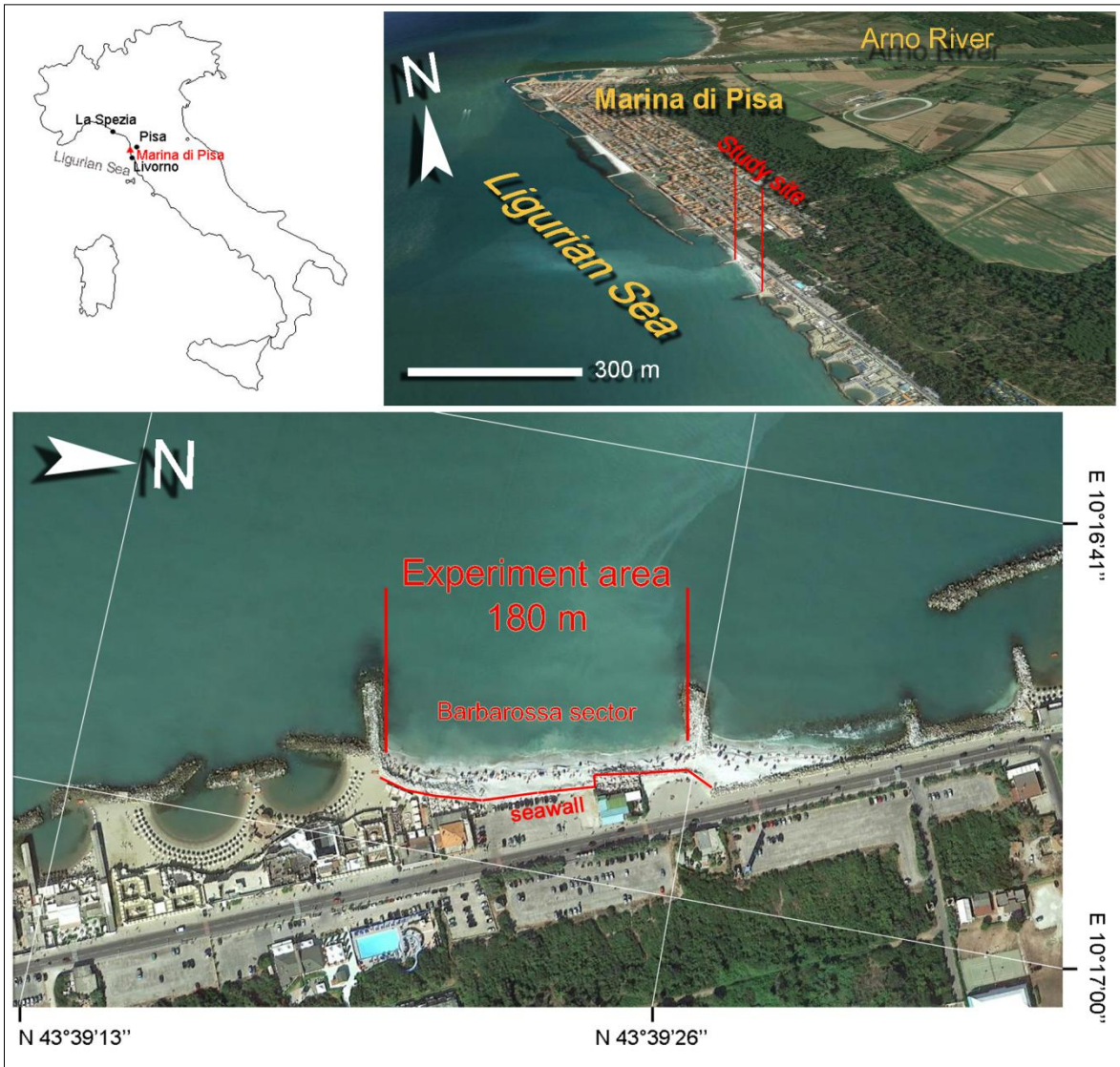


Figure 2-4. Marina di Pisa study area.



Figure 2-5. Overall look of Barbarossa beach during the experiment. View towards N (A) and towards S (B).

Barbarossa beach can be classified as reflective in accordance with the classification by Wright and Short (1984) and it can be defined as a composite gravel beach according to the classification of Jennings and Shulmeister (2002). The littoral drift along this sector of the coast is southward-trending (Cipriani et al. 2001; Pranzini, 2004; Bertoni and Sarti 2011) but this does not affect the sediment dynamics in the Barbarossa sector because of its longshore boundaries. The tide regime is semidiurnal and the maximum tidal range measured at spring tide at Livorno station is 0.38 m (Nordstrom et al., 2008). The waves most frequently approach the coastline from the southwest (Cipriani et al., 2001), and the major storms are commonly driven by south-westerly winds (Libeccio wind) as also measured between 1989 and 2007 by the wave buoy deployed by ISPRA (ISPRA - Servizio Mareografico “Rete Ondametrica Nazionale”, Bencivenga et al., 2012) off La Spezia (Figure 2-4, Figure 2-6).

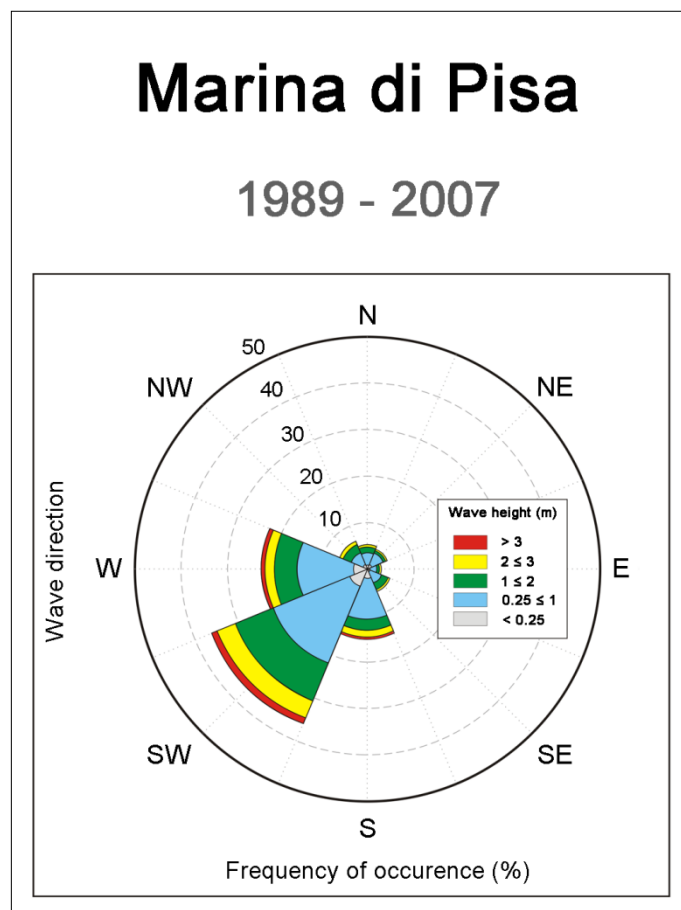


Figure 2-6. Multiyear wave climate for Marina di Pisa (recording period from 1989 to 2007). Wave data recorded by ISPRA buoy of La Spezia (ISPRA - Servizio Mareografico “Rete Ondametrica Nazionale”).

### ***3. Materials and methods***



### **3.1 - Radio tracers: RFID technology**

The pebble displacement was investigated by means of RFID technology. RFID technology is one of the most widely used automatic identification techniques and the term RFID stands for Radio Frequency IDentification. Basically, an RFID system consists of two components: the transponder (or tag), which is the effective identification device positioned on the item to be identified (Figure 3-1), and the reader (or radio signal antenna), which generates the interrogating electromagnetic field that performs the location and identification operations (Benelli et al., 2012, Figure 3-3). Each tag has an alphanumeric code that is required to unequivocally identify the item (the pebble in our case) to which is coupled. The antenna is connected to a laptop (Figure 3-2), where the tag code is shown once a tracer is detected; in addition, an acoustic signal is emitted by the RFID reader coupled with a light signal as additional warning signs of pebble detection. In order to track the pebbles underwater low frequency (125 kHz) passive transponders were used. Benelli et al. 2011 made also some tests using high frequency (13.56 MHz) transponders but the signal attenuation due to the water was too high, with a substantial decrease of the reading range. RFID technology was initially designed for subaerial pebble tracking (Allan et al. 2006, Figure 3-2) and recently improved to work in the underwater environment (Bertoni et al. 2010, Figure 3-2 B) by embedding the reader inside a waterproof plastic box (Figure 3-3 A). The electro-magnetic field generated by the antenna has a spherical shape with a 40 cm radius, which represents the maximum detection range possible (Figure 3-2). In order to prevent shorter displacements wrongly caused by the RFID antenna detection range, tracer displacements were considered significant if greater than 0.5 m in XY. The tracers were prepared by drilling each pebble to create a hole suitable to accommodate the tag (Figure 3-1 C); the hole was sealed with a waterproof resin. The tagged pebbles were randomly collected from the beach surface (backshore and beachface), the only limitation being the size, which needed to be coarse enough to be drilled. In our three experiments we used cylinder glass tags of different sizes (Figure 3-1 A, B).

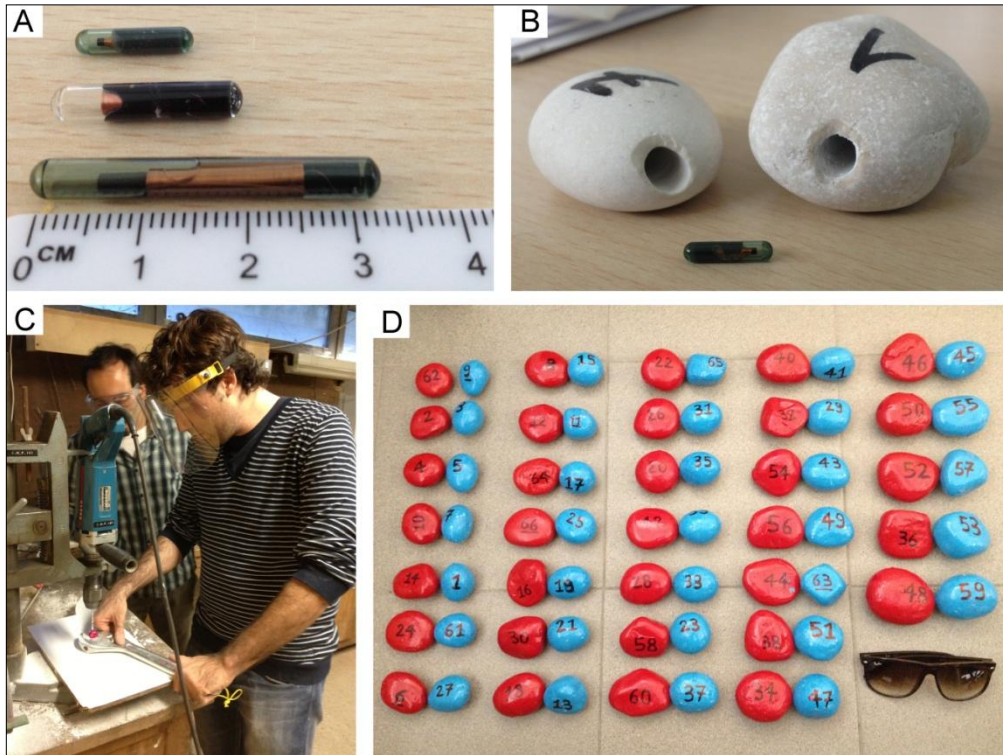


Figure 3-1. A) Cylinder tags adopted to track pebbles; B) samples of drilled pebbles; C) drilling operations by means of the vertical driller; D) Pebbles sealed and painted: the reds are disc shaped, the blue are sphere shaped. These two categories were used in the second experiment in Portonovo.

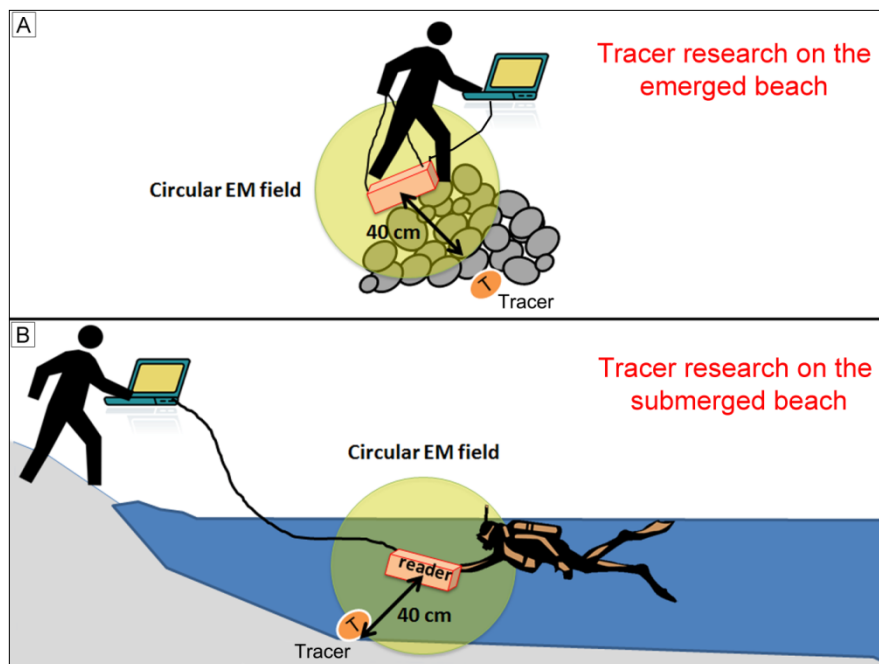


Figure 3-2. Research technique of tracers on A) the emerged beach and B) the submerged beach.

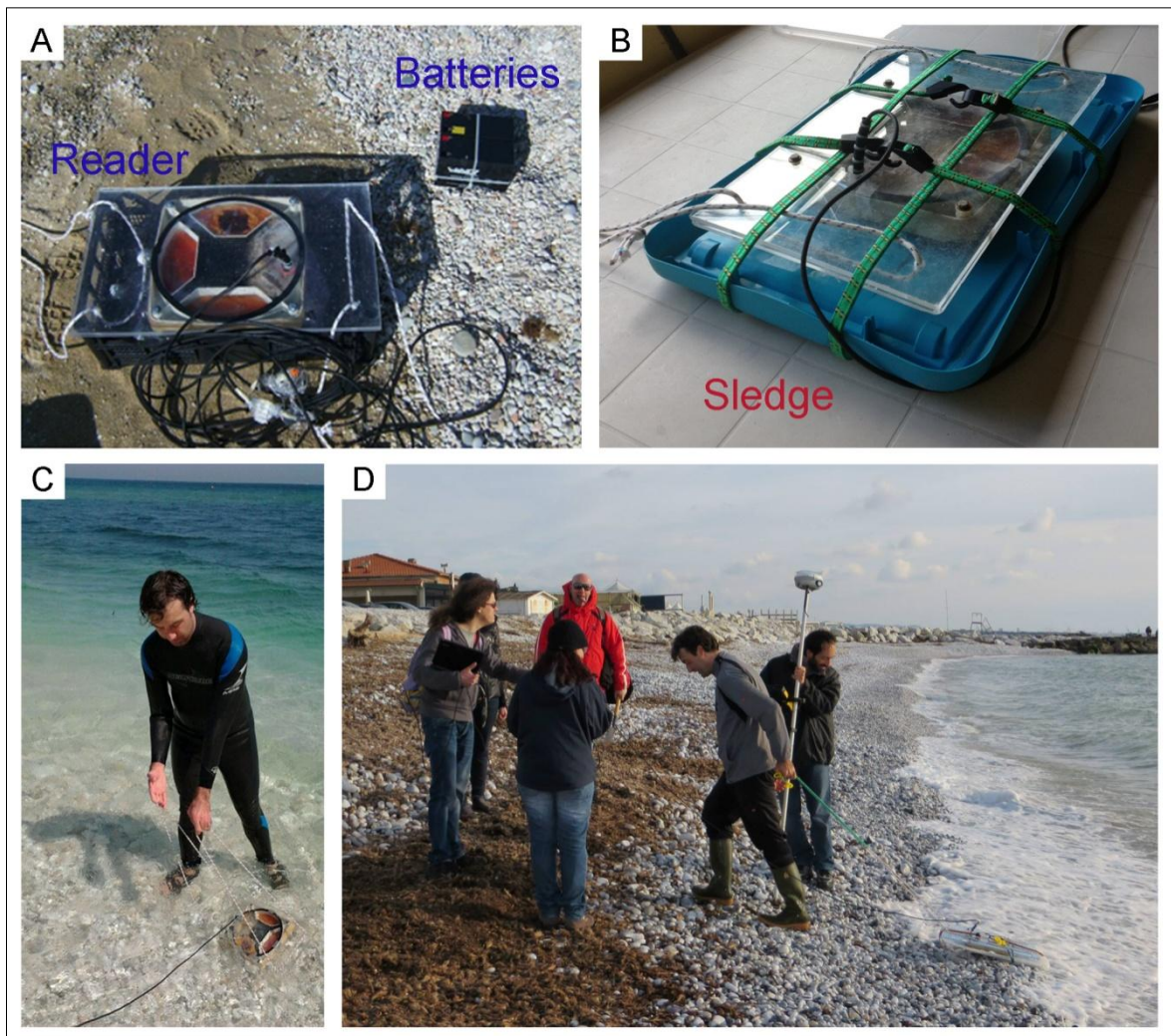


Figure 3-3. A) Reader and batteries: two plexiglass sheets render the reader waterproof ; B) Reader set up on a plastic sledge to easily drag it on the emerged beach ; C) dragging operations on a steep beachface; D) Trailing the reader on the beach surface by means of sledge.

### 3.2 - Experiment set up

Three radio tracer experiments were carried out to investigate the short term displacement of pebbles in the two beaches. Two experiments were realized in Portonovo beach and one in the Barbarossa sector of Marina di Pisa. All the experiments followed the same injection scheme which involved the deployment of tracers along cross-shore transects in the swash zone. The marked pebbles were released on three critical profile locations: on the fair-weather berm, in the swash zone mid-point, and on the step crest; following the morphological terminology of Bauer and Allen (1995). The pebbles were not just dropped on the beach surface at the three injection points, but were carefully positioned in a stable

position amid the ambient sediment, in order to facilitate a movement as natural as possible. The recovery campaigns were performed 6 and 24 h after the injection, covering both the subaerial and underwater portions of the beaches. Tracer dispersion was studied adopting the spatial integration method (SIM), method already tested on beaches by many authors (Komar and Inman, 1970; Bray et al., 1996; VanWellen et al., 1999a; Lee et al., 2000; Ciavola, 2004). The pebble displacements were measured by means of an RTK-DGPS (Trimble R6, instrument accuracy approximately  $\pm 2$  cm). In Portonovo a continuative research of marked pebbles was constantly carried out over one year time span to monitor the long term displacement of tracers.

### *3.2.1 - Portonovo experiments*

Two tracer experiments involved the same beach sector at Portonovo beach (Figure 2-1). The marked pebbles were deployed in the swash zone along 29 cross-shore transects (Figure 3-7 A) and recovered 6 and 24 hours after the injection. During both experiments, the wave characteristics were recorded by means of an InterOcean S4 directional wave gauge (Figure 3-4; Figure 2-2). The device was deployed on the bed seaward of the beachface (-1.5 m below the Mean Sea Level) to keep it underwater for the entire acquisition time (Figure 3-4; Figure 3-7 A; Figure 2-2 A). Two time series of 20 min per hour were provided, measuring the water level and wave parameters at a frequency of 2 Hz. The device was operative through the entire experiment duration.

The first tracer experiment was carried out in the early spring of 2012. The pebbles were sampled on March 17<sup>th</sup>, two weeks before the experiment: no significant topographic modifications occurred on the beach (Figure 3-5). At 10:00 am on March 29<sup>th</sup>, 145 marked pebbles were injected in the swash zone according to the following order for each transect: one tracer was deployed on the fair weather berm crest; two tracers at the swash zone mid-point; and two tracers on the step crest (Figure 3-7 A, B). Five marked pebbles were injected along each profile without taking their size or shape into account (Figure 3-7 B). Because no sediment tracer tests had ever been performed up to that date at the Portonovo beach, two marked pebbles were injected in the swash zone and on the step crest along the transects, in order to check the consistency of the resulting displacement trends.

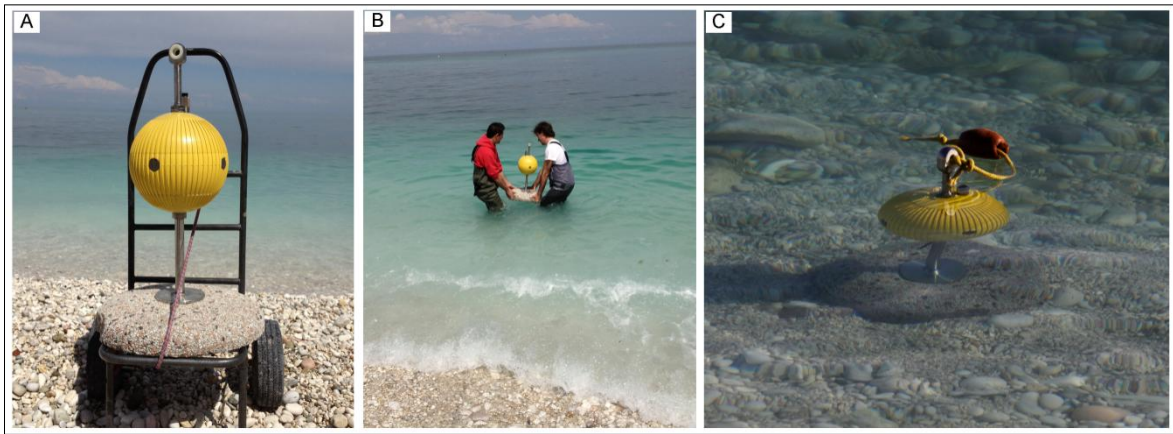


Figure 3-4. InterOcean S4 directional wave gauge.

At the time of the injection, the tracers released on the fair-weather berm (75 mm) and in the swash zone (73 mm) were characterized by average mean diameters that were not equivalent to those of the beach sediments (6 and 9 mm, respectively, Table 3-1). Beach sediment (65 mm) and tracer (79 mm) grain sizes were similar in the step area (Table 3-1). Information on the beach sediments was obtained from surface sampling carried out the day before the experiment.

The second tracer experiment was realised in mid-spring of 2013. The pebbles were sampled on March 22<sup>nd</sup>, one month before the experiment: no significant topographic modifications occurred on the beach (Figure 3-5). At 10:00 am on April 23<sup>rd</sup>, 116 tagged pebbles were deployed on every profile following the scheme: one pebble on the fair weather berm crest; two tracers at the swash zone mid-point; and one pebble on the step crest (Figure 3-7 B). No tracer subdivision in terms of shape was conducted at the injection; they were only sorted by the grain size. The mean diameter considered for tracer size subdivision was the b-axis, obtained from sieving at 0.5 phi. Three classes of size were considered: the "Small" class, characterised by a mean diameter with values between -4.5 and -5 phi (coarse pebbles according to the Udden-Wentworth grain size scale, 24 to 32 mm); the "Medium" class, characterised by a mean diameter with values between -5 and -5.5 phi (very coarse pebble according to the Udden-Wentworth grain size scale, 32 to 48 mm); and the "Big" size, characterised by a mean diameter with values between -5.5 and -6.5 phi (very coarse pebble and small cobbles according to the Udden-Wentworth grain size scale, 48 to 96 mm). One "Small" pebble was injected on the fair weather berm crest, one "Small" tracer and one "Medium" tracer were released on the swash zone mid-point, and one "Big" marked pebble was placed on the step crest (Figure 3-7 C). Four marked

pebbles were deployed on each profile (Figure 3-7 C). This type of injection scheme was conceived to understand whether a selective transport, based on the different size of the tracers, operates under low energy conditions. Due to the frequent variation of the sediment grain size in the swash zone, two different pebble sizes were released at its mid-point (“Small” and “Medium” classes) to better represent the most typical grain sizes. The tracers deployed on the step were compatible with the sediment normally present on that portion of the beach; pebbles slightly coarser than those characterising the natural sediment berm were injected on the fair-weather berm (Table 3-1). Because of the logistic limitations of the drilling operation, a mean diameter between -4.5 and -5 phi was the smallest size that could be drilled. Information on the beach sediments was obtained from surface sampling carried out the day before the experiment. A tracer distribution based on shape and size is shown in Figure 3-6 for both experiments.

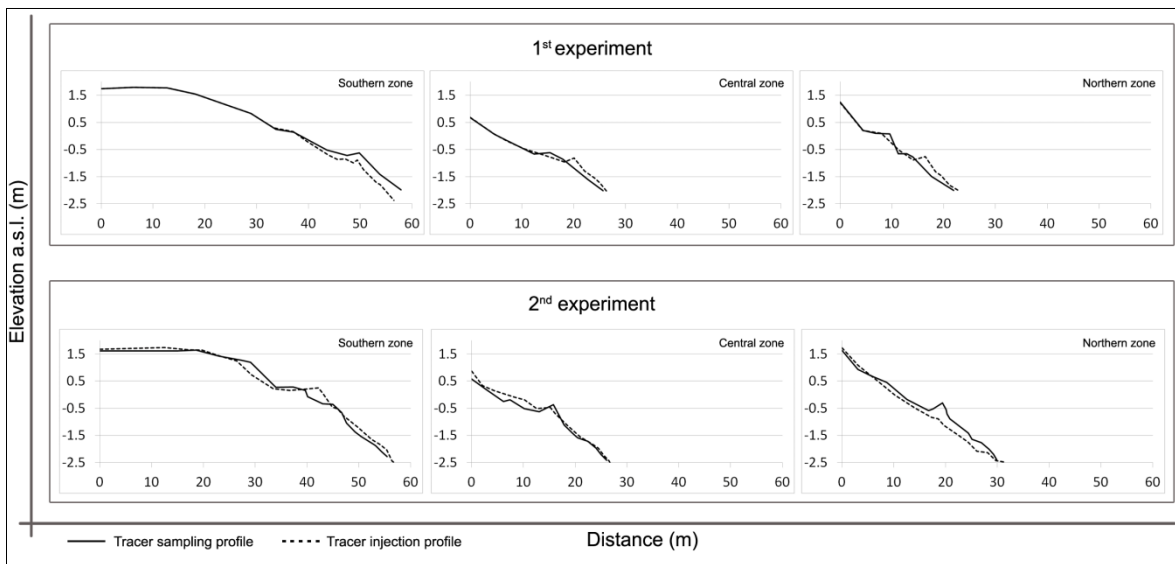


Figure 3-5. Beach profile comparison between the tracer sampling and the tracer injection for both the experiments.

Morphological feature	Marked pebbles (size mm)		Beach sediments (size mm)	
	1 <sup>st</sup> experiment	2 <sup>nd</sup> experiment	1 <sup>st</sup> experiment	2 <sup>nd</sup> experiment
Berm	75	30	6	13
Swash	73	37	9	18
Step	79	71	65	-

Table 3-1. Mean diameter comparison between the natural beach sediment and the marked pebbles. The average values showed are in mm for each morphological feature. No step crest samples were collected during the second experiment.

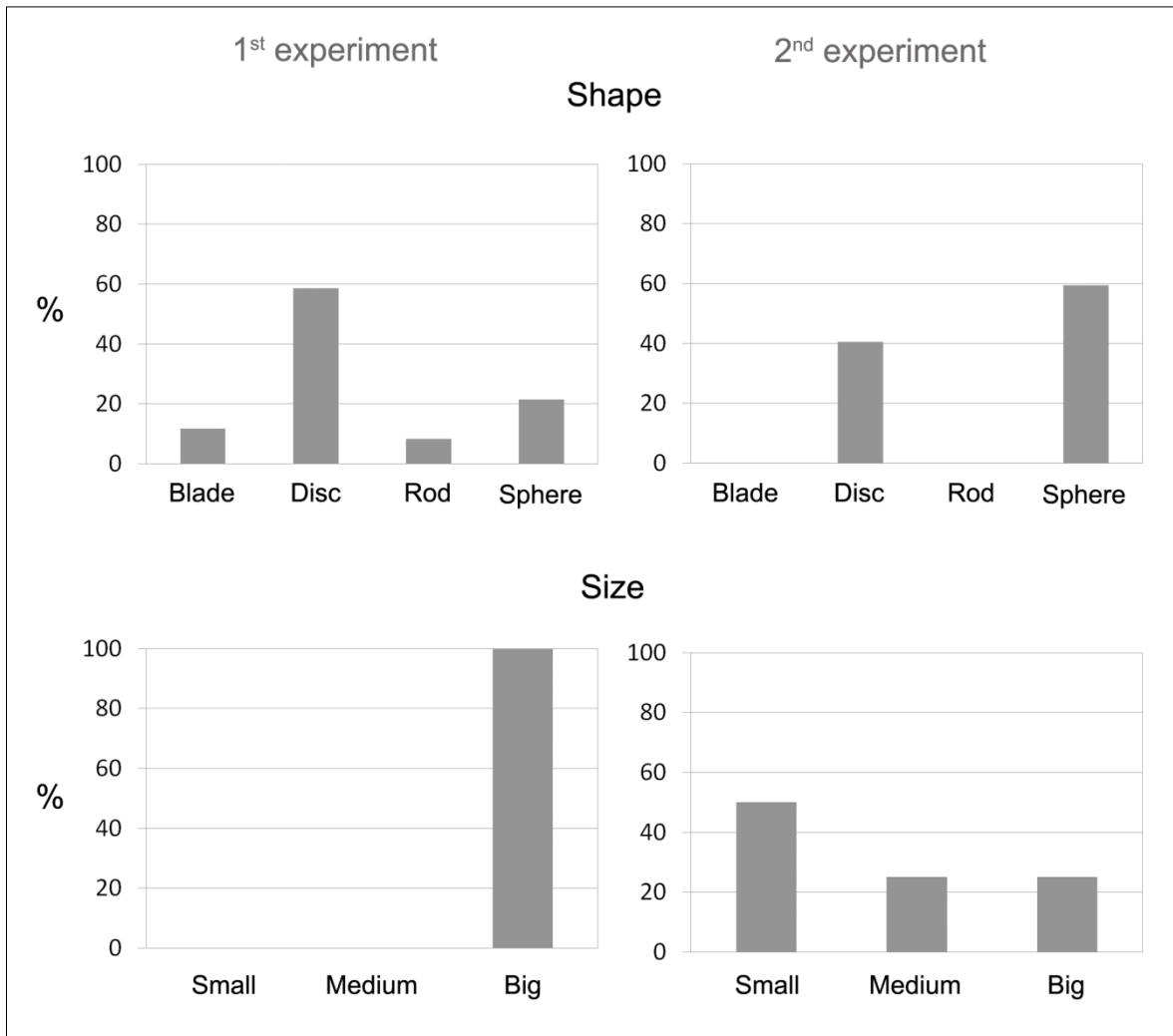


Figure 3-6. Distribution of tracer used in the experiments according to their shape and size.

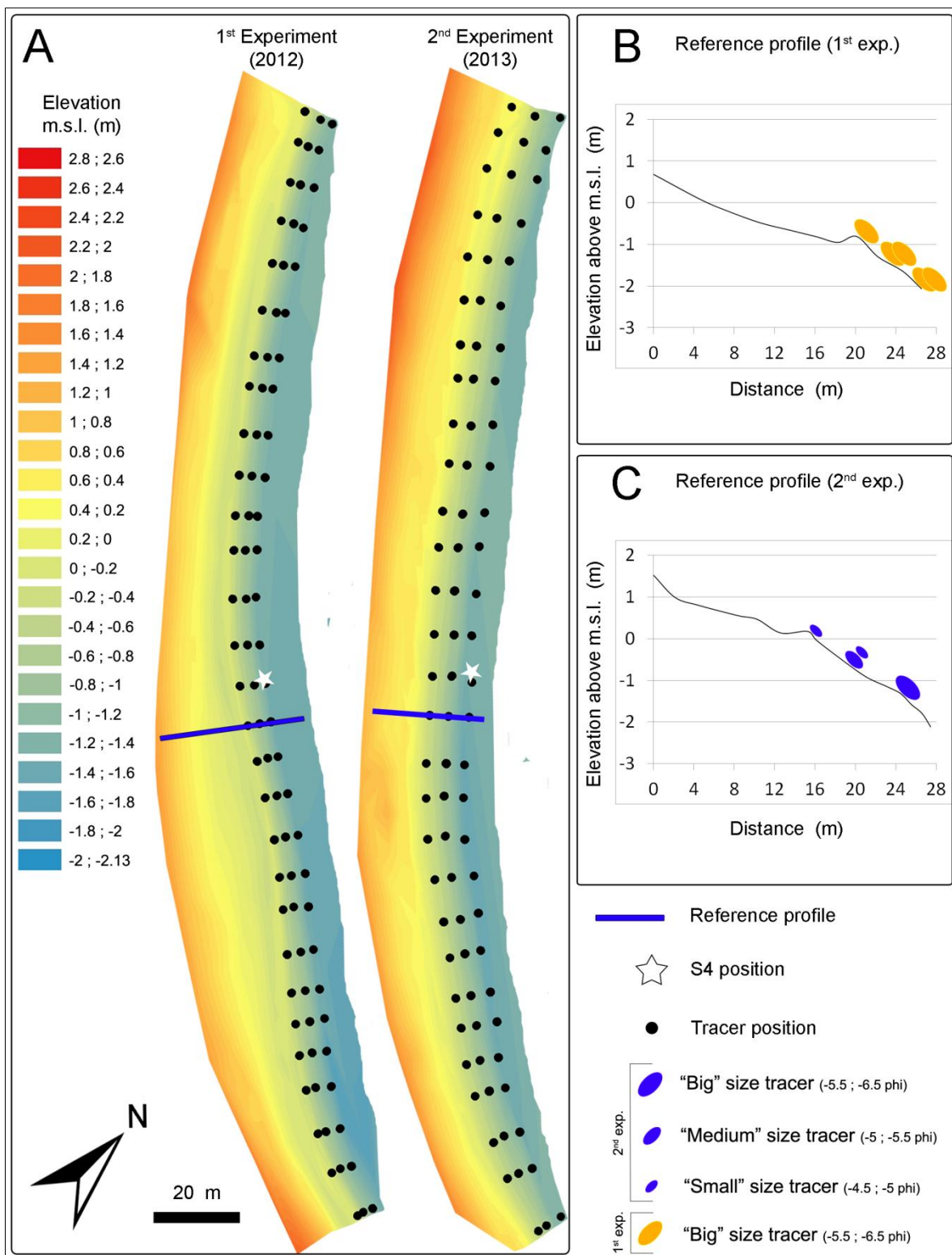


Figure 3-7. Experiment setup at Portonovo beach. A) S4 device and injection positions of tracers over an elevation surface for both experiments. Tracer injection scheme of the first (B) and second experiment (C).



During the second experiment a evaluation of the mixing depth was carried out. Three piles of 15 painted pebbles were inserted at the back side of the fair-weather berm in order to appreciate the layer of sediments interested by wave reworking after one day (Figure 3-8 A). Piles were located at three different sites along the beach: southern edge, mid sector and northern edge (Figure 3-8 B). Disc shaped pebbles were chosen in order to build a more stable pile; they were painted in blue and enumerated from 1 to 15 for each pile (the 15<sup>th</sup> pebble at the pile bottom, the 1<sup>st</sup> at the top, Figure 3-8 C). The resulting height was reckoned adding the *c axis* of each pebble which was previously measured with a caliper.

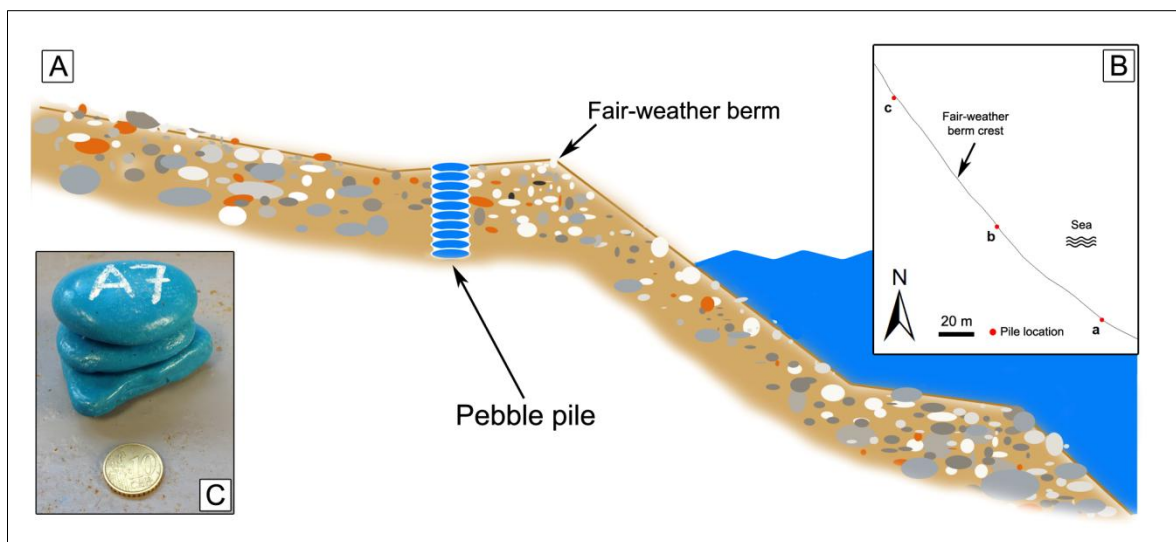


Figure 3-8. Scheme of the mixing depth evaluation conceived during the second experiment (A). Pebble pile locations in three significant beach points (B). Painted pebbles of disc shape used for the mixing depth evaluation (C).

### 3.2.2 - Marina di Pisa experiment

The marked pebbles were placed on the Barbarossa beach on 15 September 2011 along 26 cross-shore transects approximately spaced 7 m. One tracer was deployed on the fair-weather berm, one on the swash zone mid-point and one on the step crest (Figure 3-9 B), for a total of 78 pebbles. The number of tracer used is less than that released in Portonovo because Barbarossa beach is shorter and a few radio tracer experiments were previously performed (Bertoni et al., 2012a, 2012b, 2013). The wave climate at Marina di Pisa was recorded twice per hour by a wave buoy of the Tuscany Hydrographic Office located 40 km offshore (43°34.2'N, 09°57.4'E), comprising significant height, period, and direction. The water level was measured by the ISPRA (ISPRA - Servizio Mareografico “Rete Mareografica Nazionale”) tide gauge located at Livorno, 12 km south of Marina di Pisa (Figure 2-4). The dimensions of marked pebbles injected in the swash zone mid-point were quite different from those of the beach sediments present at the time of the injection (Table 3-2). By contrast, the tracers released on the fair-weather berm (82 mm) and on the step (86 mm) were homogeneous with the beach sediments at those locations (75 and 80 mm, respectively, Table 3-2). The beach sediment values are derived from samplings realised two years before in Bertoni’s experiments.

	Marked pebbles	Beach sediments
Fair-weather berm	82	75
Swash	86	35
Step	86	80

Table 3-2. Mean diameter comparison between the natural beach sediment and the marked pebbles. The averaged values are in mm for each morphological feature.

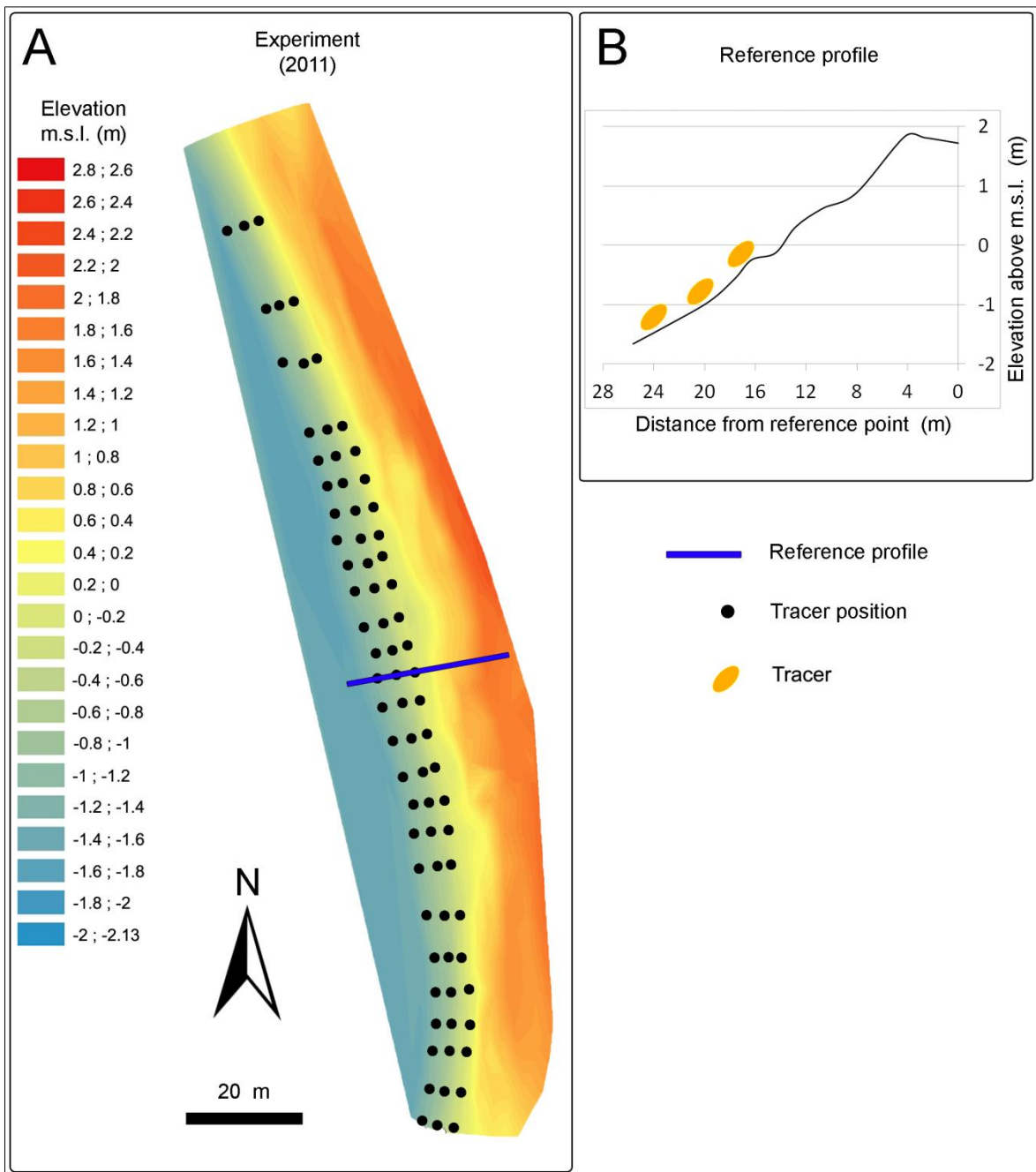


Figure 3-9. Experiment set up at Marina di Pisa. A) Injection positions of tracers over an elevation surface for the experiment at Marina di Pisa, Barbarossa sector.; B) reference profile at Barbarossa beach at the time of the injection.

### **3.3 - Surface samplings and grain size analyses**

Six surface sediment samplings were performed at Portonovo (Figure 3-10 B) beach at 3 to 4 cross-shore locations along 14 transects (Figure 3-10 A, C). Locations were selected on the basis of morphological features observed on the first sampling (Figure 3-10 A, C): the fair-weather berm crest, the back of the fair-weather berm, the storm berm crest and the backshore (Figure 3-10 C). The sample number varied from 3 to 4 on each profile depending on the presence of the storm berm. From March 2012 and April 2013, 306 samples were collected in six times (March 2012, April 2012; May 2012; October 2012; December 2012; April 2013), 51 samples were gathered at each sampling campaign performing the same sampling grid. The methodology allowed to monitor the surface sediment variability of the beach within one year span time.

Grain size analyses were performed by dry sieving using sieves of 1phi interval. The sediments were dried in an electric oven at 105 C° and the mechanical sieve shaker (Figure 3-11 A) was set to 15 minutes shaking for each sample. Every sieve was emptied (Figure 3-10 C) and then weighed by means of a precision scale (Figure 3-10 B). Grain size parameters (mean diameter, sorting, skewness, kurtosis) were calculated following the formulae proposed by the graphical method by Folk and Ward (1957) and obtained by means of software Gradistat (Blott and Pye, 2001). Beach sediments were classified according to the Udden-Wentworth granulometric scale (Udden, 1914; Wentworth, 1922a; later modified adding the phi scale by Krumbein, 1934).

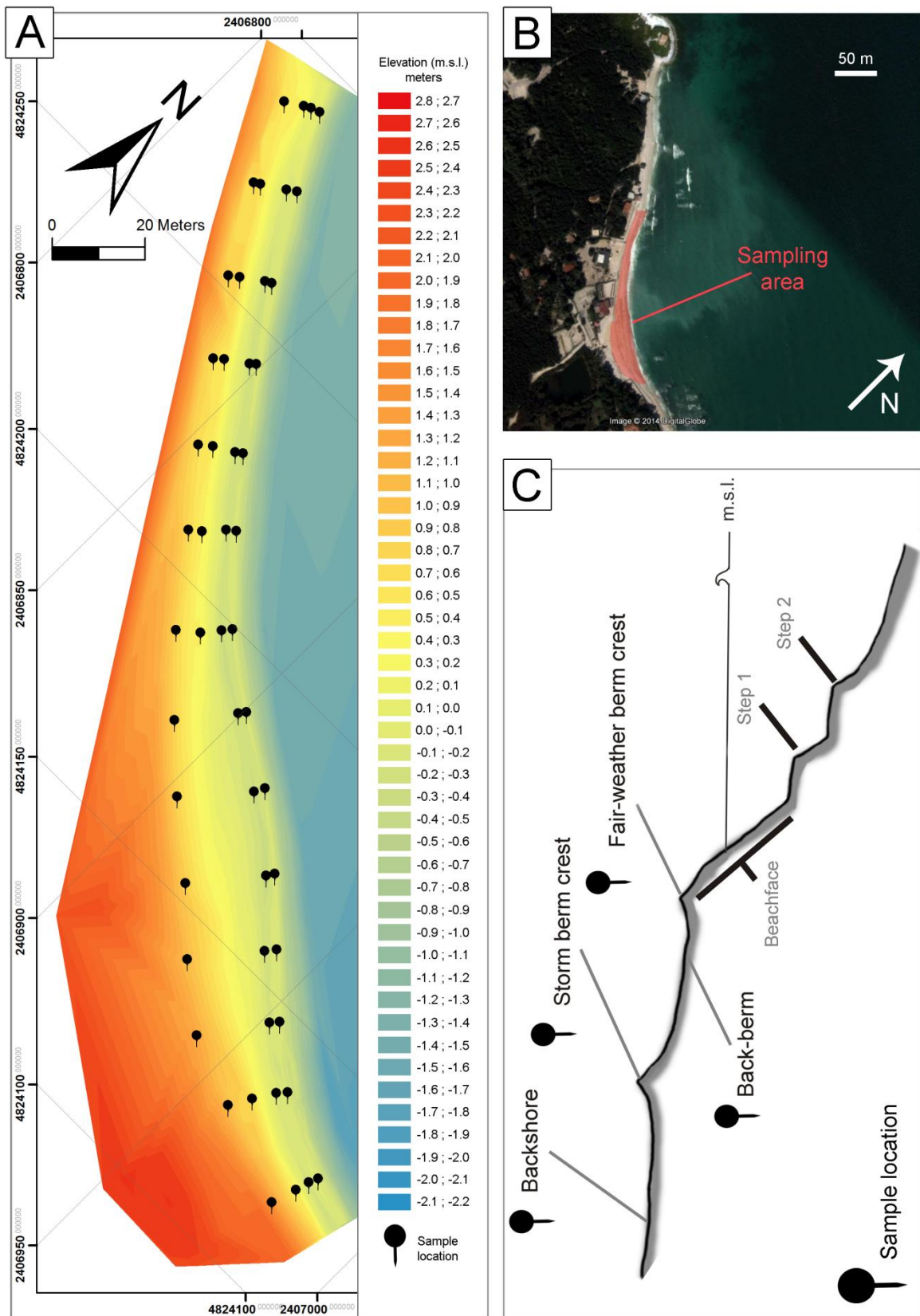


Figure 3-10. A) Sample locations of 14 cross-shore transects on topographic surface; B) Sampling area; C) Surface sampling scheme held in Portonovo and based on the morphologies found on the first sampling campaign.

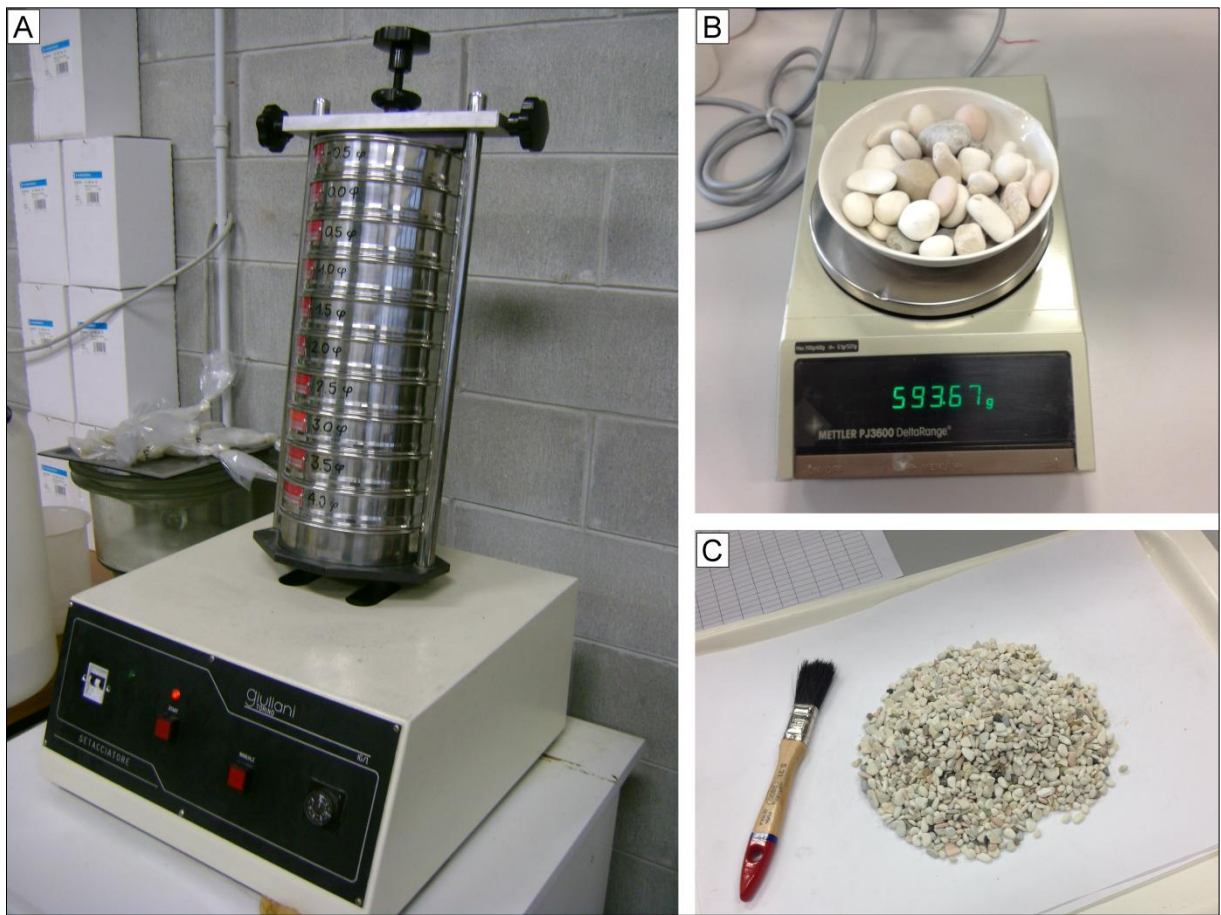


Figure 3-11. A) Mechanical sieve shaker; B) precision scale; C) example of granule content from a sieve.

### 3.4 - Topographic surveys

The beach morphology was monitored measuring cross-shore transects by means of an RTK-DGPS (Trimble R6, instrument accuracy is approximately  $\pm 2$  cm). The monitoring of beach topography was constantly (monthly to seasonally) realised only on Portonovo beach where the profile spacing is approximately 10 m for a total number of 50 profiles. After an initial monitoring that covered just the experiment and sampling area which consists of 29 profiles (Figure 3-12; Figure 3-10 A, B; Figure 2-1), from May 2012 the beach surveys covered the entire beach length (approximately 500m, Figure 2-1). Thirteen topographic surveys were measured from March 2012 to February 2014 (March 2012, April 2012, May 2012, October 2012a, October 2012b, November 2012, December 2012, January 2013, February 2013, March 2013, April 2013, May 2013, February 2013) covering a whole period of almost two years (see also Appendix A). Five profiles will be

selected and discussed in Chapter 6 to appreciate variation of beach topography during the study period (Figure 3-12).

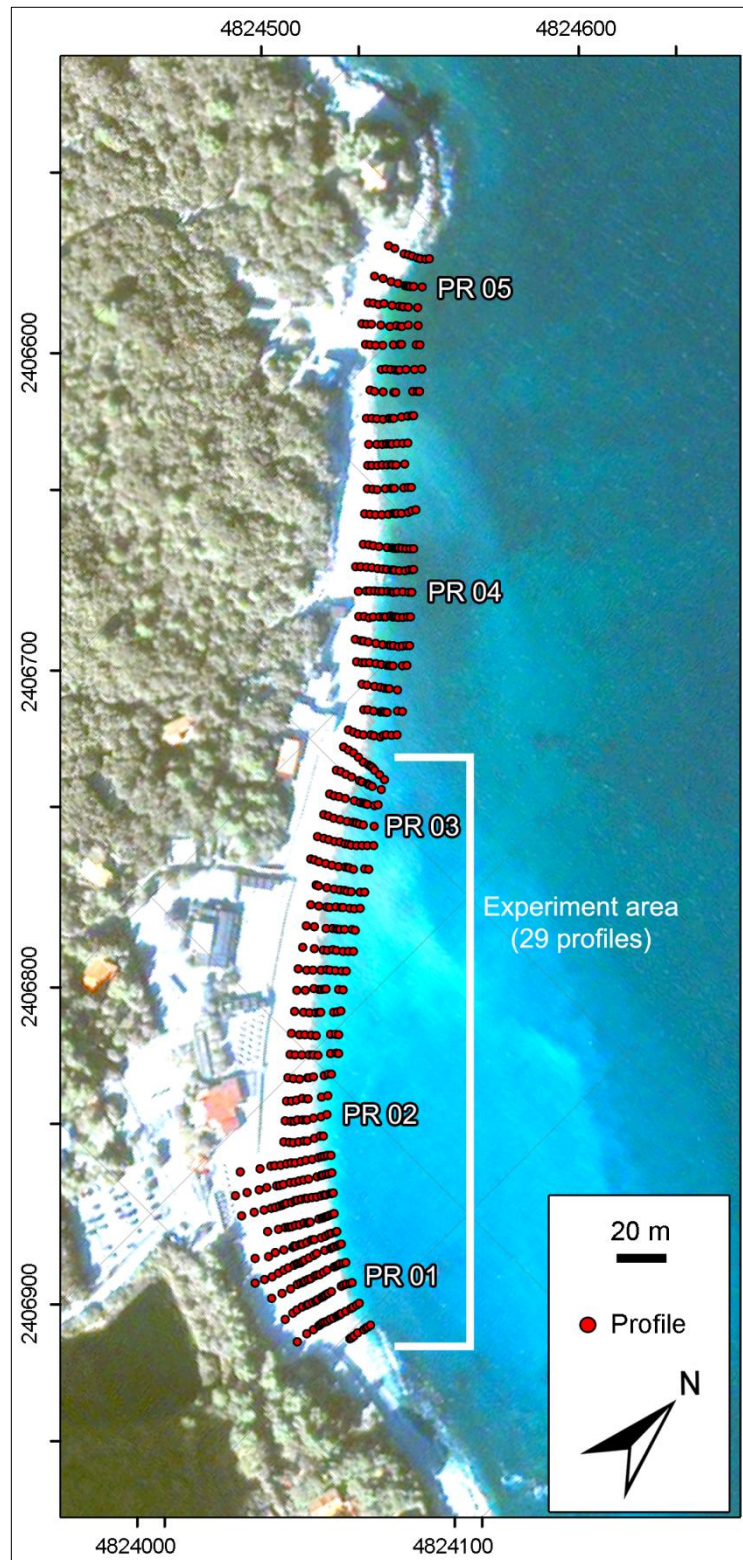


Figure 3-12. Profile locations on Portonovo beach. Topographic network repeated during each survey from May 2012 to February 2014. In bold are indicated the reference profiles shown and discussed in Chapter 6.

### **3.5 - Volume variation estimation**

Volumetric changes observed during the topographic surveys were calculated by means of the ArcGIS tool 3D Analyst. In order to exclude bad interpolated areas, a polygon mask was created for each survey based on the measured points. Then it was chosen to compute the volume from above -1.4 m, which represented the lowest elevation reached during topographic surveys and at least reached during every survey. The tool finally calculated the volume comprised between -1.4 m and the beach surface for each survey.

### **3.6 - Shoreline variation estimation**

Shoreline changes occurred during the topographic monitoring were computed by means of the ArcGIS extension DSAS 4.2 (Digital Shoreline Analysis System) created by Thieler et al. (2009). Shoreline design from GPS survey was possible using query expressions in ArcGIS in order to select measured elevation values within  $\pm 0.2$  m. Elevation measured by GPS is referred to the mean sea level position. Thirteen shorelines were digitized based on topographic surveys realised throughout the two years of measurements. Three different statistical methods were used to calculate shoreline changes by mean of DSAS 4.2: Shoreline Change Envelope (SCE), End Point Rate (EPR) and Net Shoreline Movement (NSM). The Shoreline Change Envelope (SCE) returns the distance between the farthest and the closest shoreline. The End Point Rate (EPR) returns a rate of erosion or accretion between the oldest and the most recent shoreline. The Net Shoreline Movement (NSM) reports the distance between the youngest and the oldest shoreline. NSM was computed both for the whole period of two years and for the time passed from each survey to another. SCE and EPR were only calculated for the entire monitoring time of two years, from spring 2012 to spring 2014. DSAS tool requires a number of cross-sections to be set on the GUI; to be consistent with the topographic network measured with the GPS a total of 50 transects were specified before the computation.



### 3.7 - Storm events identification

The results reported in the next chapters which deal with long term variations of sediment transport, beach topography, shoreline rotation or surface patterns variability of sediment observed in Portonovo (Chapters 5, 6, 7) will be discussed considering their relationship with the wave conditions experienced through the whole period of study (see also Appendix B). The offshore wave data were kindly provided by the ISPRA (ISPRA - Servizio Mareografico “Rete Ondametrica Nazionale”, Bencivenga et. al., 2012) and refer to the buoy located 28 km offshore Ancona. Storm events were identified following the method described by Armaroli et al. (2012). The method considers a significant wave height greater than 1.5 m which lasted for at least 6 consecutive hours. According to Armaroli et al. (2012) two storms are considered separate if the significant wave height decays below that threshold for 3 or more consecutive hours. For each storm was also calculated the severity class following the scale of Mendoza et al. (2011) which is based on the storm energy definition of Dolan and Davis (1992). The authors define the storm energy as the square of the significant wave height observed during the storm event:


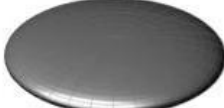


$$E = \int_{t_1}^{t_2} H_s^2 dt \quad (3.1)$$

### 3.8 - Analysis of tracer characteristics

#### 3.8.1 - Statistical analysis

Statistical analysis was performed by means of T-tests and box plots on both the pebble shape and size of tracers which were used in the Portonovo experiments. Box plots were used to describe the distributions of the pebble displacements according to shape and size separately and also to their combinational effect. The recovery distributions after 6 and 24 hours were compared for each experiment. The size classes were divided according to the scheme used for the second experiment injection (Paragraph 3.2.1, Figure 3-7 C). The shape categories were established according to the Zingg diagram (Zingg, 1935, Figure 3-13). Each shape type was represented in the population used for the first experiment. Rods and blades were subordinate to discs and spheres in terms of appearance. Due to their small quantity, the rods and blades were incorporated with the discs to compare elongated

shapes with spheres. In the second experiment, all the tracers belonged to the sphere and disc shapes. Whether a differential displacement was statistically significant between the different shape and size classes of marked sediments (0.05 significance level) T-tests were performed. Because no size discrimination was adopted on the marked pebbles of the first experiment (they all belong to the "Big" class, which ranges from -5.5 phi to -6.5 phi, Paragraph 3.2.1, Figure 3-7 B), only the second experiment size data have been used for the T-tests. T-tests were not used to analyse the combinational effect of shape and size given the scarce quantity of data that would have resulted from an additional partition that takes into account both characteristics.

<b>ZINGG CLASSES</b>	$b/a < 2/3$	$b/a > 2/3$
$c/b < 2/3$	<b>BLADE</b> 	<b>DISC</b> 
$c/b > 2/3$	<b>ROD</b> 	<b>SPHERE</b> 

**Zingg classes**  
 $a > b > c$ : axis lengths of the ellipsoid

Figure 3-13. Shape categories of pebbles according to Zingg (1935). Shape classes are based on different ratios of axis lengths.

### 3.9.2 - Threshold of tracer motion

Estimations of the threshold wave orbital velocity for motion of pebble were computed and compared with the tracer displacements that were actually measured during both experiments. S4 data have been used to determine the threshold orbital velocity which was obtained using the graphical method of Soulsby (1997), shown in Figure 3-14.

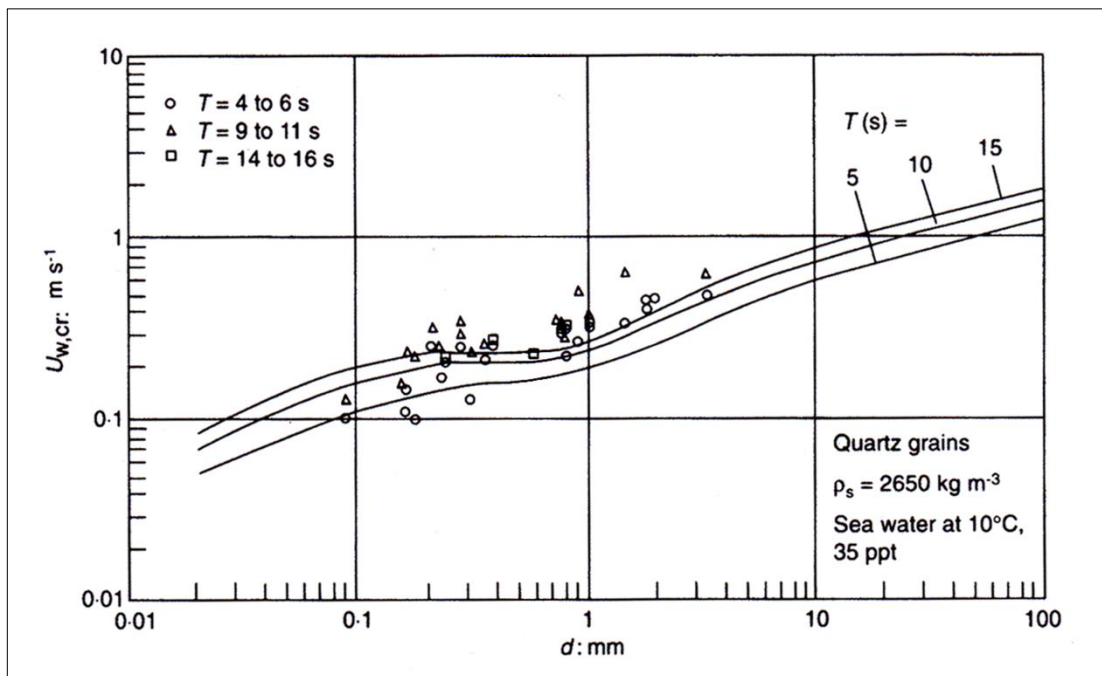


Figure 3-14. Threshold orbital velocity for motion of sediment by waves (from Soulsby, 1997).

# ***4. Pebble transport: displacements on the short and long term***

This chapter is part of the published paper: Bertoni, D., Grottoli, E., Ciavola, P., Sarti, G., Benelli, G., Pozzebon, A., 2013. On the displacement of marked pebbles on two coarse-clastic beaches during short fair-weather periods (Marina di Pisa and Portonovo, Italy). *GeoMarine Letters*, 33, 463-476.

## 4.1 - Portonovo beach

### 4.1.1 - Short term tracer recovery

In the first experiment (spring 2012) at Portonovo beach there was virtually no wave action during the two test days. The average wave height was barely 0.1 m (max value 0.15 m), and an averaged peak wave period of 4.3 s within the experiment duration. Plunging breakers were observed during the experiment. The wave direction was strongly variable: no dominant direction was recognisable even though the most frequent direction was NE (Figure 4-1). Tracer recovery after 6 hours was 99%, which slightly decreased to 93% after 24 hours (Figure 4-1). Only a few tracers moved more than 0.5 m (17% of the whole, Figure 4-1) after the first recovery, with a maximum displacement of 2.6 m. Only 1% of the detected pebbles shifted over a different morphological feature. After 24 hours, 39% of the recovered tracers moved more than 0.5 m and the maximum measured displacement was 20 m. The amount of tracers which moved to a different morphological feature increased at 17% after 24 hours. Basically, most of the tracers were dragged down the beach face, moving from the fair weather berm to the swash or the step zone (Figure 4-2 b; Figure 4-3; Figure 5-4 B). The swash zone at Portonovo beach represented the area characterized by the highest transport rate: 36% of the tracers released on the swash zone moved over 0.5 m just 6 h after the injection (Table 4-1). The highest rate among the three injection locations at Portonovo beach after 24 h was observed on the fair-weather berm where 76% of the pebbles showed displacement distances of over 0.5 m (Table 4-1). The step crest was the area least affected by transport processes: no pebbles were lost during the entire experiment and only 10% moved over 0.5 m (Table 4-1). In all cases, the preferential direction of movement was cross-shore and offshore (Figure 4-3): 14 marked pebbles moved toward the beach step already 6 h after the injection, as opposed to six showing an onshore pattern. After 24 h the difference was sharper, as only two tracers were transported onshore and 33 offshore. Longshore displacement was very low during the first 6 h (four pebbles), but increased to 21 tracers after 24 h. After the first recovery campaign (6 h), the pebbles initially released on the swash zone shifted preferentially downslope (Figure 4-3; Figure 4-2 b). After 24 h the tracer transport rate also increased at the other injection sites, i.e., the step and the fair-weather berm (Figure 4-3; Figure 4-2 c). The step crest turned out to be the area least affected by wave action: every tracer injected at the step was detected even after 24 h. The longshore component was barely active at Portonovo during the first hours of the experiment, as no tracers moved alongshore for

more than 3 m and just one for 2 m. The number of pebbles that shifted alongshore increased during the next hours: 11 tracers showed a southward-trending displacement of more than 3 m, and nine over 5 m (Figure 4-3). However, the cross-shore transport component was prevalent to the longshore component, given that the majority of pebbles injected on the fair-weather berm crest felt down the swash zone (Figure 4-3; Figure 4-2; Figure 5-4 B). No differences in transport trend were noted at the sites where two marked pebbles were injected simultaneously, both tracers undergoing similar displacement.

In the second experiment (spring 2013) at Portonovo beach the energy conditions were higher compared to those of the first one. An average wave height of 0.25 m (max value 0.38 m) with an averaged peak wave period of 6 s was measured throughout the experiment. The significant wave height hovered at approximately 0.3 and 0.4 m during the first ten hours. The wave direction was basically stable within the ENE sector with a strong predominance from E, which lasted 18 hours (Figure 4-1). Pebble recovery was 34% after 6 hours and increased to 47% after 24 hours (Table 4-1). These lower percentages, compared to the first experiment, are connected to longer paths travelled by the tracers: the maximum displacements measured after 6 and 24 hours were, respectively, 52 and 54 m. After the first recovery, 90% of the detected pebbles exceeded the displacement threshold of 0.5 m (31% of the injected pebbles, Table 4-1), which reached 89% after 24 hours (44% of the injected pebbles, Table 4-1). The percentage of shifting to a different morphological feature was 38% after 6 hours and 49% after 24 hours. The tracers did not show any peculiar trend in terms of direction after 6 hours (Figure 5-4 C). A prevalent movement direction stands out after 24 hours: pebbles released at the swash zone's mid-point essentially split towards the up-slope and down-slope locations (Figure 5-4 D). All the pebbles moved from south to north, with shorter displacements in the southern part of the beach and greater displacements in the northern sector (Figure 5-4 C, D).

In both Portonovo experiments, even though a main trend was recognisable after one day, not every part of the beach showed the same displacement patterns among the pebbles. The southern part of the beach, where the swash zone is steep and narrow, seems to be distinguished by shorter pebble displacements compared to the northern section. The latter is more exposed to wave action and looks like a "transfer zone", where a wider and milder sloping swash zone creates a more comfortable space for pebble transportation.

	Portonovo (1 <sup>st</sup> experiment)				Portonovo (2 <sup>nd</sup> experiment)			
	Recovery rate		Tracers moved (> 0.5 m)		Recovery rate		Tracers moved (> 0.5 m)	
	6h	24h	6h	24h	6h	24h	6h	24h
Injection position	6h	24h	6h	24h	6h	24h	6h	24h
Fair-weather berm	97%	83%	14%	76%	41%	41%	38%	38%
Swash zone	100%	91%	36%	50%	28%	48%	28%	48%
Step	100%	100%	0%	10%	41%	59%	31%	41%
<b>Total</b>	<b>99%</b>	<b>93%</b>	<b>17%</b>	<b>39%</b>	<b>34%</b>	<b>47%</b>	<b>31%</b>	<b>44%</b>

Table 4-1. Recovery percentages of tracers after the first (6 h) and the second (24 h) survey for both experiments at Portonovo beach. Percentages are expressed according to the injection position of tracers. Only displacements greater than 0.5 m were retained significant given the RFID antenna accuracy of about 40 cm. The last row shows the total recovery percentages without considering the injection position of tracers.

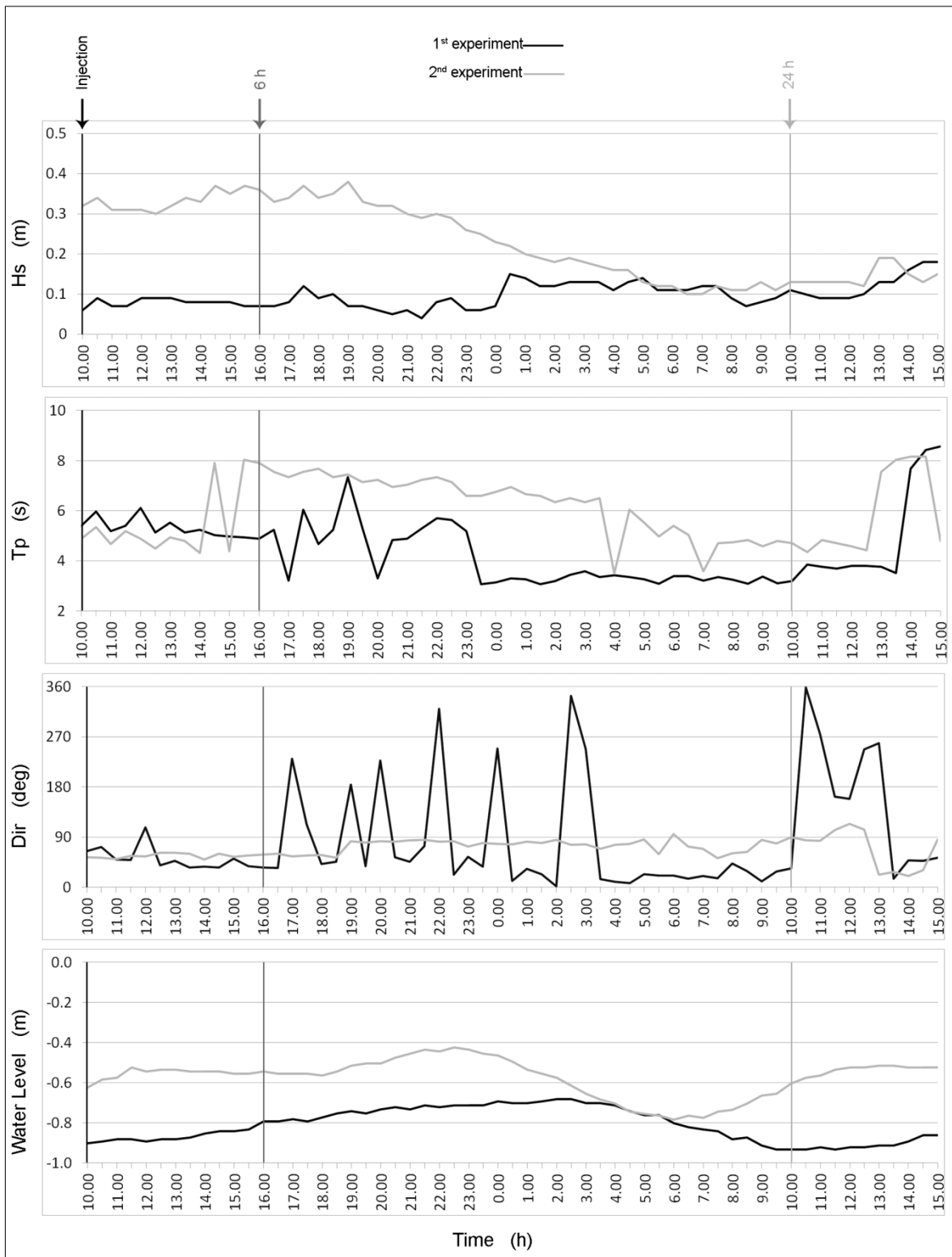


Figure 4-1. Wave climate during both the Portonovo experiments recorded by the S4 directional wave gauge.



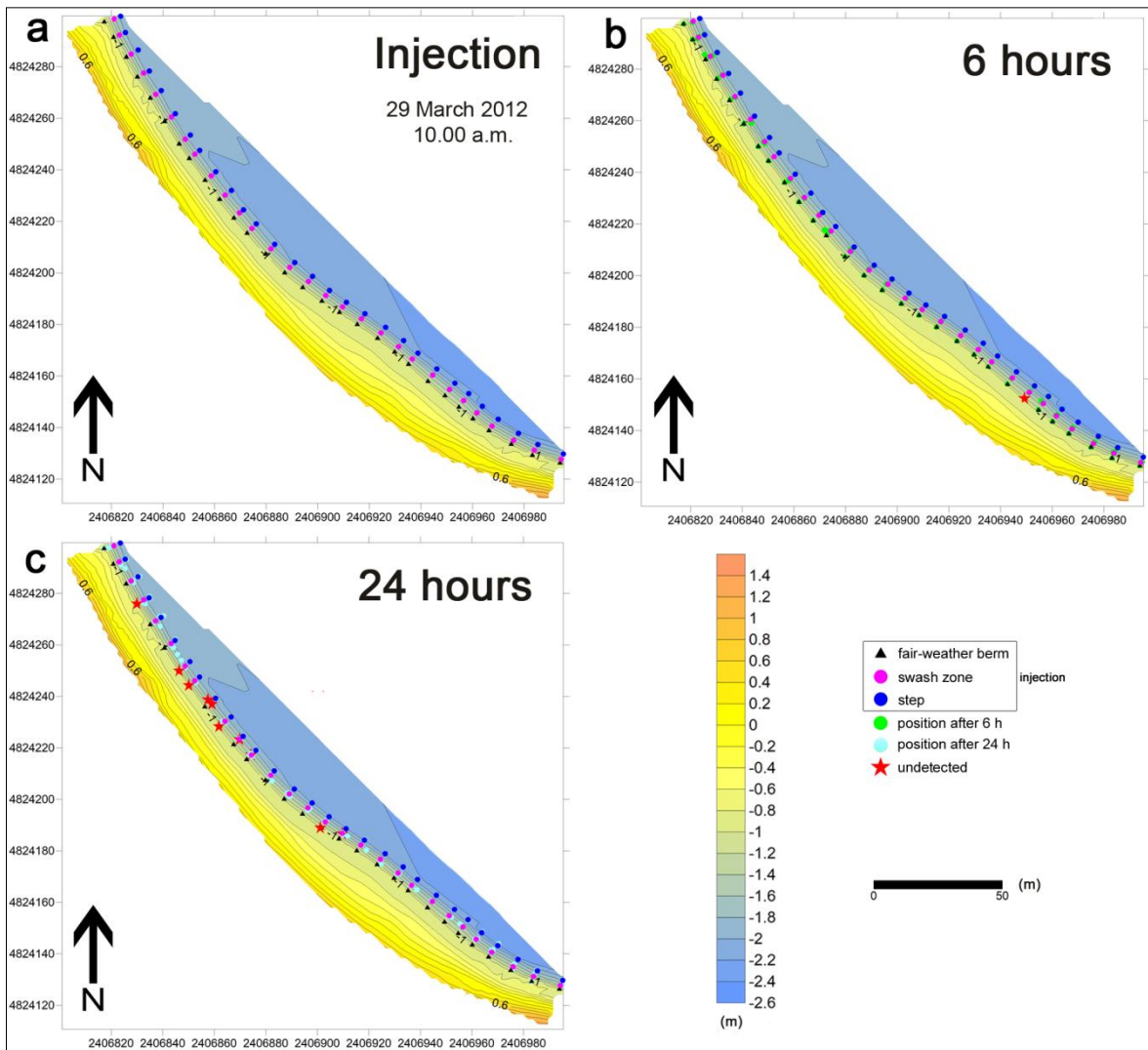


Figure 4-2. Tracer displacement within the time frame of the 1st experiment at Portonovo beach: a) injection position of each marked pebble; b) position of each detected pebble 6 h after the injection; c) position of each detected pebble 24 h after the injection.

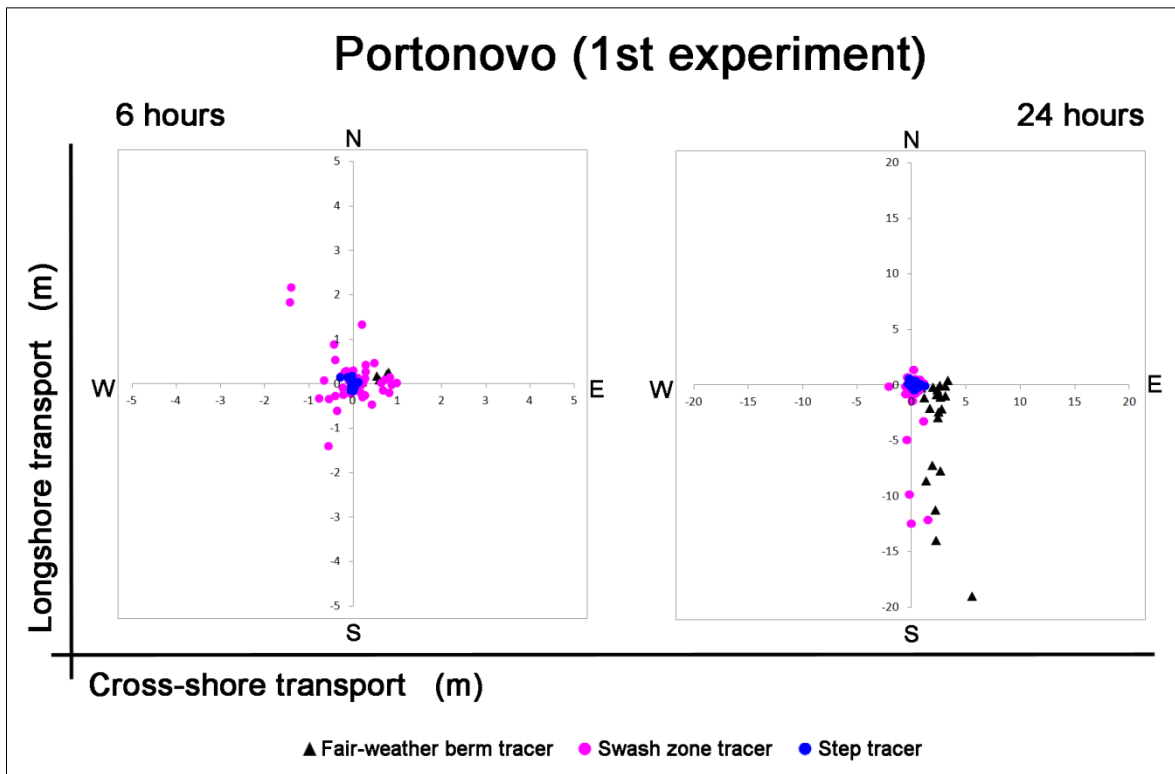


Figure 4-3. Diagrams showing cross-shore versus longshore transport for the experiment at Portonovo.

The mixing depth evaluation carried out during the second experiment gave the following results. After one day two of the three blue pebble piles were completely dismantled. As showed in Table 4-2, only the “a” pile was not entirely wiped out because the 15<sup>th</sup> pebble, initially placed at the pile bottom, was recovered in situ even after 24 hours. Therefore, a mixing depth of at least 30 cm was observed for the central and the northern sectors of the beach, whereas a slightly lower layer of sediments was reworked at the southern edge of the beach (about 25 cm, Table 4-2).

	Pile height (cm)		Mixing depth (cm)
	Injection	24 hours	
Pile a	26.15	1.5	24.65
Pile b	28.95	0	28.95 (at least)
Pile c	28.35	0	28.35 (at least)

Table 4-2. Mixing depth results for the three beach locations.

#### 4.1.2 - Long term tracer recovery

Since the 1<sup>st</sup> experiment injection (spring 2012), tracer research was repeated a few times all over the Portonovo beach. Recovery campaigns were performed on May 2012, October 2012 and April 2013 in order to monitor the tracer transport even after storm events occurred throughout one year time span. As expected, the number of tracer recovered decreased over time (Figure 4-4). During each recovery campaign tracers were searched all over the emerged and submerged beach, up to -5 m below mean sea level. No tracers were never found beyond the two physical longshore limits that delimit the beach or offshore (except for one pebble that was found during the October 2012 recovery campaign at -2.2 m below sea level), hence decrease over time of tracer recovery was possible due to burial by other sediments moved by energetic storms. Because the RFID reader detection range does not exceed 40 cm is quite easy to think that stormy waves can pile up sediment with thickness higher than 40 cm (Figure 7-6).

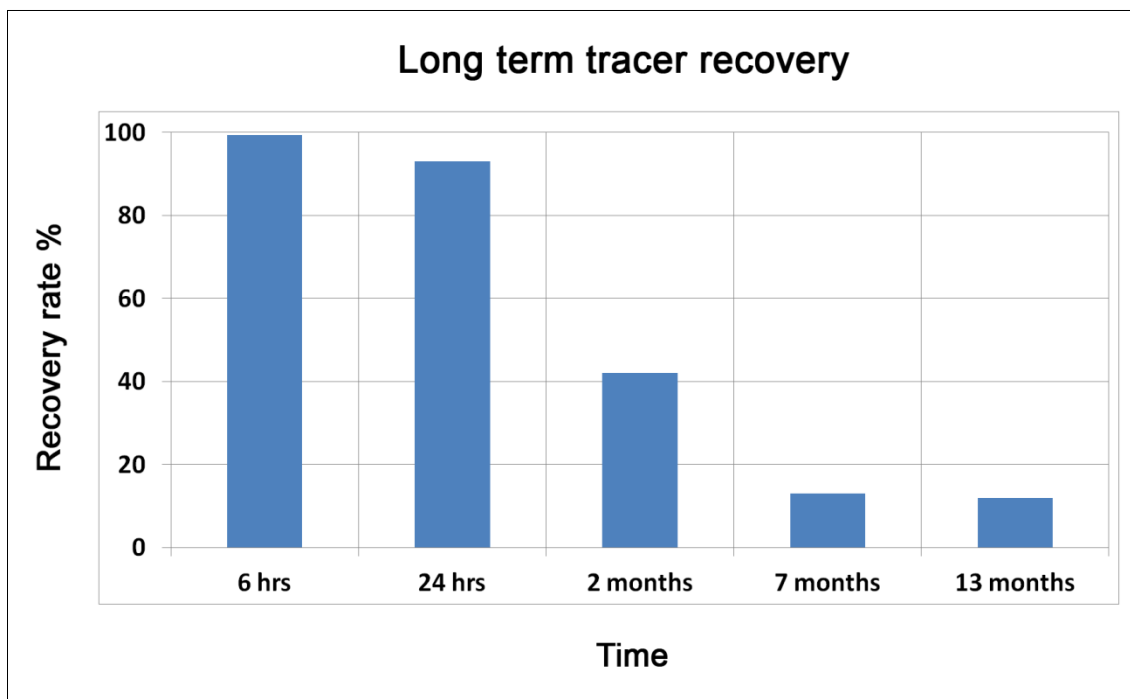


Figure 4-4. Recovery rates of tracers after one year at Portonovo beach.

The most relevant result from long term research of tracers emerged during the campaign of May 2012, two months after the injection, 61 marked pebbles were found (42 % of the injected tracers, Figure 4-4). The average displacement length was 189 m, whereas the largest was 445 m (Table 4-3), value which basically corresponds to the entire beach length. The majority of the tracers ended up on the backshore and the foreshore of the

northern sector of the beach, shifted toward NW direction relative to the injection locations (Figure 4-5). Only six pebbles moved toward SE (Figure 4-5 B) even though some of them with significant displacement length (Table 4-3). At each recovery campaign, independently from the rate of recovery, the marked pebbles were mainly found at beach edges and they were basically never recovered, except for a few, in the central sector of the beach. The latter is the narrowest area of Portonovo beach (Figure 2-1) since the backshore is delimited by a longshore seawall and acts like a transfer zone for longshore sediment transport toward the beach limits. It is interesting that basically no variations were noted between 7 and 13 months in terms of recovery rate of the tracers, i.e. 13 and 12 % respectively (Figure 4-4), and that almost all marked pebbles were different among the two recovery campaigns (only 2 pebbles were found both times). According to the morphological feature which the marked pebbles were injected on, tracers that came from the step resulted the most recovered two months after the injection, then follow the tracers from the swash zone and those from the fair-weather berm respectively. After one year the situation appeared reversed: the highest recovery rate referred to the tracers injected on the fair-weather berm while the lowest to the step tracers (Table 4-4). These findings suggest that a continuous process of accumulation and erosion of relevant sediment thickness take place according to the last storm direction and energy occurred.

Injection position	Towards NW			Towards SE		
	Displacement length (m)			Displacement length (m)		
	Min.	Ave.	Max.	Min.	Ave.	Max.
Fair-weather berm	52	190	306	40	73	105
Swash zone	15	211	445	-	-	-
Step	36	184	440	26	137	264
<b>Total</b>	<b>15</b>	<b>197</b>	<b>445</b>	<b>26</b>	<b>116</b>	<b>264</b>

Table 4-3. Displacement length covered by tracers two months after the injection according to the two longshore directions. Values are shown according to the morphological feature where tracers were injected.

Injection position	2 months	7 months	13 months
Fair-weather berm	31%	14%	24%
Swash zone	41%	10%	12%
Step	47%	16%	7%

Table 4-4. Recovery rates of tracers throughout one year time span based on the injection position of pebbles.

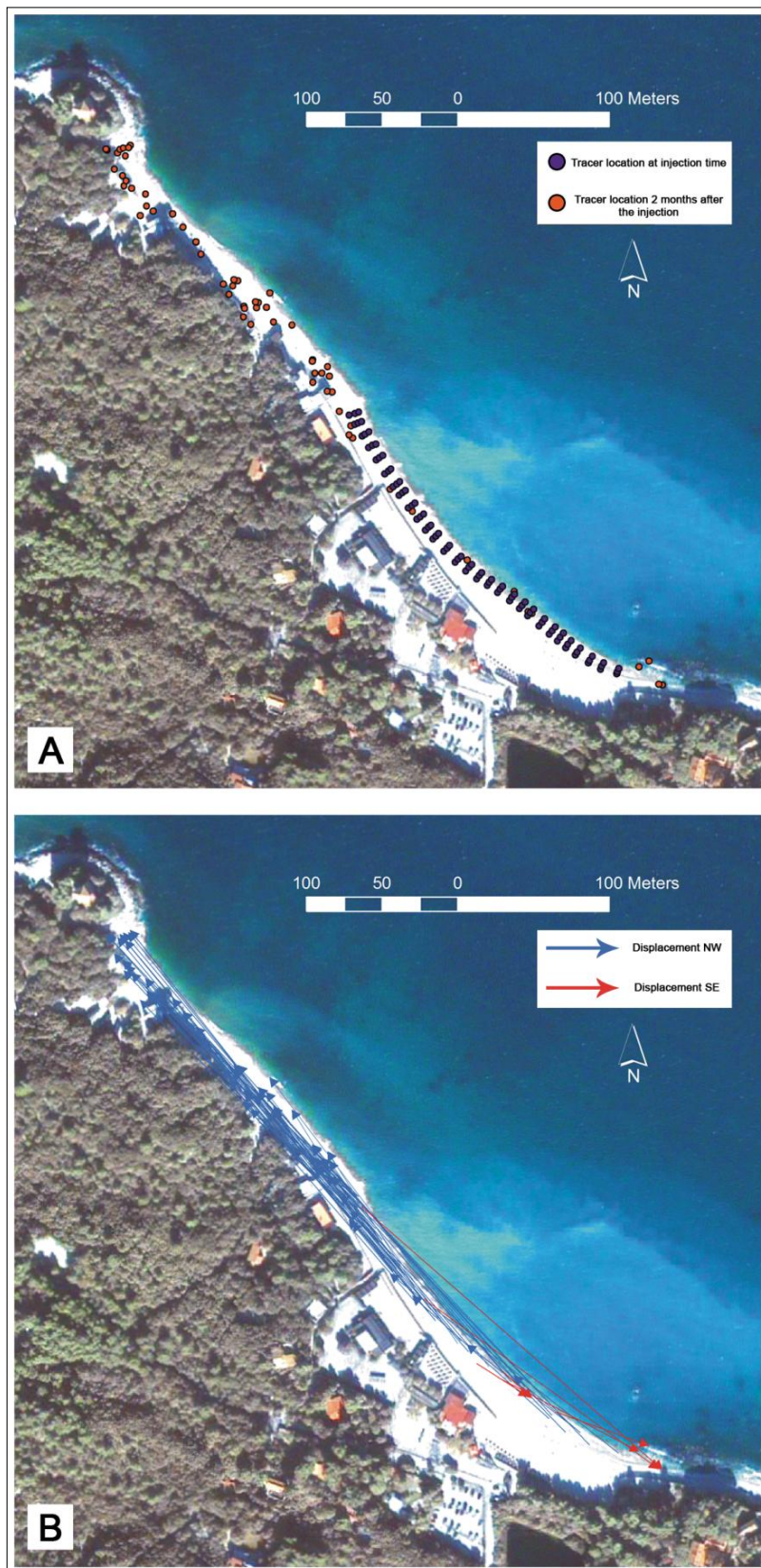


Figure 4-5. Tracer displacement two months after the injection: A) Comparison between the injection and the recovery locations; B) Displacement magnitude toward the two longshore directions (i.e. NW and SE).

## 4.2 - Marina di Pisa beach

### 4.2.1 - Short term tracer recovery

Wave motion at Marina di Pisa was very low during the entire duration of the experiment. The significant wave height never exceeded 0.32 m, with an average height of 0.22 m and an averaged wave peak period of 5.5 s. Waves broke as plunging breakers directly on the beachface. During the experiment waves approached from SW most of the time (Figure 4-6). After the first recovery campaign (6 h), 92% of the injected pebbles were detected; after the second survey (24 h), the recovery rate decreased to 85% (Table 4-5). If one compares the recovery positions with the release ones (Table 4-5), it is evident that the swash zone is the part of the beach where pebbles showed greatest mobility (keeping in mind that 19% and 27% of the tracers went undetected after 6 and 24 h, respectively). This observation is further confirmed by the percentage of pebbles that moved more than 0.5 m, which is well over 60% already 6 h after the injection (Table 4-5). On the other hand, no tracers released on the step moved over 0.5 m 6 h after the injection; this value increased to 35% after 24 h, while the percentages for the other two injection locations increased considerably less (8% to 19% for the fair-weather berm, and 65% to 69% for the step crest, Table 4-5). Among the tracers that moved over 0.5 m, only three showed onshore transport after 6 h, whereas 13 marked pebbles were displaced toward the step. After 24 h, the number of pebbles subjected to onshore movement did not change (three); those that moved offshore increased to 15. Longshore transport reached similar values to the onshore movement: three and five tracers after 6 and 24 h, respectively. After the first recovery campaign (6 h), the pebbles initially released on the swash zone shifted preferentially downslope (Figure 4-8; Figure 4-7 a, b). After 24 h the tracer transport rate also increased at the other injection sites, i.e., the step and the fair-weather berm (Figure 4-8; Figure 4-7 c). The step crest turned out to be the area least affected by wave action also in Marina di Pisa. The cross-shore transport component clearly dominated over the longshore component (Figure 4-8): only three pebbles moved over 3 m in a longshore direction after 24 h, and just one after 6 h. No unexpected transport tendency was observed at Marina di Pisa, even though the results show that transport processes were more active here than at Portonovo beach (93% and 85% of pebble recovery after 6 and 24 h, respectively, as opposed to 99% and 93%).

Marina di Pisa				
Injection position	Recovery rate		Tracers moved	
	6h	24h	6h	24h
Fair-weather berm	100%	85%	8%	19%
Swash zone	81%	73%	65%	69%
Step	96%	96%	0%	35%
<b>Total</b>	<b>92%</b>	<b>85%</b>	<b>24%</b>	<b>41%</b>

Table 4-5. Recovery percentages of tracers after the first (6 h) and the second (24 h) survey for the experiment at Marina di Pisa. Percentages are expressed according to the injection position of tracers. Only displacements greater than 0.5 m were retained significant given the RFID antenna accuracy of about 40 cm. The last row shows the total recovery percentages without considering the injection position of tracers.



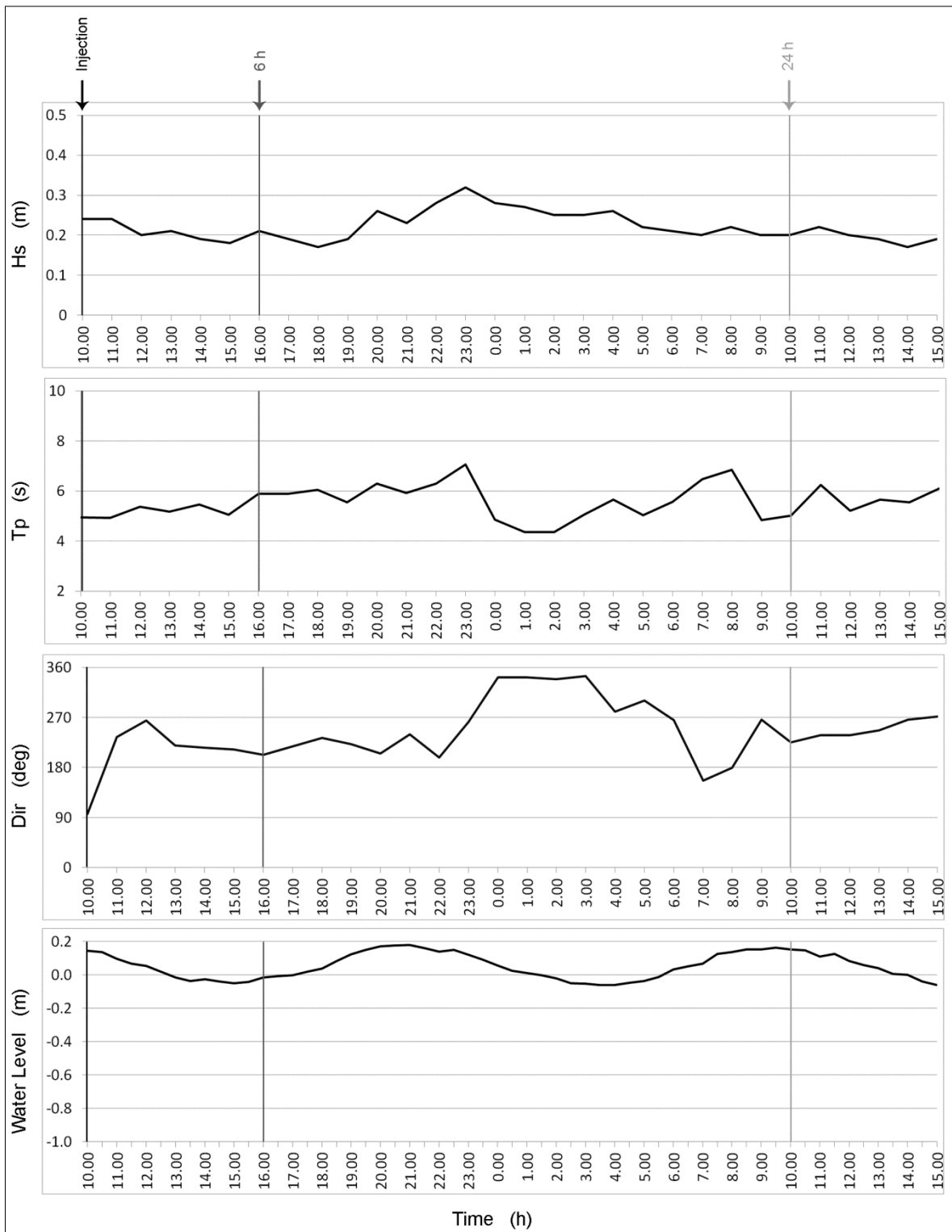


Figure 4-6. Wave climate during the Marina di Pisa experiment (wave data were provided by the Tuscany Hydrographic Office; water level data were recorded by the ISPRA tide gauge located at Livorno).

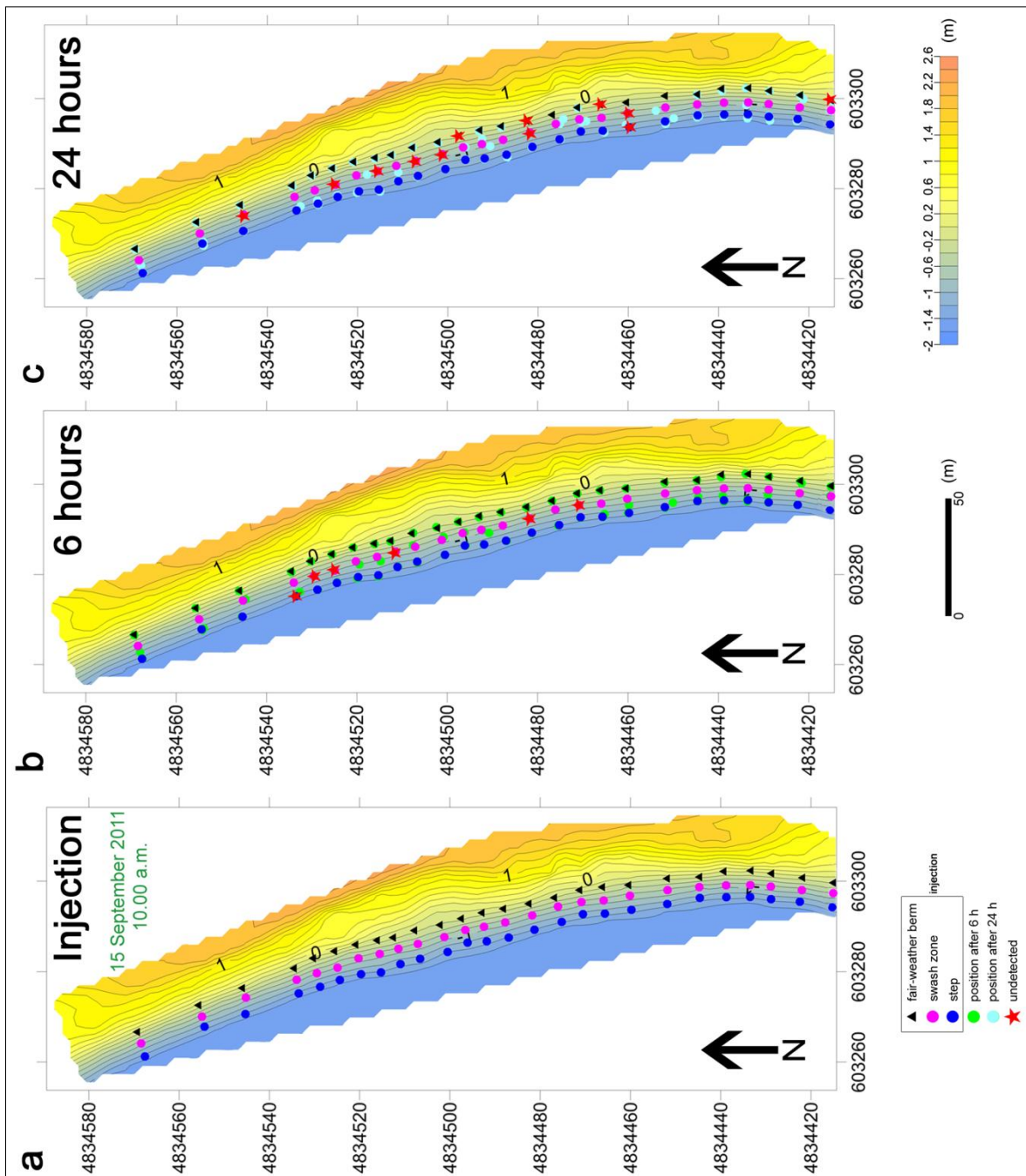


Figure 4-7. Tracer displacement within the time frame of the experiment at Marina di Pisa, Barbarossa sector: a) injection position of each marked pebble; b) position of each detected pebble 6 h after the injection; c) position of each detected pebble 24 h after the injection.

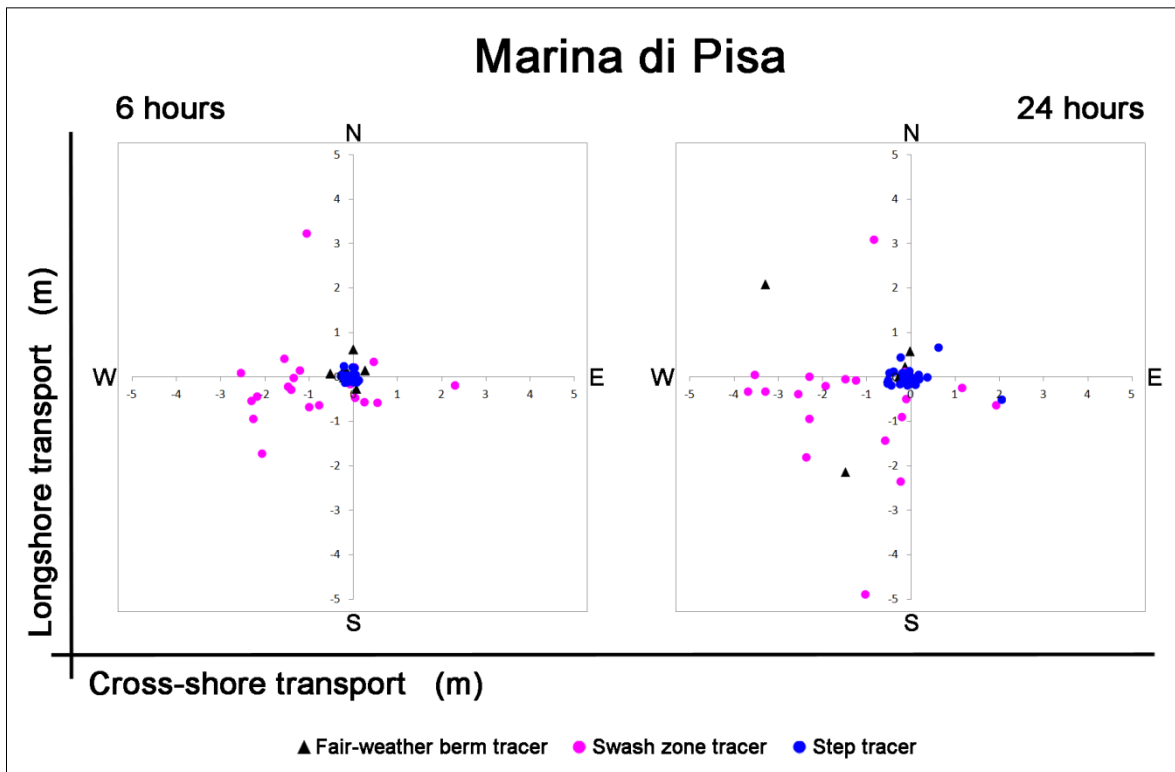


Figure 4-8. Diagrams showing cross-shore versus longshore transport for the experiment at Marina di Pisa.

### 4.3 - Discussion

Despite the low wave energy experienced during the field tests, the tracers underwent significant displacement already after 6 h, in particular in the swash zone. The fluctuations of the maximum water level within the time frame of the experiments (Figure 4-1; Figure 4-6; Figure 4-10) were a major factor affecting pebble transport because they defined the area where swash processes were most active. This point is related to the contribution of wave run-up, which in microtidal environments of the type studied here plays a key role, also overriding the influence of the tide. The persistence of uprush and backwash action at a certain elevation on the beach was found to be a key factor in controlling beach morphodynamics, even under low wave energy conditions (e.g., Sedrati et al., 2009). Since swash processes are probably the main force driving the movement of the tracers, direct measurements of the run-up velocity would have been a key parameter to explain the transport rate reached in just 24 h. However, as this was not undertaken, an estimate was made using the formula of Van der Meer and Breteler (1990) for the run-up velocity ( $v_{up}$ ):

$$v_{up} = \sqrt{\frac{1}{2\pi s}} \sqrt{gH} \sqrt{1 - \frac{z}{R_u}} \quad (4.1)$$

where  $s$  is the wave steepness ( $H/L$ ),  $g$  the gravity acceleration,  $H$  the wave height,  $z$  the location on the slope referred to as the still water level, and  $R_u$  the level of maximum run-up. The limit for the application of this formula is a beach slope of about 0.33. Considering that the beach at Marina di Pisa has a slope of 0.13 and at Portonovo of 0.1, the equation can be applied within its range of validity.  $R_u$  was calculated using three different formulae:

$$R_{max} = 2.32H_0\xi^{0.77} \quad (4.2)$$

$$R_{2\%} = (0.83\xi + 0.2)H_0 \quad (4.3)$$

$$R_{2\%} = 0.73\beta\sqrt{H_0L_0} \quad (4.4)$$

Where  $H_0$  is the deep water significant wave height,  $\xi$  the Iribarren number (Battjes 1974),  $\beta$  the beach slope, and  $L_0$  the deep water wave length. The formula of Mase (1989; Formula 4.2), although only reliable for friction-less and impermeable beds and hence not applicable to the present case, nevertheless provides the exact value of maximum run-up. The formulae of Holman (1986; Formula 4.3) and Stockdon et al. (2006; Formula 4.4) do not compute the exact level of maximum run-up ( $R_u$ ), but the 2% surplus of the peak run-up height ( $R_{2\%}$ ). However, they have the advantage of being based on field observations, albeit not on coarse beaches. Before carrying out any further work (e.g., the calculation of bed shear stress on the particles) a comparison was made with the comprehensive field dataset collected by Austin et al. (2011) on a macrotidal gravel beach. Those authors measured run-up velocities between 1 and 2 m/s, while the estimates for the present experiments were one order of magnitude higher and therefore not credible. Thus, no further work on the mechanics of pebble displacement could unfortunately be carried out, but this remains a topic to be investigated in future experiments. The tracers shifted preferentially offshore because they were quickly entrained by swash and backwash fluxes (swash grazing). Swash grazing was responsible for their seaward displacement as an additional factor to gravity processes. The slope of the beachface contributed to the downslope movement of the marked pebbles, which was triggered by the swash and then

amplified by gravity and backwash. The tracers basically needed just a small energy impulse to be destabilized before moving preferentially in the offshore (downslope) direction. The run-up levels reached during the experiments are consistent with the movement of the marked pebbles because every tracer was swept and then mobilized by the swash (Figure 4-9 a, b). For instance, using the Holman (1986) and Stockdon et al. (2006) formulae (Figure 4-9 b) at Portonovo, the run-up levels computed using the offshore data (Ancona wave buoy) increased with time and reached a maximum during the night. While during the first hours of the experiment the run-up level was below or barely over the maximum elevation reached by the tracers along the beach profile, it experienced a definite increase during the night, which is also coincident with the rise in water level. Run-up level computations using the two formulae follow similar patterns even if the Holman formula provides higher values than the one of Stockdon and colleagues (Figure 4-9 a, b). On the other hand, if run-up levels are computed using as input data those provided by the S4 directional wave gauge, there is closer agreement within the Portonovo dataset (Figure 4-9 b). Recent observations on reflective beaches in southern Portugal confirmed that run-up levels need to be computed using offshore wave data rather than nearshore wave data (Vousdoukas et al. 2009). However, when energy conditions are very low as in the case of Portonovo, offshore waves may not coincide with local wave conditions at the beach step and this may explain why the estimations of the formulae coincide better using the S4 dataset. To be truly correct, the local waves should be back-shoaled offshore using, for example, linear wave theory as suggested by Stockdon et al. (2006) themselves. However, given the wave conditions, even backtracking into deep water condition would not change the picture very much because for coarse-grained beaches there are a number of factors that complicate the applicability of run-up formulae. First, bed friction is higher than on finer grained sand slopes. Second, because the beach is highly permeable, energy is lost through percolation. This may explain why data analysis using Formula 4.2 provided entirely unrealistic results. Moreover, the choice of the beach slope for use in the formulae very much controls the results because it either appears directly in the equations or in the Iribarren number. Stockdon et al. (2006) suggest that this should be the foreshore slope and not just the beachface slope. In the present case the former was used, including the beach step and the seabed slope at the base. A comparison between Formula 4.4 and the generalized expression contained in the paper of Stockdon et al. (2006) showed that the simplified version was in better agreement with the observations of tracer elevation displacement. According to those authors, this is sufficient for reflective conditions, keeping in mind that in their datasets they observed a high root mean square

error between predictions and observations. However, their datasets were generally derived from beaches with slopes gentler than the foreshores at Marina di Pisa (0.13) and Portonovo (0.10), with the exception of the datasets collected at the Duck pier (NC, USA), which are in any case from a coarse sandy and a gravelly beach (Stockdon et al. 2006).

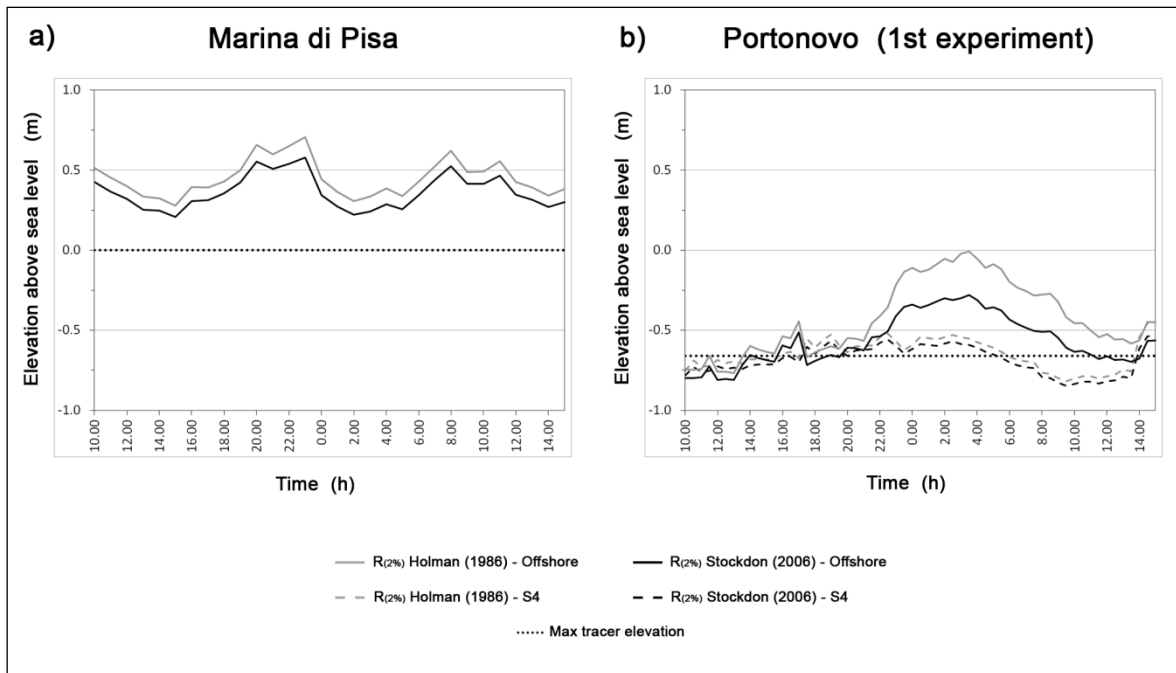


Figure 4-9. Plots of the run-up levels computed for Marina di Pisa (a) and Portonovo 1st experiment (b) using the formulae of Holman (1986) and Stockdon et al. (2006), compared to the maximum tracer elevation (horizontal dashed line).

The preferential mobilization of swash zone pebbles on both beaches may also be related to the difference in grain sizes between beach sediment and tracers at the time of the injection. Under low-energy conditions, the winnowing of finer sediments can expose underlying pebbles and thereby promote their displacement. This is particularly evident at Marina di Pisa where the tagged pebbles of the swash zone were clearly the tracers that moved more vigorously than those at any other injection site where the grain-size difference between beach sediment and marked pebbles was negligible. Conversely, at Portonovo the swash zone was composed of very fine pebbles and gravel, which enabled the coarser pebbles to be moved first, as reflected by higher displacement rates with a subordinate alongshore transport (Figure 4-3). Nine pebbles showed a south-trending alongshore component (Figure 4-3), which is consistent with the dominant wave direction recorded by the S4 device (Figure 4-1). None of these tracers was injected on the step, and their average mean diameter was significantly smaller compared to that of the rest of the

marked pebbles released at the same injection level (62 mm as opposed to 75 mm on the fair-weather berm, and 61 mm as opposed to 73 mm in the swash zone). Their finer dimensions probably favoured greater displacement. Once the tracers reached the step crest, they usually settled there, possibly because onshore wave forces were too weak to move them upslope against gravity. As a matter of fact, swash zone pebbles that showed displacement over 0.5 m after the second recovery campaign (24 h) were lower in number than those that reached the same position after 6 h. After 24 h the transport rates of tracers injected on the fair-weather berm increased. This tendency was not caused by higher wave energy, but rather by incessant swash action reworking the foreshore. The rise in water level recorded during the night enabled swash action to reach higher elevations along the beach profile (Figure 4-10 a, b). This trend is particularly evident at Portonovo, where the fair-weather berm was first eroded and then reformed by swash action (Figure 4-10 b). The pebbles released on the berm showed higher transport rates after 24 h than after 6 h. They basically moved toward the step crest during the erosion of the berm. This trend was not so evident at Marina di Pisa because the berm was composed by coarser sediment. Here the beach profile did not show any modifications during the experiment (Figure 4-10 a), which explains why the pebbles that moved the most were those released in the swash zone. The average mean diameter of these pebbles (86 mm) was substantially different from that of the sediment present at the time of the injection (35 mm). This determined the preferential shift of the coarser fraction but did not imply major modifications of the beachface. The datasets of the present study represent a further step toward filling the gap in knowledge for low-energy relative to high-energy coarse-clastic beaches. In fact, previous studies on coarse sediment transport were mostly carried out on high-energy beaches (Deguchi et al. 1998; Mason and Coates 2001; Buscombe and Masselink 2006; Curoy 2012). In all these cases a dominant onshore transport was observed, which is in sharp contrast with the prevailing downslope movement of the tracers released at Marina di Pisa and Portonovo. A previous study performed at Marina di Pisa (Barbarossa sector) also observed a prevalent onshore movement of sediment, but that investigation was performed after several storms in the course of 1 year (Bertoni and Sarti, 2011). Other fieldwork carried out on the beaches of Marina di Pisa during 2-month-long experiments (Bertoni et al. 2010, 2012a) confirmed the predominance of onshore movement as opposed to offshore movement, but the dominant overall displacement was alongshore. Onshore displacement of sediment was also reported by Ellis and Cappiotti (2013) during tests on a laboratory model of the Marina di Pisa gravel beaches simulating strong storms. These findings support the notion that the downslope movement of pebble-sized sediment occurs preferably during fair-

weather periods. The present results are in accordance with those of Saini et al. (2012) from an estuarine coarse-clastic beach, which was characterized by wave-energy conditions similar to those at Marina di Pisa and Portonovo, at least in the short term. Downslope displacement of coarse sediment potentially causing erosion in the short term was also reported by Austin et al. (2011) from a macrotidal gravel beach in the UK (Slapton). Those findings confirm the tendency observed at the Marina di Pisa and Portonovo beaches, which are composed of respectively coarser and finer sediment than that at Slapton. Although 24 h is not a long enough time span to cause any weight loss of the tracers by attrition, the results of the experiments may have repercussions for abrasion issues. In an experiment carried out at Marina di Pisa (Barbarossa sector), Bertoni et al. (2012b) found that pebbles of the same size as those released in the present study on average lost more than 10% of their mass in just 2 months. Considering that (1) only three storms occurred in that span of time, and (2) the transport rate reported by the present experiment in only 1 day, it is reasonable to expect that frequent movement during fair-weather periods should also have contributed to the observed wear of the pebbles.



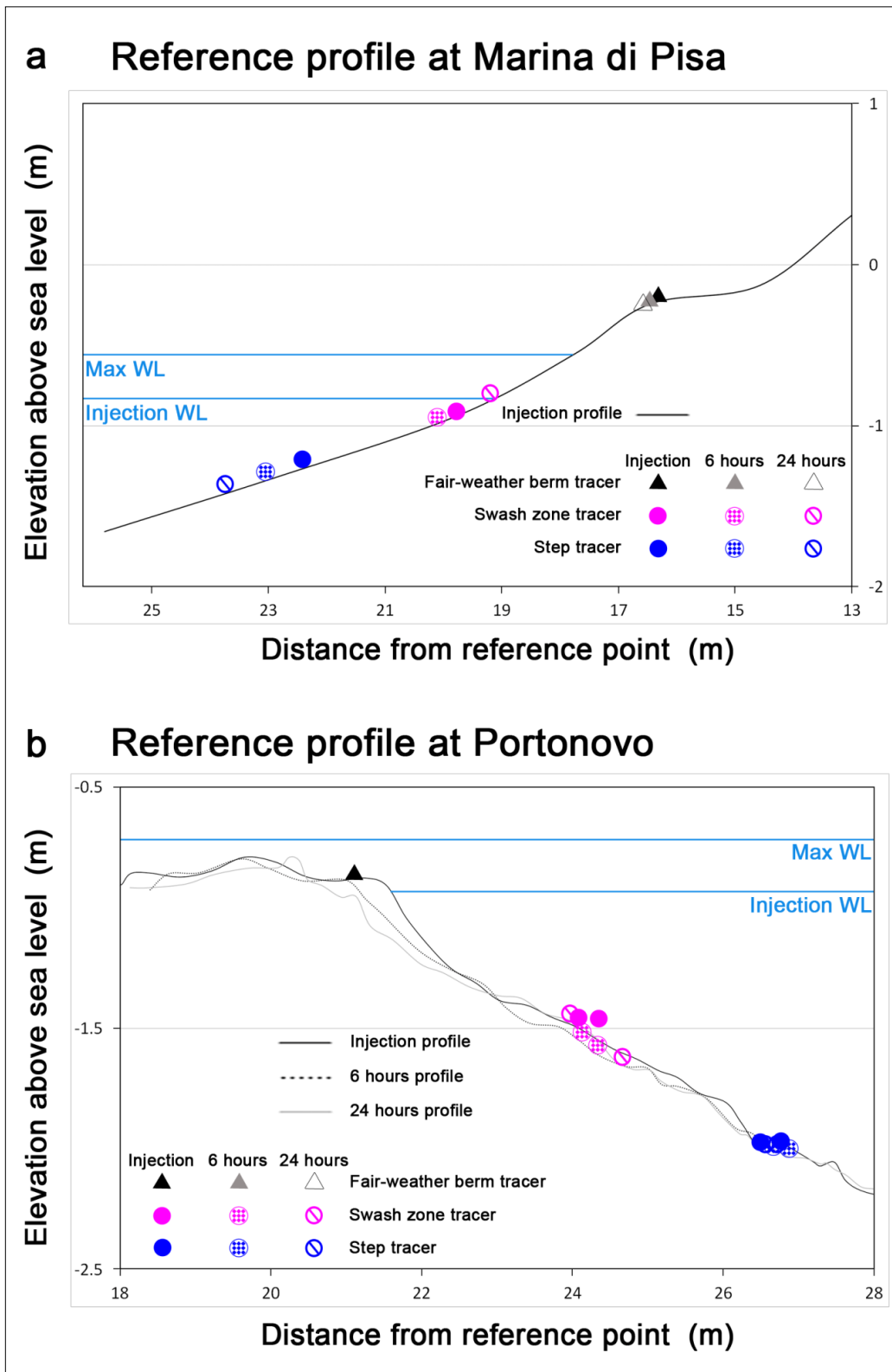


Figure 4-10. Evolution of the beach profiles taken as a reference during the experiments on the two beaches; tracer positions at the time of the injection and after 6 and 24 h are also illustrated. a) Marina di Pisa, Barbarossa sector: only one profile is shown because no change was recorded during the experiment. b) Portonovo beach (1st experiment). Injection WL Water level at the time of the injection, Max WL maximum water level reached during the experiment.

The long term monitoring of tracer displacement allowed to highlight some specific insights on pebble transport. The NW-SE orientation of Portonovo beach maintains the system exposed to storm driven by “Bora” (NNE) and “Scirocco” (SE) facilitating the transportation of sediments from one edge to another of the beach over the entire length of 500 m. This order of displacement magnitude was observed also by Curoy (2012): after seven months a maximum longshore displacement of 469 m was recorded on the mixed (MSG) beach of Birling Gap (East Sussex, UK). An averaged value of 500 m was also measured by Dickson et al. (2011) over eight month monitoring. In Portonovo a maximum displacement of 445 m was measured from SE to NW just after two months. Is not easy to identify which storm was responsible of the tracer displacements observed two months after the injection. Eight storms from opposite directions occurred from March (injection) to May 2012 (Table 4-6; Figure 4-5). The first two storms approached from NE sector and likely moved tracers towards the southern beach end. Then two storms driven by SE sector probably transported the marked pebbles towards the northern edge and again other few storms from NE and NW sectors probably relocated sediments on the southern zone of the beach. Unfortunately surveys of the entire beach length started from May 2012 (Appendix A) therefore only partial data are available about beach topography of that period (topographic data referred only to the southern embayment *aka* “experiment area”, see Figure 2-1). From March to May 2012 the southern embayment of the beach showed changes in topography more focused on its central and northern areas (Figure 4-11). The southern beach end exhibited mild topographic variations limited to the swash zone. In the whole surveyed area the beach elevation resulted higher in May 2012, therefore the last storm occurred from ESE (see VIII event in Table 4-6), though of mild energy, was able to transport a relevant amount of sediments towards the northern compartment of the beach. The tracers found on the north zone of the beach (Figure 4-5) were the majority by far, therefore is quite probable that the last storm from ESE was able to move marked pebbles longshore towards NW. The opposite hypothesis could be the exhumation of tracers done by the previous storms driven by NE sector, but considering the highest elevation measured on May 2012 this option is unlikely (Figure 4-11). Furthermore, according to the tracer displacements experienced under low to moderate conditions during the second experiment in Portonovo (see Chapter 5) the large displacements measured two months after the injection could also be ascribed to the swash grazing may occurred towards NW after the VII storm. In that case the last storm (VIII event, Table 4-6) driven from ESE completed the ultimate displacements.

Events	Storm characteristics				
	Hs max (m)	Dir	Duration (h)	E (m <sup>2</sup> h)	Severity
I (1/04/2012)	2.3	ENE	6	31	weak
II (8/04/2012)	2.9	NNE	24	195	weak
III (11/04/2012)	2	ESE	10	42	weak
IV (13/04/2012)	2.2	ESE	17.5	82	weak
V (17/04/2012)	2	ENE	10	41	weak
VI (13/05/2012)	3.1	NNE	44	428	moderate
VII (16/05/2012)	3.9	NNW	22	333	moderate
VIII (21/05/2012)	2.1	ESE	8	35	weak

Table 4-6. Storm events occurred between the injection (March 2012) and the first tracer recovery carried out two months later (May 2012).

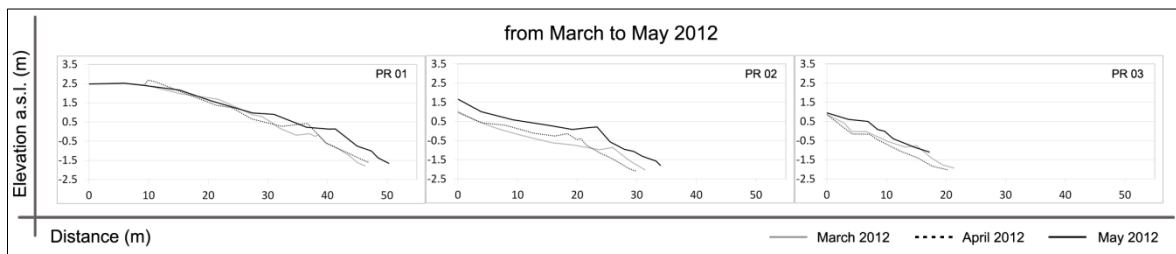


Figure 4-11. Beach topography variation from March 2012 (tracer injection) to May 2012 (2 month recovery). Profile numbers refers to the south limit (PR 01), central zone (PR 02) and north limit (PR 03) of the southern embayment (see Figure 3-12).

On the other hand the few marked pebbles recovered in the southern area (Figure 4-5) were probably not entrained by the waves of the last storm driven from ESE. A different beach exposure to wave motion of the southern edge of the beach was confirmed by the mixing depth evaluation carried out during the 2013 experiment (Figure 3-8; Table 4-2). Only the pebble pile inserted at the southern beach end was not completely dismantled after one day, while at least 30 cm of sediments were surely removed by waves in the central and northern sectors (Table 4-2). Wave direction during that experiment lasted for 18 consecutive hours from E ( $H_s$  between 0.3 and 0.1 m) and tracers moved towards NW (Figure 4-1, see also Chapter 5). The swash zone slope basically did not show any difference from south to north during that experiment (0.13-0.16, Figure 3-5), but the higher exposure to wave action of the central and northern beach portions likely allowed sediments to travel longer distances in those areas. As confirmed by Bluck's works (Bluck 1967, 1999), if the beach system is in swash-alignment the cross-shore transport can dominate regardless of wave energy (see Nash Point facies type). Portonovo beach does not show a perfect swash alignment and its slight embayment of the southern beach edge, which is also protected by a longshore seawall defending an historical building, creates inconsistency on pebble displacements from south to north. Hence, longshore transport can easily occur in the more exposed areas of the beach (central and northern zone) as also experienced analysing the transport of tracers in long term. Regarding the recovery rate of tracers, a value of 42% after two months represented a significant result. Curoy (2012) after the same time span could recover almost the 5 % of tracers in Birling Gap (UK). It is crystal clear that in the case of Portonovo the longshore limits of the beach played a major role on the high recovery percentages. Birling Gap is a macrotidal open beach where significant displacement of pebbles (145 m) were measured already after one tide cycle (Curoy et al., 2007). Dickson et al. (2011) observed at three different sites recovery rate of 10-35 % after two months and 0-30 % seven months after the injection. Allan et al. (2006) measured significantly high percentages of recovery, from 90 % eight months after the injection to 18 % after 17 months. The latter is basically the same rate experienced after 13 months in Portonovo (Figure 4-4). The high recovery rates observed by Allan et al. (2006) were related to the larger detection range of their RFID antenna which was able to detect tracers up to 1 m below the beach surface (versus 40 cm supported by our RFID antenna). It is likely that the undetected part of our tracers was buried under a layer of sediments thicker than 40 cm. Because the major part of the tracers was recovered on the northern zone of the beach is likely that also the undetected pebbles were buried in that part of the beach.

# ***5. Pebble transport in the short term: influence of size and shape of particles (Portonovo beach)***

This chapter is part of the paper in phase of review: Grottoli, E., Bertoni, D., Ciavola, P., Pozzebon, A., (XXXX). Short term displacements of marked pebbles in the swash zone: focus on particle shape and size. Marine Geology X, XX-XX.

## **5.1 - The role of size**

### *5.1.1 - Displacement and recovery of pebbles based on their size*

An analysis of a selective transport based on the pebble size was possible only in the second experiment, where a size discrimination of the marked pebbles was made at the injection time. "Small" and "Medium" classes seemed to move significantly even after 6 hours towards various directions (Figure 5-1 A). All the sizes increased their displacements after 24 hours (Figure 5-1 B), even though the "Big" class was the least mobile. Many "Small"-sized tracers, initially located at the swash zone mid-point or on the fair-weather berm crest, reached the back of the fair-weather berm after 24 hours (Figure 5-1 B). "Medium"-sized pebbles essentially split from the swash zone mid-point either up-slope towards the berm or down-slope to the step crest (Figure 5-1 B). "Big"-sized tracers basically moved with short longshore paths in the southern part of the beach, never climbing up the swash zone slope (Figure 5-1 B). On the contrary, the "Big"-sized tracers in the northern sector showed longer displacements and in a few cases moved onshore, almost reaching the fair-weather berm (Figure 5-1 B). In the first experiment all tracers were comprised in the "Big" size class, characterised by a mean diameter with values between -5.5 and -6.5 phi (very coarse pebble and small cobbles according to the Udden-Wentworth grain size scale, 48 to 96 mm). Given the size uniformity, no selective transport based on the pebble dimension could be made for the first experiment held in Portonovo.

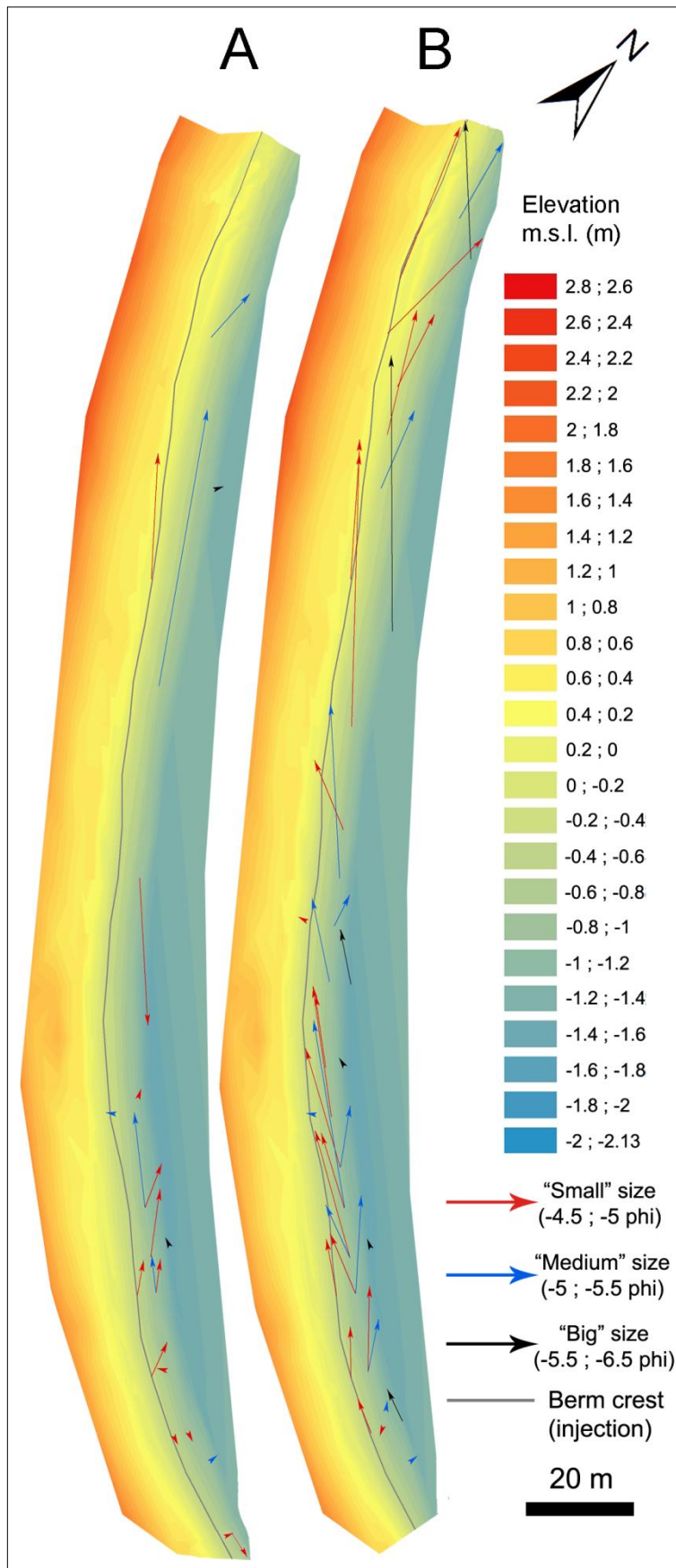


Figure 5-1. Tracer displacement in terms of size (only 2nd experiment): A) 6 hour displacements; and B) 24 hour displacements.

### 5.1.2 - Statistical analyses

After the 6 hour recoveries of both experiments, all the size box plots are skewed to the right except for "Big"-sized pebbles (Figure 5-2 a, b). The "Small" and "Medium" tracers moved significantly more compared to the "Big" ones, having a larger distribution interval compared to the biggest size (Figure 5-2 b). Their median values are initially closer to the box bottom and then increase towards the end of the experiment. This does not happen to the "Big" class, which seems to be quite stable at low displacement values, especially for the median values. At the 6 hour recovery period, the "Medium" class has slightly longer displacements compared to the "Small" one. After 24 hours, the "Small"-sized tracers have the largest range, skewness and median values (without outliers) of any size class. The "Medium" class has the most stable range throughout the 24 hours, although the median value increases in the second recovery; on the other hand, the "Small" class has the largest stretch after one day, making it the most dynamic class (Figure 5-2 b). The box plots of pebble displacement show that the "Big" class is less susceptible to large movements, both 6 and 24 hours after tracer release. Although some "Big" pebbles moved up to 5 m from their initial position 24 hours after the injection, their median values are quite low and gravitate towards the bottom of the box (Figure 5-2 a, b). "Big"-sized sediments seem to have a similar behaviour in both experiments.



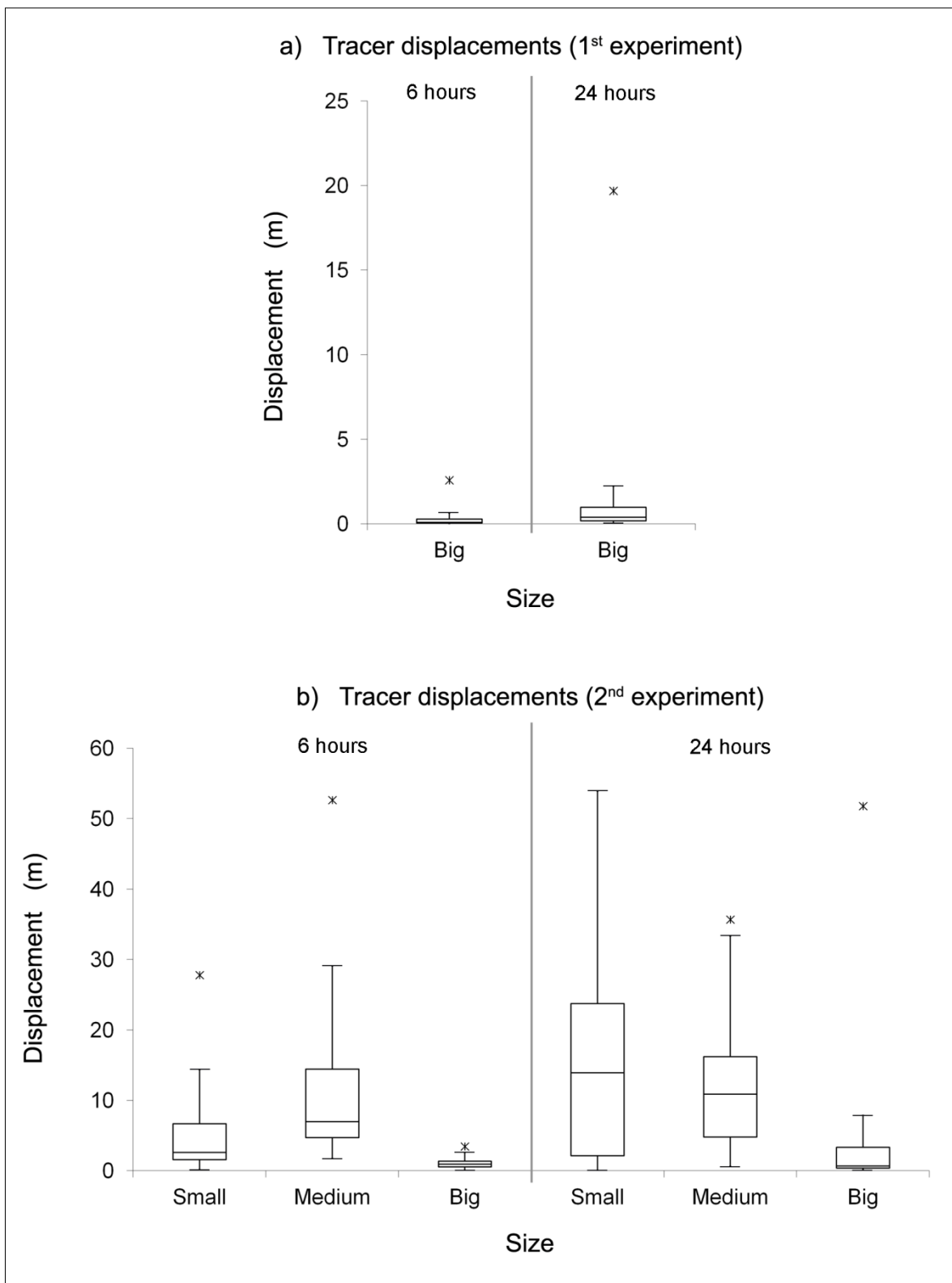


Figure 5-2. Box plots showing the displacement magnitude after the 6 and 24 hour recoveries according to the size subdivision of the tracers: a) box plots referring to the first experiment; and b) box plots refer to the second experiment: here, a size discrimination was taken into account prior to pebble injection.

T-tests on the pebble size data (Table 5-1) reveal that the "Big" tracers have significantly different displacements compared to the "Medium" and "Small" pebbles, except after 24 hours, where no substantial difference is noted. On the other hand, the "Small" and "Medium" tracer displacements are not significantly different either after the two recoveries or considering the experiment as a whole. Accounting for the 6 hour recovery the "Big"-sized sediments show a significant dissimilarity compared to the other sizes (Table 5-1).

Size ( $p < 0.05$ )	2 <sup>nd</sup> exp. - 6 h	2 <sup>nd</sup> exp. - 24 h
Small vs. Medium	0.088	0.704
Medium vs. Big	<b>0.019</b>	0.142
Small vs. Big	<b>0.031</b>	0.058

Table 5-1. Probability values calculated by means of T-tests. The pebble displacements measured for different sizes are compared. The bold numbers represent a significant difference between the two categories considered in each row. A significance level of  $p < 0.05$  was used.

### 5.1.3 - Threshold of tracer motion

The estimation of the thresholds of motion using the graphical method of Soulsby (1997) gave the following results. Considering the first experiment, the graphical method gives a value of  $1.1 \text{ ms}^{-1}$  for the "Big" class, which was the only present at that experiment. For the second experiment, the Soulsby's method provides a value of  $1.2 \text{ ms}^{-1}$  for the "Big"-sized pebbles,  $1 \text{ ms}^{-1}$  for the "Medium" class and  $0.9 \text{ ms}^{-1}$  for the "Small" class (Figure 5-3). The graphical method of Soulsby (1997) resulted fairly close to the actual wave orbital velocities measured by the S4 wave gauge (Figure 5-3).

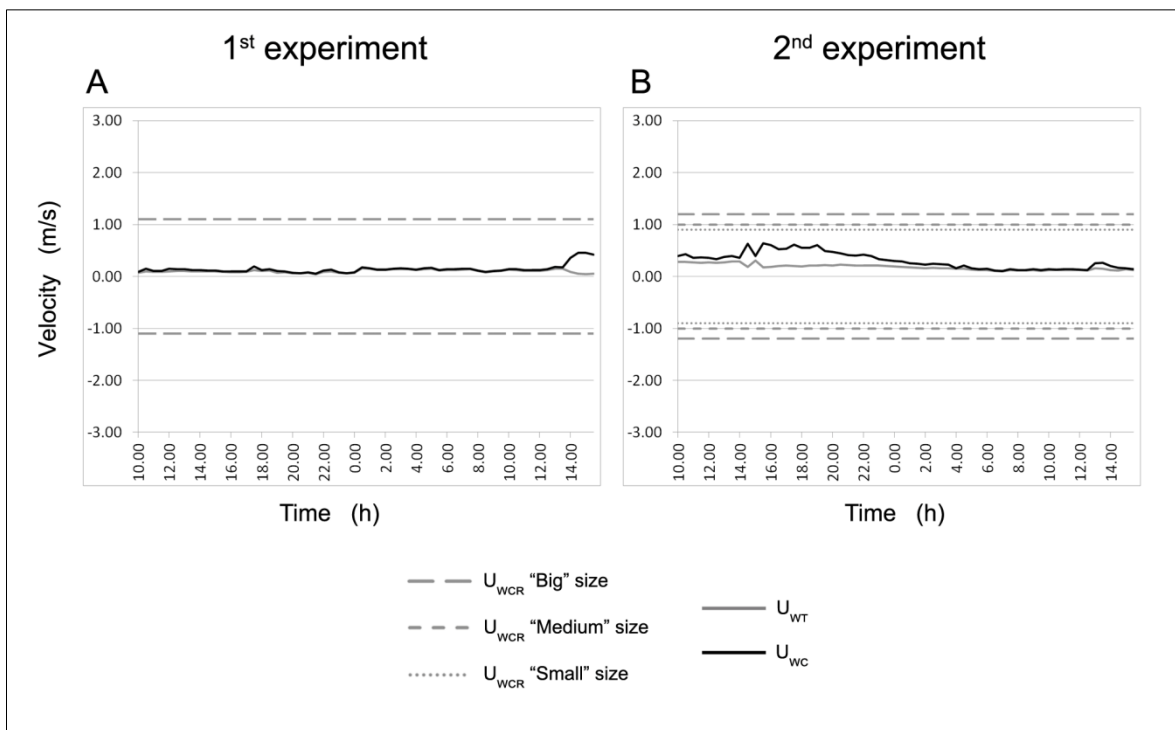


Figure 5-3. Threshold of motion for marked pebbles estimated by the graphic method of Soulsby (1997). Calculations shown for the first (A) and the second (B) experiment.

## 5.2 - The role of shape

### 5.2.1 - Displacement and recovery of pebbles based on their shape.

In the first experiment, most of the tracers were dragged down the beach face, moving from the fair weather berm to the swash or the step zone (Figure 5-4 B). Such a trend affected every shape because no differences in the displacement direction related to pebble shape were noted. The tracer displacements reached greater magnitudes on the northern sector of the beach with a stronger longshore component compared to the southern sector. During the second experiment, all the shapes moved from south to north, with shorter displacements in the southern part of the beach and greater displacements in the northern sector (Figure 5-4 C, D). Disc-shaped pebbles travelled longer distances, and many of them ended up on the back of the berm. Spheres covered shorter paths after 24 hours and did not move landward of the fair-weather berm (Figure 5-4 C, D).

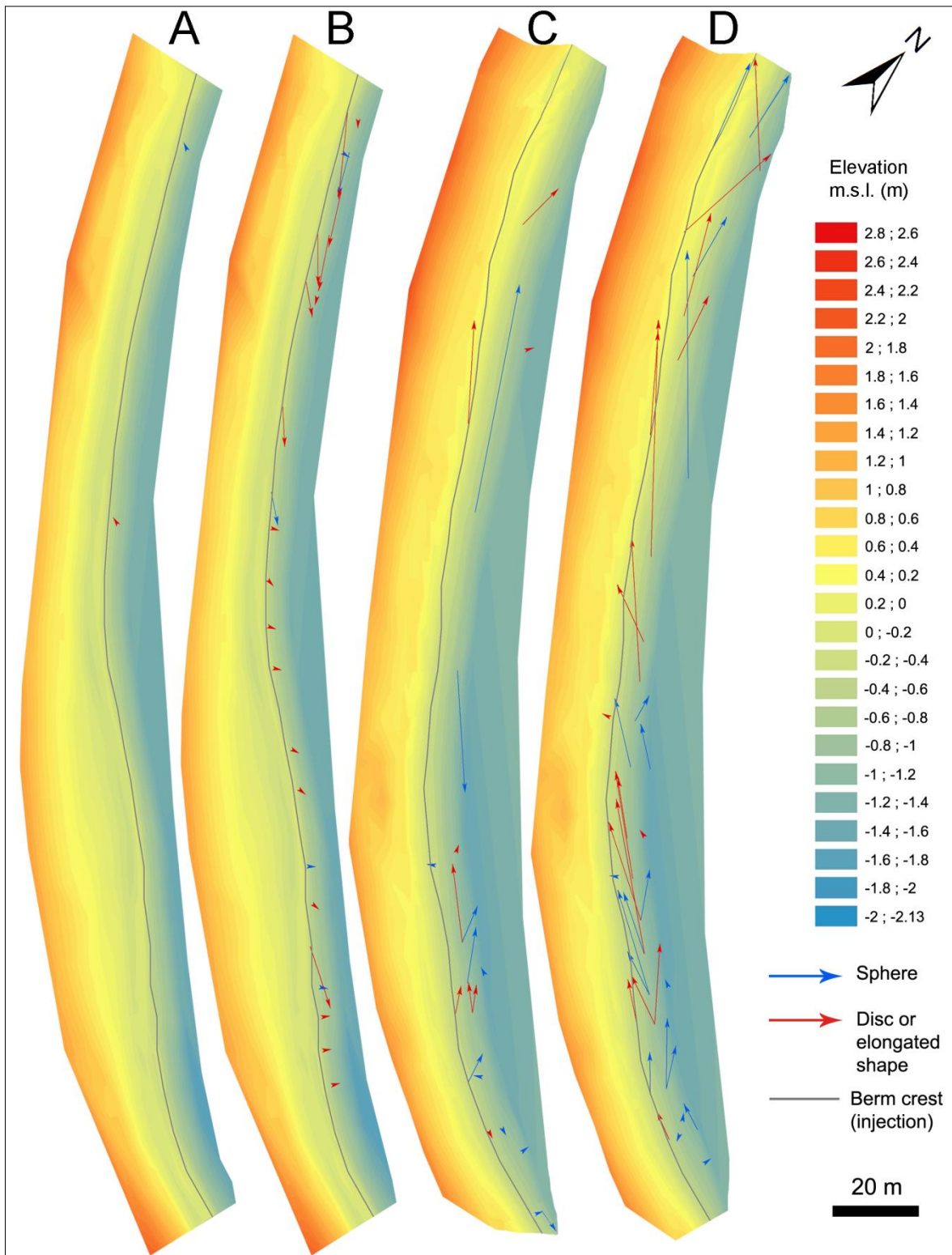


Figure 5-4. Tracer displacement in terms of shape: A) First experiment 6 hour displacements; B) First experiment 24 hour displacements; C) Second experiment 6 hour displacements; and D) Second experiment 24 hour displacements.

### 5.2.2 - Statistical analyses

Box plots of pebble shape are fairly different from one experiment to the other. In the first one, there is no remarkable difference between elongated and spherical shapes. After 6 hours, the spheres reach larger displacements compared to the elongated shapes, but they maintain roughly the same interval after 24 hours. The elongated shapes look more static at first but then show a quite similar to slightly larger range compared to the spheres after one day (Figure 5-5 a). In each case, the median values are constantly close to the box bottom (Figure 5-5 a). The intervals of the box plots are much larger in the second experiment (Figure 5-5 b). Although the displacements are larger, the discs and spheres behave as they did during the first experiment. After 6 hours, the disc-shaped pebbles are less inclined to motion than the spheres. The spheres show slightly greater median values and larger intervals. After 24 hours, both shapes record larger displacements because of increased wave energy, but the discs have a wider range than the spheres. Furthermore, the disc box plot is skewed far to the right with a median value strongly adherent to the bottom. The sphere box plot seems to be more balanced with a more limited interval and a median value perfectly set in the middle of the interquartile range (Figure 5-5 b).

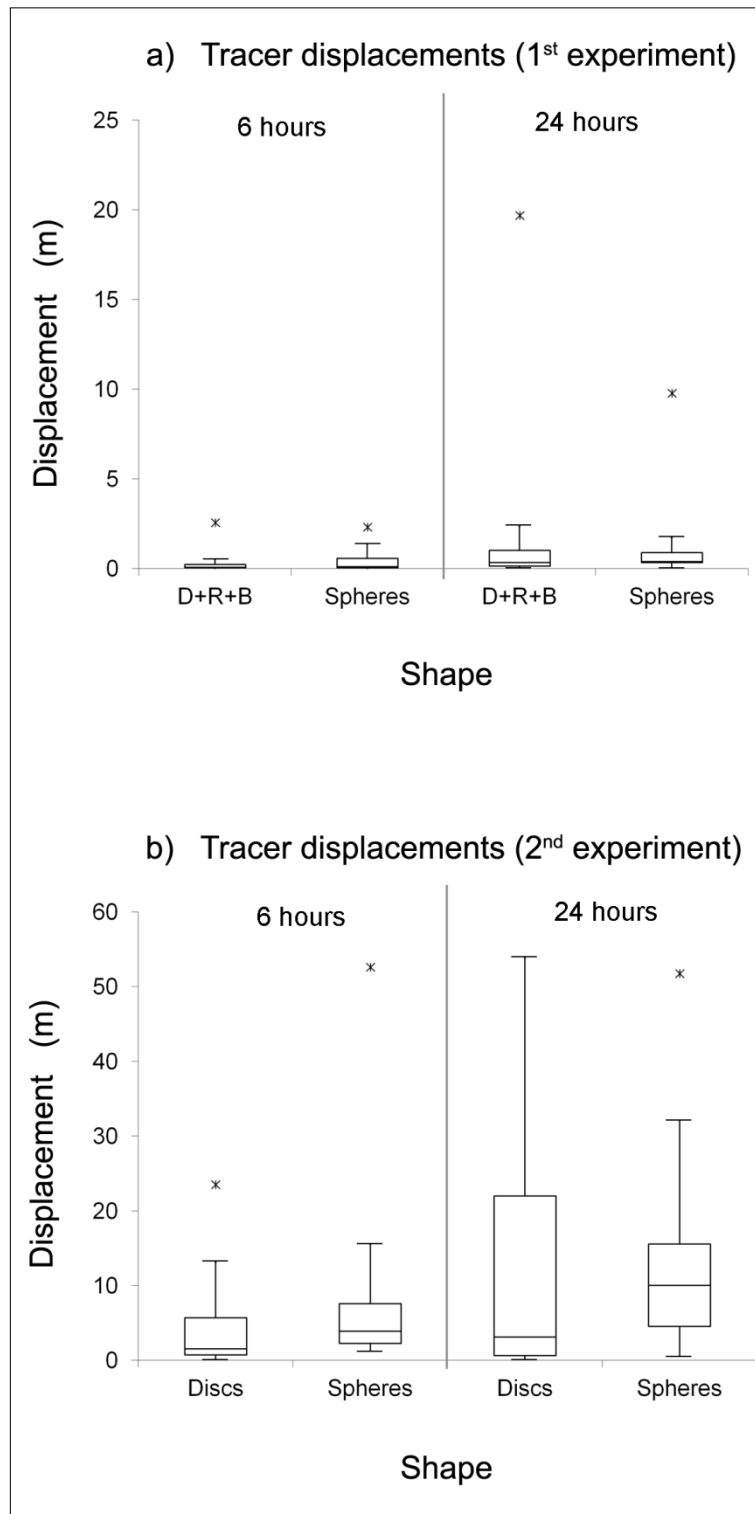


Figure 5-5. Box plots showing the pebble displacement magnitude after 6 and 24 hours according to the shape subdivision of the tracers: a) box plots referring to the first experiment, where the elongated shapes are joined together (D = Disc, B = Blade, R = Rod); and b) box plots referring to the second experiment, where only the disc and sphere shapes were present.

Statistically significant differences are not present in Table 5-2 according to the shape of the marked pebbles. There is no movement discrimination of the pebbles in terms of their shape for any recovery time, except for the first experiment among the discs and spheres 6 hours after the injection (Table 5-2).

Shape (p < 0.05)	1 <sup>st</sup> exp. 6 h	1 <sup>st</sup> exp. 24 h	2 <sup>nd</sup> exp. 6 h	2 <sup>nd</sup> exp. 24 h
Disc vs. Sphere	<b>0.028</b>	0.889	0.121	0.821
Elongated (D+R+B) vs. Sphere	0.212	0.650	-	-

Table 5-2. Probability values calculated by means of T-tests. The pebble displacements measured for different shapes are compared. The bold numbers represent a significant difference between the two categories considered in each row (D = Discs; B = Blades; R = Rods; S = Spheres). A significance level of  $p < 0.05$  was used.

### 5.3 - The combinational role of size and shape

#### 5.3.1 - Displacement of pebbles based on the combinational effect of size and shape

Regarding the second experiment it was also possible to analyse the combinational effect of shape and size. “Big” class did not show any displacement difference between spheres and discs (Figure 5-6 A, B). “Medium”-sized tracers did not exhibit any peculiar movement according to shape, both during the 6 and 24 hour recoveries (Figure 5-6 C, D). “Small” class of tracers showed slight differences: especially 24 hours after the injection disc shaped pebbles moved behind the berm crest, reaching higher positions if compared to the “Small” spheres (Figure 5-6 E, F).

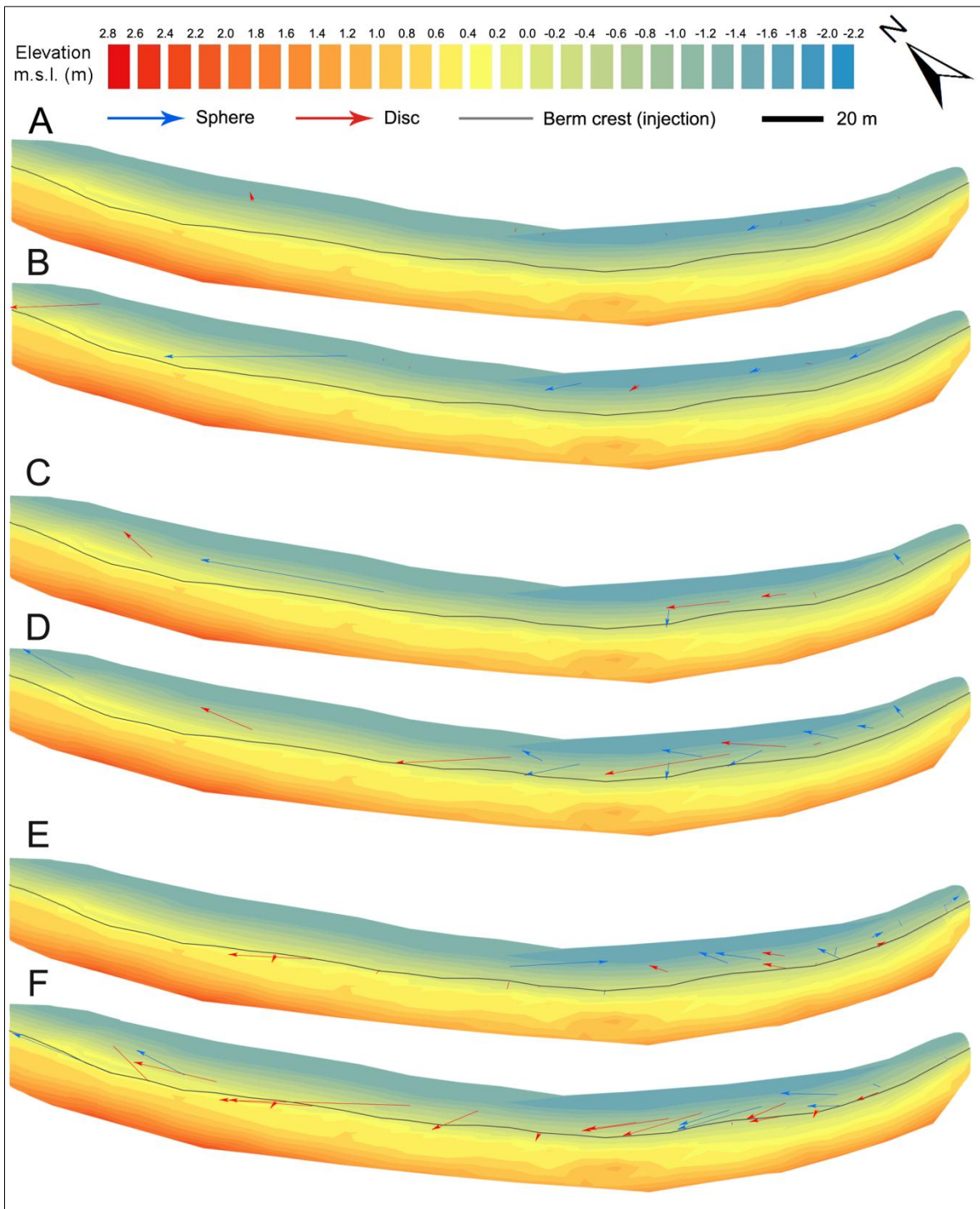


Figure 5-6. Tracer displacement based on the combined effect of size and shape (only 2<sup>nd</sup> experiment): “Big” class displacements 6 hours (A) and 24 hours (B) after the injection; “Medium” class displacements 6 hours (C) and 24 hours (D) after the injection; and “Small” class displacements 6 hours (E) and 24 hours (F) after the injection.



#### *5.4 - Statistical analyses*

Taking into account the combinational effect of shape and size some other peculiar behaviour of pebbles can be appreciated from box plots of the second experiment. “Big” spheres resulted more dynamic than discs since the first recovery. The larger displacements of “Big” spheres appeared fairly clear 24 hours after the injection, when most of them moved from the injection position of approximately 10 m (median value) and some of them up to 20 m (Figure 5-7 A). The displacement interval of “Big” discs remained basically the same even after 24 hours, with the box steadily stuck at the bottom and maximum displacements of approximately 5 m (Figure 5-7 A). “Medium”-sized discs recorded lower displacements than “Medium” spheres 6 hours after the injection. This situation was completely overturned after one day (Figure 5-7 B). The interquartile range of “Medium” discs after 24 hours was the same produced by spheres of the same size already after 6 hours even though the median values differed consistently (Figure 5-7 B). “Small”-sized spheres confirmed larger displacements if compared to the discs 6 hours after the injection. After one day the situation was overturned as already shown by the “Medium” class even though with larger displacements (Figure 5-7 C).

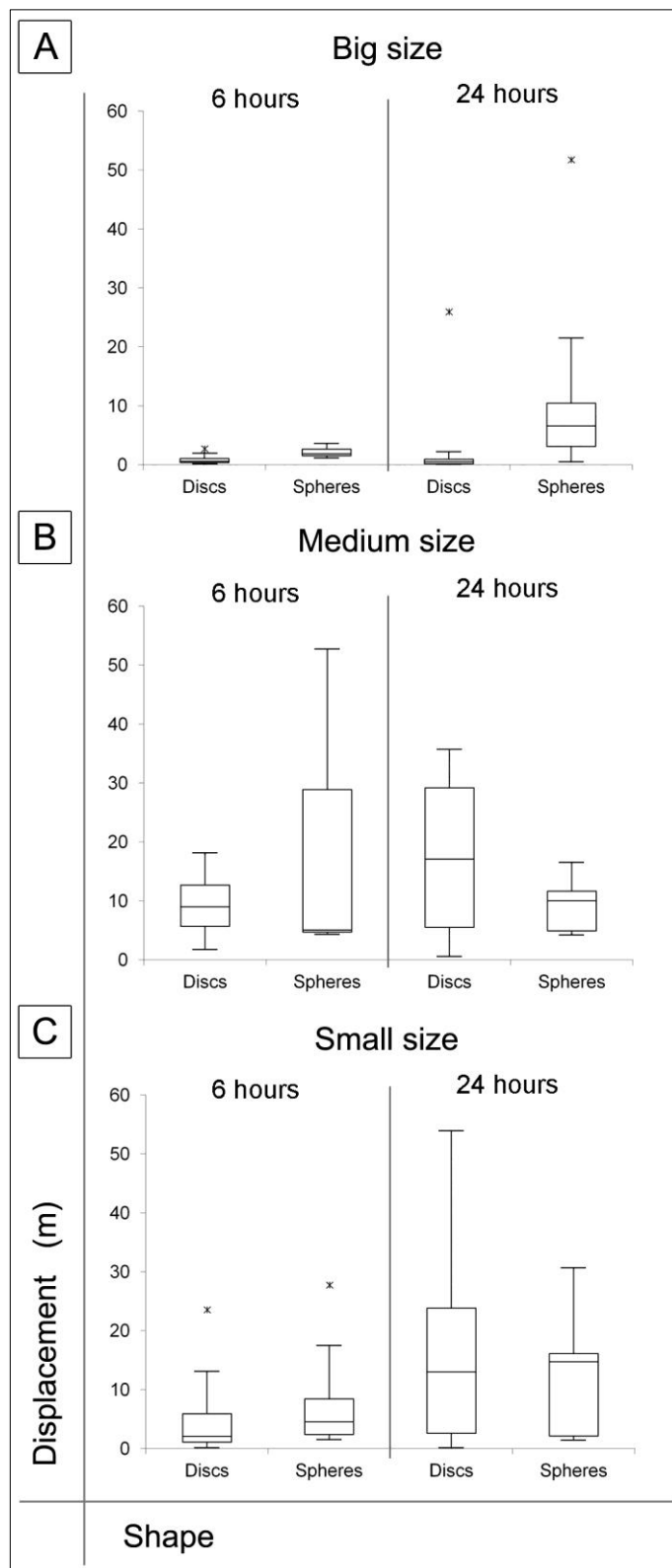


Figure 5-7. Box plots showing the pebble displacement magnitude after 6 and 24 hours based on the combined effect of size and shape. A) “Big”-sized discs and spheres comparison; B) “Medium”-size discs and spheres comparison; C) “Small”-sized discs and spheres comparison.

## 5.5 - Discussion

The results of the first experiment suggest that shape does not represent a discriminating factor for pebble movement: very low energy conditions combined with "Big"-sized tracers facilitated a pebble down dragging. Dissimilarities in the pebble displacements among different shapes of particles are more evident when analysing the outcome of the second experiment, where smaller tracers were investigated and higher wave energy occurred. This disparity seems to confirm what was already stated by McLean and Kirk (1969), that is, size is the primary factor controlling the sorting trends of sediments and shape is a second order factor. In the second experiment, many disc-shaped pebbles ended up on the back of the berm, while this did not happen to the spheres. As stated by Ciavola and Castiglione (2009) during an experiment conducted in a nearby sand-gravel mixed beach (Porto Recanati beach) under equivalent energy conditions, the uprush is able to drag large, flat pebbles up onto the beachface. Once the pebble reaches the berm, the backwash dissipates because of infiltration and the flattest pebbles are left there, while the more spherical ones roll down the slope. This was also observed by Bluck (1967) and Isla (1993) based on surface sampling and beach observations on macrotidal coarse-grained beaches; the same process was already described by Dobkins and Folk (1970) on some mixed beaches under low and high energy conditions (Table 5-3). Spherical and discoidal shapes behaved consistently during each experiment in terms of the displacement length. After 6 hours, the spheres moved further from the injection points than the discs, but after 24 hours the discs covered longer paths than the spheres. This trend was confirmed by box plots focused on the combinational effect of shape and size except for the "Big"-sized pebbles. Wave motion recorded during the second experiment was not strong enough to entrain discs of bigger size; whereas it was able to move spheres of the same size probably taking advantage from their capability to roll. Some authors found that discs have lower pivotability than spheres (Shepard and Young, 1964; Bluck, 1967), the latter move more easily in traction (Bluck, 1967) by taking advantage of their spherical shape. Also Orford (1975) found that discs can be moved further landward by waves, having better suspension properties than spheres. The longer distances covered by discs after 24 hours do not mean that this shape is more dynamic compared to the spheres. As noted by Isla and Bujaleski (1993), spheres are preferentially set into "saltation", although the bed is dominated by discs, blades and rods, which means that spheres keep moving until they find a stable location to be incorporated into the sediments that constitute the beach (Caldwell, 1981), moving more quickly through the pores of the beach surface than other shapes (Bluck,

1967). The resulting difference in the behaviour of the two shapes at 6 and 24 hours cannot be imputed to an increase in the wave energy because higher waves occurred within 10 hours of the injection during the second experiment (the significant wave height remained between 0.3 and 0.4 m), while the first experiment was characterised by quite low waves (average significant wave height of 0.09 m; max value 0.15 m). According to Orford (1975), the influence of shape depends not only on the wave energy but also on the wave phase and breaker type. The results from the shape displacements are not sufficient to say that there is a correlation between the shape and distance travelled by pebbles, as Carr (1971) already noted. Another aspect in need of in-depth investigation is the relationship between the shape of the pebbles and the characteristics of the surface over which they move (Carr et al., 1970; Caldwell, 1981): an irregular coarse bottom determines different types of pebble movements (Isla, 1993), and pebbles are preferentially entrained over sandy surfaces (Nordstrom and Jackson, 1993). According to Bertoni et al. (2012b), the primary factor controlling the pebble displacement is the modification of incident waves induced by irregularities in the morphology of the sea bottom. A zonation of particle shape was not observed on the Portonovo swash zone, but shape very likely exerts an influence on pebble transport at least under low energy conditions and in the short term. As noted by Orford (1975), the roles of size and shape cannot be easily separated, and it is easier to use both factors to discern possible pebble zonation on a beach. The choice of focusing separately or combining the effect of size and shape on pebble movement should be done considering the energy conditions when the displacement takes place. Williams and Caldwell (1988) proposed a model wherein the influence of particle size is more important on sorting when energy conditions are high and particle shape predominates when energy conditions are low (Table 5-3). At the Portonovo beach, according to the size subdivision established only for the second experiment, only "Big" sized pebbles (-5.5 - -6.5 phi class) showed a different behaviour relative to the two finer classes. Pebbles of "Small" and "Medium" sizes (-4.5 - 5 phi and -5 - -5.5 phi classes, respectively) actually travelled greater distances than those belonging to the "Big" class; in addition, this difference in displacement was statistically significant, especially after 6 hours. The first 6 hours were characterised by moderate wave height (approximately 0.3 to 0.4 m up to 10 hours after the injection) that was not able to move "Big"-sized pebbles over the fair-weather berm. According to the paths of the marked pebbles, no relationship between their size and the elevation along the beach where they were detected was noted, which means that wave height is a subordinate factor controlling pebble displacement under very low energy conditions (first experiment) and under low-to-moderate energy conditions (second

experiment). The swash zone slope, swash fluxes, run up levels and gravity play a major role in dragging down or moving up the pebbles along the swash zone. Coarser pebbles basically moved toward the step, not reaching the backshore under low-to-moderate energy conditions. As stated by Carr (1969), coarser material on the backshore is presumably "stranded" during longshore transport only under severe storm conditions. Later, Carr (1971) found a linear correlation between pebble size and the longshore movement in the short term, which becomes exponential in the long term. A sort of longshore size sorting caused by the vector imparted by the direction of the wave's approach can be recognised at the end of the second experiment, given that "Small"- and "Medium"-sized tracers moved farther from their injection positions compared to the "Big" pebbles (Figure 4-1; Figure 5-1). Because the conventional techniques (i.e., sediment samplings, beach observations) commonly provide an opportunity to recognise complex patterns on beach surfaces related to the size and shape of pebbles (McLean, 1970; Kirk, 1980), coarse tracer research needs to be supported by more sophisticated methods to improve the knowledge about the natural sieving of pebbles. Cross-shore transport was prevalent in the first experiment, while longshore paths were more evident in the second resulting from the higher energy conditions experienced. A short list of past studies concerning the relationship between pebble transport and their characteristics is presented in Table 5-3.

<b>Author</b>	<b>Focus on</b>	<b>Sediment size and type</b>	<b>Tidal regime</b>	<b>Wave energy</b>	<b>Beach type</b>	<b>Study method</b>
<b>Bluck (1967)</b>	Pebble shapes and their sorting on the beach	Glacial pebbles (Subgreywacke, quartzite, limestone and sandstone) from 6 to 200 mm	Macro- or mesotidal (not specified)	High	Mixed wide and flat beaches	Long term study Long term samplings
<b>Carr (1969)</b>	Pebble characteristics and their sorting under different wave conditions	Quartzite and flint/chert pebbles	Mesotidal	High	Limited by two cliffs 26 km long and 150-200 m wide	1 year of surface and borehole samplings
<b>McLean and Kirk (1969)</b>	Importance of size and shape of sediments on controlling beach morphology	Gravel size between 0.25 and 16 mm, greywacke derived	Mesotidal	High (mean Hs 1-2 m; storm Hs 5-6 m)	Mixed sand-shingle beaches	1 year of repeated samplings on a monthly basis
<b>Carr et al. (1970)</b>	Pebble characteristics and the importance of the type of sub-strata which pebbles movement takes place	Quartzite and flint/chert pebbles	Mesotidal	High	Limited by two cliffs 26 km long and 150-200 m wide	1 year of repeated surface samplings
<b>Dobkins and Folk (1970)</b>	Different pebble displacements relative to their shapes	From sand to cobble derived from basalt rocks	Micro	High and low	Mixed beaches	Samplings
<b>McLean (1970)</b>	Sediment transport trends according to the size and sorting sediments	From medium sand to medium pebble derived from greywacke	Mesotidal	High	Mixed beaches, Rivers supply material	Surface sampling and topographic profiles

<b>Author</b>	<b>Focus on</b>	<b>Sediment size and type</b>	<b>Tidal regime</b>	<b>Wave energy</b>	<b>Beach type</b>	<b>Study method</b>
<b>Carr (1971)</b>	Relationships between distance travelled by pebbles and their size and shape characteristics	Quartzite and flint/chert pebbles	Mesotidal	Medium/high (Hs max 1.2 m and mean Hs 0.5 m during the tracer experiment)	Limited by two cliffs 26 km long and 150-200 m wide	Tracer experiments with non-native material
<b>Orford (1975)</b>	Role of shape and size of particles related to sediment zonation and wave parameters	From gravel to boulders in a sandy-silt matrix. Mudstone and greywacke	Meso- or macrotidal (not specified)	Not described	Embayed mixed beach	1 year of repeated samplings
<b>Williams and Caldwell (1988)</b>	Beach model based on the influence of particle size and shape	Limestone pebbles	Macro	High and low	Wide and gently sloping foreshore	1 year of repeated samplings.
<b>Isla (1993)</b>	Displacement and arrangement of different sized pebbles and shapes	Glacial pebbles and cobbles	Macro	High (Hs normally greater than 1.2 m)	Coarse-clastic beaches	Surface samplings
<b>Isla and Bujalesky (1993)</b>	Transport processes affecting different pebble shapes	Glacial pebbles and cobbles	Macro	High	Gravel spit	Samples collected by traps after tidal cycles
<b>Ciavola and Castiglione (2009)</b>	Displacement of different pebble shapes under low and medium energy conditions	From medium sand to cobbles	Micro	Low to medium (Hs from 0.1 to 0.45 m during the experiment)	Mixed sand and gravel beach 1 km long	Short term tracer experiment with fluorescent paint

Table 5-3. List of the most recent studies on the role of particle size and shape on coarse-clastic and mixed beaches.

Mixed beaches are dominated by swash action and the interaction between these flows and wave breakers (Kirk, 1980). Uprush-backwash systems are responsible for most of the activity on these beaches (Kirk, 1980). Kirk (1975) measured swash velocities on some mixed sand and gravel beaches: the mean velocity at the swash zone mid-point was  $1.68 \text{ ms}^{-1}$ ; the maximum swash velocity was  $2.5 \text{ ms}^{-1}$ . The backwash velocities averaged  $1.40 \text{ ms}^{-1}$ . Other studies observed a higher uprush velocity of  $3.5 \text{ ms}^{-1}$  on sandy steep beaches (Hughes et al., 1997; Masselink and Hughes, 1998). These velocities are comparable with the estimations conducted by Komar and Miller (1974) and Soulsby's (1997) methods used in this study. As already noted by Kirk (1975), those velocity values are adequate to enable high transport rates for any sediment size on the foreshore. Because the majority of the injected pebbles recorded larger displacements after 24 hours in both experiments, the estimation of Soulsby (1997) seems to be more plausible given that the threshold of motion for each size is closer to the wave orbital velocities computed from the S4 data. Because nearshore wave heights were used (the S4 was located very close to the shoreline, but not on the swash zone), the wave heights at the breaker line would be preferred to improve the accuracy of wave orbital velocity estimation. Williams and Caldwell (1988) provided insights on the relationship between pebble shape and swash flows. According to the authors, when swash velocities (either uprush or backwash) approach the critical threshold for transport, more easily suspended oblate sediments are thrown forward during the short-lived energy peak of the swash. When non-marginal swash velocities occur, mass is more important than shape in determining sediment transport (cross-shore or alongshore) (Williams and Caldwell, 1988). Regarding the interaction between pebble size and swash fluxes, Isla (1993) supposed that an armoured deposit forms as flow decreases (during the backwash), producing an inverse grading of the sediment (coarser sediments over the finer ones). As expected and confirmed by many authors (Kirk, 1980; Van Wellen et al., 2000; Mason and Coates, 2001; Bertoni et al., 2013), the swash zone was the most dynamic part of the beach even under low energy conditions.



## ***6. Beach evolution (Portonovo beach)***

## 6.1 - Topographic variation

Every morphodynamic study of beaches, independently from the aspects which the researcher is focusing on, needs a strong background of topographic surveys to ensure a comprehensive analysis of the collected data. As already explained in the Paragraph 3.4, after a short period of monitoring, limited to the experiment and sampling area (March 2012 and April 2012 surveys, Figure 2-1; Figure 3-10), from May 2012 the topographic measurements were extended to the whole beach length. Hence, here are presented and discussed the morphological variations recorded from May 2012 (3<sup>rd</sup> survey) to February 2014 (13<sup>th</sup> survey) which interested the entire beach extent.

In May 2012 (3<sup>rd</sup> topographic survey), the beach width varied from peak values of 50 m in the southern end (Figure 6-1 A; Figure 6-2 A) to a minimum of 15 m in the northern part (Figure 6-1 A; Figure 6-1 E). The southern portion exhibit also an higher elevation, about 1 m more than the rest of the beach which reached 1.5 m as highest value (Figure 6-1 A; Figure 6-2 A to compare to Figure 6-2 B, C, D, E). The southern end is characterized by two storm berm tiers and a well developed step approximately located at -1 m below mean sea level (Figure 6-2 A). An embryonic bulge form started to develop in the second profile (PR 02, Figure 6-1 A; Figure 6-2 B). The latter is delineated by a steep beachface and a more flattened step if compared to PR 01, no storm berms were present (Figure 6-2 B). A general milder topography characterized the northern portion of the beach, with no particular storm berms or steps (Figure 6-1 A; Figure 6-2 C, D, E).

From May to the first survey of October 2012 (i.e. October 2012 a), huge modifications of beach topography were not observed. The beach width did not experienced substantial variations except for the bulge form which became more prominent toward the sea, developing a higher sharp crest and a better defined step (Figure 6-1, Figure 6-3 B). Beach elevation remained basically the same of the previous survey. Few features were nevertheless notable: the formation of a berm 1 m high in the southern end (PR 01, Figure 6-3 A; Figure 6-1 B); the increase of irregular topography showed from the central to the northern part of the beach (PR 03, 04, 05; Figure 6-3 C, D, E; Figure 6-1 B).

From October a to October b 2012, not relevant morphological changes were observed. The beach width slightly decreased in the southern portion (approximately retreat 3-5 m) and enlarged by few meters in the northern part (Figure 6-1 C; Figure 6-4). Beach

elevation remained stable except for two new storm berms emerged in the central compartment (PR 04, Figure 6-1 C; Figure 6-4 D) and the growth in elevation of the bulge form of PR 02 (Figure 6-1 C; Figure 6-4 B) with a crest flattening associated.

From the second survey of October 2012 to November 2012 huge variations affected the beach in each compartment. In the southern end the beach appeared clearly “cut” by an erosive scarp: the central and the lowest part of the profile were reduced in elevation of 1 to 1.5 m and retreated approximately 15 m relative to the previous survey (PR 01, Figure 6-1 D; Figure 6-5 A). Similar situation was experienced in the profile PR 02, where, the larger distance from the southern protecting limit, caused 15 to 20 m of retreatment and 1 to 2 m of surface lowering (Figure 6-1 D; Figure 6-5 B). On the other hand, the central and northern beach portions were interested by a substantial accretion toward sea and increase in elevation (Figure 6-1 D; Figure 6-5 C, D, E). The width increase was of lower magnitude if compared to the retreatment in the southern area, because part of the transported material went up to the beach to create significant storm berms. A singular storm berm parallel to the shoreline is clearly visible from Figure 6-1 D: its shape became sharper from PR 03 to PR 04 (Figure 6-5 C, D) and was distinctly separated from the higher landward storm berm (Figure 6-1 D; Figure 6-5 D). The two storm berm orders were just the symptom of the huge amount of material deposited at the northern end (PR 05, Figure 6-1 D; Figure 6-5 E). Due to shifted material from south to north the beach topography in PR 05 was from 1 to 2 m higher than previous survey of October 2012 b (Figure 6-5 E). In this stage the prominent bulge form disappeared completely (Figure 6-1 D; Figure 6-5 B) and no well developed steps were recognized on the surveyed beach profiles (Figure 6-5).

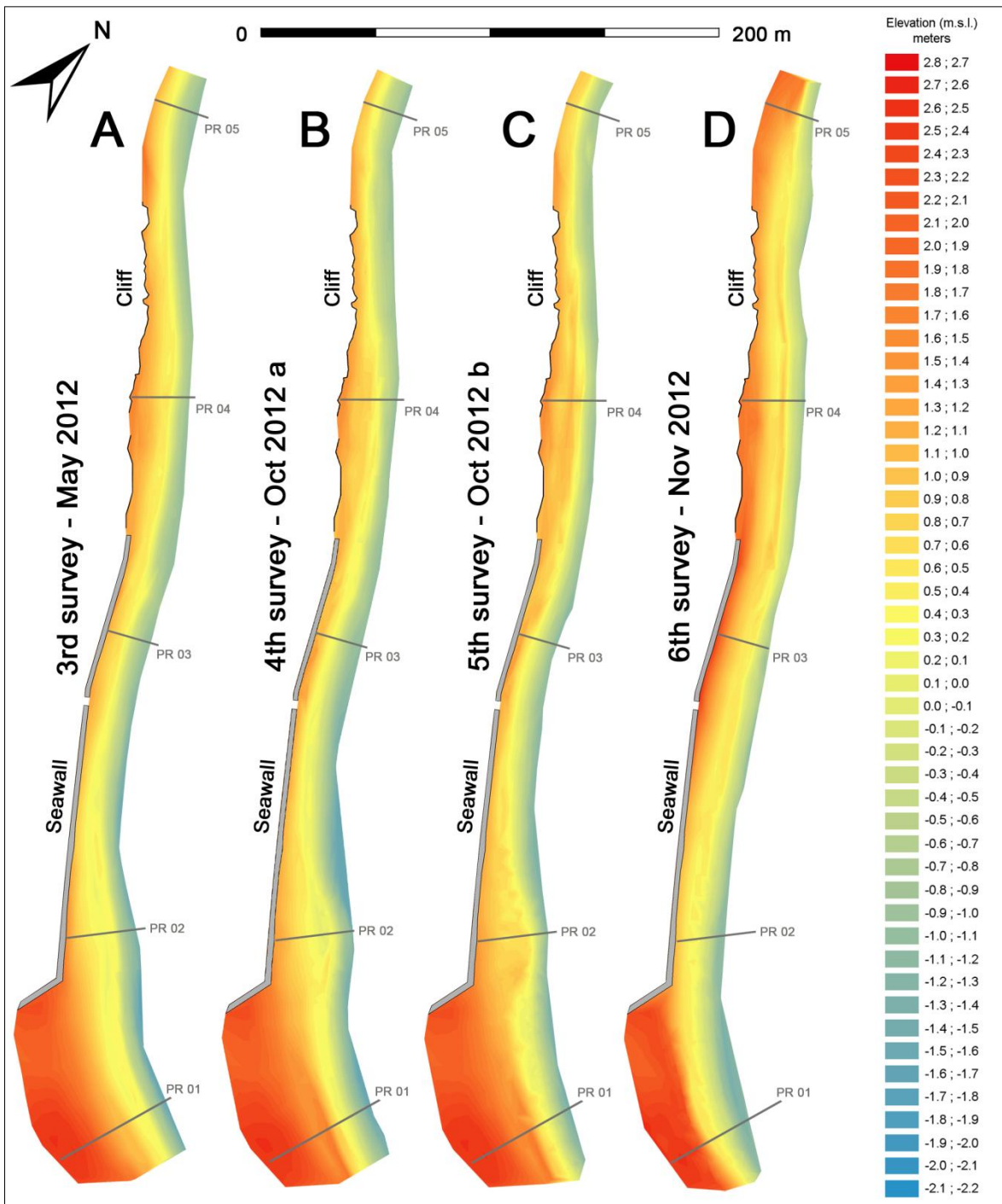


Figure 6-1. Topographic surfaces of Portonovo beach from May 2012 to November 2012: (A) May 2012; B) October 2012 a; C) October 2012 b; D) November 2012). The seawall and the cliff toe are shown on each topographic surface.

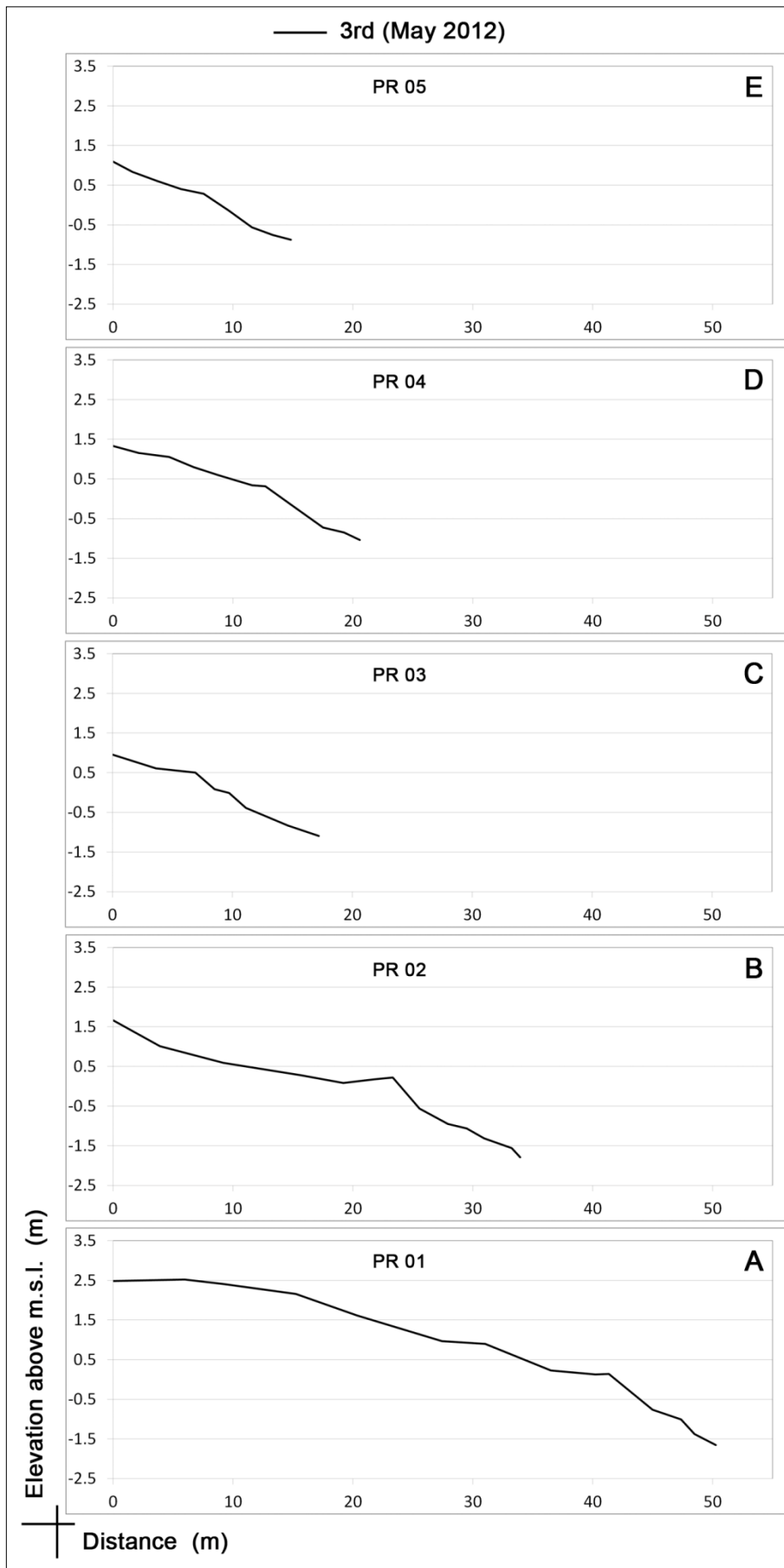


Figure 6-2. Profile variation of the entire beach in May 2012.

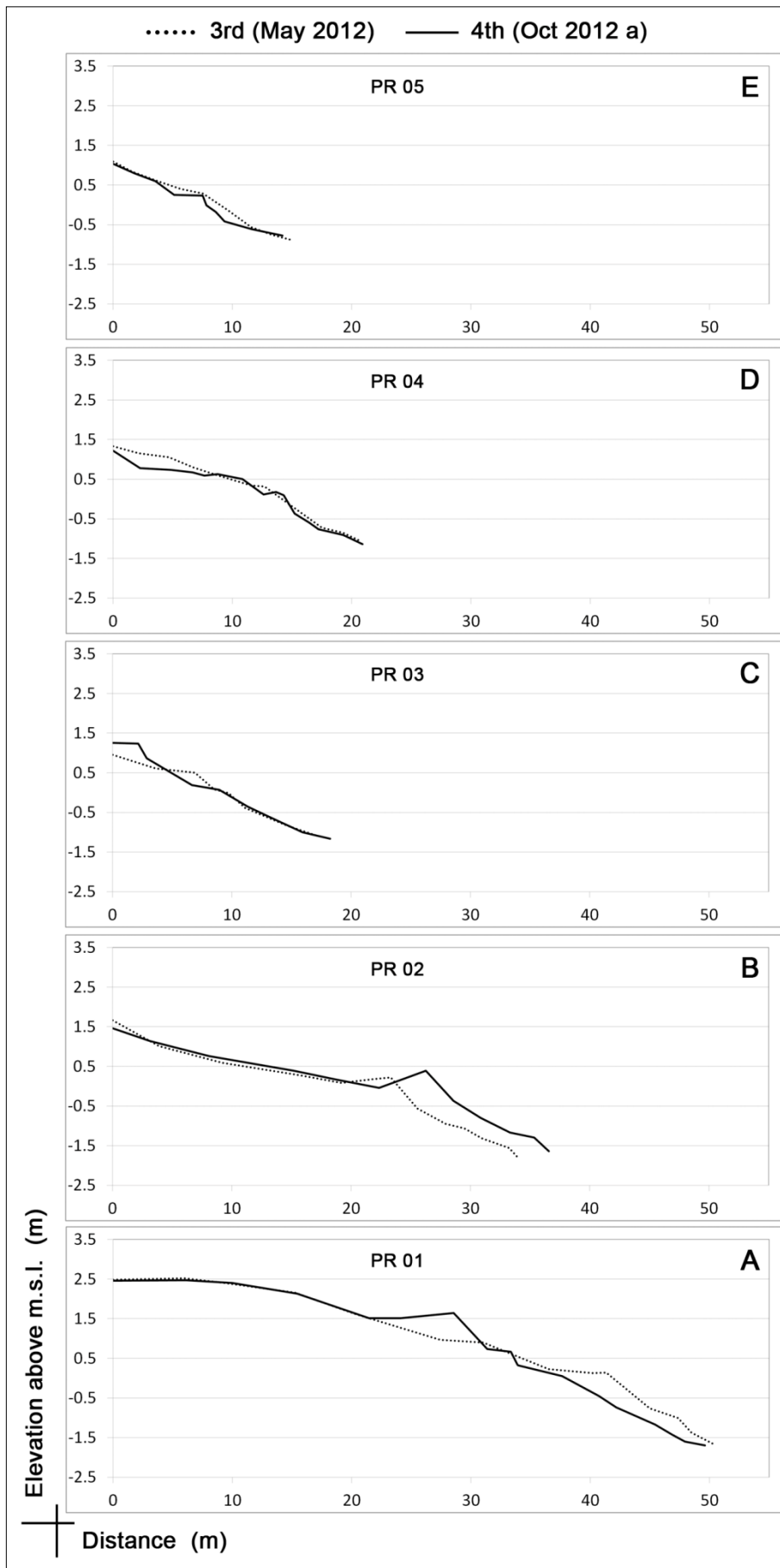


Figure 6-3. Profile variation of the entire beach from May 2012 to October 2012 a.

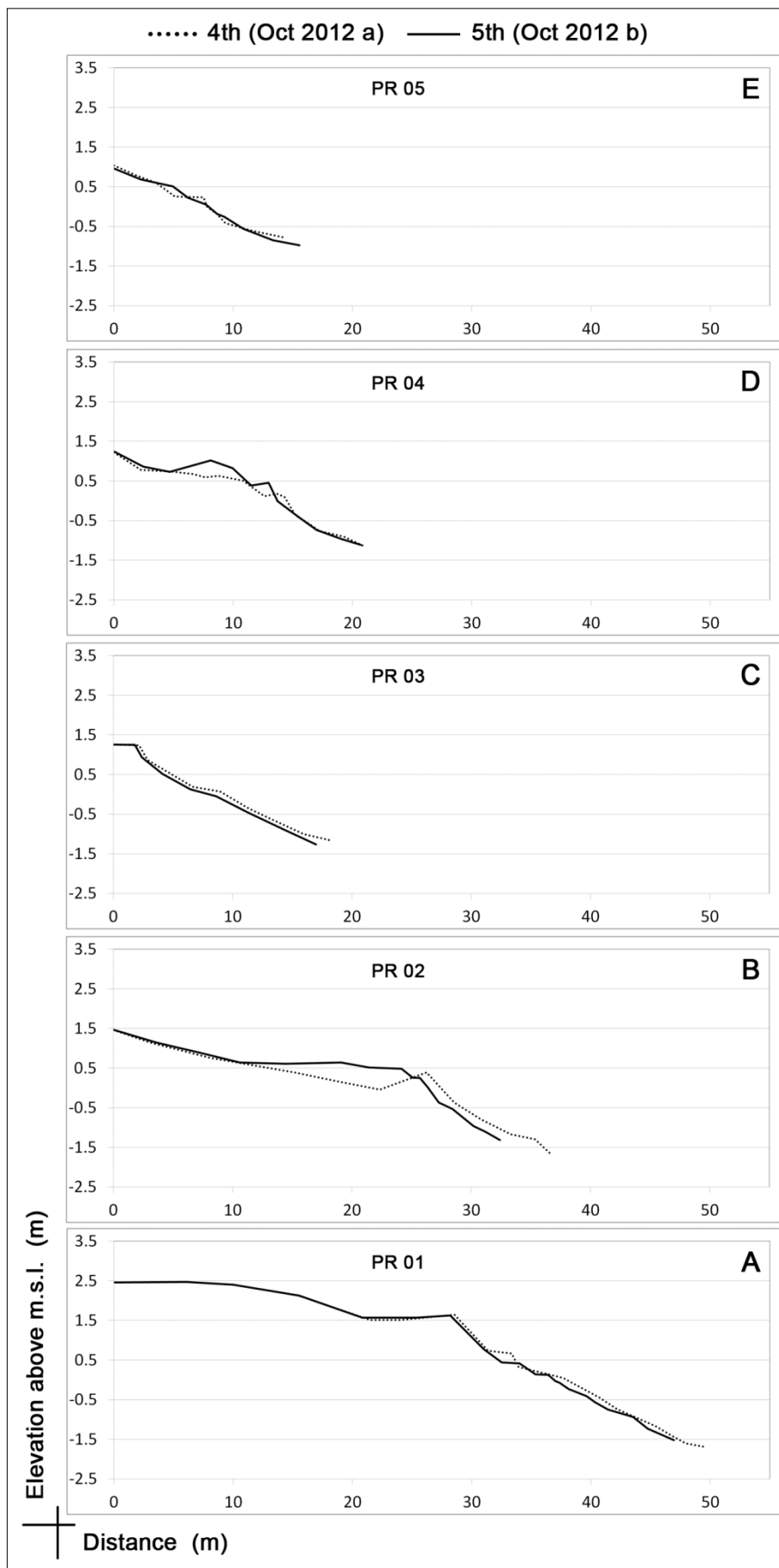


Figure 6-4. Profile variation of the entire beach from October 2012 a to October 2012 b.

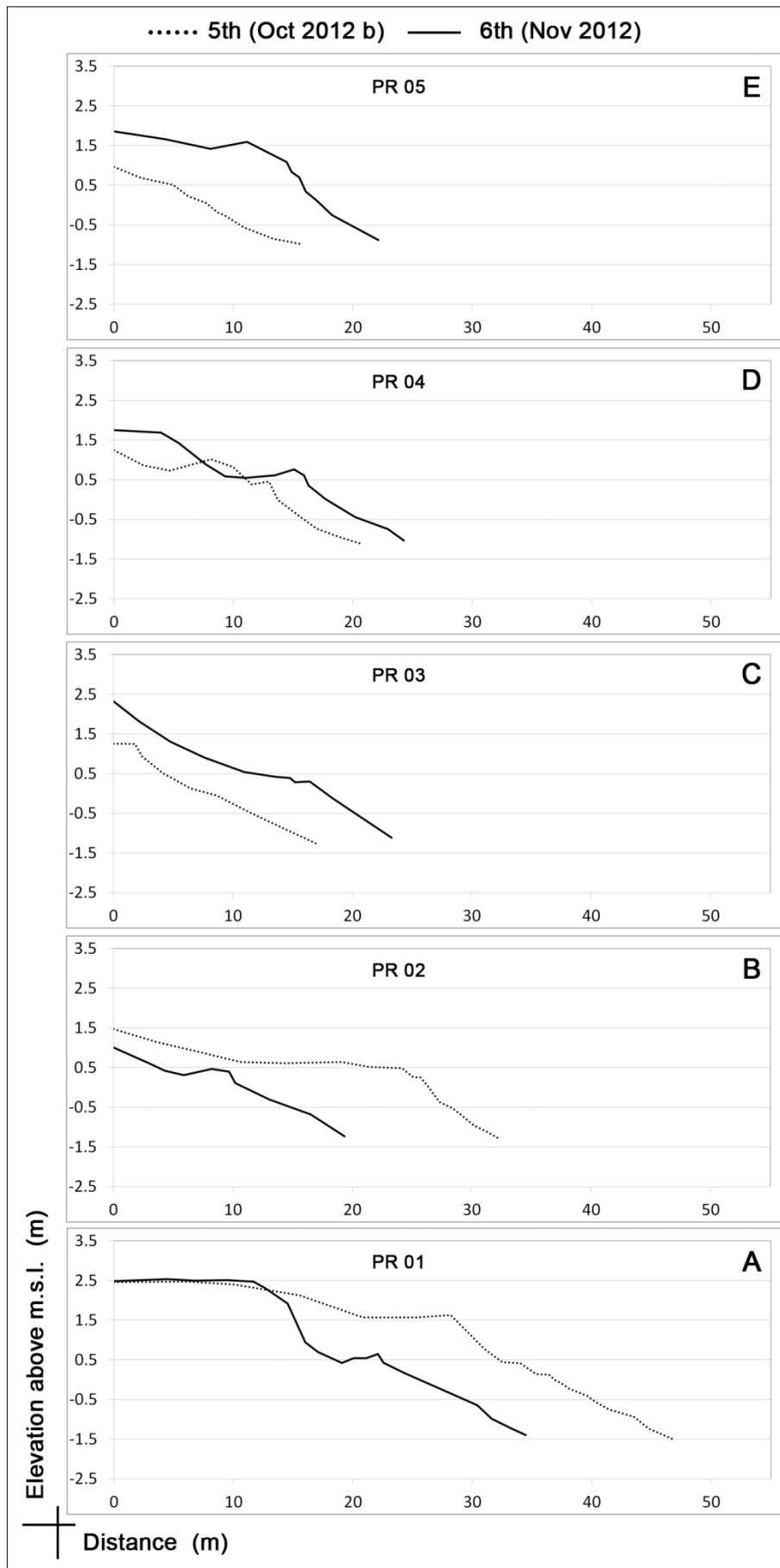


Figure 6-5. Profile variation of the entire beach from October 2012 b to November 2012.



From November to December 2012 the beach returned to a more balanced stage. The southern portion recovered again its typical width nearly 50 m (Figure 6-6 A; Figure 6-7 A) and presented two tiers of flat shaped storm berms (Figure 6-7 A). The second cross section (PR 02) recovered in elevation assuming a milder slope in comparison to the previous survey (Figure 6-1 D; Figure 6-6 A; Figure 6-7 B). In the central and northern compartment all the previous storm berms and morphological features were flattened (Figure 6-7 C, D, E); the beach profile was subjected to lowering especially in the PR 05 where the beach elevation was reduced of about 1-2 m (exactly the accretion quantity experienced from October to November 2012, Figure 6-7 E; Figure 6-6 A).

From December 2012 to January 2013 the beach was subjected to an accumulation of material on the upper part of the entire beach: this can be better observed from Figure 6-6 B rather than Figure 6-8. Nevertheless, an increase of approximately 0.5 m is clearly evident in PR 02 (Figure 6-8 B) and this occurred in the entire southern compartment (Figure 6-6 B). Higher elevation was even experienced from the centre to the north of the beach, especially in the area that runs along the cliff toe (Figure 6-6 B). Relative to the previous survey, a steeper beach face was recognized in the central and southern part of the beach (Figure 6-8 A, B, C; Figure 6-6 B).

From January to February 2013 the beach surface had enriched of morphological features (Figure 6-6 C; Figure 6-9). Different tiers storm berms, distinguished the southern beach portion (Figure 6-9 A; Figure 6-6 C). Storm berms were present even in the rest of the beach area, basically through a single line which mostly ran from PR 03 to PR 04 (Figure 6-6 C; Figure 6-9 C, D). Storm berm showed the sharpest shape in PR 04 (Figure 6-9 D). The northern end appeared completely “filled” relatively to the previous survey, an increase of 1 m occurred (Figure 6-6 C; Figure 6-9 E). The entire beach was not subjected to strong retreat (Figure 6-9).

From February to March 2013 many remarkable changes affected the beach. A retreat of approximately 5 m affected the southern beach end (Figure 6-10 A) which became milder in cross section PR 02 (Figure 6-10 B). Furthermore, a general lowering of the beach surface was experienced in those sections (Figure 6-10 A, B; Figure 6-6 D). Whereas, from profile PR 03 to PR 05 an increase in beach elevation was recorded (Figure 6-10 C, D, E) with a peak value of 1 m measured at the northern beach end (PR 05, Figure 6-10 E). Consequently to this fluctuation of beach surface, erosive scarps were located south and

great storm berms occupied the central and north portion of the beach, with a steep side facing the sea (Figure 6-10 D, E).

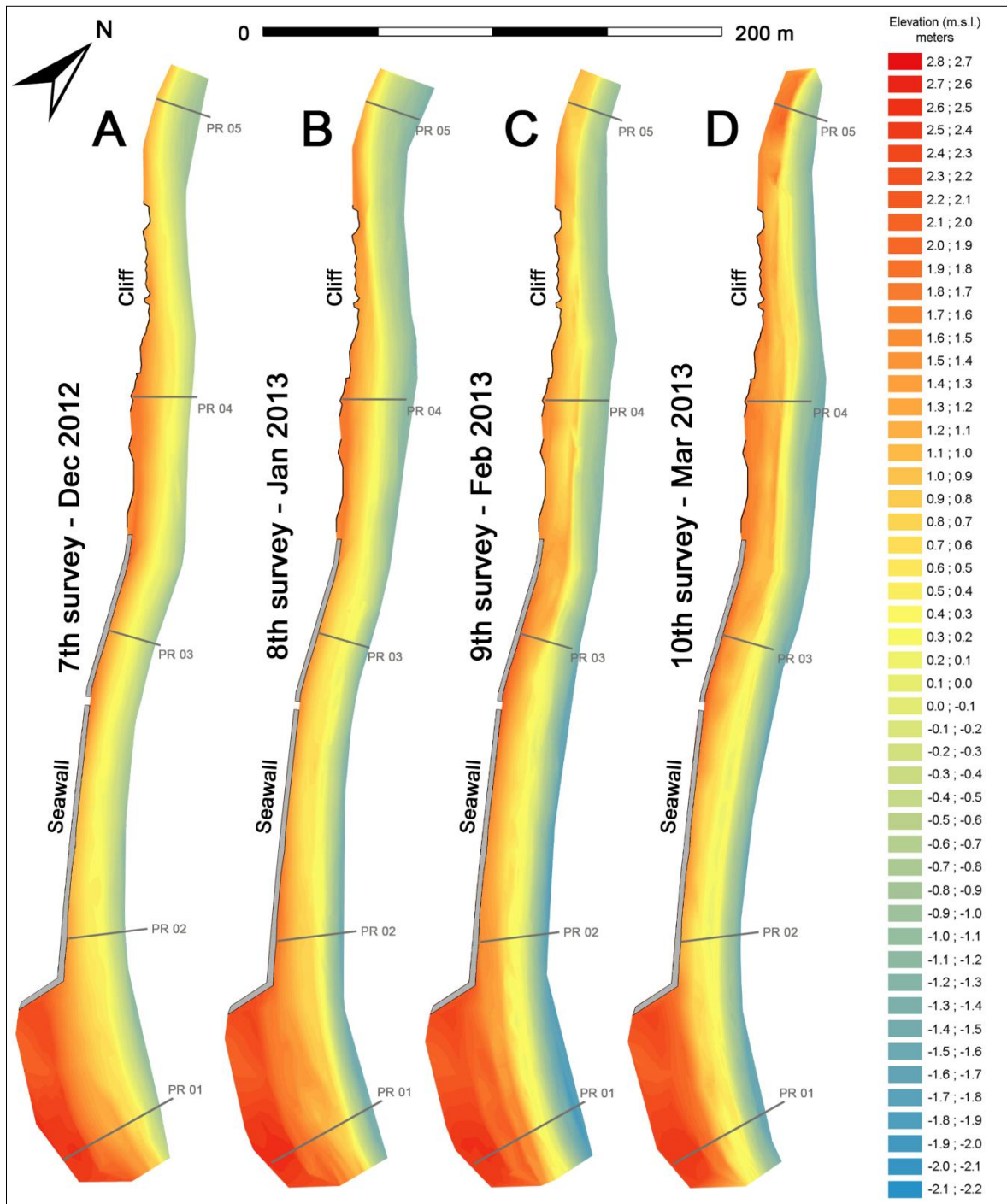


Figure 6-6. Topographic surfaces of Portonovo beach from December 2012 to March 2013 (A) December 2012; B) January 2013; C) February 2013; D) March 2013). The seawall and the cliff toe are shown on each topographic surface.

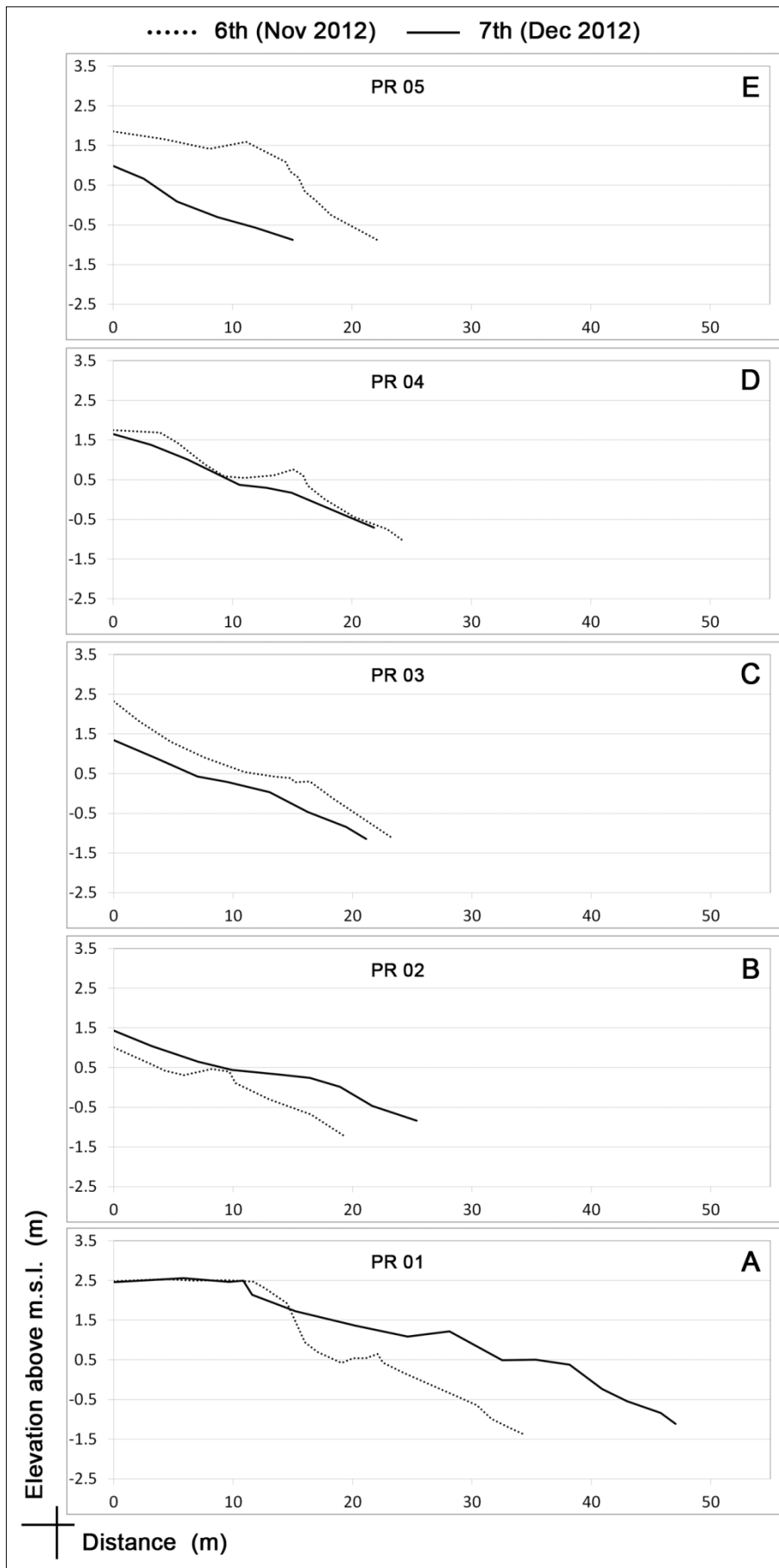


Figure 6-7. Profile variation of the entire beach from November 2012 to December 2012.

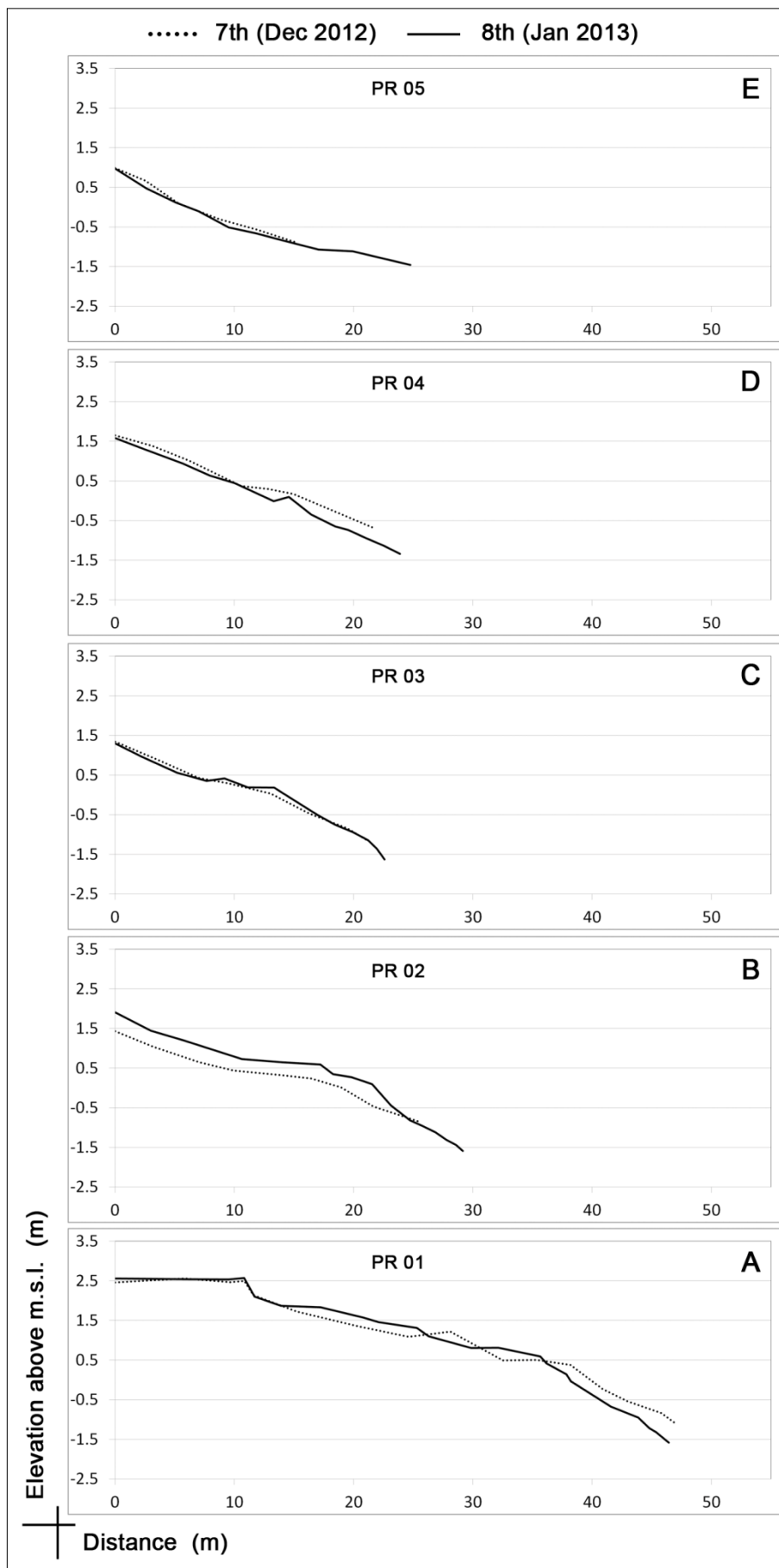


Figure 6-8. Profile variation of the entire beach from December 2012 to January 2013.

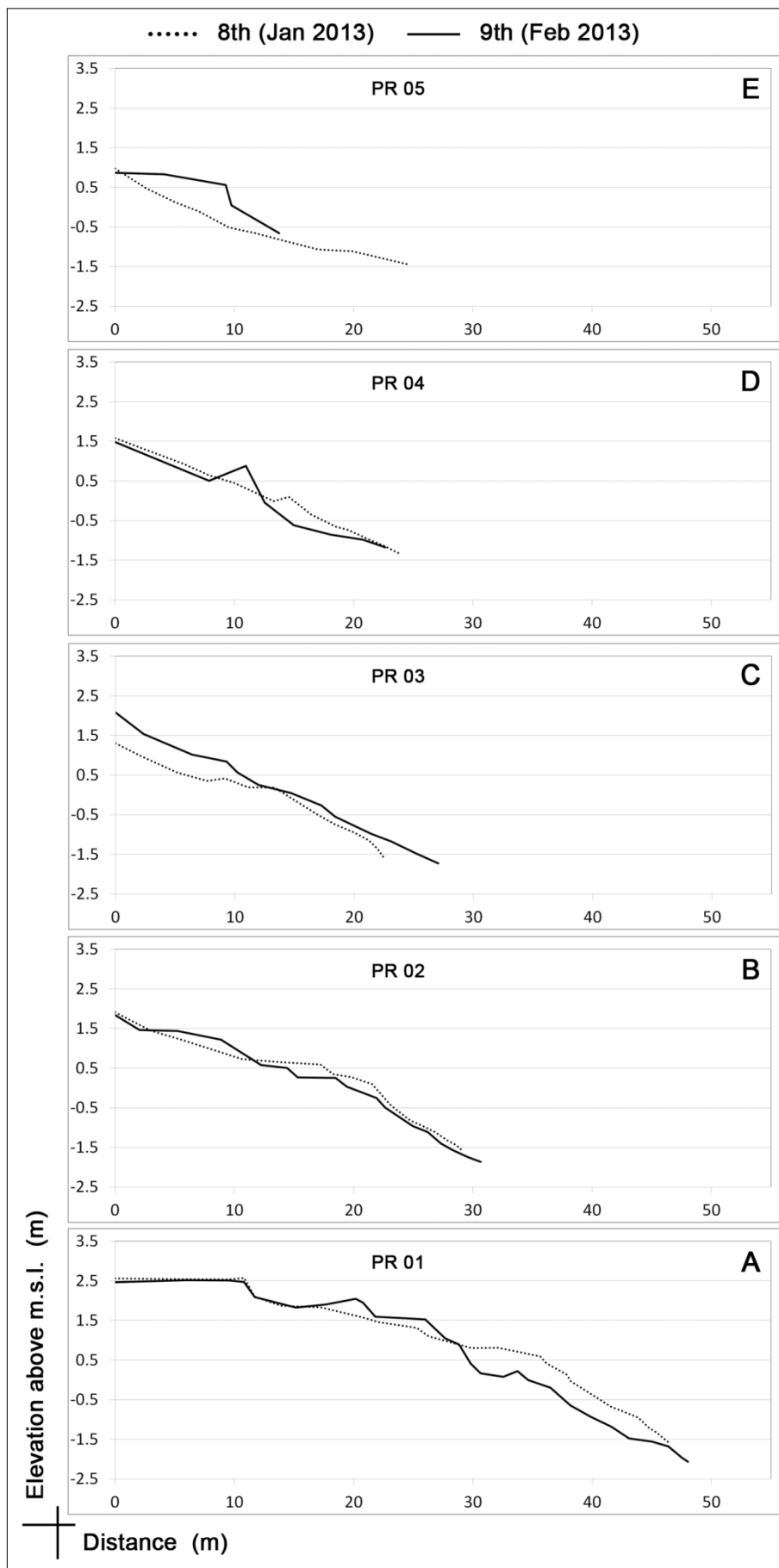


Figure 6-9. Profile variation of the entire beach from January 2013 to February 2013.

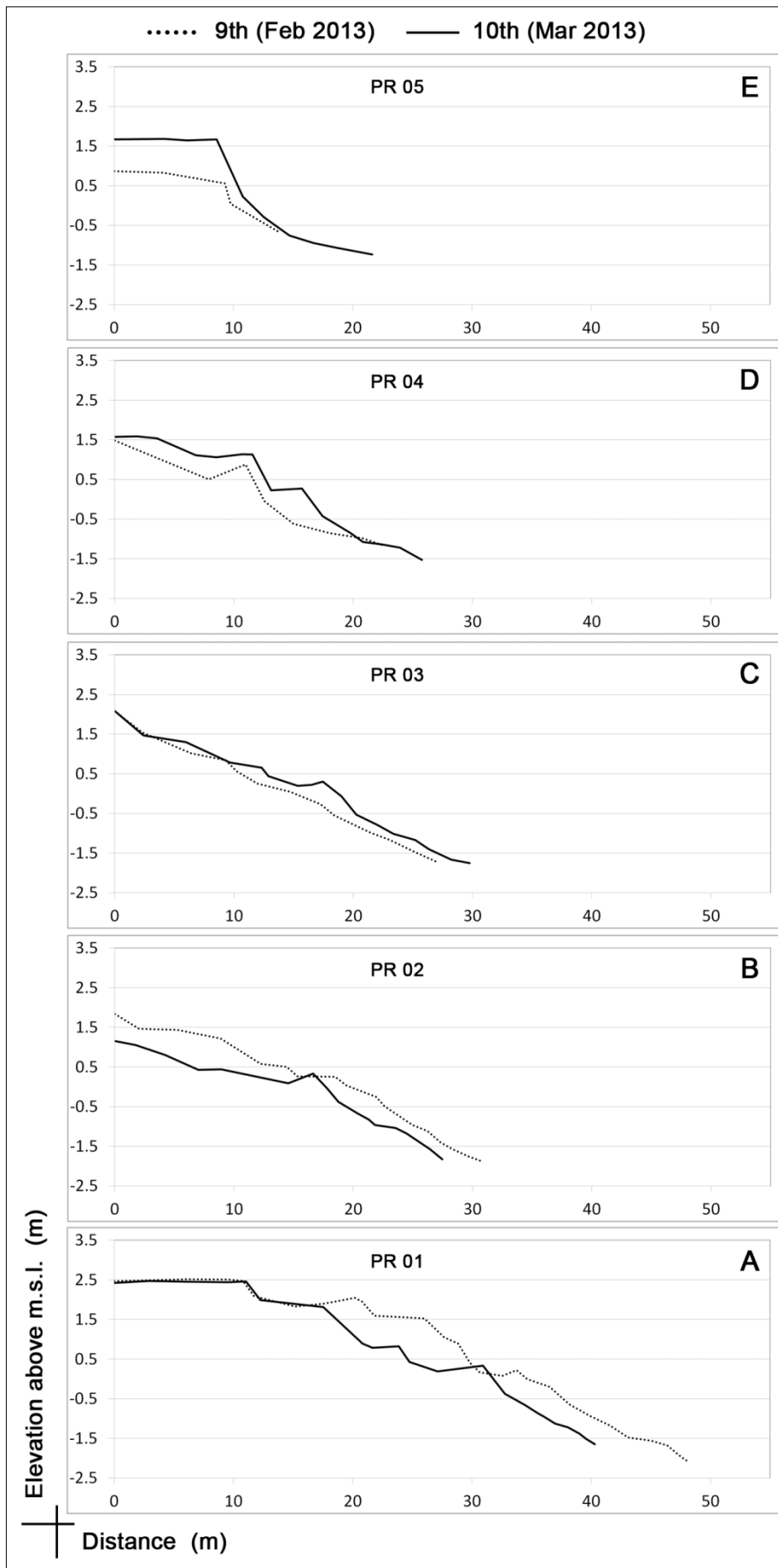


Figure 6-10. Profile variation of the entire beach from February 2013 to March 2013.

From March to April 2013, a general transport of material from the upper to the lower part of the beach was experienced (Figure 6-11 A to compare to Figure 6-6 D; Figure 6-12). This process was clearly visible mostly all over the beach and in particular in the profile PR 01 (Figure 6-12 A). The material displaced to lower areas and the lowering in beach elevation produced a decrease in beachface sloping (Figure 6-12 A, C, E). No particular change was observed in beach width (Figure 6-12).

From April to May 2013 remarkable changes were noted only in some beach portions (Figure 6-11 A, B; Figure 6-13). The southern compartment of the beach was affected by a slight retreat (2-3 m) and lowering of beach which interested only the beach face and the submerged beach (Figure 6-13 A, B). A notable flattening was experienced in PR 01 (Figure 6-13 A), whereas substantially unchanged appeared the PR 03 and PR 04 relative to the previous survey (Figure 6-13 C, D). A significant increase in beach topography was measured at the northern beach end where a maximum increase of 1 m was recorded in the lower part of the profile PR 05 (Figure 6-13 E).

From May 2013 to February 2014 the beach look completely different from south to north (Figure 6-11 B, C; Figure 6-14). The southern part was retreated of approximately 10 m (Figure 6-14 A, B) and the “cut” aspect was confirmed by the presence of erosive scarps (Figure 6-11 C; Figure 6-14 A, B). The central compartment was the only beach portion which did not experienced notable changes (Figure 6-14 C). On the other hand, the northern sector experienced a large accretion, with more than 10 m of increase in width at the very northern end (PR 05, Figure 6-14 E). A higher elevation was recorded in PR 04 and PR 05, with an outstanding peak value of 3 m more than the previous survey at PR 05 (Figure 6-14 D, E; Figure 6-11 C). The great material amount accumulated in the northern portion of the beach was highlighted by the presence of several tiers of storm berms (Figure 6-11 C; Figure 6-14 D, E). As a consequence, the beach slope was steeper in the southern and milder in the northern part of the beach (Figure 6-14; Figure 6-11 C).

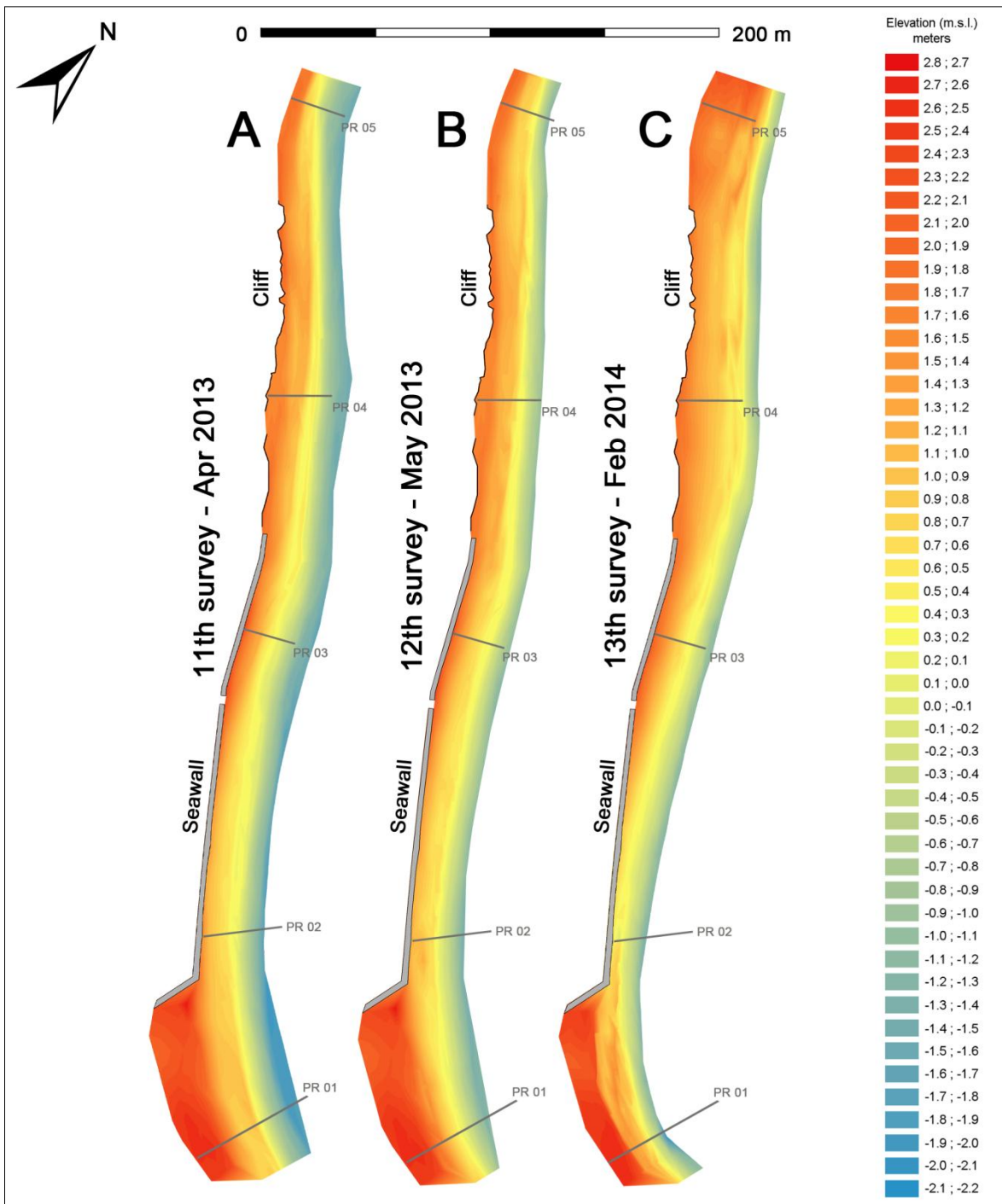


Figure 6-11. Topographic surfaces of Portonovo beach from April 2013 to February 2014 (A) April 2013; B) May 2013; C) February 2014). The seawall and the cliff toe are shown on each topographic surface.



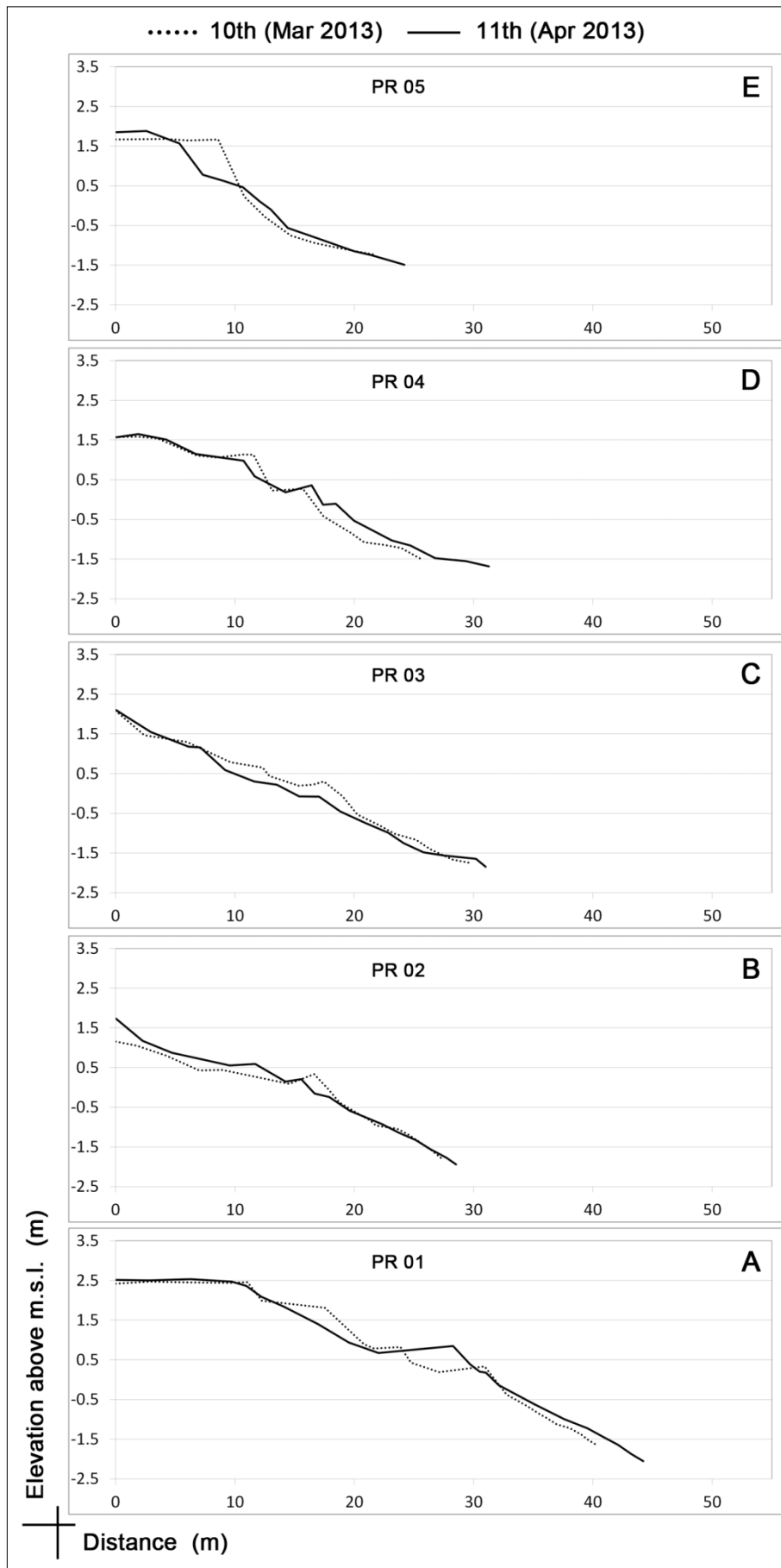


Figure 6-12. Profile variation of the entire beach from March 2013 to April 2013.

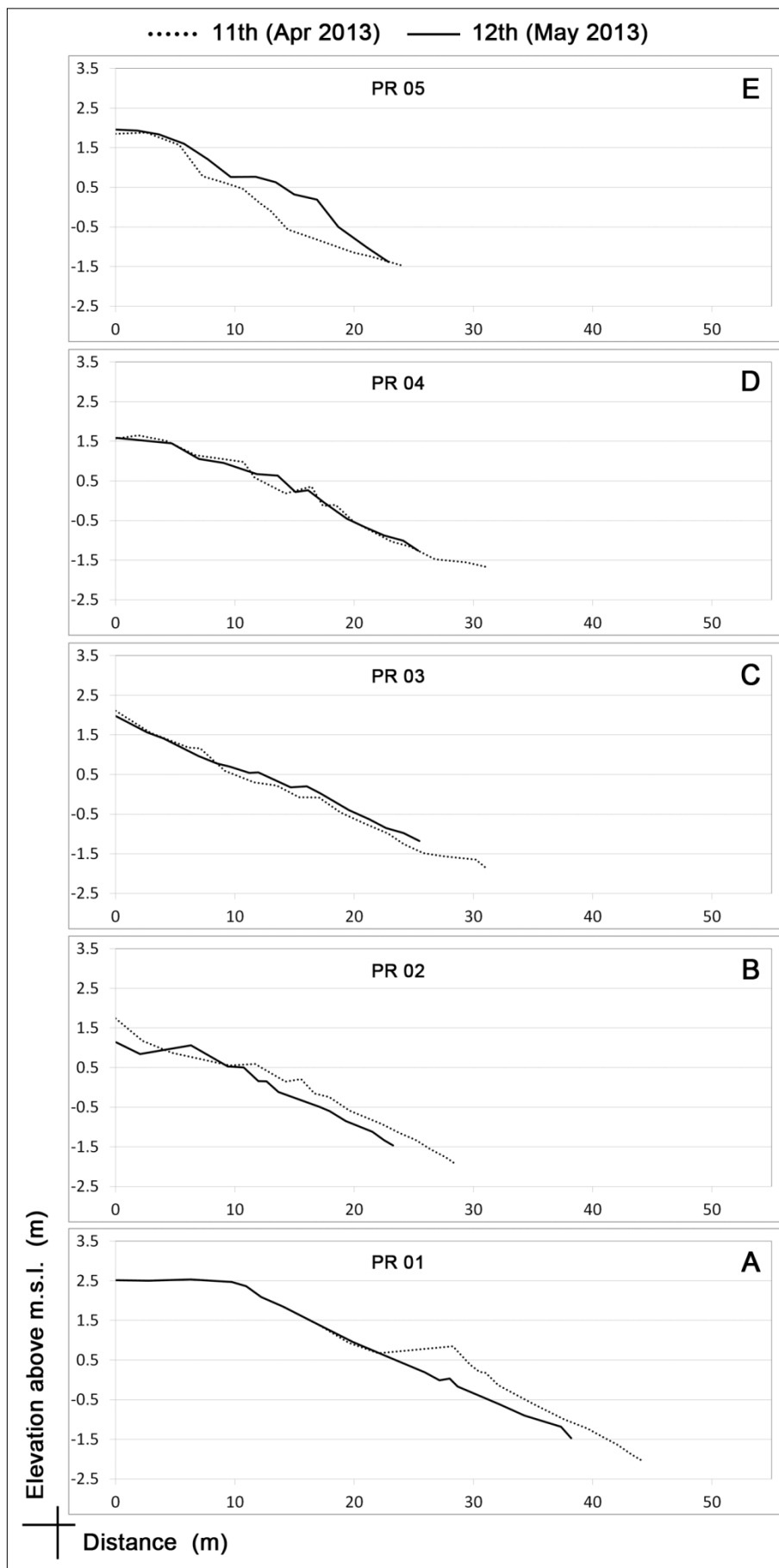


Figure 6-13. Profile variation of the entire beach from April 2013 to May 2013.

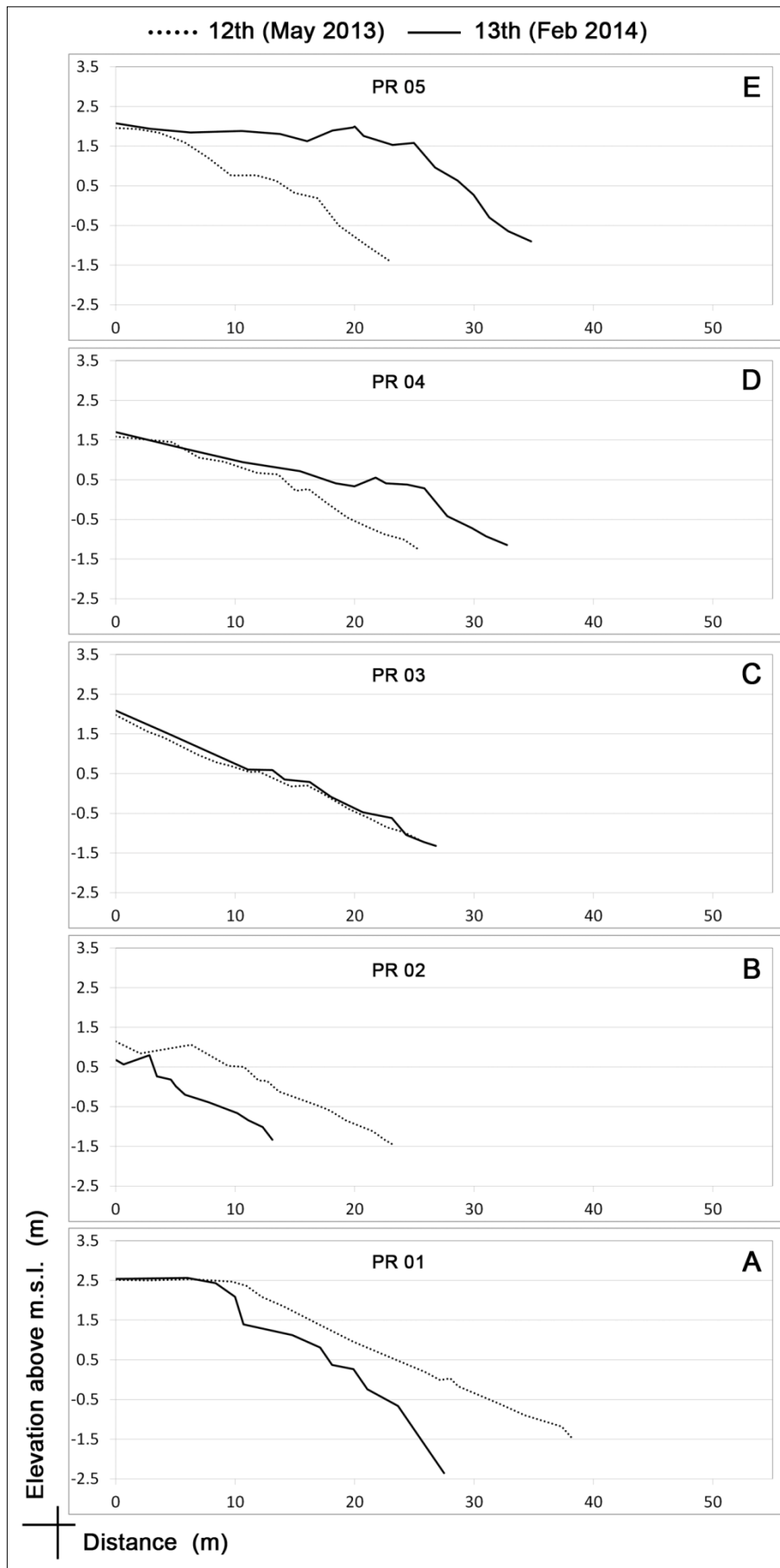


Figure 6-14. Profile variation of the entire beach from April 2013 to May 2013.

## **6.2 - Shoreline variation**

As already explained in the Paragraph 3.4, after a short monitoring period, limited to the experiment and sampling area (March 2012 and April 2012 surveys, Figure 2-1; Figure 3-10), from May 2012 the topographic measurements were extended to the whole beach length. In this paragraph are presented the shoreline variations recorded from May 2012 (3<sup>rd</sup> survey) to February 2014 (13<sup>th</sup> survey) which interested a time span of almost two years. From May 2012 to the first survey of October 2012 (i.e. October 2012 a) the beach presented some eroded and accreted areas. The largest shoreline advancement occurred in the southern zone with values close to 10 m which created a bulge form in the middle of the embayment (Figure 6-15). No consistent change arose in the central compartment of the beach. A shoreline retreat of almost 5 m took place in the northern beach sector and in the southern beach limit (Figure 6-15).

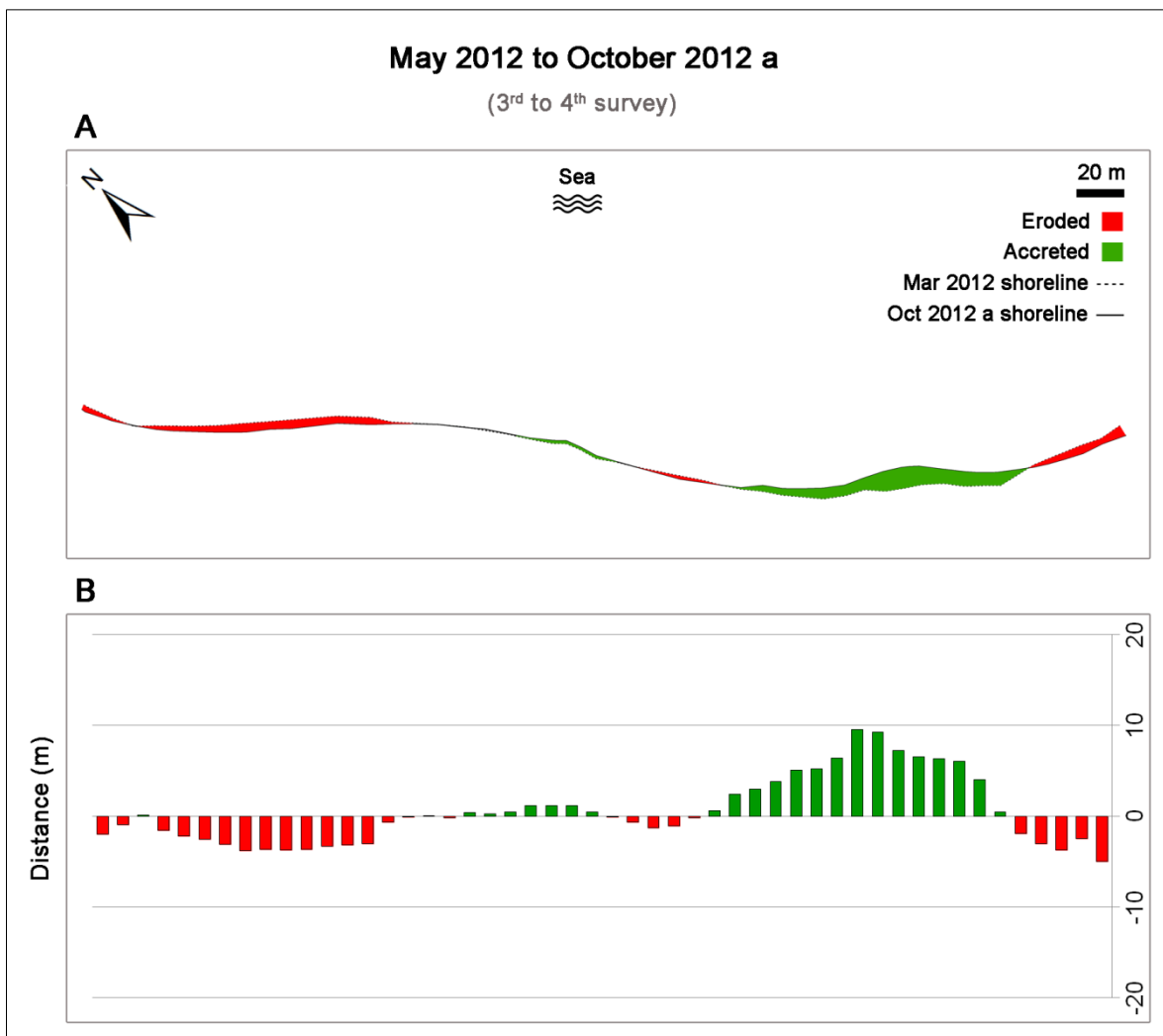


Figure 6-15. Shoreline variation from May 2012 to October 2012 a (3<sup>rd</sup> to 4<sup>th</sup> survey): accretion/erosion map (A) and Net Shoreline Movement (NSM) computed by the ArcGIS tool DSAS (B).

From the first to the second survey of October 2012 (i.e. October 2012 a and October 2012 b) very little variations occurred. Little accretion interested the beach edges and limited erosion was observed in the central area. Variation all over the beach did not exceed 2 m (Figure 6-16). In the southern embayment the bulge form was still present even though less prominent and slightly wider given the moderate accretion that affected both its sides (Figure 6-16).

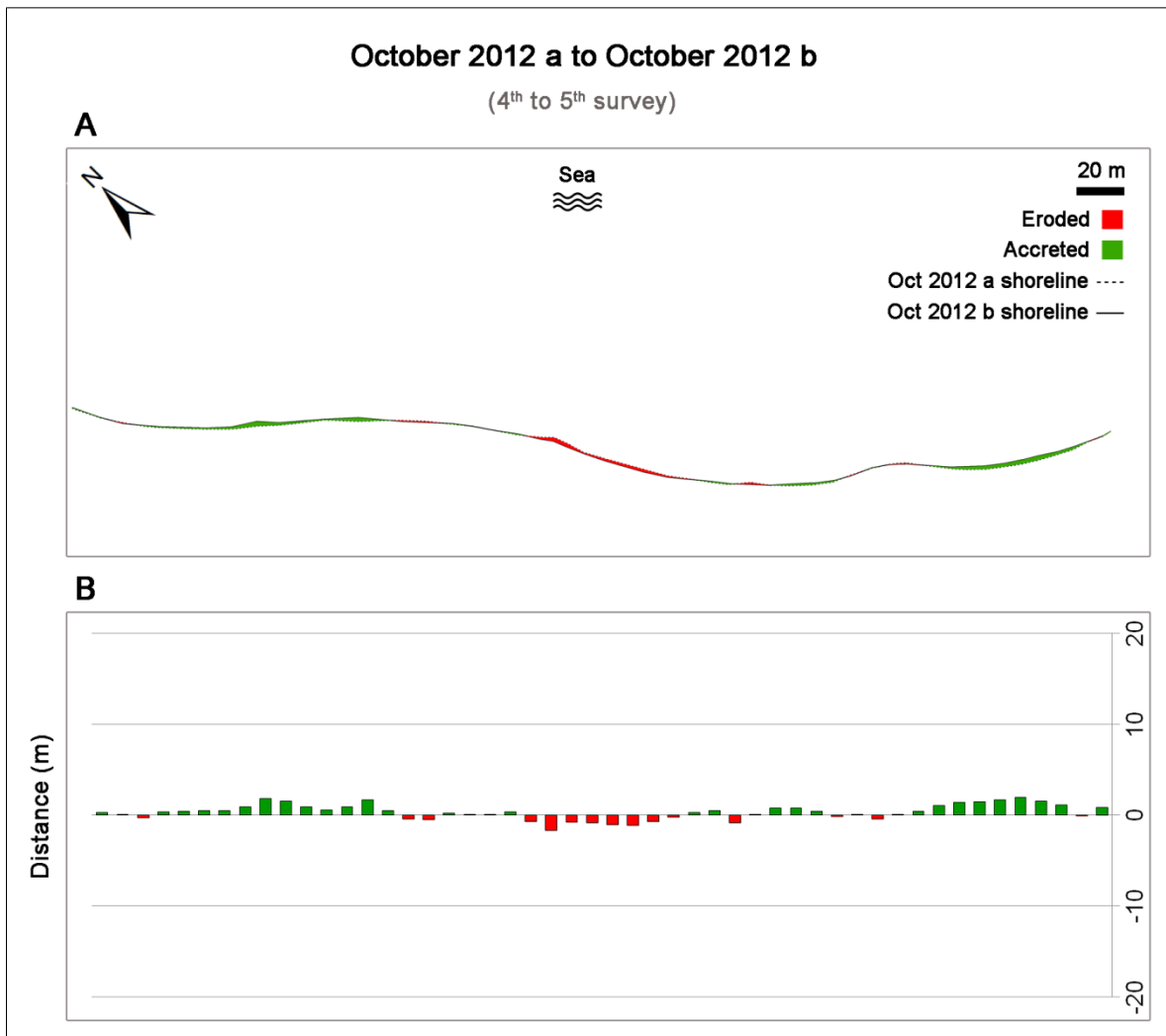


Figure 6-16. Shoreline variation from October 2012 a to October 2012 b (4<sup>th</sup> to 5<sup>th</sup> survey): accretion/erosion map (A) and Net Shoreline Movement (NSM) computed by the ArcGIS tool DSAS (B).

From the second survey of October (i.e. October 2012 b) to November 2012 Portonovo beach was subjected to the first significant variation of its shoreline. The southern part retreated approximately of 16 m which meant the complete erosion of the bulge form that was present in the southern embayment (Figure 6-17). On the other hand the central and the northern compartments gained 10 m seaward.

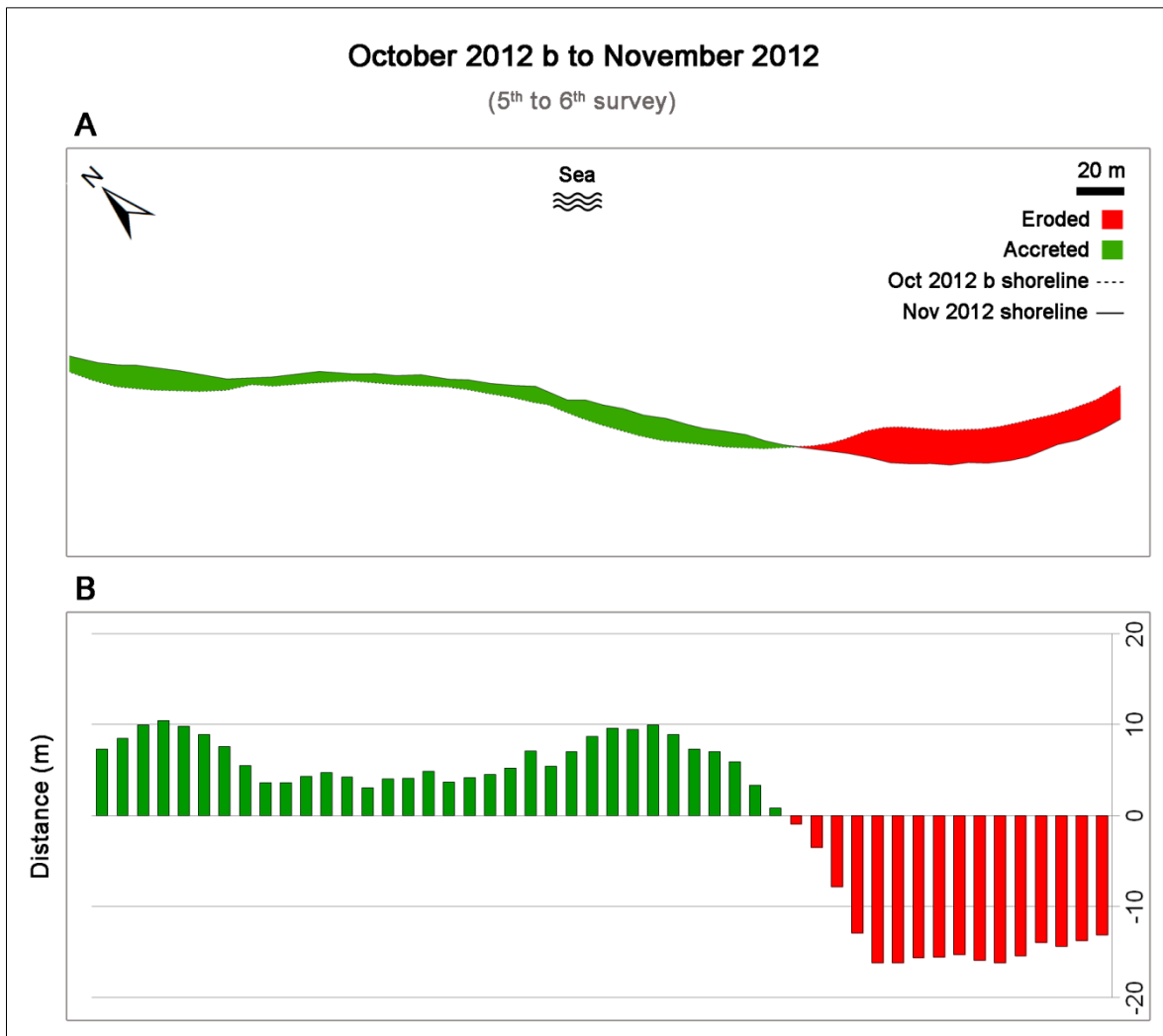


Figure 6-17. Shoreline variation from October 2012 b to November 2012 (5<sup>th</sup> to 6<sup>th</sup> survey): accretion/erosion map (A) and Net Shoreline Movement (NSM) computed by the ArcGIS tool DSAS (B).

From November to December 2012 another relevant shoreline variation occurred. At this time the eroded and accreted areas were exactly overturned relative to the previous stage. Shoreline retreat of approximately 12 m interested the northern zone of the beach. Slightly limited erosion affected the beach in its central area (up to 6 m) while the highest values of shoreline variation were observed in the southern edge. Here the coastline advanced up to 16-17 m, entirely recovering the same area previously lost. A clear clockwise rotation affected the beach at this stage (Figure 6-18).

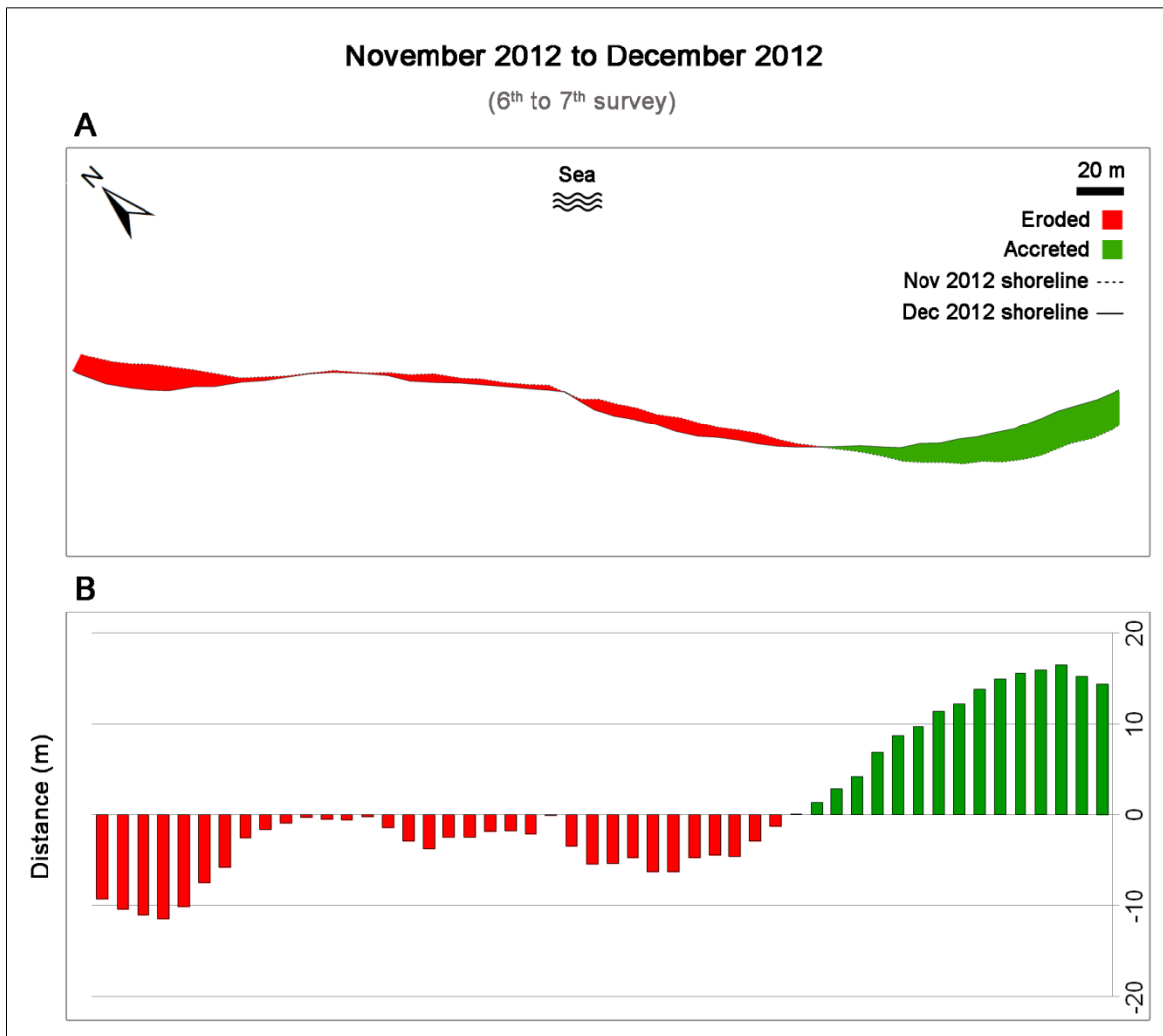


Figure 6-18. Shoreline variation from November 2012 to December 2012 (6<sup>th</sup> to 7<sup>th</sup> survey): accretion/erosion map (A) and Net Shoreline Movement (NSM) computed by the ArcGIS tool DSAS (B).

From December 2012 to January 2013 the beach was in a phase of post-storm recovery. Shoreline variations of approximately 5 m interested the entire beach length with an accretion focused on the southern embayment and mild erosion intensified in the northern compartment. A counter-clockwise rotation affected the beach at this time (Figure 6-19), even though less pronounced if compared to the previous two (Figure 6-17; Figure 6-18).



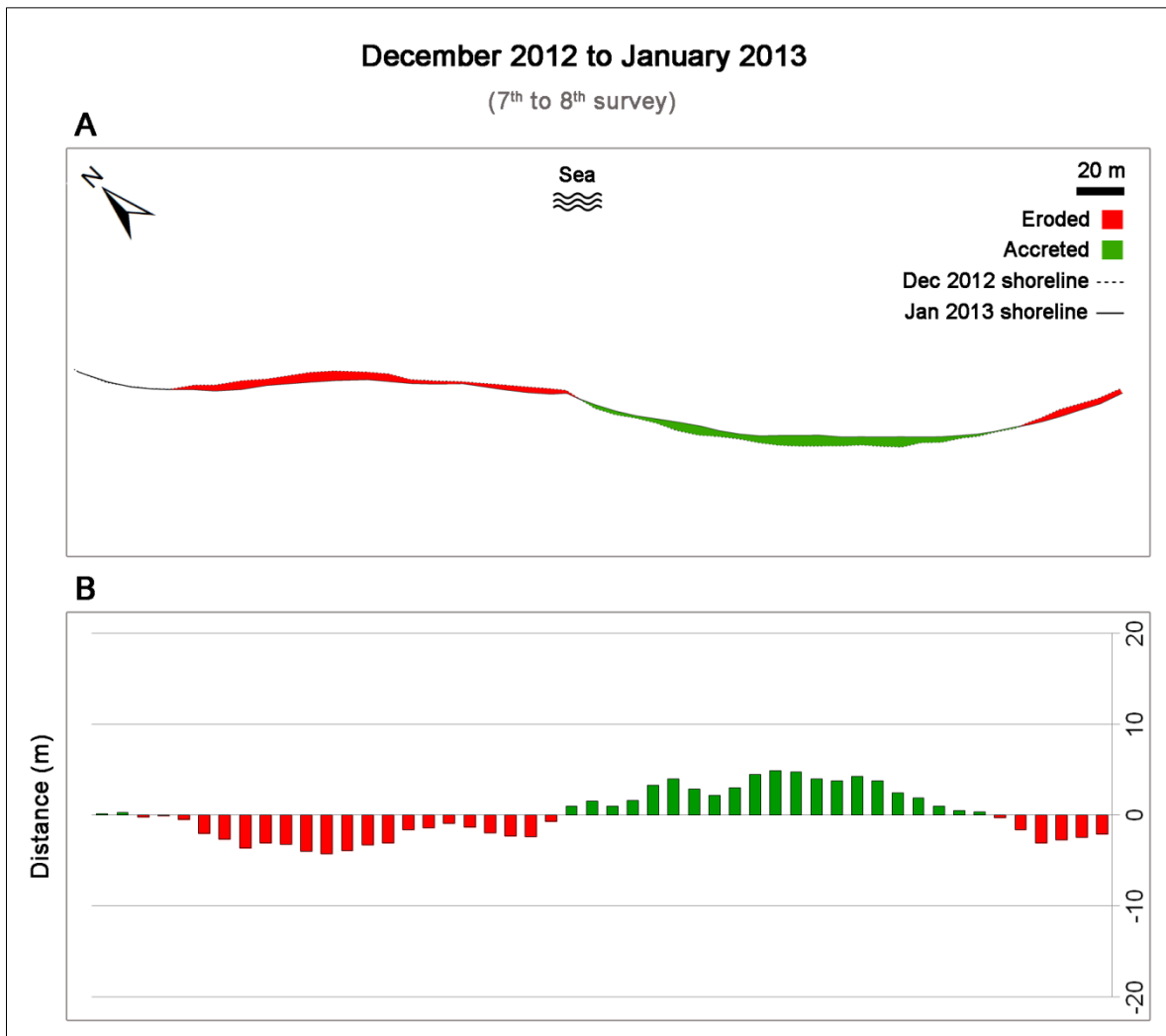


Figure 6-19. Shoreline variation from December 2012 to January 2013 (7<sup>th</sup> to 8<sup>th</sup> survey): accretion/erosion map (A) and Net Shoreline Movement (NSM) computed by the ArcGIS tool DSAS (B).

From January to February 2013 the magnitude of shoreline change slightly decreased to 2-3 m. Small accretion and erosion areas can be distinguished all over the beach, with a more pronounced erosion in the southern beach end and a mild accretion in the northern compartment (Figure 6-20). The shoreline situation was basically comparable to the previous stage.

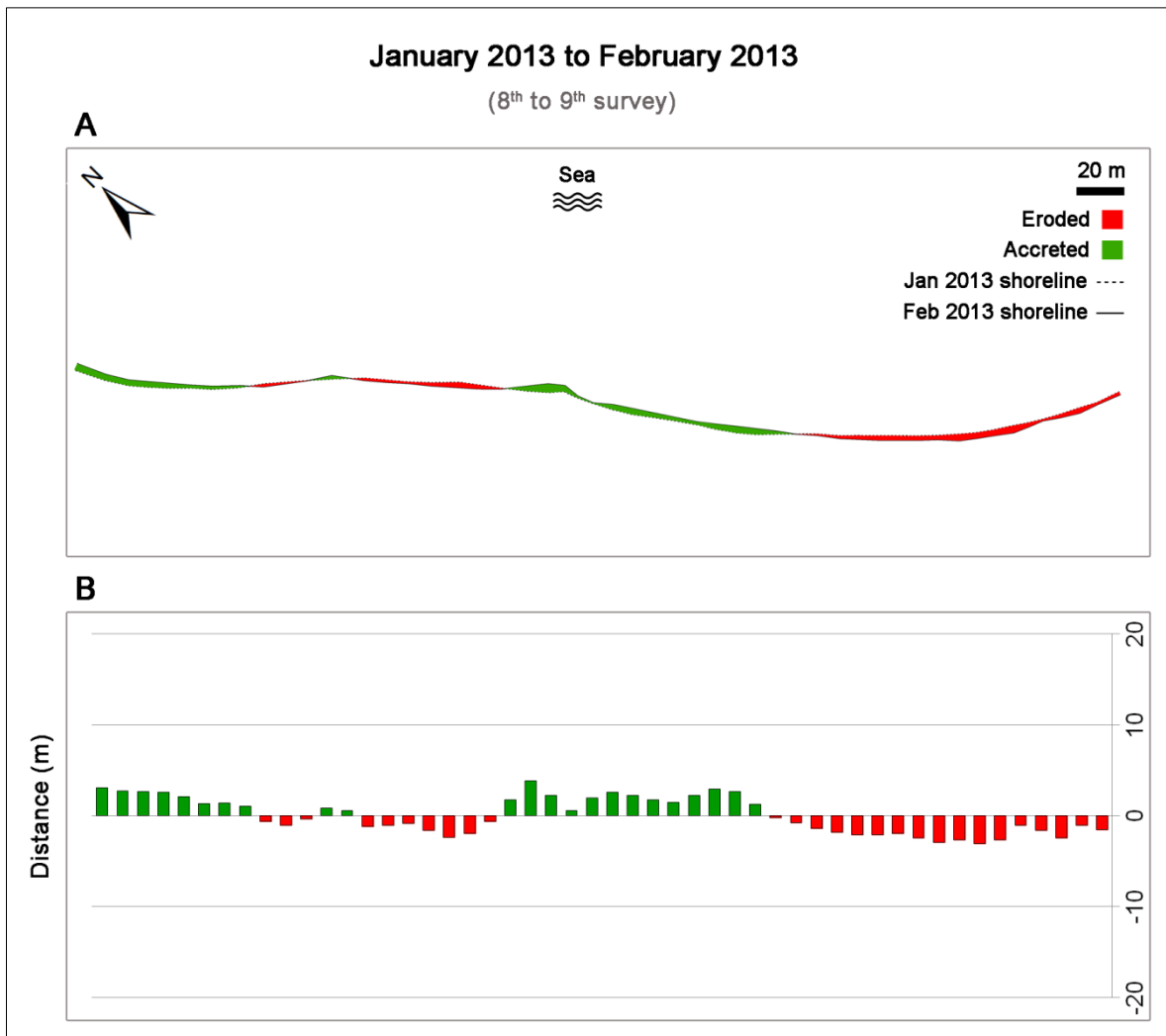


Figure 6-20. Shoreline variation from January 2013 to February 2013 (8<sup>th</sup> to 9<sup>th</sup> survey): accretion/erosion map (A) and Net Shoreline Movement (NSM) computed by the ArcGIS tool DSAS (B).

From February to March 2013 relevant shoreline changes were recorded. In the southern zone the largest retreat was approximately 10 m while in the northern compartment of the beach a maximum advance of 7 m was recorded. A clear clockwise rotation of the beach occurred at this stage (Figure 6-21).

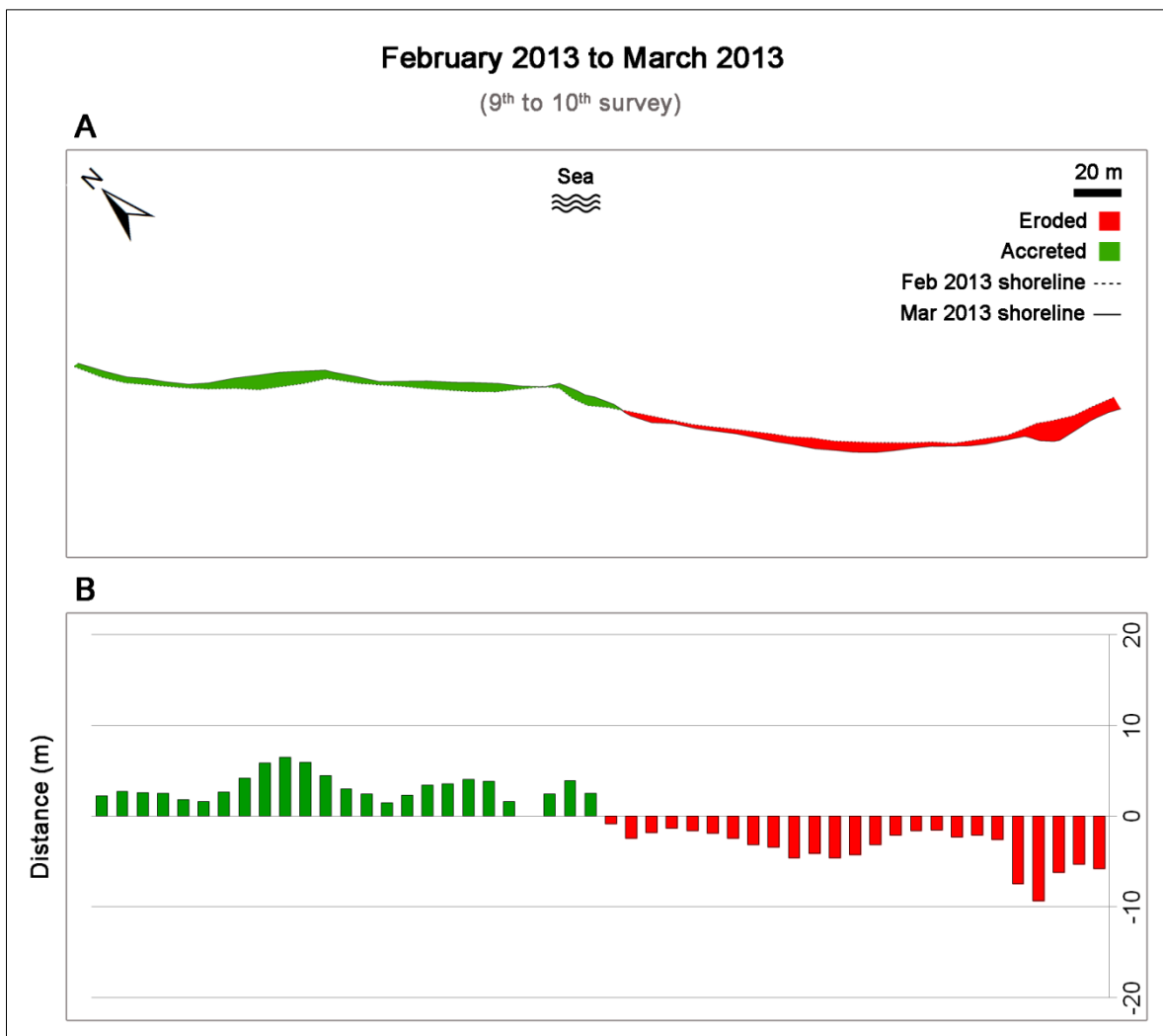


Figure 6-21. Shoreline variation from February 2013 to March 2013 (9<sup>th</sup> to 10<sup>th</sup> survey): accretion/erosion map (A) and Net Shoreline Movement (NSM) computed by the ArcGIS tool DSAS (B).

From March to April 2013 the beach was interested by a general recovery process. The northern part of the beach gained 6 m and up to 4 m in the southern zone (Figure 6-22).

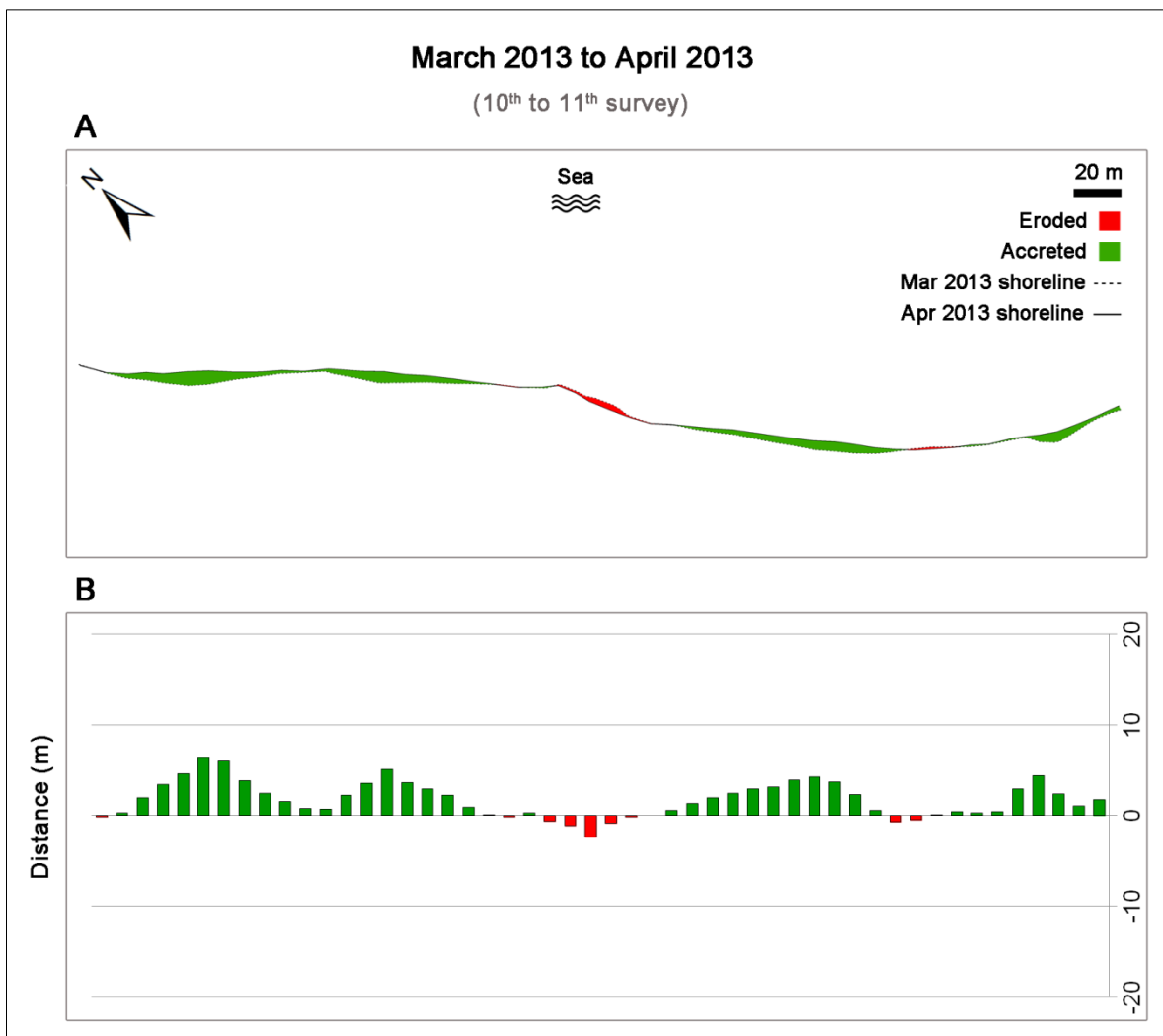


Figure 6-22. Shoreline variation from March 2013 to April 2013 (10<sup>th</sup> to 11<sup>th</sup> survey): accretion/erosion map (A) and Net Shoreline Movement (NSM) computed by the ArcGIS tool DSAS (B).

From April to May 2013 shoreline repositioning was milder. The southern embayment was affected by a retreat of approximately 4 m while the rest of the beach showed eroded and accreted areas. A peak value of advancement of 6 m was recorded at the northern beach end (Figure 6-23).

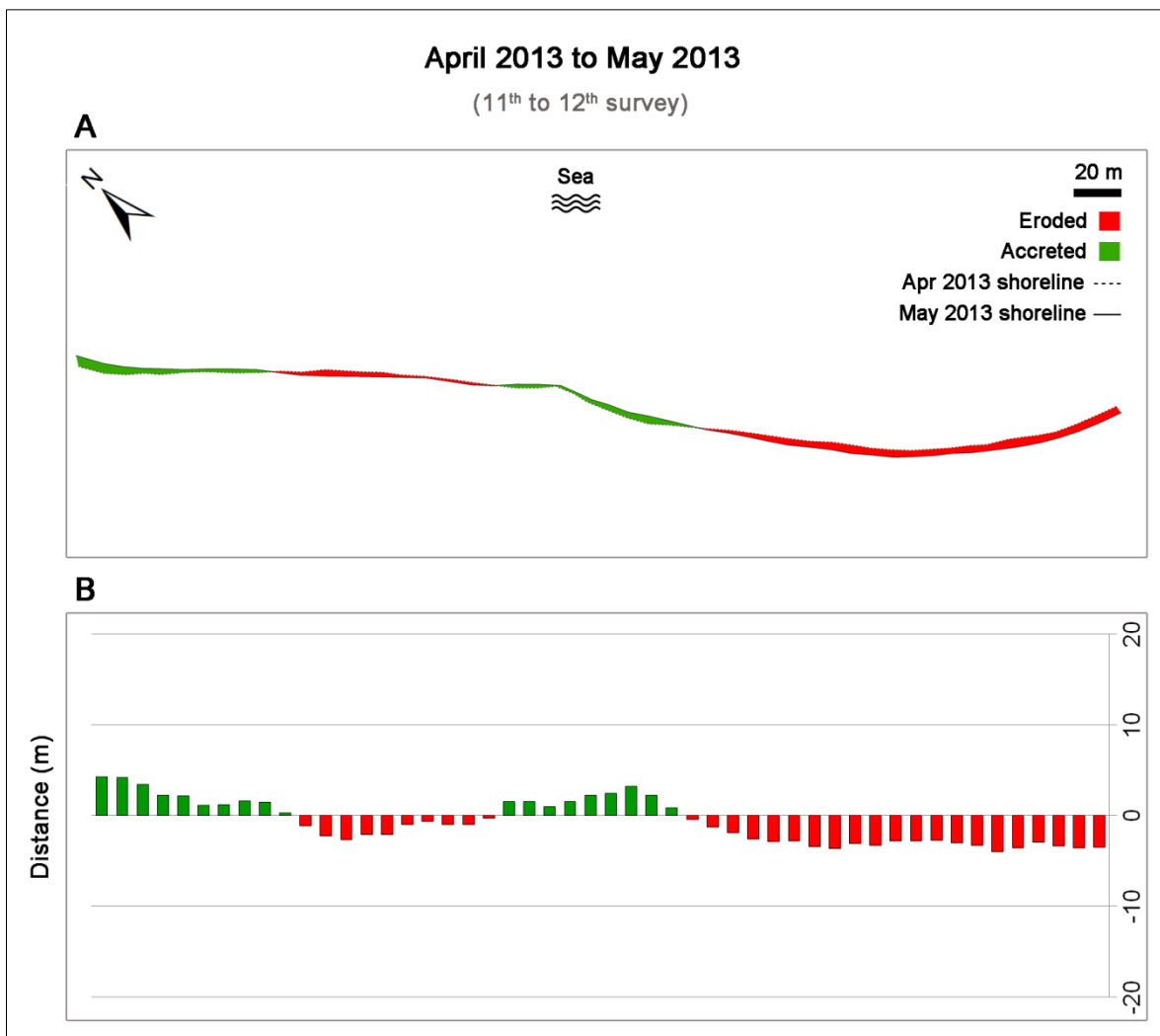


Figure 6-23. Shoreline variation from April 2013 to May 2013 (11<sup>th</sup> to 12<sup>th</sup> survey): accretion/erosion map (A) and Net Shoreline Movement (NSM) computed by the ArcGIS tool DSAS (B).

From May 2013 to February 2014 large variations affected the shoreline. A clear clockwise beach rotation occurred: 10 m retreat affected the southern embayment while a considerable accretion involved the northern compartment, with a peak value of 14 m (Figure 6-24). Little variations were experienced in the central part of the beach since behaved as pivotal point for rotation.

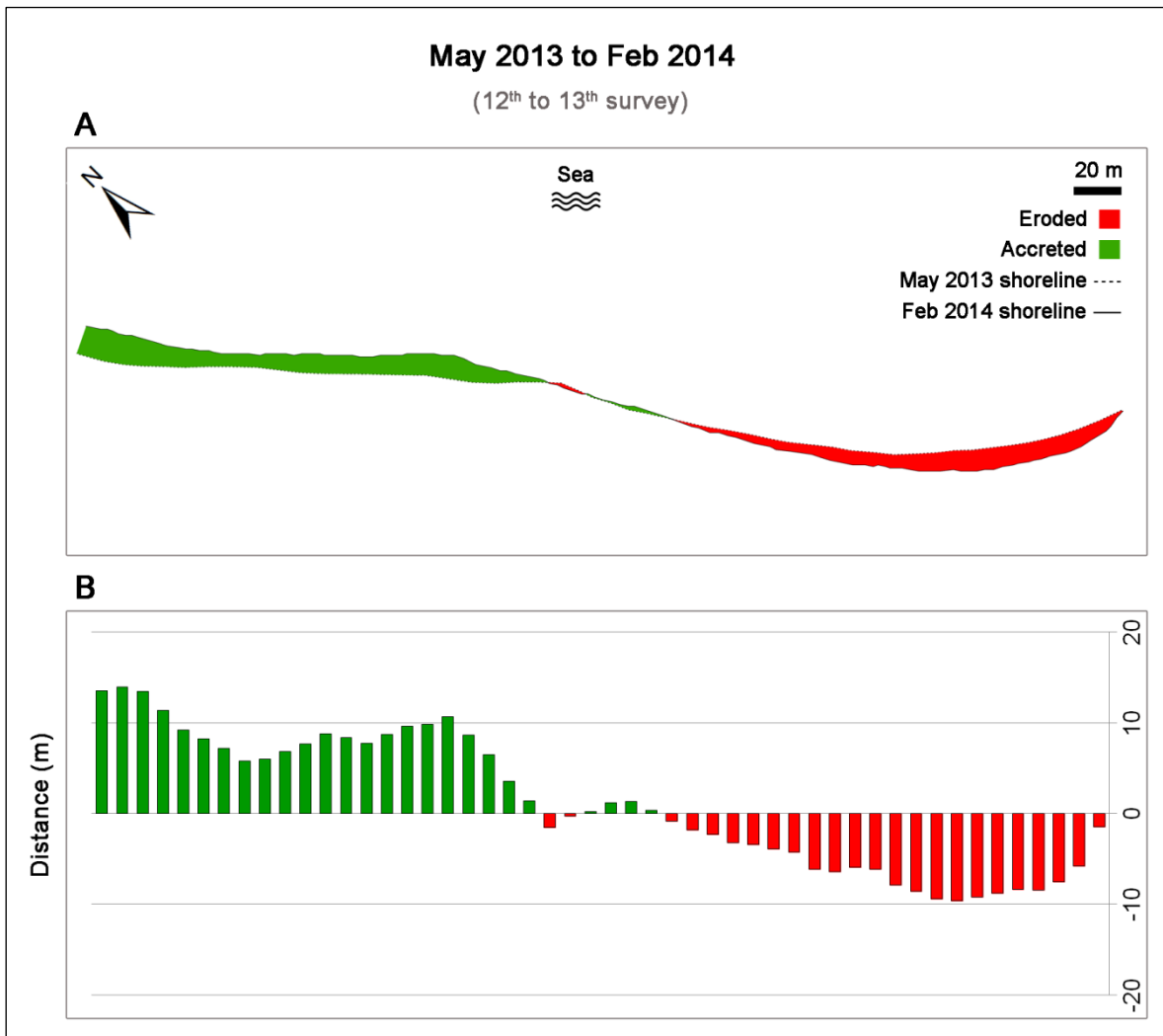


Figure 6-24. Shoreline variation from May 2013 to February 2014 (12<sup>th</sup> to 13<sup>th</sup> survey): accretion/erosion map (A) and Net Shoreline Movement (NSM) computed by the ArcGIS tool DSAS (B).

Considering the two years monitoring period (from May 2012 to February 2014) the shoreline in Portonovo had recorded significant variations. The SCE estimation (Shoreline Change Envelope, see Paragraph 3.6) had reported the largest shoreline changes at both beach ends, with maximum values of 25 m in the northern compartment and 21 m in the southern zone while a minimum value of almost 8 m was recorded in the central part of the beach (Figure 6-25 C). The values computed by the SCE should not be taken as accretionary or erosive amounts but as maximum distances experienced by shoreline repositioning in two years. According to the NSM calculations (Net Shoreline Movement, see Paragraph 3.6) from the first to the last topographic survey the shoreline advanced in the central and northern compartment while consistent retreat affected the southern embayment of the beach (Figure 6-25 A, B). The final beach configuration was the result of a clear clockwise rotation which produced advancement values up to 23 m in the northern zone and 21 m of shoreline retreat at the southern end (Figure 6-25 B). As computed by the EPR tool (End Point Rate, see Paragraph 3.6) in almost two years the rate of shoreline retreat in the southern area was 12 m (peak value, Figure 6-25 D) while the accretion rate in the northern zone was approximately 13 m (peak value, Figure 6-25 D). The most limited shoreline variability was recorded in the central zone of the beach (Figure 6-25 C) where usually the pivotal point of beach rotation is located.

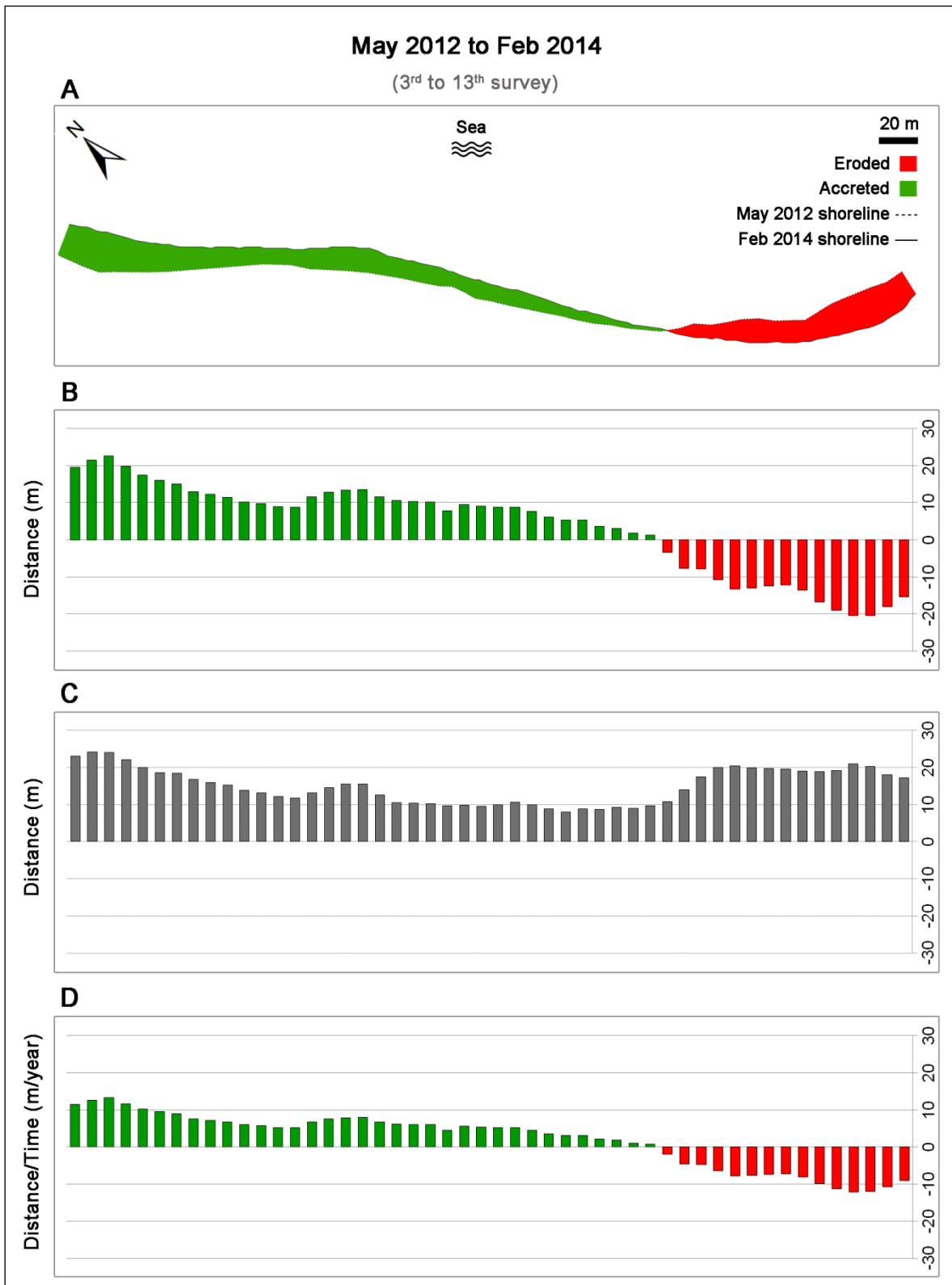


Figure 6-25. Shoreline variation for the whole period of almost two years (from May 2012 to February 2014; 3<sup>rd</sup> to 13<sup>th</sup> survey): accretion/erosion map (A), (NSM) Net Shoreline Movement (B), (SCE) Shoreline Change Envelope (C) and (EPR) End Point Rate (D) computed by the ArcGIS tool DSAS.



### 6.3 - Volumetric variation

The volume calculated from the surveyed beach, during almost two years span time, ranged from a minimum of 25148 m<sup>3</sup> (October 2012 a, Figure 6-14) to a maximum of 29158 m<sup>3</sup> (February 2014, Figure 6-14). From the first topographic survey (May 2012) to the last one (February 2014), a total gain of 3790 m<sup>3</sup> was estimated. According to this data the beach does not present problems of material loss. The largest variation was recorded between December 2012 and January 2013 (Figure 6-14; Figure 6-26) which represented a break point between the 2012 period, with volume values oscillating approximately between 25100 and 26500 m<sup>3</sup>, and the later interval (2013-2014) with constantly higher values comprised approximately between 27600 and almost 29100 m<sup>3</sup> (Figure 6-14). Variation in volume can be relevant from one survey to another: four volume losses were observed (from May to October 2012 a, from November to December 2012, from February to March 2013 and from March to April 2013, Figure 6-26). The entity of volume lost during those surveys varied from 220 to 844 m<sup>3</sup>, rather much larger was the quantity of material gained by the beach in the remaining six time intervals, from a minimum of 113 m<sup>3</sup> (gain reached between the two October 2012 surveys, Figure 6-26) to a peak value of 2355 m<sup>3</sup> (occurred from December 2012 to January 2013, Figure 6-26).

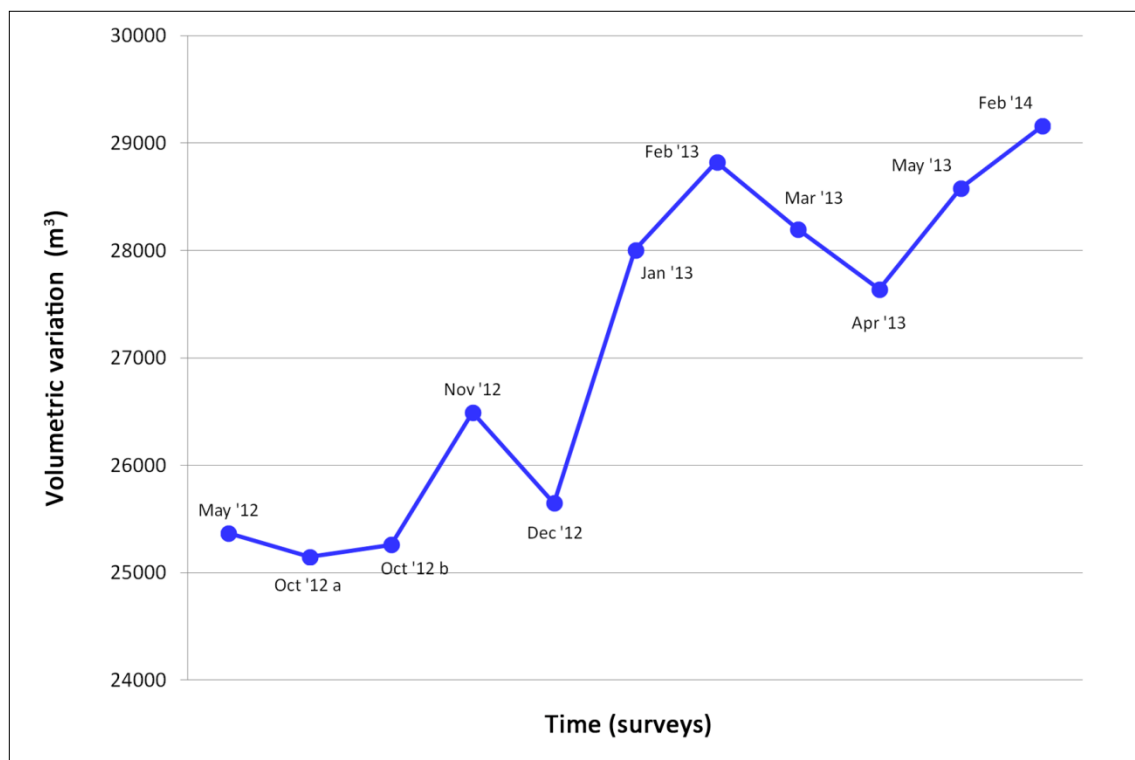


Figure 6-26. Volumetric variation in almost two year time span.

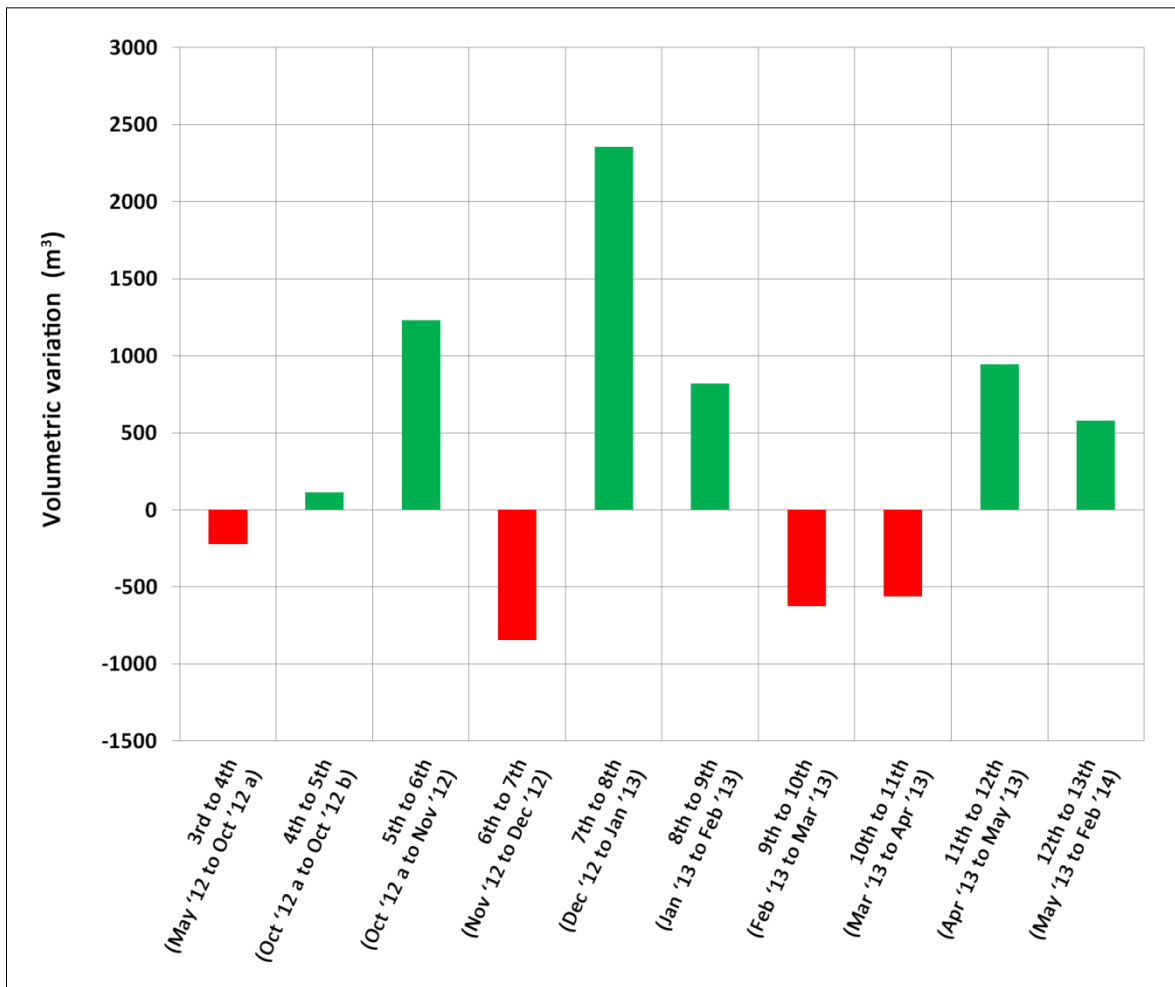


Figure 6-27. Volumetric variation from one survey to another in almost two year time span.

#### 6.4 - Discussion

Portonovo beach had experienced significant shoreline variability during the two years of monitoring. Beach rotation often occurs in response of the direction of major storms. In Table 6-1 are shown the characteristics of the last storm occurred before each topographic survey. Storm events prior to each survey were identified following the method described by Armaroli et al. (2012). In Table 6-1 is also shown the severity class of each storm following the scale of Mendoza et al. (2011) (see also Paragraph 3.7). Beach rotation arises during winter periods (Table 6-1) and the sense of rotation can be easily reversed if a storm from the opposite direction of the previous one occurs (compare Figure 6-17 with Figure 6-18). A clockwise rotation of the beach happens each time a storm from ESE takes place while a counter-clockwise rotation occurs if a storm approaches from NE or NW sectors.

Among all the measured surveys is fairly clear that the last storm is the event accountable for beach rotation when this process occurs (Table 6-1). March 2013 represents the only exception since a counter-clockwise rotation was clear after the survey even though the direction of the last storm (NW) was supposed to produce a clockwise rotation. In this case the last storm was too weak to cover the rotation occurred with the next to last storm which was stronger (Hs: 3.5 m, Dir: SE, Duration: 43.5 h, E: 545 m<sup>2</sup>h) and was scaled as “significant” according to Mendoza et al. (2011) storm severity scale.

Survey	Evidence of beach rotation	Last storm occurred				
		Hs max (m)	Dir	Duration (h)	E (m <sup>2</sup> h)	Severity
Oct 2012 a	none	-	-	-	-	-
Oct 2012 b	none	-	-	-	-	-
Nov 2012	yes (clockwise)	4	ESE	38	602	significant
Dec 2012	yes (counter-clockwise)	2.4	NNW	50.5	291	weak
Jan 2013	yes (counter-clockwise)	2.9	NNE	54	451	moderate
Feb 2013	none	2	ESE	12.5	52	weak
Mar 2013	yes (clockwise)	2	NW	10.5	40	weak
Apr 2013	none	2.2	ENE	9.5	45	weak
May 2013	none	2.2	ESE	6	28	weak
Feb 2014	yes (clockwise)	4.1	ESE	103	1859	extreme

Table 6-1. Evidence of beach rotation observed in Portonovo beach during the two year monitoring. Characteristics of the last storm occurred before each survey are shown from offshore wave data (ISPRA - Servizio Mareografico “Rete Ondametrica Nazionale”). Severity class of each storm is calculated according to the storm severity scale of Mendoza et al. (2011).

Shortest values of shoreline variation were usually recorded in the central zone of the beach or in the middle of the southern embayment (see all figures where evidence of beach rotation is shown, Figure 6-17; Figure 6-18; Figure 6-19; Figure 6-21; Figure 6-24). The central area of Portonovo beach is the pivotal point for shoreline rotation process. Portonovo seems to act like a pocket beach even though is not a natural pocket beach given its longshore boulder armours protecting historical buildings (Figure 2-1). The behaviour is quite similar to another beach located few kilometres southward in the village of Sirolo (San Michele-Sassi Neri beach). Harley et al. (2014) demonstrated the rotation occurring in the beach of San Michele-Sassi Neri by means of a low cost video-monitoring system set up to observe the beach response to a gravel nourishment project. According to Harley et al. (2014) the clockwise rotation in Sirolo is driven by ESE storms while the counter-clockwise rotation is the result of the natural readjustment to ESE events. In Portonovo the beach orientation is approximately NW-SE, and differently from Sirolo, storms approaching from NNE or NNW force counter-clockwise rotation which are able to delete previous evidence created by storms drove by SE sector. Subsequent storms occurring from opposite directions are quite frequent in Portonovo and the NW-SE orientation induces the beach to undergo both “Bora” and “Scirocco” driven events.

According to volumetric variation during almost two year time span, the beach does not present serious problems of material loss. Several “cut” and “fill” processes were observed in response of the main storms but the final budget showed a volume gain of almost 4000 m<sup>3</sup> (Figure 6-26). When a storm from SE direction approaches, the southern portion of the beach is cut and several erosive scarps of remarkable height (approximately 1.5 m) are created (Figure 6-28). On the other hand, the northern sector of the beach is “filled” by material (generally coarse, Figure 7-6 C) combined to well developed storm berms (Figure 6-28). This “Cut and fill” process occurs in response to each energetic storm and is combined to the downdrift coarsening of sediments which will be discussed in Chapter 7. The topographic data presented in the previous paragraph confirm that only the very landward portion of the southern part of the beach was never subjected to changes because never reached by storm waves (all Figures related to PR 01). The lower part of the profiles showed a quick recover after the major storms. In case of subsequent storm of comparable magnitude occurred in the opposite direction, also the upper portion of the beach can quickly recover. The other area less affected by remarkable morphological variation is the central compartment of the beach: as already discussed in Chapter 4, this portion of the beach act as “transfer zone” for sediment transport, probably due to wave reflection given

by the presence of the seawall (Figure 6-1; Figure 6-6; Figure 6-11). Furthermore, as demonstrated by shoreline variability, the central area of Portonovo beach is where the “pivotal point” is located when a beach rotation occurs. The two beach edges appeared as the most dynamic areas: decrease or increase of beach width and elevation in these sectors are produced in response to the last storm direction. One more time, it is confirmed that the major forcing condition controlling the beach morphology and sediment pattern is the storm event. Lorang et al. (1999) supported the thesis according to intense storms characterised by high waves and long duration have the greatest opportunity to pile material to the highest elevation. Also Ibrahim et al. (2006) found that accretion is more pronounced on the upper portion of beach profile when an increase in wave height occurs. In Portonovo the highest changes in elevation had surely arisen after the most energetic storms: crystal clear example are the profile changes occurred from May 2013 to February 2014 (Figure 6-14) after the strongest storm occurred in the whole monitoring period which was classified as extreme (Table 6-1). Another example were the topographic changes arose from October to November 2012 (Figure 6-5; Figure 6-1 C, D) after the “Halloween 2012” storm assessed as significant severity (Table 6-1). Storms not so energetic can similarly produce significant variability in beach elevation: from November to December 2012 a storm driven by NNW, classified as weak severity (Table 6-1), completely overturned the beach configuration generated by the “Halloween 2012” storm (Figure 6-7; compare also Figure 6-1 D with Figure 6-6 A). This process is to ascribe to the NW-SE beach orientation and to the availability of material on the northern beach end which was driven by the weak NNW storm towards the southern beach portion, filling the space previously eroded by the “Halloween” storm (Figure 6-7). The importance of material supply was highlighted by Lorang et al. (1999). According to the authors the height to which waves can pile material is dependent also on a sufficient quantity of material in the proper size and density ranges.

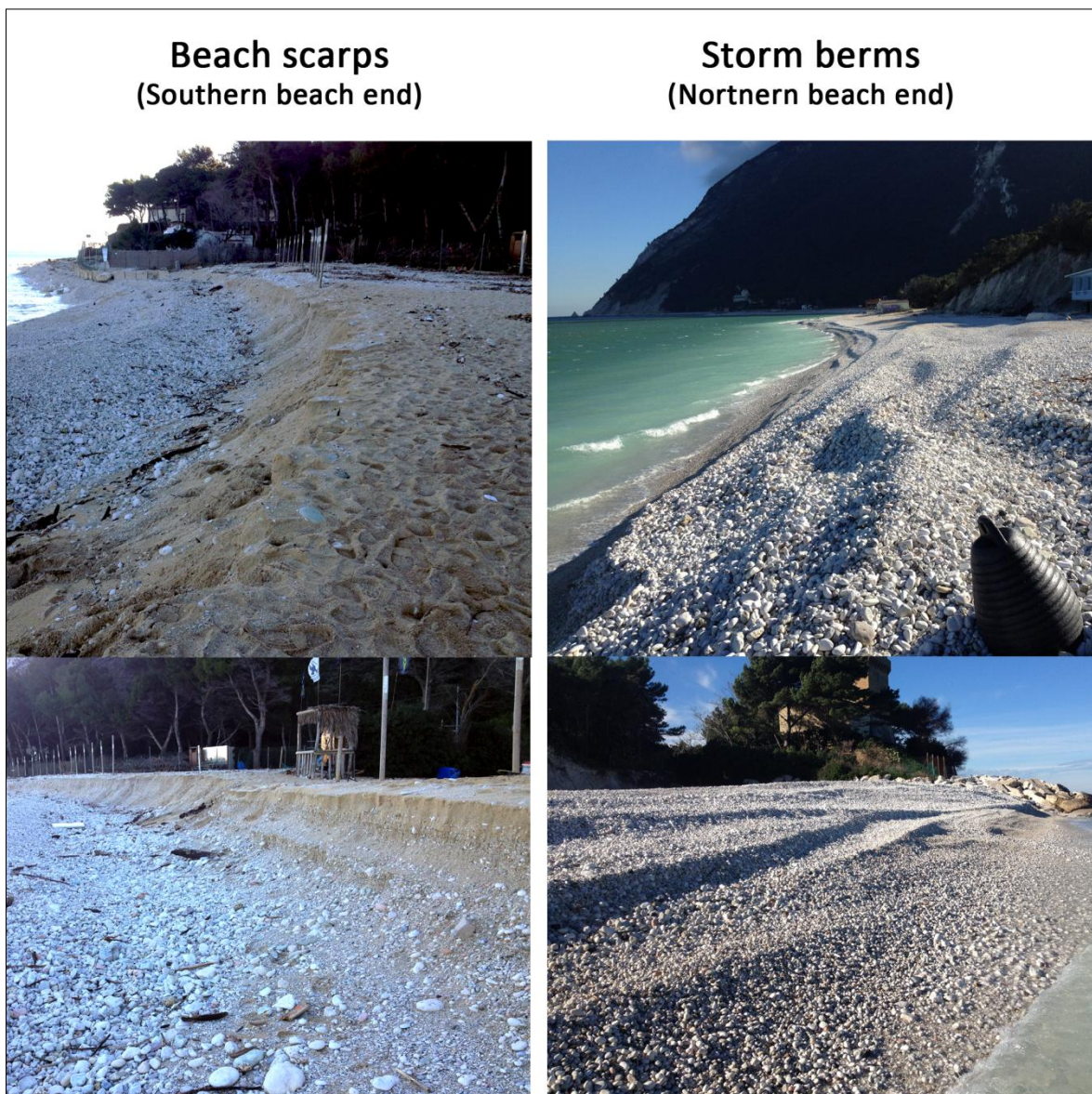


Figure 6-28. “Cut and fill” process observed in Portonovo beach after a storm approached from SE. On the left the “Cut” southern part of the beach is shown, with erosive scarps. On the right, the “Filled” northern beach area, with several tiers of storm berms deposited.

***7. Surface sediment  
variability (Portonovo  
beach)***

## 7.1 - One-year variability

The one year monitoring of surface sediment variability allowed to state that gravel sediments are prevalent over sandy ones in Portonovo beach (Figure 7-1), since the sand-gravel ratio resulted less than 0.5 in each sampling campaign (Figure 7-1 G). The sand-gravel ratio did not vary significantly during one year sampling period (Figure 7-1 G), that means the beach is approximately constituted by gravel for three-fourths and by sand for the remaining one-fourth. The most frequent grain size categories resulted granules and also fine and medium pebbles (Figure 7-1 A; B; C; D; E; F), while the less recurrent fractions were cobble and medium sand, which even appeared in some surveys (Figure 7-1 A; B; C; D; E; F). The largest variety of grain size classes was present on May 2012, while the smallest emerged from the first sampling on March 2012 (Figure 7-1 A), with only five grain size classes. The highest sand-gravel ratio was recorded in the second sampling campaign (April 2012, Figure 7-1 G) with a 32 % of sandy sediments of the whole (Figure 7-1 B). The lowest sand-gravel ratio percentage was experienced during the last sampling campaign, in April 2013 (Figure 7-1 G) with a scarce 16 % of sandy sediments (Figure 7-1 F).



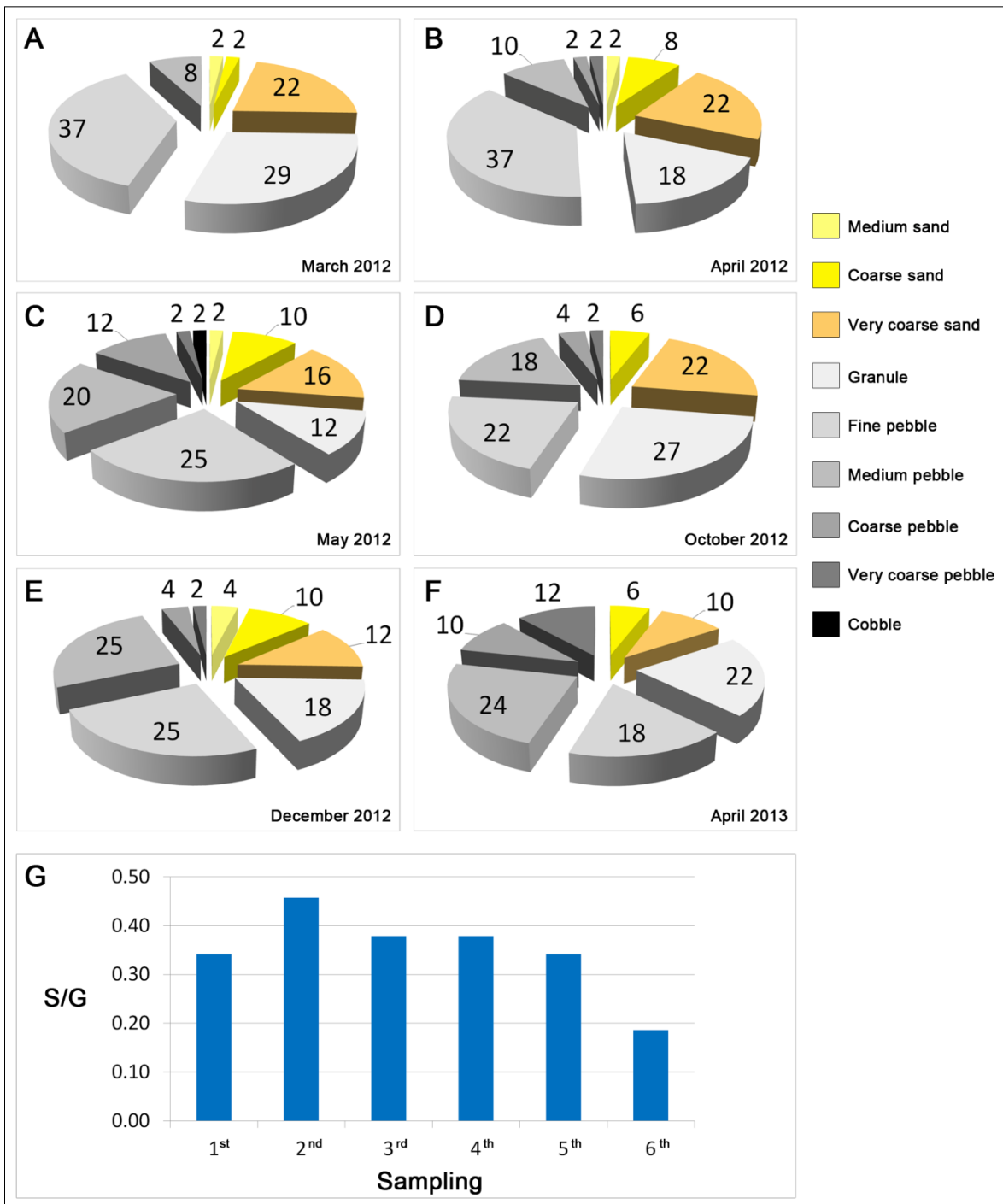


Figure 7-1. Surface sediment variability during one year span time. Pie charts with percentage values relative to: A) 1st sampling - March 2012; B) 2nd sampling - April 2012; C) 3rd sampling - May 2012; D) 4th sampling - October 2012; E) 5th sampling - December 2012; F) 6th sampling - April 2013. Sand-Gravel ratio variability during the six sampling campaigns (G).

## 7.2 - Analysis of sediment parameters: dispersion maps

### 7.2.1 - Mean diameter ( $M_z$ ) variability

The best analysis method to successfully discuss sediment patterns on a beach surface is to provide a spatial view of sediment variability. In Figure 7-2 the mean diameter ( $M_z$ ) variation on Portonovo beach is shown. Some recurrent characteristics can be accepted: the swash zone and the submerged beach are always constituted by gravel which is generally ranging from granules to fine or medium pebbles. The other frequently occurred circumstance is the presence of sandy stripes covering the landward limit of the backshore, both in the large southern portion of the beach and often leaned against the seawall that runs parallel to the shoreline in the central sector of the beach (Figure 7-2; Figure 2-1). A general seaward coarsening trend of the mean diameter is also recognizable mostly in each survey (Figure 7-2). A longshore coarsening of sediment is also clearly visible (Figure 7-2 A; C; F) as response of the last storm direction experienced before each sampling.

### 7.2.2 - Sorting ( $\sigma_1$ ) variability

The other relevant parameter which needs to be displayed is the sorting ( $\sigma_1$ ) variation of beach surface sediment. Being a mixed sand and gravel beach, the extremely heterogeneous sediment which constitutes the Portonovo beach reflects poor values of sorting. A general patchy aspect, with peaks of better and worse size sorting, characterizes the beach. There is no clear separation between areas well or moderately well sorted and parts worse sorted (value 1 discriminates these two categories, Figure 7-3). The beach normally looks like an irregular juxtaposition of poorly sorted and moderately sorted areas (Figure 7-3). The only case with a well spatially defined limit of sediment sorting was in the first sampling campaign of March 2012, where a net separation of sediment sorting ran along the shoreline (Figure 7-3 A). Poorly sorted sediments, covering the emerged beach, were clearly separated from better sorted which were lied in the submerged part. In the other surveys, bodies of sediments, from moderately to poor sorted, were stretching for maximum 100 m. Some peaks of very poor sorted sediment were present during the surveys of March 2012, April 2012 and December 2012 (i.e. Figure 7-3 A; B; E). Peaks of well sorted sediment emerged from the third and sixth sampling (i.e. May 2012 and April

2013, Figure 7-3 C; F) and the best sorting value was recorded always in the last sampling of April 2013 in an area, approximately 30 m long of very well sorted deposit (Figure 7-3 F).

### 7.2.3 - *Skewness ( $S_k$ ) variability*

Skewness ( $S_k$ ) values allowed to state if the sample grain size distribution was symmetrical or contained a surplus of coarse or fine sediments. Given the general moderate to poor sorting of sediment which characterised all the sampling campaigns (Figure 7-4); also the skewness values displayed a patchy variation throughout the beach (Figure 7-4). Some surveys were characterised by barely homogeneous tendencies, like the negative skewed values of December 2012 (5<sup>th</sup> sampling, Figure 7-4 E). In October 2012, the skewness values were the most uniform and fairly symmetrical of the entire monitored year (except for a strongly negative skewed area in the northern part of the beach, Figure 7-4 D). Nevertheless a patchy aspect seems to have distinguished each survey, with no cross-shore or longshore trends clearly recognizable. A more complete discussion of skewness value will be presented in the next paragraph comparing it with sorting and mean diameter of sediments and the wave characteristics recorded between the sampling campaigns.

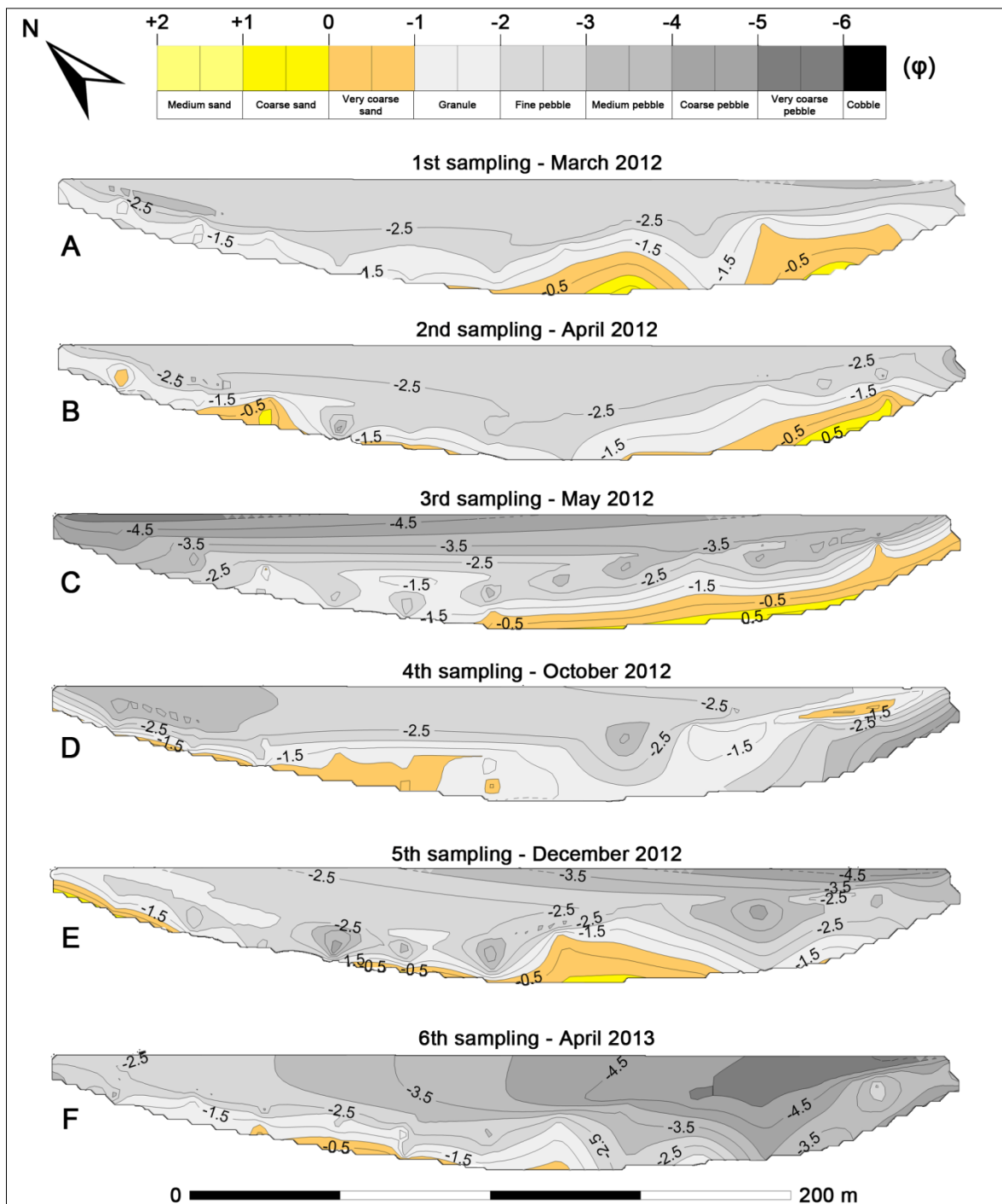


Figure 7-2. Mean diameter ( $M_z$ ) dispersion map through one year span time: all the six sampling campaigns are represented.

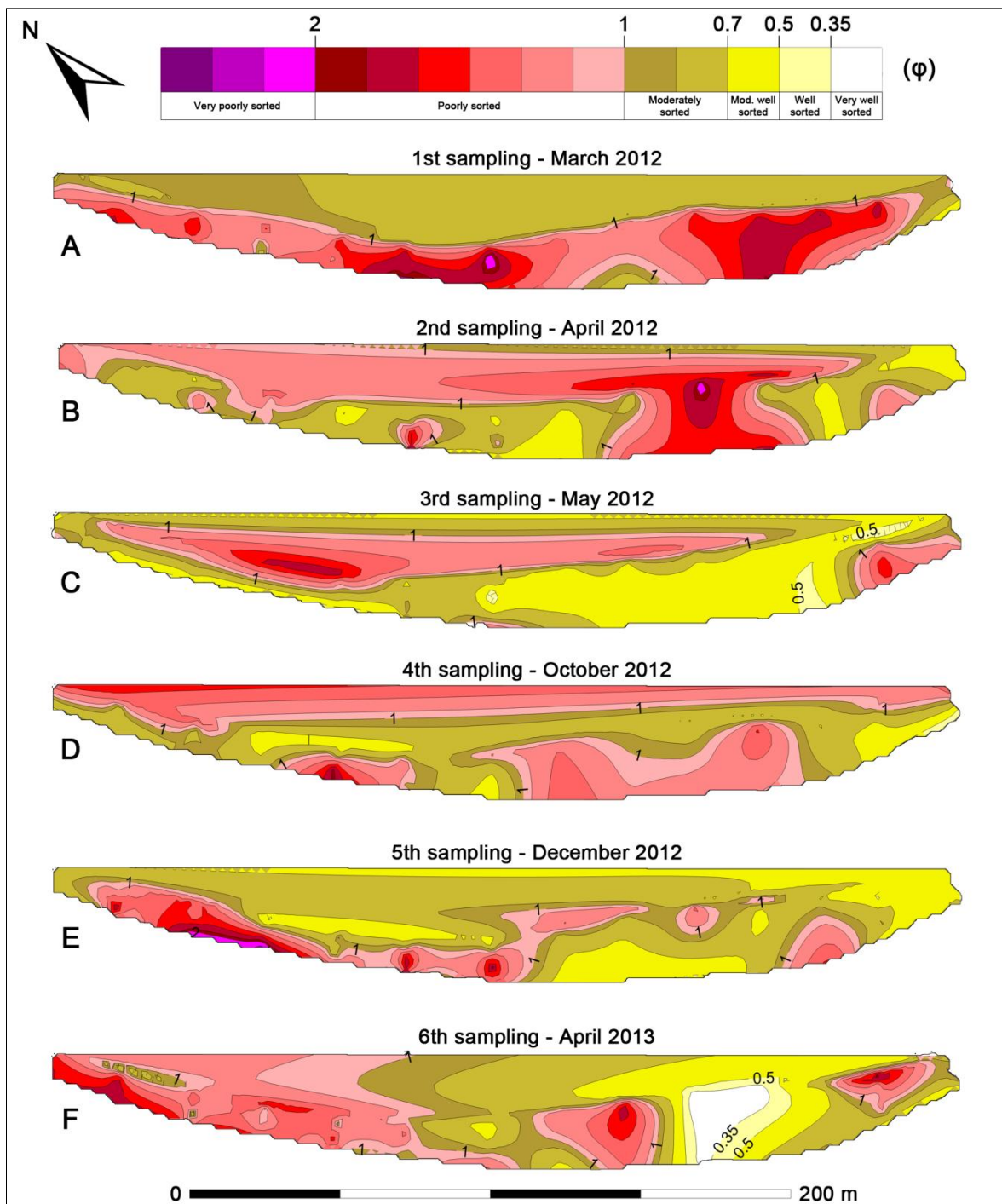


Figure 7-3. Sorting ( $\sigma_1$ ) dispersion map through one year span time: all the six sampling campaigns are represented.

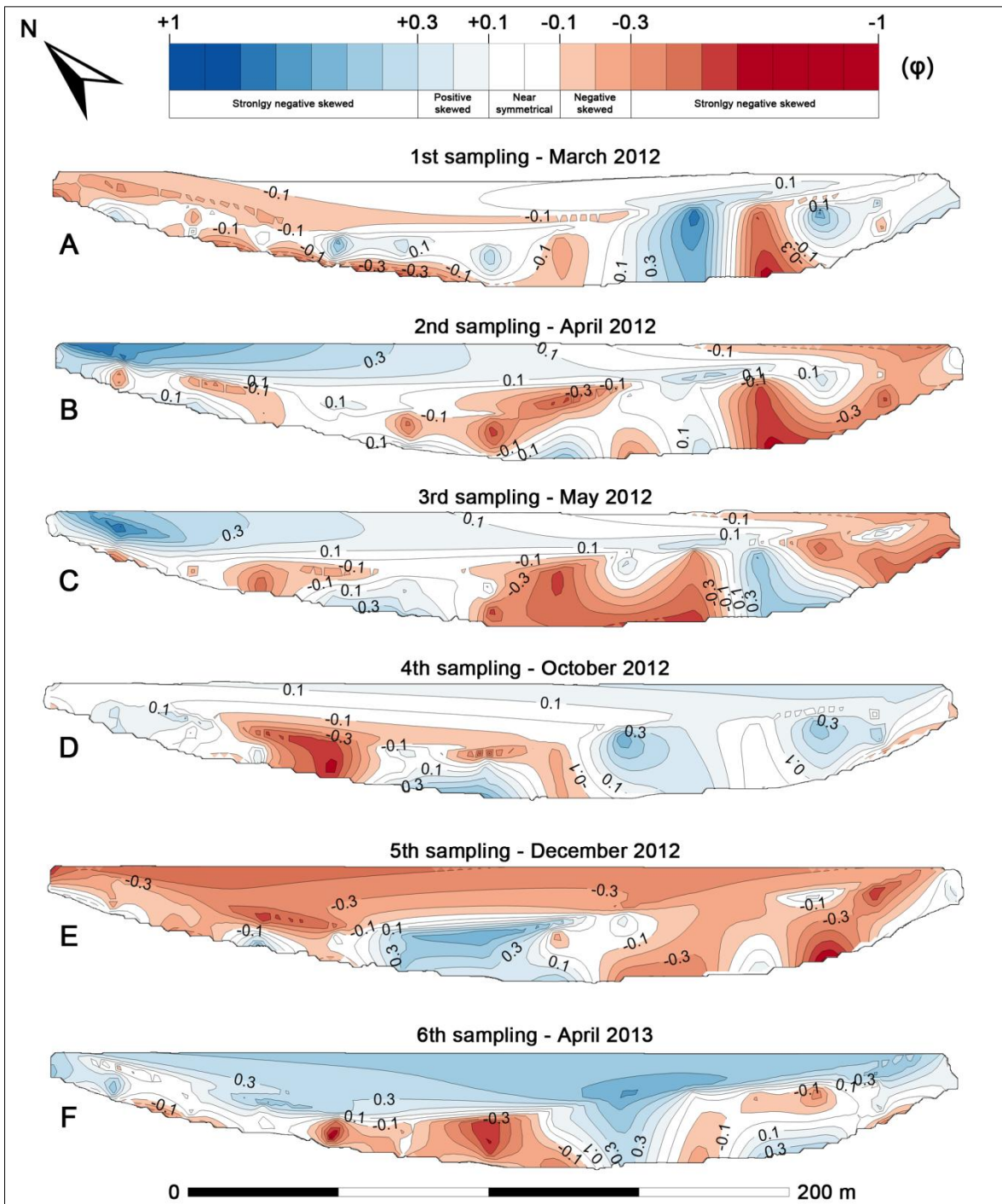


Figure 7-4. Skewness ( $S_k$ ) dispersion map through one year span time: all the six sampling campaigns are represented.

### 7.3 - Discussion

According to Kirk (1980), the most complex aspect on mixed beaches relates to sediment characteristics and the way to how sources and processes within the beach environment interact to distribute the material both across and along shore. Keeping in mind that just half of the Portonovo beach was sampled during one year time span (Figure 3-10 B), some good correspondences with what already accepted in literature can be found. The sediment pattern covering a beach surface is the result of a transport exerted by several hydrodynamic agents. In Portonovo beach, the forcing condition which controls the sediment and the topographic variability is the storm event. Hence is crucial to correlate the sediment parameters showed in the previous paragraphs with the wave conditions experienced from one survey to another. As already explained in Paragraph 3.7, storm events were identified according to the method of Armaroli et al. (2012) while the storm severity was calculated following the scale of Mendoza et al. (2011).

March 2012 was characterised by a fairly uniform surface sediment pattern. Coarser gravel (medium and coarse pebbles, Figure 7-2 A) was covering the swash zone while granules and medium pebbles were on the berm and in the lower part of the backshore. Sand was mainly located on the upper part of the backshore of the southern zone of the beach (Figure 7-2 A). This surface sediment configuration was produced by a general fair weather wave climate except for a weak storms approached from NE sectors (Table 7-1, see also Appendix B). Sorting was moderately sorted in the swash zone and poorly sorted on the backshore (Figure 7-2 A).

From March 2012 to April 2012 few storms occurred (highest  $H_s = 2.9$  m from NNE, Figure 7-5). The last storm of weak severity approached from ENE (Table 7-1; Figure 7-5). Storms of weak intensity did not produce any distinct downdrift coarsening at this stage (Figure 7-2 B). A grain size separation between the upper backshore limit (sandy) and the remaining part of the beach (gravelly) was recognizable (Figure 7-2 B). In terms of sorting, the worst sorted sediments were deposited in the submerged beach (Figure 7-3 B). The southern compartment, which was also distinguished by a strongly negative skewness values, confirm a bad sorting and a surplus of coarse sediments (Figure 7-4 B). A slightly sorting improvement was related to the entire emerged beach if compared to the same beach area of the previous survey (Figure 7-3 A; B). The most positive skewness values were indentified at the northern edge (Figure 7-4 B).

Sampling	Evidence of surface sediment pattern		Last storm occurred				
	Sediment size	Sorting	H <sub>s</sub> max (m)	Dir	Duration (h)	E (m <sup>2</sup> h)	Severity
Mar 2012	Sufficiently uniform (following to parallel stripes)	Net separation between swash zone (better sorted) and upper beach (worse sorted)	1.9	NNE	6.5	24	weak
Apr 2012	Swash zone and lower backshore covered by gravel	Worst selected sediment in the submerged beach	2	ENE	10	40	weak
May 2012	Downdrift coarsening (towards NW)	Downdrift worsening (towards NW)	2.1	ESE	8	35	weak
Oct 2012	Size coarsening affected the entire beach	Better sorting in the lower part of the backshore	-	-	-	-	-
Dec 2012	Downdrift coarsening (towards SE)	Downdrift worsening (towards SE)	2.4	NNW	50.5	291	significant
Apr 2013	Downdrift coarsening (towards SE)	No clear trend	2.2	ENE	9.5	45	weak

Table 7-1. Evidence of surface sediment patterns observed in Portonovo beach during the one year sampling. Characteristics of the last storm occurred before each sampling are shown from offshore wave data (ISPRA - Servizio Mareografico “Rete Ondametrica Nazionale”). Severity class of each storm is calculated according to the storm severity scale of Mendoza et al. (2011).



From April 2012 to May 2012 few storms occurred (highest  $H_s = 3.9$  m from NNW, Figure 7-5). The last storm occurred from ESE direction and classified as weak severity (Figure 7-5, Table 7-1) generated a coarsening of sediments at the northern end (increasing toward the limit, Figure 7-2 C). A clear separation between the upper backshore (sandy) and the remaining part of the beach (gravelly) was present, even though this situation characterised only the central and the southern part of the shore. On regard to the sediment sorting, the coarser sediment, that occupied the northern beach end, was also the worst sorted (Figure 7-3 C), also marked by a positive skewness which determines a fine sediment surplus presence in that area (Figure 7-4 C).

From May 2012 to October 2012 no storms occurred (Figure 7-5; Table 7-1; see also Appendix B). During the summer, an increase of grain size in the southern end (Figure 7-2 D) was combined to a general improvement in terms of sorting (moderately sorted, Figure 7-3 D) and skewness (from symmetrical to slightly negative or positive skewed, Figure 7-4 D) of the swash zone and the lower part of the backshore.

From October 2012 to December 2012, many storms occurred (highest  $H_s = 5.2$  m from ESE, *aka* “Halloween 2012 storm”, Figure 7-5). Last storm of significant severity approached from NNW direction (Figure 7-5; Table 7-1). One more time a downdrift coarsening of sediment was noticed in response to the last storm direction (i.e. storm direction from NNW and subsequent deposition of coarser sediments in the southern part of the beach, Figure 7-2 E). In terms of sorting and skewness, a deterioration of values took place, probably caused by storms that reworked the sediments reasonably well sorted during the previous summer (Figure 7-3 D; Figure 7-4 D).

From December 2012 to April 2013 many storms occurred (highest  $H_s = 5.3$  m from ESE, Figure 7-5; Table 7-1). Last storm of weak severity was driven from ENE direction (Table 7-1; Figure 7-5). Coarser grain size was again accumulated on the southern end of the beach due to the last storm direction (Figure 7-2 F). The beach was more gravelly than the five previous samplings (Figure 7-2 F compare to Figure 7-2 A; B; C; D; E). The deposits conveyed to the southern part of the beach were characterized by areas well and very well sorted and others poorly sorted (Figure 7-3 F). Skewness values were barely good except for the central sector of the backshore (Figure 7-4 F).

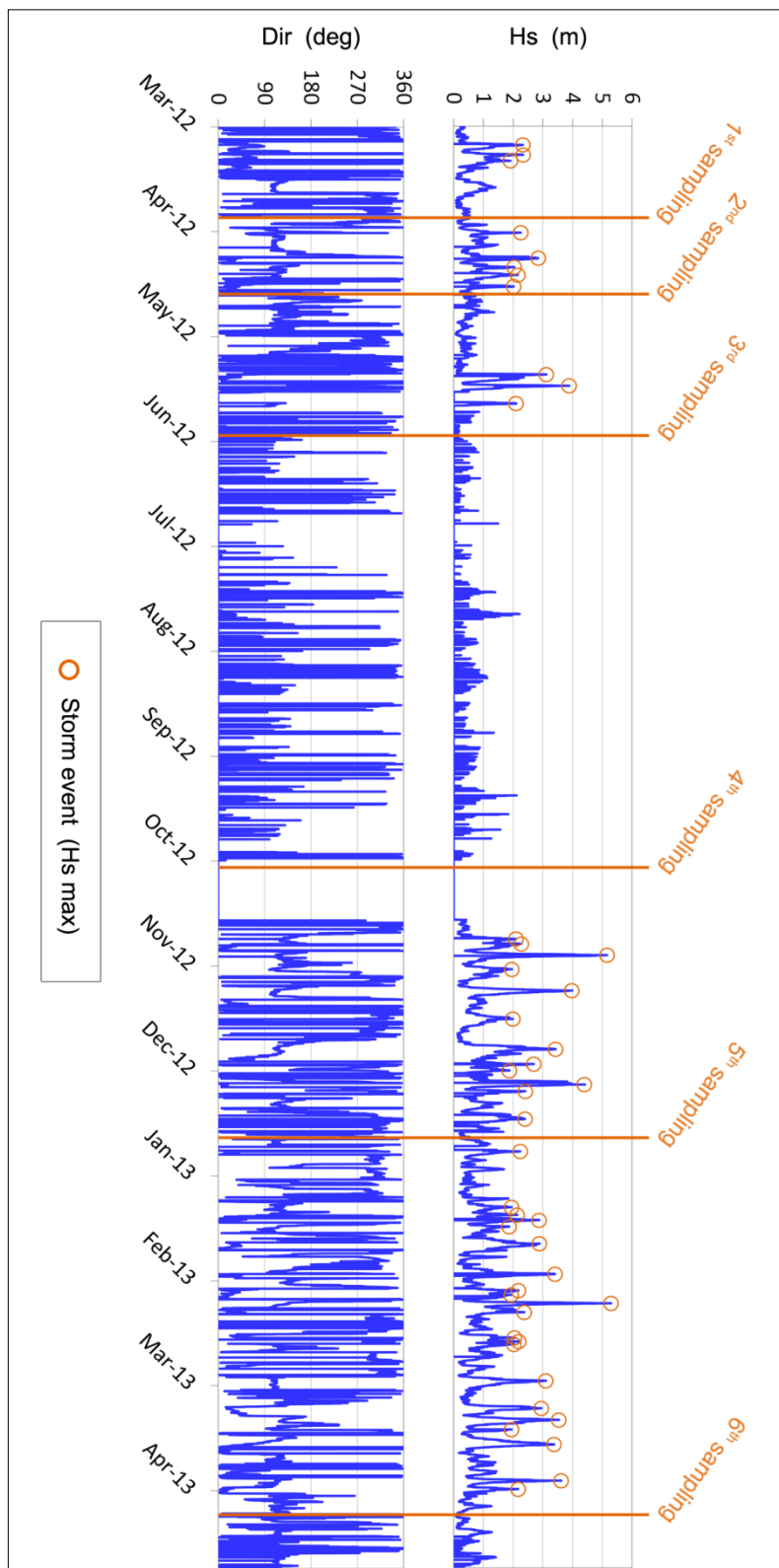


Figure 7-5. Significant wave height ( $H_s$ ) and wave direction (Dir) recorded by the Ancona offshore buoy (ISPRA - Servizio Mareografico “Rete Ondametrica Nazionale”) throughout the entire period of samplings.

In a mixed sand-gravel beach longshore transport directions could be identified with difficulty among large local fluctuations in size and sorting values by use of average trends (McLean and Kirk, 1969). Complex spatial patterns usually characterize sediments of mixed beaches in terms of sorting and size (McLean, 1970). Analyzing the dispersion maps of the previous paragraph (Figure 7-2; Figure 7-3; Figure 7-4), these authors were right, but some recurrent aspects can be highlighted. Firstly, a downdrift coarsening of sediments in response to storms was recognized in every sampling campaign, and in particular this happened in accordance to the last storm direction. Carr (1969) already noted this behavior in Chesil Beach (UK), by means of a repeated sampling in one year span time. According to the author, coarser material is stranded on the backshore by longshore transport under severe storm conditions. Carr (1971) stated that there is a longshore size sorting achieved by the vector imparted by the direction of wave approach. Furthermore, it is fairly usual to find the coarsest material towards the beach ends (McLean, 1970). To highlight this finding, a qualitative example is represented in Figure 7-6 where is shown the same beach end after two storms approached from opposite directions (eroded sandy portion, Figure 7-6 B and large pebble accumulation, Figure 7-6 C of the same beach portion).

The most clear aspect resulted by sediment analyses is the evident surface pattern left by the storms. Watt et al. (2005), studying the surface distribution of sediments across three mixed beaches, already noted that higher wave energy conditions (wave height higher than 2 m) produce distinct surface sediment grain size patterns. According to the authors finer sediments can be commonly found on the upper beach after storms while coarser ones accumulate in the lower part of it. A similar behavior was found by Sarti and Bertoni (2007) in some mixed beaches of northern Tuscany. In Portonovo a clear sediment diversification can be made mostly longshore rather than cross-shore. Coarse sediment usually was piled up on the upper beach in response of the last storm direction. A downdrift coarsening of sediment was observed after each storm.

Secondary, it is the last storm, even though not the most energetic, to control the sediment pattern all over the beach surface. During phases of fair-weather, wave action tend to improve the sorting and the skewness values of sediments covering the swash zone and the lower part of the backshore; this is also combined to a general coarsening of sediments occupying those areas. According to Gleason and Hardcastle (1973) sorting process is to ascribe to small, low frequency waves, which leave coarser material on the surface and

provide a readily-available population for longshore drift that takes place with higher energy conditions.

Periods of fair weather or without severe storm occurring develop a striped pattern of surface sediments. Stripes of different grain size run parallel to the shoreline: with the swash zone and the fair-weather berm normally characterized by gravel (granules or fine pebbles) and scattered non continuous stripes of sand that cover the landward part of the backshore (Figure 7-2 A, B, D). During these periods of low to moderate wave energy a better sorting of sediments which cover the swash zone and the lower part of the backshore also occurs.

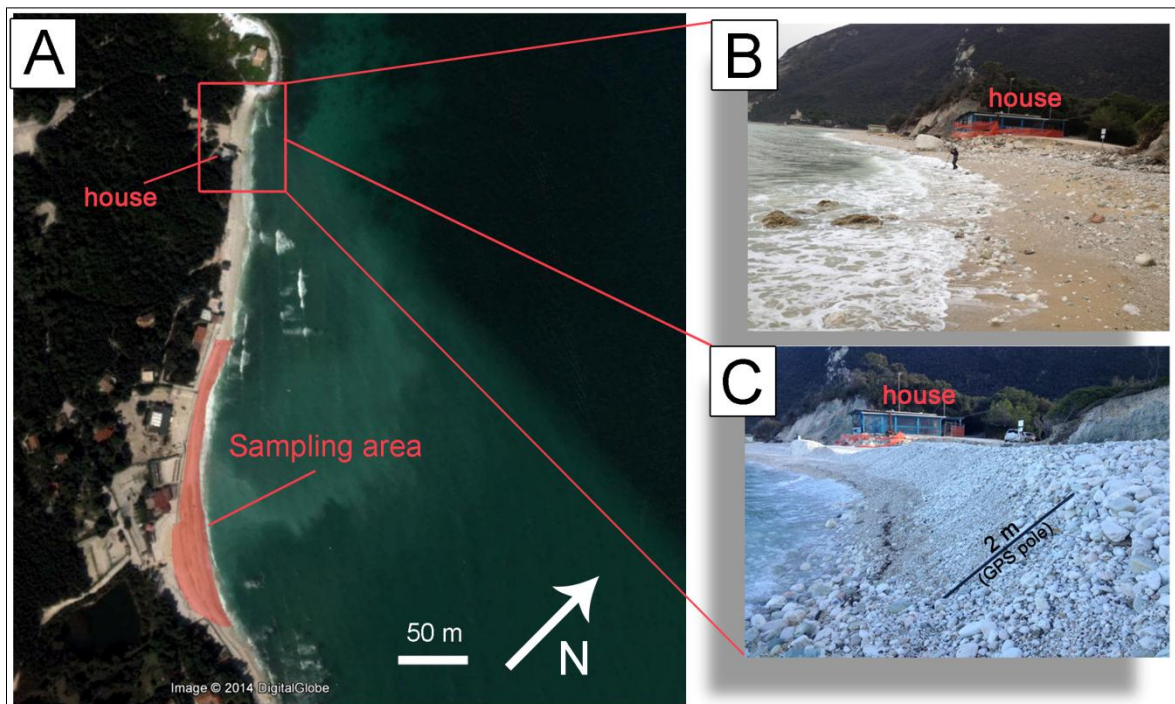


Figure 7-6. Representation of the same beach end (northern) after a storm approached from NE direction in December 2012 (B) and a storm reached from SE direction in March 2013 (C). In A is shown the location where the pictures were taken relatively to the sampling area.

***8. Considerations on fill  
material characteristics for  
nourishment purposes***

## 8.1 - Italian and worldwide overview on gravel nourishment projects

Beach nourishment is a “soft” defensive practice consisting of refilling beach sectors, in advanced state of erosion, with material of different nature (i.e. beach sand, beach gravel, off-shore deposits, alluvial material, quarry waste, etc.). It is considered a “soft” approach of coastal protection because usually any construction of hard structure is provided. Coarse grained and mixed beaches, although they are quite common at high latitudes or in proximity to high coasts, have been less studied than the sandy ones. In the last 15 years, the scientific interest on these beaches is growth due to nourishment practices realized to contrast erosive processes also in these kind of beaches (Takagi et al., 2000; Masselink and Hughes, 2003; Cammelli et al., 2006; Kumada et al., 2010; Noshi et al., 2011). Gravel is increasingly being used for beach nourishment (e.g., Moses and Williams, 2009); therefore, there is a real need for field investigations on gravel beach morphodynamics to increase our understanding of these coastal systems (Masselink et al., 2010). The Marche Region was one of the first local municipalities in Italy to adopt coarse material to replenish sector of the coast. Some beaches of Conero Headland were involved in replenishment schemes: Portonovo, where 18500 m<sup>3</sup> of gravel and pebbles were transported mainly on the western side of the town between 2006 and 2011 (personal communication by the Regione Marche); Sirolo (San Michele - Sassi Neri beach), where 156000 m<sup>3</sup> were transferred at different stages by dredges between 2009 and 2010 (Harley et al., 2014); Numana (Marcelli beach), which represented the largest project with 225000 m<sup>3</sup> of gravel deposited between 2009 and 2010 (personal communication by the Regione Marche). Other cases can be found along the Italian peninsula, e.g. several sectors of Marina di Pisa shore (Cammelli et al., 2006; Bertoni and Sarti, 2009), Barbarossa sector included, where the gravelly fill material was placed on the native sandy beach. Some other examples from Italy come from Liguria region. Interesting is the case of Bregeggi where a gravel refill carried out during the 1960’s created a new beach (Sirene beach) at the cliff toe where the beach was never present naturally (Fierro et al., 2010). Several examples can also be found worldwide: in Japan many monitoring studies of replenished beaches have been produced (Takagi et al., 2000; Kumada et al., 2010; Noshi et al., 2011); in France, especially in the Les Bas-Champes area (since 1969), in the Gulf of Lion in 1984 (Hanson et al., 2002) or recently in Nice (Anthony et al., 2011); in New Zealand, on Washdyke beach where a nourishment project was monitored for five years (Kirk, 1992); in Ireland, in the Dublin area during the 1990s (Hanson et al., 2002); in South-West of England, nearby Dungeness, nourishment projects with shingle material were realised to

prevent the local nuclear power station from flooding damage (Maddrell, 1996). UK is certainly the leader country since the first nourishment works with shingle material were realised in the 1950s (McFarland et al., 1995; Whitcombe 1996). It was calculated that approximately 4.25M m<sup>3</sup> of gravel (about 170.000 m<sup>3</sup> per year) were transferred along the England coastline between 1970 and 1994 (Hanson et al., 2002). The success of refill schemes on beaches led to a significant growth demand of gravel for future projects which was estimated for the period 1995-2015 in 209M m<sup>3</sup> to refill Wales and England coasts (Hanson et al., 2002). Beyond the classical purposes of beach protection, some other objectives can be related to nourishment projects. Many scientists have focused on the environmental impact of beach feeding, dealing with the ecological consequences for fauna habitats populating beaches (Nordstrom, 2005; Jackson et al., 2007; 2010) or with the slope stability of cliffs subjected to erosive processes under storm conditions (Harley et al., 2014). Others remarkable objectives of nourishment projects could be tourism improvement and consolidation or maintenance of both natural and recreational values (the cases of Conero beaches and Marina di Pisa).

## **8.2 - Which fill material?**

Sediment characteristics and sources are the key components of nourishment projects for several reasons. First of all, nourishment project requires periodic maintenance that means to plan all the future refill and monitoring of feed material (transport, abrasion rate, loss rate) and mostly to find an adequate sediment source. The most accepted advantage of nourishment practice, which allows to define nourishment as a “soft” protection method, is to refill beach portions with natural sediment. All beaches have specific sediment characteristics which the fill material should meet, such as size, colour, roundness, sorting, mineralogical composition, etc. Furthermore a mixed beach, as shown from the results of Chapter 7, is not a homogeneous texture of sediments and varies several times during the year after each storm. Find a clear trend of particles characteristics valid all over the beach seems to be impracticable. Trying to fulfil all those requirements makes the research of fill material a hard challenge. The Regione Marche for its nourishment project in Portonovo provided a refill material as close as possible to the native sediment (Table 8-1; Figure 8-1). The fill material was extracted from inland quarries on alluvial deposits (mainly limestone) then was subjected to fragmentation and washing stages and finally was divided

in proper size percentages (not mono-dimensional) in order to obtain particles of similar size to the beach sediment (informal communication by the Regione Marche, Table 8-1; Figure 8-1). Washing and sizing phases are essential to reject undesirable clay and finer particles (Smith and Collis, 1993).

	Source	Mineralogical composition	Size	Roundness	Shape (Zingg diagram)	Note
<b>Native material</b>	Cliff erosion	Limestone and marls	Medium sand to cobble  (1 to 256 mm)	Well rounded	Disc and spheres (mainly)	-
<b>Nourishment material</b>	Inland quarries on alluvial deposits	90% Limestone	Fine pebble to cobble  (4 to 100 mm)	Subangular	Disc	Washed before deposition

Table 8-1 - Comparison between native sediment and fill material characteristics for Portonovo beach.



Figure 8-1- Comparison between a fill nourishment material adopted in Portonovo beach (A) and the native natural sediment (B).



Select the appropriate material is crucial for gravel nourishment project since is not unusual to observe problems related to fill material. For examples cliffing issues could easily appear on replenished mixed beaches if an overestimated quantity of sand is included in the supply (She et al., 2006; Ciavola and Castiglione, 2009). According to She et al. (2006) even when the fill material is quite similar to the native one, the sand fraction tends to accumulate on the backshore leading to the cliff development in correspondence of the high water mark. In Portonovo it is quite common to find sand stripes on the upper part of the backshore even though cliffing phenomena were never seen during the monitoring period. When the sand percentage is greater than 30 % the hydraulic performance of a mixed sand and gravel beach become similar to a pure sandy beach and the advantage of a coarse grained beach (see *permeability*) is completely lost (López de San Román-Blanco, 2006; She et al., 2006). According to Ibrahim et al., (2006) the location of the water level in the beach profile has an important role in determining erosion or accretion processes and its position is surely depending from the size of sediments (sand versus gravel) and this is another reason why recharge material should be similar to the natural one.

Different from Portonovo was the case of Barbarossa beach in Marina di Pisa where the native sandy beach profile was covered by marble pebbles and cobbles (60 to 100 mm in diameter) derived from quarry waste. In this case local authorities could prevent to fulfil specific requirements to meet the natural sediment of the beach. Gray marble was the selected material for these replenishments given its large availability from local quarries and its relative limited costs. Furthermore, gray marble resulted more resistant to abrasion relative to the white type (Nordstrom et al., 2008). A net separation between native sandy sediment and highly coarser fill material can cause the incorporation of sand into the gravel matrix, combined, in places, with removal of the larger particles by concessionaires causes them to lose their distinctiveness rapidly (Nordstrom et al., 2008). Whitcombe (1996) observed that artificially replenished gravel beaches do not necessarily exhibit the same characteristics of a natural gravel beaches. These kind of beaches tend to be more compact (McFarland et al., 1995), process that was also noted at Barbarossa beach from time to time, and the consequent lack of permeability of fill material may not respond to wave attack in the same way of a natural gravel beach (Whitcombe, 1996). Some laboratory tests have been conducted in order to better understand the behavior of fill material in response to the wave action even in presence of protective structures (D'Elisio et al., 2008; Van Wellen et al., 1999b), trying to predict the artificial replenished beach profile with

available formulae and models (Van der Meer, 1988; Powell, 1990; Lorang, 2002). To analyse the fill material displacement a monitoring study is always recommended. Coarser gravel is less mobile than finer one, but unfortunately really coarse gravel (i.e. pebbles and cobbles) are usually in short supply (Williams and Moses, 2005). Cases of nourishment project with gravel are shown in Table 8-2 where is highlighted if the recharge material had met the native one from case to case. Only few cases are shown since data collected are often incomplete or fragmentary. In many cases gravel replenishment is used to create beaches where these were not existent previously. When the recharge material is quite similar to the native one in term of size, little consideration is usually given to particle shape.

Site	Fill material				Compatible with native material
	Source	Particle size	Particle shape - Roundness	Lithology	
<u>Portonovo</u> (Italy)	Quarry on alluvial material	4 - 100 mm (M <sub>z</sub> )	Disc Subangular	Limestone	Yes
<u>Marina di Pisa</u> (Italy)	Quarry waste	60 - 100 mm (M <sub>z</sub> )	Disc Subangular	Grey marble	No (sandy beach or not existent before)
Sirolo (Italy)	Quarry on alluvial material	8 mm (D <sub>50</sub> )	-	Limestone	Yes
Numana (Italy)	Quarry on alluvial material	6 mm (D <sub>50</sub> )	-	Limestone	Yes
Ancona (Italy)	Quarry on alluvial material	60 mm (D <sub>50</sub> )	-	-	No (beach not existent before)

Bergeggi (Italy)	Waste material from construction	-	-	-	No (beach not existent before)
Fuji coast (Japan)	“Crushed stones”	50 - 150 mm (M <sub>z</sub> )	“Angular shape”	-	-
Saltdean and Telscombe (U.K.)	Marine deposits	Pebbles	Subangular to subrounded	Flint	Yes

Table 8-2. Fill material characteristics adopted in some Italian and worldwide nourishment projects.

### 8.2.1 - Recommendations on fill material for the case studies.

In Portonovo beach, the ideal fill material for a nourishment project should be comprised of pebbles with a spherical shape. During short fair-weather periods sediment characteristics can exert a notable influence on particle transport (Chapter 5), the same has not been demonstrated under severe storm conditions. It fairly clear that spherical and well rounded material is not easy to find, but in natural offshore deposits or after long laboratory treatment, keeping in mind that these two alternatives are highly expensive (Nunny and Chillingworth, 1986; Smith and Collis, 1993). According to the results of Chapter 5, disc shaped pebbles can reach larger displacement even though the spherical pebbles are more dynamic, therefore the spherical shape would be preferred for pebble nourishment. A bulk of spherical pebbles would be starting to move before and in a more homogeneous way than disc shapes. Furthermore, thanks to their less mobility, disc could be transported towards the beach limits during storm events and be resumed less easily rather than spherical pebbles once they reach the upper beach profile. An ideal beach comprised of spherical pebbles would always kept in moving with no “permanent” erosive or augmentative areas that could be more frequent adopting discoidal pebbles. Regarding the size to adopt for pebble replenishment, a dimension comprised between -5.5 and -6.5 phi (“Big” size, very coarse pebble and small cobbles according to the Udden-Wentworth grain size scale, 48 to 96 mm) is to avoid given its low mobility. “Big”-sized pebbles could

be used to build step feature or anything that would supposed to be more stable. “Medium” and “Small”-sized pebbles (coarse and very coarse pebbles, -4.5 to -5.5 phi or 24 to 48 mm according to the Udden-Wentworth grain size scale) should be preferred for feeding the swash zone and the emerged beach in order to keep the system free to interact actively with several wave conditions. Furthermore, the use of sand as part of fill material is not recommended: cliffing issues may could occur even though sandy fraction is approximately one fourth of the whole sediment grain size constituting the beach. Regarding the beach studied in Marina di Pisa (Barbarossa sector) there are less information about the influence of pebble characteristics on transport. As confirmed by the previous paragraph, local authorities usually give little consideration to particle shape in their nourishment projects. This can be surely overcome by the significant abrasion rates which were also measured in some of the cases listed in Table 8-2. Bertoni et al. 2012a measured a rate of abrasion of 8.5 % in two months at Barbarossa sector. A rate of abrasion of 2.4 % was observed in a close beach even in Marina di Pisa (Cella 7) in the same time span. Cella 7 was part of the same recharging project of Barbarossa beach and was built with the same material used to recharge Barbarossa. The smaller rate of abrasion was mainly due to the presence of both longshore and cross-shore protecting the beach (Bertoni et al., 2012a). Is not clear if change of shape could occur, even though a significant increase in roundness was experienced in both cases studied at Marina di Pisa (Bertoni et al., 2012a). Studies dealing with rate of abrasion should be conceived even in Portonovo given the high rate of abrasion experienced by other authors on limestone pebbles. Dornbush et al. (2002) measured a mean weight loss over a period of 10 months of 0.36% for quartzite pebbles compared with 1.44% for limestones. Some authors cyclically remark the loss of nourishment gravel after a certain time since the end of replenishment (Takagi et al., 2000; Maddrell, 1996; Limber and Warren, 2006). Loss of nourishment material in case of pebble nourishment could also be related to loss of volume due abrasion processes. In other cases additional material does not produces significant beach enlargement. Harley et al. (2014) focused on the response of a gravel nourishment project to beach rotation processes in a beach close to Portonovo (Sirolo, San Michele - Sassi Neri). Despite the additional gravel recharge, only moderate increases in the average dry beach width and dry beach area were observed by the authors. Since shoreline rotation affect also Portonovo beach (see Paragraph 6.2) and pocket beaches in general, another aspect to take in account surely is beach rotation process. Given the issues and the actual processes that may occur on replenishment material, is always recommended the use of natural sediment which should meet as more as possible the native one. Furthermore a

better understanding of sediment characteristics and its relationship with hydrodynamics is crucial for future nourishment purposes together with a long term monitoring on how these characteristics can vary over time.

## ***9. Conclusions***

The study here presented is an original contribution to the understanding of influence of pebble characteristics on sediment transport. It also leads to a more complete interpretation of mixed beaches response to different wave conditions in terms of grain size and topographic variability.

Under low energy conditions gravel and pebbles need just a small quantity of energy to be destabilized: in both experiments (Marina di Pisa and the first Portonovo experiment) swash action provided that energy, considering that the run-up levels exceeded the maximum tracer elevation for almost the entire duration of the experiments. Once that threshold is reached, marked pebbles can be displaced away from the injection point even though wave motion and swash processes are at minimum.

Discs can cover greater distances than spheres but are less dynamic. Once lifted and shifted by swash flows, the discs can travel long paths, reaching a stable location characterized by feeble forces under low wave energy conditions (e.g., the back side of the fair-weather berm or slope break between the swash zone and the beach step). On the other hand the threshold to initiate movement for spheres is lower so it is more difficult for them to find more stable position on beach profile.

"Big"-sized pebbles (-5.5 to -6.5 phi) are less dynamic compared to the finer classes ("Medium", -5 to -5.5 phi; "Small", -4.5 to -5 phi). They are not able to reach the back of the fair-weather berm if initially released at the step crest, but they can be easily dragged down to the swash or step zone if released on the berm crest, even under very low energy conditions. Nevertheless the "Big"-sized spheres resulted slight more dynamic than discs of the same size.

There is no statistical relationship between the shape of pebbles and their displacements, although different shapes respond to different forces. "Big"-sized sediments had a similar behaviour in both experiments, which was significantly different from that of the "Medium" and "Small" classes. Further investigations focusing on particle shape are needed to identify the possible primary factors that control pebble movement (e.g., surface where displacement takes place, beach slope, permeability in the swash zone, wave breakers, swash velocities, etc.).

Very low and steady energy conditions facilitate pebble cross-shore and offshore movement rather than longshore. In that case, beach exposure, beach morphology and water level fluctuations play a prevalent role on pebble movement than wave height. A slight increase in wave height produces a predominant longshore transport characterized by non-negligible displacements. Furthermore, low to moderate energy conditions trigger some trend displacements based on pebble shape: discs end up on the back side of the fair-weather berm; spheres keep on moving throughout the swash zone driven by swash grazing.

Actual measurements of swash velocities, which are able to initiate pebble movement, should be obtained in order to improve threshold velocity formulae, which currently do not involve any shape parameter. It is believed that shape can be a discriminating factor for coarse and very coarse pebble transport (from 16 to 64 mm according to Udden-Wentworth grain size scale) at least under low energy conditions.

Portonovo beach seemed to be a close system regarding at least pebble transport, as no tracers were ever found beyond the longshore beach limits and not even offshore. Tracer loss is mainly to ascribe to burial by other sediments and is also related to the limited detection range of RFID antenna (about 40 cm).

The central sector of the beach is a transfer zone for pebble motion during storms. No tracers were found here during any recovery; the most was always found at beach edges. Weak storms combined to swash grazing are able to move pebbles and cobbles alongshore with great displacements (mean displacement 190 m; max 445 m; min 15 m ; 2 months after the injection of the first experiment at Portonovo).

The central sector is also the narrowest sector and less affected by morphological changes. The southern beach edge, in its upper part, was never reached by storm waves, thus is the only sector never showing morphological changes. A different beach exposure to wave action of the southern embayment was observed by means of a mixing depth evaluation. This was also confirmed by shorter displacements always experienced in this part of the beach.

Beach rotation is a common phenomenon in Portonovo. The system seems to act like a pocket beach: erosion (defined with scarps) and accretion areas (defined with storm berms)



change in accordance to the most frequent direction of each storm (SE “Scirocco” and NNE “Bora”). The central area of the beach represents the pivotal point for beach rotation.

Despite the high grain size heterogeneity, at Portonovo the sediment pattern is the result of the last storm direction: storms are the forcing conditions controlling the beach surface sediment variability. Evident downdrift coarsening of sediments in response to storms normally occurs. In the long term, longshore transport is more clearly visible than cross-shore transport, according to grain size locations on the beach and to the long term tracer recoveries.

Periods of fair weather (with at least very weak storms) develop a striped pattern of surface sediments. Stripes of different grain size run parallel to the shoreline: the swash zone and the lower part of the backshore increase their sediment size becoming gravelly (granules or fine pebbles) and better sorted, while scattered and non continuous stripes of sand cover the landward and the upper part of the backshore. Storm waves produce weak values of sorting and skewness.

The fill material for nourishment purposes should fit as best as possible the native sediment, evaluating costs of material supply and its possible treatment to make it compatible.

At Marina di Pisa the material used for beach refill was sufficiently good: covering the natural sandy backshore with pebbles and cobbles did not prevent users from going to the beach. Deeper studies on coarse sediment abrasion rate are needed for better assessment on replenishment material and to better estimate contingent loss of volume in the refill material.

At Portonovo beach, the material provided by local authorities for nourishment projects is quite compatible with the native one. In order to have an even more compatible material the use of spherical pebbles is suggested, to take advantage of their higher dynamicity relative to the discs. A size comprised between -4.5 and -5.5 phi (24 to 48 mm) should be preferred since spheres of that size are more dynamic than discs and tend to prevent the formation of permanent areas in erosion or in strong accumulation on the beach.

# *References*

- Allan, J.C., Hart, R., Tranquilli, J.V., 2006. The use of Passive Integrated Transponder (PIT) tags to trace cobble transport in a mixed sand and-gravel beach on the high-energy Oregon coast, USA. *Marine Geology* 232, 63–86.
- Anthony, E.J., Cohen, O., Sabatier, F., 2011. Chronic offshore loss of nourishment on Nice beach, French Riviera: a case of overnourishment of a steep beach. *Coastal Engineering* 58, 374-383.
- Armaroli, C., Ciavola, P., Perini, L., Calabrese, L., Lorito, S., Valentini, A., Masina, M., 2012. Critical storm thresholds for significant morphological changes and damage along the Emilia-Romagna coastline, Italy. *Geomorphology* 143-144, 34-51.
- Austin, M.J., Masselink, G., Russell, P.E., Turner, I.L., Blenkinsopp, C.E., 2011. Alongshore fluid motions in the swash zone of a sandy and gravel beach. *Coastal Engineering*, 58, 690–705.
- Battjes, J.A., 1974. Surf similarity. *Proceedings of 14th Conference of Coastal Engineering*, ASCE, Copenhagen, 466–480.
- Bauer, B.O., Allen, J.R., 1995. Beach steps: an evolutionary perspective. *Marine Geology*, 123, 143–166.
- Benavente, J., Gracia, F.J., Anfuso G., Lopez-Aguayo, F., 2005. Temporal assessment of sediment transport from beach nourishments by using foraminifera as natural tracers. *Coastal Engineering*, 52, 205-219.
- Bencivenga, M., Nardone, G., Ruggiero, F., Calore, D., 2012. The Italian data buoy network (RON). *Proc. Advances in Fluid Mechanics IX*, 321-332.
- Benelli, G., Pozzebon, A., Raguseo, G., Bertoni, D., Sarti, G., 2009. An RFID based system for the underwater tracking of pebbles on artificial coarse beaches. *Proceedings of the 3rd International Conference on Sensor Technologies and Applications*, Athens, 294–299.

Benelli, G., Panzardi, E., Pozzebon, A., Bertoni, D., Sarti, G. 2011. An analysis on the use of LF RFID for the tracking of different typologies of pebbles on beaches. 2011 IEEE International Conference on RFID-Technologies and Applications, 426-431.

Benelli, G., Pozzebon, A., Bertoni D., Sarti, G. 2012. An RFID-based toolbox for the study of under and outside-water movement of pebbles on coarse-grained beaches. *IEEE Journal of Selected Topics in Applied Earth Observations and Remote Sensing*, 5, 1474-1482.

Bertoni, D., Sarti, G., Benelli, G., Pozzebon, A., Raguseo, G., 2010. Radio Frequency Identification (RFID) technology applied to the definition of underwater and subaerial coarse sediment movement. *Sedimentary Geology*, 228, 140-150.

Bertoni, D., Sarti, G., 2011. On the profile evolution of three artificial pebble beaches at Marina di Pisa, Italy. *Geomorphology* 130, 244–254.

Bertoni, D., Sarti, G., Benelli, G., Pozzebon, A., 2012a. In situ abrasion of marked pebbles on two coarse clastic beaches (Marina di Pisa, Italy). *Italian Journal of Geoscience*, 131, 205-214.

Bertoni, D., Sarti, G., Benelli, G., Pozzebon, A., Raguseo, G., 2012b. Transport trajectories of “smart” pebbles on an artificial coarse-grained beach at Marina di Pisa (Italy): Implications for beach morphodynamics. *Marine Geology* 291-294, 227-235.

Bertoni, D., Grottoli, E., Ciavola, P., Sarti, G., Benelli, G., Pozzebon, A., 2013. On the displacement of marked pebbles on two coarse-clastic beaches during short fair-weather periods (Marina di Pisa and Portonovo, Italy). *GeoMarine Letters*, 33, 463-476.

Bluck, B.J., 1967. Sedimentation of beach gravels: examples from South Wales. *Journal of Sedimentary Petrology*, 37, 128-156.

Bluck, B.J., 1999. Clast assembling, bed forms and structure in gravel beaches. *Trans. Roy. Soc. Edinb. Earth Sci.* 89, 291–323.

Bluck, B.J., 2011. Structure of gravel beaches and their relationship to tidal range. *Sedimentology* 58, 994-1006.

Brambati, A., Bregant, D., Lenardon, G., Stolfa, D., 1973. Transport and sedimentation in the Adriatic Sea. Museo Friulano di storia naturale, 20, Udine.

Brambati, A., Ciabatti, M., Fanzutti, G.P., Marabini, F., Marocco, R., 1983. A new sedimentological textural map of the northern and central Adriatic Sea. Boll. Oceano. Teor. Appl. 1, 267-271.

Brampton, A.H., Motyka, J.M., 1987. Recent examples of mathematical models of UK beaches. Proceedings of Coastal Sediments '91 (American Society of Civil Engineers), 515-530.

Bray, M.J., Workman, M., Smith, J., Pope, D., 1996. Field measurements of shingle transport using electronic tracers. Proceedings of the 31<sup>st</sup> MAFF Conference of River and Coastal Engineers. Ministry of Agriculture, Fisheries and Food, London, pp. 10.4.1–10.4.13.

Bujalesky, G.G. Gonzalez-Bonorino, G., 1991. Gravel spit stabilized by unusual (?) high-energy wave climate in Bay Side, Tierra del Fuego. Proceedings of Coastal Sediments '91 (American Society of Civil Engineers), 960-974.

Buscombe, D., Masselink, G., 2006. Concepts in gravel dynamics. Earth-Science Reviews 79, 33-52.

Caldwell, N.E., 1981. Relationship between tracers and background beach material. Journal of Sedimentary Research 51, 1163-1168.

Caldwell, N.E., Williams, A.T., 1985. The use of beach profile configuration in discrimination between differing depositional environments affecting coarse clastic beaches. Journal of Coastal Research, 1, 129-139.

Cammelli, C., Jackson, N.L., Nordstrom, K.F., Pranzini, E., 2006. Assessment of a gravel nourishment project fronting a seawall at Marina di Pisa, Italy. Journal of Coastal Research, S.I. 39, 770 - 775.

Carr, A.P., 1969. Size grading along a pebble beach: Chesil Beach, England. Journal of Sedimentary Petrology 39, 297-311.

- Carr, A.P., Gleason, R., King, A., 1970. Significance of pebble size and shape in sorting by waves. *Sedimentary Geology* 4, 89-101.
- Carr, A.P., 1971. Experiments on longshore transport and sorting of pebbles; Chesil Beach, England. *Journal of Sedimentary Research* 41, 1084-1104.
- Carter, R.W.G., Orford, J.D., 1991. The sedimentary organisation and behaviour of drift aligned gravel barriers. *Proceedings of Coastal Sediments '91 (ASCE)*, 934-948.
- Carter, R.W.G., Orford, J.D., 1993. The morphodynamics of coarse clastic beaches and barriers: a short- and long-term perspective. *Journal of Coastal Research*, SI 15, 158-179.
- Ciavola, P., Castiglione, E., 2009. Sediment dynamics of mixed sand and gravel beaches at short timescales. *Journal of Coastal Research S.I.* 56, 1751-1755.
- Ciavola, P., Taborda, R., Ferreira, O., Dias, J.M.A., 1997. Field measurements of longshore sand transport and control processes on a steep mesotidal beach in Portugal. *Journal of Coastal Research*, 13, 1119–1129.
- Ciavola, P., Taborda, R., Ferreira, O., Dias, J.M.A., 1997. Field measurements of longshore sand transport and control processes on a steep mesotidal beach in Portugal. *Journal of Coastal Research*, 13, 1119-1129.
- Ciavola, P., Dias, N., Ferreira, O., Taborda, R., Dias, J.M.A., 1998. Fluorescent sands for measurements of longshore transport rates: a case study from Praia de Faro in southern Portugal. *Geo-Marine Letters*, 18, 19-47.
- Ciavola, P., 2004. Tracers. In: Schwartz, M., (Eds), *Encyclopedia of Coastal Sciences*. Kluwer Academic Publishers, Dordrecht, pp. 1253-1258.
- Cipriani, L.E., Ferri, S., Iannotta, P., Paolieri, F., Pranzini, E., 2001. Morfologia e dinamica dei sedimenti del litorale della Toscana settentrionale. *Studi Costieri*, 4, 119-156.
- Coccioni, R., Moretti, E., Nesci, O., Savelli, D., Tramontana, M., Veneri, F., Astracedi, M., 1997. Carta geologica con itinerari geologico-escursionistici, Parco Naturale del Conero, scala 1:20.000. Selca Edizioni, Firenze.

Colantoni, p., Mencucci, D., Baldelli, G., 2003. Idrologia e idraulica costiere processi litorali attuali e deposizione dei sedimenti. In: Coccioni, R., (Eds.), Verso la gestione integrata della costa del Monte San Bartolo: risultati di un progetto pilota, Quaderni del Centro di Geobiologia dell'Università degli Studi di Urbino, Urbino, 15-37.

Curoy, J., Moses, C.A., Robinson, D.A., 2007. Longshore sediment transport on a macrotidal mixed sediment beach, Birling Gap, United Kingdom. EGU General Assembly Conference Abstracts 14, 5856.

Curoy, J., 2012. Morphological and longshore sediment transport processes on mixed beaches. PhD Thesis, University of Sussex.

Curtiss, G.M., Osborne, P.D., Horner-Devine, A.R., 2009. Seasonal patterns of coarse sediment transport on a mixed sand and gravel beach due to vessel wakes, wind waves, and tidal currents. *Marine Geology*, 259, 73-85.

Curzi, P.V., 1986. Cenni di geologia dell'Adriatico nel tratto marchigiano. In: Centamore, E., Deiana, G., (Eds.), *La geologia delle Marche*. Università di Camerino, Camerino, 135-145.

Curzi, P.V., Tomadin, L., 1987. Dinamica della sedimentazione pelitica attuale ed olocenica nell'Adriatico centrale. *Giornale di Geologia*, 49, 101-111.

Deguchi, I., Ono, M., Araki, S., Sawaragi, T., 1998. Motions of pebbles on pebble beach. *Proceedings of 26th International Conference of Coastal Engineering, ASCE, Copenhagen*, 2654-2667.

Dickson, M.E., Kench, P.S., Kantor, M.S., 2011. Longshore transport of cobbles on a mixed sand and gravel beach, southern Hawke Bay, New Zealand. *Marine Geology* 287, 41-42.

Dobkins, J.E., Folk, R.L., 1970. Shape development on Tahiti-nui. *Journal of Sedimentary Petrology*, 40, 1167-1203.

Dolan, R., Davis, R.E., 1992. An intensity scale for Atlantic coast northeast storms. *Journal of Coastal Research* 8, 840-853.

- Dornbush, U., Williams, R.G.B., Moses, C., Robinson, D.A., 2002. Life expectancy of shingle beaches: measuring in situ abrasion. *Journal of Coastal Research* s.i. 36, 249-255.
- Ellis, J.T., Cappiotti, L., 2013. Storm-driven hydrodynamics and sedimentological impacts to an engineered coast. *Journal of Coastal Research*, 65, 1461-1466.
- Fierro, G., Berriolo, G., Ferrari, M., 2010. Le spiagge della Liguria occidentale. Regione Liguria (Eds.).
- Folk, R.L., Ward, W.C., 1957. Brazos River bar: a study in the significance of grain size parameters. *Journal of Sedimentary Petrology*, 27, 3-26.
- Gleason, R., Hardcastle, P.J., 1973. The significance of wave parameters in the sorting of beach pebbles. *Estuarine and Coastal Marine Science*, 1, 11-18.
- Harley, M.D., Andriolo, U., Armaroli, C., Ciavola, P., 2014. Shoreline rotation and response to nourishment of a gravel embayed beach using a low-cost video monitoring technique: San Michele-Sassi Neri, Central Italy. *Journal of Coastal Conservation* 18, 551-565.
- Hayes, M.O., Michel, J., Betenbaugh, D.V., 2010. The intermittently exposed, coarse-grained gravel beaches of Prince William Sound, Alaska: comparison with open-ocean gravel beaches. *Journal of Coastal Research* 26, 4-30.
- Hill, P.R., 1990. Coastal geology of the King Point Area, Yukon Territory, Canada. *Marine Geology*, 91, 93-111.
- Holman, R.A., 1986. Extreme value statistics for wave run-up on a natural beach. *Coastal Engineering*, 9, 527-544.
- Hughes, M.G., Masselink, G., Brander, R.W., 1997. Flow velocity and sediment transport in the swash zone of a steep beach. *Marine Geology*, 138, 91-103.
- Ibbeken, H., Schleyer, R., 1991. *Source and sediment*. Springer, Berlin



- Ibrahim, J.C., Holmes, P., Blanco, B., 2006. Response of a gravel beach to swash zone hydrodynamics. *Journal of Coastal Research* s.i. 39, 1685-1690.
- Isla, F.I., 1993. Overpassing and armouring phenomena on gravel beaches. *Marine Geology*, 110, 369-376.
- Isla, F.I., Bujalesky, G.G., 1993. Saltation on gravel beaches, Tierra del Fuego, Argentina. *Marine Geology*, 115, 263-270.
- Jackson, N.L., Smith, D.R., Tiyyarattanachai, R., Nordstrom, K.F., 2007. Evaluation of a small beach nourishment project to enhance habitat suitability for horseshoe crabs. *Geomorphology* 89, 172-185.
- Jackson, N.L., Nordstrom, K.F., Saini, S., Smith, D.R., 2010. Effects of nourishment on the form and function of an estuarine beach. *Ecological Engineering* 36, 1709-1718.
- Jennings, R., Shulmeister, J., 2002. A field based classification scheme for gravel beaches. *Marine Geology*, 186, 211-228.
- Kirk, R.M., 1975. Aspects of surf and runup processes on mixed sand and gravel beaches. *Geografiska Annaler. Series A. Physical Geography*, 57, 117-133.
- Kirk, R.M., 1980. Mixed sand and gravel beaches: morphology, processes and sediments. *Progress in Physical Geography*, 4, 189-210.
- Kirk, R.M., 1992. Experimental beach reconstruction-renourishment on mixed sand and gravel beaches, Washdyke Lagoon, South Canterbury, New Zealand. *Coastal Engineering* 17, 253-277
- Komar, P.D., Inman, D.L., 1970. Longshore sand transport on beaches. *Journal of Geophysical Research*, 75, 5914-5927.
- Komar, P.D., Miller, M.C., 1974. Sediment threshold under oscillatory water waves. *Journal of Sedimentary Petrology*, 43, 1101-1110.

- Krumbein, W.C., 1934. Size frequency distributions of sediments. *Journal of Sedimentary Petrology*, 4, 65-77.
- Kumada, T., Uda, T., Matsu-ura, T., Sumiya, M., 2010. Field experiment on beach nourishment using gravel at Jinkoji coast. *Coastal Engineering*, 1 - 13.
- Lee, M.W.E., Bray, M., Workman, M., Collins, M.B, Pope, D., 2000. Coastal shingle tracing: a case study using the Electronic Tracer System (ETS). In: Foster, I. (Ed.), *Tracers in Geomorphology*. John Wiley and Sons Ltd, Chichester, UK, pp. 413-435.
- Limber, P., Warren, J., 2006. Development of sediment criteria regulations for beach fill projects along North Carolina's Atlantic Coast. North Carolina Division of Coastal Management CRC 06-01.
- López de San Román Blanco, B., Coates, T.T., Holmes, P., Chadwick, A.J., Bradbury, A., Baldock, .E., Pedrozo-Acuña, A., Lawrence, J., Grüne, J., 2006. Large scale experiments on gravel and mixed beaches: Experimental procedure, data documentation and initial results. *Coastal Engineering* 53, 349-362.
- Lorang, M.S., Namikas, S.L., McDermott, J.P., Sherman, D.J., 1999. El Niño storms and the morphodynamic response of two cobble beaches. *Coastal Sediments 1999*, 922-937.
- Lorang, M.S., 2002. Predicting the crest height of a gravel beach. *Geomorphology*, 48, 87-101.
- Maddrell, R.J., 1996. Managed coastal retreat, reducing flood risks and protection costs, Dungeness Nuclear Power Station, UK. *Coastal Engineering* 28, 1-15.
- McFarland, S., Whitcombe, L.J., Collins, M.B., 1995. Recent shingle beach renourishment schemes in the UK: Some preliminary observations. *Ocean and Coastal Management*, 25, 143-149.
- Mase, H., 1989. Random wave runup height on gentle slope. *J Waterw Port Coast Ocean Eng*, 115, 649-661.

- Mason, T., Coates, T.T., 2001. Sediment transport processes on mixed beaches: a review for shoreline management. *Journal of Coastal Research*, 17, 645-657.
- Masselink, G., Hughes, M.G., 1998. Field investigations of sediment transport in the swash zone. *Continental Shelf Research*, 19, 1179-1199.
- Masselink, G., Hughes, M.G., 2003. *Introduction to coastal processes & geomorphology*. Arnold, London
- Masselink, G., Puleo, J., 2006. Swash zone morphodynamics. *Continental Shelf Research*, 26, 661–680.
- Masselink, G., Russel, P., Blenkinsopp, C., Turner, I., 2010. Swash zone sediment transport, step dynamics and morphological response on a gravel beach. *Marine Geology*, 274, 50-68.
- McCave, I.N., 1978. Grain size trends and transport along beaches: example from eastern England. *Marine Geology*, 28, M43–M51.
- McKay, P.J., Terich, T.A., 1992. Gravel barrier morphology: Olympic National Park, Washington State, USA. *Journal of Coastal Research*, 8, 813-829.
- McLean, R.F., Kirk, R.M., 1969. Relationships between grain size, size-sorting, and foreshore slope on mixed sand-shingle beaches. *New Zealand Journal of Geology and Geophysics*, 12, 138-155.
- McLean, R.F., 1970. Variations in grain-size and sorting on two Kaikoura beaches. *New Zealand Journal of Marine and Freshwater Research*, 4, 141-164.
- Mendoza, E.T., Jimenez, J.A., Mateo, J., 2011. A coastal storms intensity scale for the Catalan Sea (NW Mediterranean). *Natural Hazards Earth System Science* 11, 2453–2462.
- Miller, I.M., Warrick, J.A., Morgan, C., 2011. Observations of coarse sediment movements on the mixed beach of the Elwha Delta, Washington. *Marine Geology*, 282, 201–214.

- Moses, C.A., Williams, R.B.G., 2009. Artificial beach recharge: the south-east England experience. *Zeitschrift fur Geomorphologie* 52 (Suppl. 3), 107–124.
- Nordstrom, K.F., Jackson, N.L., 1993. Distribution of surface pebbles with changes in wave energy on a sandy estuarine beach. *Journal of Sedimentary Petrology*, 63, 1152-1159.
- Nordstrom, K.F., 2005. Beach Nourishment and coastal habitats: research needs to improve compatibility. *Restoration Ecology* 13, 215-222.
- Nordstrom, K.F., Pranzini, E., Jackson, N.L., Coli, M., 2008. The marble beaches of Tuscany. *The Geographical Review* 98, 280-300.
- Noshi, Y., Uda, T., Tsuchiko, H., Imai, K., Higano, T., 2011. Prediction of topography of stable beach produced by gravel nourishment at Jinkoji coast and further nourishment using medium sand. *Proceedings of the Coastal Sediments 2011*, 29 -42.
- Nunny, R.S., Chillingworth, P.C.H., 1986. *Marine dredging for sand and gravel*. HMSO, London.
- Orford, J.D., 1975. Discrimination of particle zonation on a pebble beach. *Sedimentology*, 22, 441-463.
- Packham, J.R., Randall, R.E., Barnes, R.S.K., Neal, A., 2001. *Ecology and geomorphology of coastal shingle*. Westbury, Otley.
- Pigorini, B., 1968. Sources and dispersion of recent sediments of the Adriatic Sea. *Marine Geology*, 6, 187-229
- Poizot, E., Anfuso, G., Méar, Y., Bellido, C., 2013. Confirmation of beach accretion by grain-size trend analysis: Camposoto beach, Cádiz, SW Spain. *Geo-Marine Letters*, 33, 263–272.
- Powell, K.A., 1990. Predicting short-term profile responses for shingle beaches. HR Wallingford laboratory SR Report, 9.

Regione Marche, 2005. Studi, indagini, modelli matematici finalizzati alla redazione del piano di difesa della costa. Bollettino Ufficiale della Regione Marche, 21, 4199–4675.

Saini, S., Jackson, N.L., Nordstrom, K.F., 2012. Characteristics of sediment in transport in the swash zone of a steep estuarine foreshore. *Sedimentology*, 59, 1001–1013.

Salomons, W., Mook, W.G., 1987. Natural tracers for sediment transport studies. *Continental Shelf Research*, 7, 1333–1343.

Sancho-García, A., Guillén, J., Ojeda, E., 2013. Storm-induced readjustment of an embayed beach after modification by protection works. *Geo-Marine Letters*, 33, 159-172.

Sarti, G., Bertoni, D., 2007. Monitoring backshore and foreshore gravel deposits on a mixed sand and gravel beach (Apuane-Versilia coast, Tuscany, Italy). *GeoActa* 6, 73-81.

Sedrati, M., Ciavola, P., Reyns, J., Armaroli, C., Sipka, V., 2009. Morphodynamics of a microtidal protected beach during low wave-energy conditions. *Journal of Coastal Research*, SI56, 198-202.

She, K., Horn, D.P., Canning, P., Thomas, I.M.R., 2006. Recharge of mixed sand and gravel beaches. *Proceedings of the 30<sup>th</sup> International Conference of Coastal Engineering 2006*, ASCE, 4092-4102.

Shepard, F.P., Young, R., 1961. Distinguishing between beach and dune sands. *Journal of Sedimentary Petrology*, 31, 196-214.

Sherman, D.J., Orford, J.D., Carter, R.W.G., 1993. Development of cusp-related, gravel size and shape facies at Malin Head, Ireland. *Sedimentology*, 40, 1139-1152.

Short, A.D., 1999. *Handbook of beach and shoreface morphodynamics*. Wiley, Chichester.

Silva, A., Taborda, R., Rodrigues, A., Duarte, J., Cascalho, J., 2007. Longshore drift estimation using fluorescent tracers: new insights from an experiment at Comporta Beach, Portugal. *Marine Geology*, 240, 137-150.

Smith, M.R., Collis, L., 1993. Aggregates. Sand, gravel and crushed rock aggregate for construction purpose. The Geological Society, London.

Soulsby, R., 1997. Dynamics of marine sands: a manual for practical applications. Thomas Telford, London.

Stockdon, H.F., Holman, R.A., Howd, P.A., Sallenger, J.A.H., 2006. Empirical parameterization of setup, swash, and runup. *Coastal Engineering*, 53, 573-588.

Sunamura, T., Aoki, H., 2000. A field experiment of cusp formation on a coarse clastic beach using a suspended video-camera system. *Earth Surface Processes Landforms*, 25, 329-333.

Takagi, T., Satoh, S., Yamamoto, K., Sakurai, W., Murano, U., Atsuzaka, Y., Ding Y., 2000. Performance of gravel nourishment for erosion control at Fuji coast. *Coastal Engineering*, 3333 - 3344.

Thieler, E.R., Himmelstoss, E.A., Zichichi, J.L., and Ergul, A., 2009. Digital Shoreline Analysis System (DSAS) version 4.0 - An ArcGIS extension for calculating shoreline change: U.S. Geological Survey Open-File Report 2008-1278.

Udden, J.A., 1914. Mechanical composition of clastic sediments. *Bulletin of the Geological Society of America*, 25, 655-744.

Van der Meer, J.W., 1988. Rock slopes and gravel beaches under wave attack. Ph.D. thesis, WL Delft Hydraulics, Delft, The Netherlands.

Van der Meer, J.W., Breteler, M.K., 1990. Measurements and computation of wave induced velocities on a smooth slope. In: *Proceedings of the 22nd International Conference of Coastal Engineering*, ASCE, Delft, 191-204.

Van Straaten, L.M.J.U., 1965. Sedimentation in the north-western part of the Adriatic Sea. *A Symposium Colston Papers*, 17, 143-162.

Van Straaten, L.M.J.U., 1970. Holocene and late Pleistocene sedimentation in the Adriatic Sea. *Geologische Rundschau*, 60, 106-131.

- Van Wellen, E., Chadwick, A.J., Lee, M.W.E., Baily, B., Morfett, J., 1999a. Evaluation of longshore sediment transport models on coarse grained beaches using field data: a preliminary investigation. Proceedings of the 26th International Conference on Coastal Engineering, 3. ASCE, Reston, VA, 2640–2653.
- Van Wellen, E., Lee, M., Baily, B., 1999b. Longshore drift evaluation on a groyned shingle beach using field data. Coastal Sediments 1999, 894-906.
- Van Wellen, E., Chadwick, A.J., Mason, T., 2000. A review and assessment of longshore sediment transport equations for coarse-grained beaches. Coastal Engineering, 40, 243-275.
- Vousdoukas, M.I., Velegrakis, A.F., Dimou, K., Zervakis, V., Conley, D.C., 2009. Wave run-up observations in microtidal, sediment-starved pocket beaches of the Eastern Mediterranean. J Mar Systems, 78 (supplement), S37-S47.
- Walker, J.R., Everts, C.H., Schmelig, S., Demirel, V., 1991. Observations of a tidal inlet on a shingle beach. Proceedings of Coastal Sediments '91 (American Society of Civil Engineers), 975-989.
- Watt, T., Dornbusch, U., Moses, C., Robinson, D., 2005. Surface sediment distribution patterns on mixed beaches in response to wave conditions. Coastal Dynamics 2005, 1-14.
- Wentworth, C.K., 1922a. A scale of grade and class terms for clastic sediments. The Journal of Geology, 30, 377-392.
- Wentworth, C.K., 1922b. The shapes of beach pebbles. US Government Printing Office.
- Wentworth, C.K., 1923. Method of measuring and plotting the shapes of pebbles. US Government Printing Office.
- Whitcombe, L.J., 1996. Behaviour of an artificially replenished shingle beach at Hayling Island, UK. Quarterly Journal of Engineering Geology, 29, 265-271.
- White, T.E., 1998. Status of measurement techniques for coastal sediment transport. Coastal Engineering, 35, 17–45.

Williams, A.T., Caldwell, N.E., 1988. Particle size and shape in pebble-beach sedimentation. *Marine Geology*, 82, 199-215.

Williams, R., Moses, C., 2005. Science report: beach recharge in Sussex and East Kent: a preliminary inventory and overview. BAR Phase I Science Report, 1-23.

Wright, D.L., Short, A.D., 1984. Morphodynamic variability of surf zones and beaches: a synthesis. *Marine Geology*, 56, 93–118.

Wright, D.L., Short, A.D., Green, M.O., 1985. Short-term changes in the morphodynamic states of beaches and surf zones: an empirical predictive model. *Marine Geology*, 62, 339–364.

Zingg, T., 1935. Beitrag zur Schotteranalyse. *Schweiz. Mineral. Petrogr. Mitt.*, 15, 39–140.



# *List of figures*

Figure 1-1. A) Construction cycle of a “Sker” type beach and B) a “Newton” type beach (Bluck, 1967). .....	8
Figure 1-2. Schematic representation of the three types of beaches proposed by Jennings and Shulmeister (2002): A) pure gravel beach, B) mixed sand and gravel beach (MSG), C) composite beach. ....	11
Figure 1-3. Typical morphology and zonation of mixed sand and gravel beach profiles according to Kirk (1980). ....	12
Figure 1-4. Conceptual morpho-sedimentary-dynamics diagram for gravel beachface. This diagram was already drafted by Masselink and Puleo (2006) and later modified by Buscombe and Masselink (2006) in the current form. The diagram illustrates interactions between and within the surf zone and the swash zone morphodynamic system. ....	13
Figure 1-5. Conceptual model of the probabilistic nature of a sediment grain transport on a gravel beach (Carter and Orford, 1993, after Carter and Orford, 1991). ....	15
Figure 2-1. Portonovo study area. ....	19
Figure 2-2. Overall view of the beach during the first (A) and the second experiment (B). ....	20
Figure 2-3. Multiyear wave climate for Portonovo (recording period from 1999 to 2006). Wave data recorded by ISPRA buoy of Ancona (ISPRA - Servizio Mareografico “Rete Ondametrica Nazionale”). ....	20
Figure 2-4. Marina di Pisa study area. ....	22
Figure 2-5. Overall look of Barbarossa beach during the experiment. View towards N (A) and towards S (B). ....	22
Figure 2-6. Multiyear wave climate for Marina di Pisa (recording period from 1989 to 2007). Wave data recorded by ISPRA buoy of La Spezia (ISPRA - Servizio Mareografico “Rete Ondametrica Nazionale”). ....	23
Figure 3-1. A) Cylinder tags adopted to track pebbles; B) samples of drilled pebbles; C) drilling operations by means of the vertical driller; D) Pebbles sealed and painted: the reds	

are disc shaped, the blue are sphere shaped. These two categories were used in the second experiment in Portonovo. ....	26
Figure 3-2. Research technique of tracers on A) the emerged beach and B) the submerged beach.....	26
Figure 3-3. A) Reader and batteries: two plexiglass sheets render the reader waterproof ; B) Reader set up on a plastic sledge to easily drag it on the emerged beach ; C) dragging operations on a steep beachface; D) Trailing the reader on the beach surface by means of sledge.....	27
Figure 3-4. InterOcean S4 directional wave gauge. ....	29
Figure 3-5. Beach profile comparison between the tracer sampling and the tracer injection for both the experiments.....	30
Figure 3-6. Distribution of tracer used in the experiments according to their shape and size. ....	31
Figure 3-7. Experiment setup at Portonovo beach. A) S4 device and injection positions of tracers over an elevation surface for both experiments. Tracer injection scheme of the first (B) and second experiment (C).....	32
Figure 3-8. Scheme of the mixing depth evaluation conceived during the second experiment (A). Pebble pile locations in three significant beach points (B). Painted pebbles of disc shape used for the mixing depth evaluation (C). ....	33
Figure 3-9. Experiment set up at Marina di Pisa. A) Injection positions of tracers over an elevation surface for the experiment at Marina di Pisa, Barbarossa sector.; B) reference profile at Barbarossa beach at the time of the injection. ....	35
Figure 3-10. A) Sample locations of 14 cross-shore transects on topographic surface; B) Sampling area; C) Surface sampling scheme held in Portonovo and based on the morphologies found on the first sampling campaign. ....	37
Figure 3-11. A) Mechanical sieve shaker; B) precision scale; C) example of granule content from a sieve.....	38

Figure 3-12. Profile locations on Portonovo beach. Topographic network repeated during each survey from May 2012 to February 2014. In bold are indicated the reference profiles shown and discussed in Chapter 6.....	39
Figure 3-13. Shape categories of pebbles according to Zingg (1935). Shape classes are based on different ratios of axis lengths. ....	42
Figure 3-14. Threshold orbital velocity for motion of sediment by waves (from Soulsby, 1997).....	43
Figure 4-1. Wave climate during both the Portonovo experiments recorded by the S4 directional wave gauge. ....	48
Figure 4-2. Tracer displacement within the time frame of the 1st experiment at Portonovo beach: a) injection position of each marked pebble; b) position of each detected pebble 6 h after the injection; c) position of each detected pebble 24 h after the injection. ....	49
Figure 4-3. Diagrams showing cross-shore versus longshore transport for the experiment at Portonovo.....	50
Figure 4-4. Recovery rates of tracers after one year at Portonovo beach.....	51
Figure 4-5. Tracer displacement two months after the injection: A) Comparison between the injection and the recovery locations; B) Displacement magnitude toward the two longshore directions (i.e. NW and SE). ....	54
Figure 4-6. Wave climate during the Marina di Pisa experiment (wave data were provided by the Tuscany Hydrographic Office; water level data were recorded by the ISPRA tide gauge located at Livorno). ....	57
Figure 4-7. Tracer displacement within the time frame of the experiment at Marina di Pisa, Barbarossa sector: a) injection position of each marked pebble; b) position of each detected pebble 6 h after the injection; c) position of each detected pebble 24 h after the injection. ....	58
Figure 4-8. Diagrams showing cross-shore versus longshore transport for the experiment at Marina di Pisa.....	59

Figure 4-9. Plots of the run-up levels computed for Marina di Pisa (a) and Portonovo 1st experiment (b) using the formulae of Holman (1986) and Stockdon et al. (2006), compared to the maximum tracer elevation (horizontal dashed line). ..... 62

Figure 4-10. Evolution of the beach profiles taken as a reference during the experiments on the two beaches; tracer positions at the time of the injection and after 6 and 24 h are also illustrated. a) Marina di Pisa, Barbarossa sector: only one profile is shown because no change was recorded during the experiment. b) Portonovo beach (1st experiment). Injection WL Water level at the time of the injection, Max WL maximum water level reached during the experiment. .... 65

Figure 4-11. Beach topography variation from March 2012 (tracer injection) to May 2012 (2 month recovery). Profile numbers refers to the south limit (PR 01), central zone (PR 02) and north limit (PR 03) of the southern embayment (see Figure 3-12)..... 67

Figure 5-1. Tracer displacement in terms of size (only 2nd experiment): A) 6 hour displacements; and B) 24 hour displacements..... 71

Figure 5-2. Box plots showing the displacement magnitude after the 6 and 24 hour recoveries according to the size subdivision of the tracers: a) box plots referring to the first experiment; and b) box plots refer to the second experiment: here, a size discrimination was taken into account prior to pebble injection. .... 73

Figure 5-3. Threshold of motion for marked pebbles estimated by the graphic method of Soulsby (1997). Calculations shown for the first (A) and the second (B) experiment..... 75

Figure 5-4. Tracer displacement in terms of shape: A) First experiment 6 hour displacements; B) First experiment 24 hour displacements; C) Second experiment 6 hour displacements; and D) Second experiment 24 hour displacements..... 76

Figure 5-5. Box plots showing the pebble displacement magnitude after 6 and 24 hours according to the shape subdivision of the tracers: a) box plots referring to the first experiment, where the elongated shapes are joined together (D = Disc, B = Blade, R = Rod); and b) box plots referring to the second experiment, where only the disc and sphere shapes were present. .... 78

Figure 5-6. Tracer displacement based on the combined effect of size and shape (only 2<sup>nd</sup> experiment): “Big” class displacements 6 hours (A) and 24 hours (B) after the injection;

“Medium” class displacements 6 hours (C) and 24 hours (D) after the injection; and “Small” class displacements 6 hours (E) and 24 hours (F) after the injection. ....	80
Figure 5-7. Box plots showing the pebble displacement magnitude after 6 and 24 hours based on the combined effect of size and shape. A) “Big”-sized discs and spheres comparison; B) “Medium”-size discs and spheres comparison; C) “Small”-sized discs and spheres comparison.....	82
Figure 6-1. Topographic surfaces of Portonovo beach from May 2012 to November 2012: (A) May 2012; B) October 2012 a; C) October 2012 b; D) November 2012). The seawall and the cliff toe are shown on each topographic surface.....	92
Figure 6-2. Profile variation of the entire beach in May 2012. ....	93
Figure 6-3. Profile variation of the entire beach from May 2012 to October 2012 a.....	94
Figure 6-4. Profile variation of the entire beach from October 2012 a to October 2012 b. ....	95
Figure 6-5. Profile variation of the entire beach from October 2012 b to November 2012.....	96
Figure 6-6. Topographic surfaces of Portonovo beach from December 2012 to March 2013 (A) December 2012; B) January 2013; C) February 2013; D) March 2013). The seawall and the cliff toe are shown on each topographic surface.....	98
Figure 6-7. Profile variation of the entire beach from November 2012 to December 2012. .....	99
Figure 6-8. Profile variation of the entire beach from December 2012 to January 2013..	100
Figure 6-9. Profile variation of the entire beach from January 2013 to February 2013....	101
Figure 6-10. Profile variation of the entire beach from February 2013 to March 2013....	102
Figure 6-11. Topographic surfaces of Portonovo beach from April 2013 to February 2014 (A) April 2013; B) May 2013; C) February 2014). The seawall and the cliff toe are shown on each topographic surface. ....	104
Figure 6-12. Profile variation of the entire beach from March 2013 to April 2013.....	105
Figure 6-13. Profile variation of the entire beach from April 2013 to May 2013. ....	106

Figure 6-14. Profile variation of the entire beach from April 2013 to May 2013. ....	107
Figure 6-15. Shoreline variation from May 2012 to October 2012 a (3 <sup>rd</sup> to 4 <sup>th</sup> survey): accretion/erosion map (A) and Net Shoreline Movement (NSM) computed by the ArcGIS tool DSAS (B). ....	109
Figure 6-16. Shoreline variation from October 2012 a to October 2012 b (4 <sup>th</sup> to 5 <sup>th</sup> survey): accretion/erosion map (A) and Net Shoreline Movement (NSM) computed by the ArcGIS tool DSAS (B). ....	110
Figure 6-17. Shoreline variation from October 2012 b to November 2012 (5 <sup>th</sup> to 6 <sup>th</sup> survey): accretion/erosion map (A) and Net Shoreline Movement (NSM) computed by the ArcGIS tool DSAS (B). ....	111
Figure 6-18. Shoreline variation from November 2012 to December 2012 (6 <sup>th</sup> to 7 <sup>th</sup> survey): accretion/erosion map (A) and Net Shoreline Movement (NSM) computed by the ArcGIS tool DSAS (B). ....	112
Figure 6-19. Shoreline variation from December 2012 to January 2013 (7 <sup>th</sup> to 8 <sup>th</sup> survey): accretion/erosion map (A) and Net Shoreline Movement (NSM) computed by the ArcGIS tool DSAS (B). ....	113
Figure 6-20. Shoreline variation from January 2013 to February 2013 (8 <sup>th</sup> to 9 <sup>th</sup> survey): accretion/erosion map (A) and Net Shoreline Movement (NSM) computed by the ArcGIS tool DSAS (B). ....	114
Figure 6-21. Shoreline variation from February 2013 to March 2013 (9 <sup>th</sup> to 10 <sup>th</sup> survey): accretion/erosion map (A) and Net Shoreline Movement (NSM) computed by the ArcGIS tool DSAS (B). ....	115
Figure 6-22. Shoreline variation from March 2013 to April 2013 (10 <sup>th</sup> to 11 <sup>th</sup> survey): accretion/erosion map (A) and Net Shoreline Movement (NSM) computed by the ArcGIS tool DSAS (B). ....	116
Figure 6-23. Shoreline variation from April 2013 to May 2013 (11 <sup>th</sup> to 12 <sup>th</sup> survey): accretion/erosion map (A) and Net Shoreline Movement (NSM) computed by the ArcGIS tool DSAS (B). ....	117

Figure 6-24. Shoreline variation from May 2013 to February 2014 (12 <sup>th</sup> to 13 <sup>th</sup> survey): accretion/erosion map (A) and Net Shoreline Movement (NSM) computed by the ArcGIS tool DSAS (B). .....	118
Figure 6-25. Shoreline variation for the whole period of almost two years (from May 2012 to February 2014; 3 <sup>rd</sup> to 13 <sup>th</sup> survey): accretion/erosion map (A), (NSM) Net Shoreline Movement (B), (SCE) Shoreline Change Envelope (C) and (EPR) End Point Rate (D) computed by the ArcGIS tool DSAS.....	120
Figure 6-26. Volumetric variation in almost two year time span.....	121
Figure 6-27. Volumetric variation from one survey to another in almost two year time span.....	122
Figure 6-28. “Cut and fill” process observed in Portonovo beach after a storm approached from SE. On the left the “Cut” southern part of the beach is shown, with erosive scarps. On the right, the “Filled” northern beach area, with several tiers of storm berms deposited..	126
Figure 7-1. Surface sediment variability during one year span time. Pie charts with percentage values relative to: A) 1st sampling - March 2012; B) 2nd sampling - April 2012; C) 3rd sampling - May 2012; D) 4th sampling - October 2012; E) 5th sampling - December 2012; F) 6th sampling - April 2013. Sand-Gravel ratio variability during the six sampling campaigns (G). .....	129
Figure 7-2. Mean diameter ( $M_z$ ) dispersion map through one year span time: all the six sampling campaigns are represented. ....	132
Figure 7-3. Sorting ( $\sigma_1$ ) dispersion map through one year span time: all the six sampling campaigns are represented.....	133
Figure 7-4. Skewness ( $S_k$ ) dispersion map through one year span time: all the six sampling campaigns are represented.....	134
Figure 7-5. Significant wave height ( $H_s$ ) and wave direction (Dir) recorded by the Ancona offshore buoy (ISPRA - Servizio Mareografico “Rete Ondametrica Nazionale”) throughout the entire period of samplings. ....	138
Figure 7-6. Representation of the same beach end (northern) after a storm approached from NE direction in December 2012 (B) and a storm reached from SE direction in March 2013	



(C). In A is shown the location where the pictures were taken relatively to the sampling area..... 140

Figure 8-1- Comparison between a fill nourishment material adopted in Portonovo beach (A) and the native natural sediment (B). ..... 144

# *List of tables*

Table 1-1. Morphological parameters of studied beaches by Jennings and Shulmeister (2002).....	10
Table 3-1. Mean diameter comparison between the natural beach sediment and the marked pebbles. The average values showed are in mm for each morphological feature. No step crest samples were collected during the second experiment. ....	31
Table 3-2. Mean diameter comparison between the natural beach sediment and the marked pebbles. The averaged values are in mm for each morphological feature. ....	34
Table 4-1. Recovery percentages of tracers after the first (6 h) and the second (24 h) survey for both experiments at Portonovo beach. Percentages are expressed according to the injection position of tracers. Only displacements greater than 0.5 m were retained significant given the RFID antenna accuracy of about 40 cm. The last row shows the total recovery percentages without considering the injection position of tracers.....	47
Table 4-2. Mixing depth results for the three beach locations. ....	50
Table 4-3. Displacement length covered by tracers two months after the injection according to the two longshore directions. Values are shown according to the morphological feature where tracers were injected.....	52
Table 4-4. Recovery rates of tracers throughout one year time span based on the injection position of pebbles.....	53
Table 4-5. Recovery percentages of tracers after the first (6 h) and the second (24 h) survey for the experiment at Marina di Pisa. Percentages are expressed according to the injection position of tracers. Only displacements greater than 0.5 m were retained significant given the RFID antenna accuracy of about 40 cm. The last row shows the total recovery percentages without considering the injection position of tracers.....	56
Table 4-6. Storm events occurred between the injection (March 2012) and the first tracer recovery carried out two months later (May 2012). ....	67
Table 5-1. Probability values calculated by means of T-tests. The pebble displacements measured for different sizes are compared. The bold numbers represent a significant difference between the two categories considered in each row. A significance level of $p < 0.05$ was used.....	74

Table 5-2. Probability values calculated by means of T-tests. The pebble displacements measured for different shapes are compared. The bold numbers represent a significant difference between the two categories considered in each row (D = Discs; B = Blades; R = Rods; S = Spheres). A significance level of $p < 0.05$ was used. ....	79
Table 5-3. List of the most recent studies on the role of particle size and shape on coarse-clastic and mixed beaches.....	87
Table 6-1. Evidence of beach rotation observed in Portonovo beach during the two year monitoring. Characteristics of the last storm occurred before each survey are shown from offshore wave data (ISPRA - Servizio Mareografico “Rete Ondametrica Nazionale”). Severity class of each storm is calculated according to the storm severity scale of Mendoza et al. (2011).....	123
Table 7-1. Evidence of surface sediment patterns observed in Portonovo beach during the one year sampling. Characteristics of the last storm occurred before each sampling are shown from offshore wave data (ISPRA - Servizio Mareografico “Rete Ondametrica Nazionale”). Severity class of each storm is calculated according to the storm severity scale of Mendoza et al. (2011).....	136
Table 8-1 - Comparison between native sediment and fill material characteristics for Portonovo beach. ....	144
Table 8-2. Fill material characteristics adopted in some Italian and worldwide nourishment projects.....	147

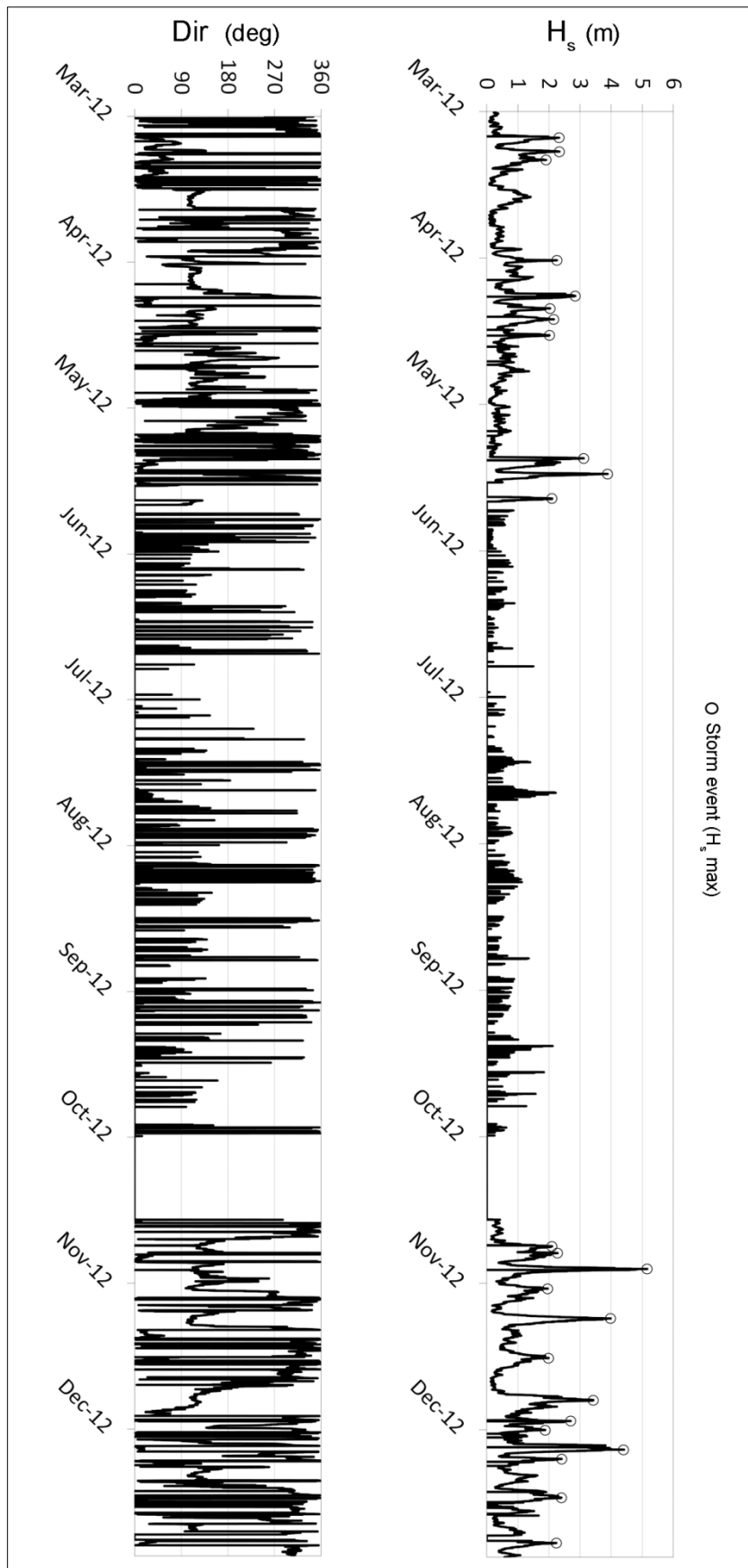
# *Appendix A - Fieldwork*

<b>Time table</b>		Beach sampling	Topographic survey	Tracer experiment	Tracer research
0	March 2012 A		half beach		
1 <sup>st</sup>	March 2012 B		half beach		
2 <sup>nd</sup>	April 2012		half beach		
3 <sup>rd</sup>	May 2012				
4 <sup>th</sup>	October 2012 A				
5 <sup>th</sup>	October 2012 B				
6 <sup>th</sup>	November 2012				
7 <sup>th</sup>	December 2012				
8 <sup>th</sup>	January 2013				
9 <sup>th</sup>	February 2012				
10 <sup>th</sup>	March 2013				
11 <sup>th</sup>	April 2013				
12 <sup>th</sup>	May 2013				
13 <sup>th</sup>	February 2014				

 done

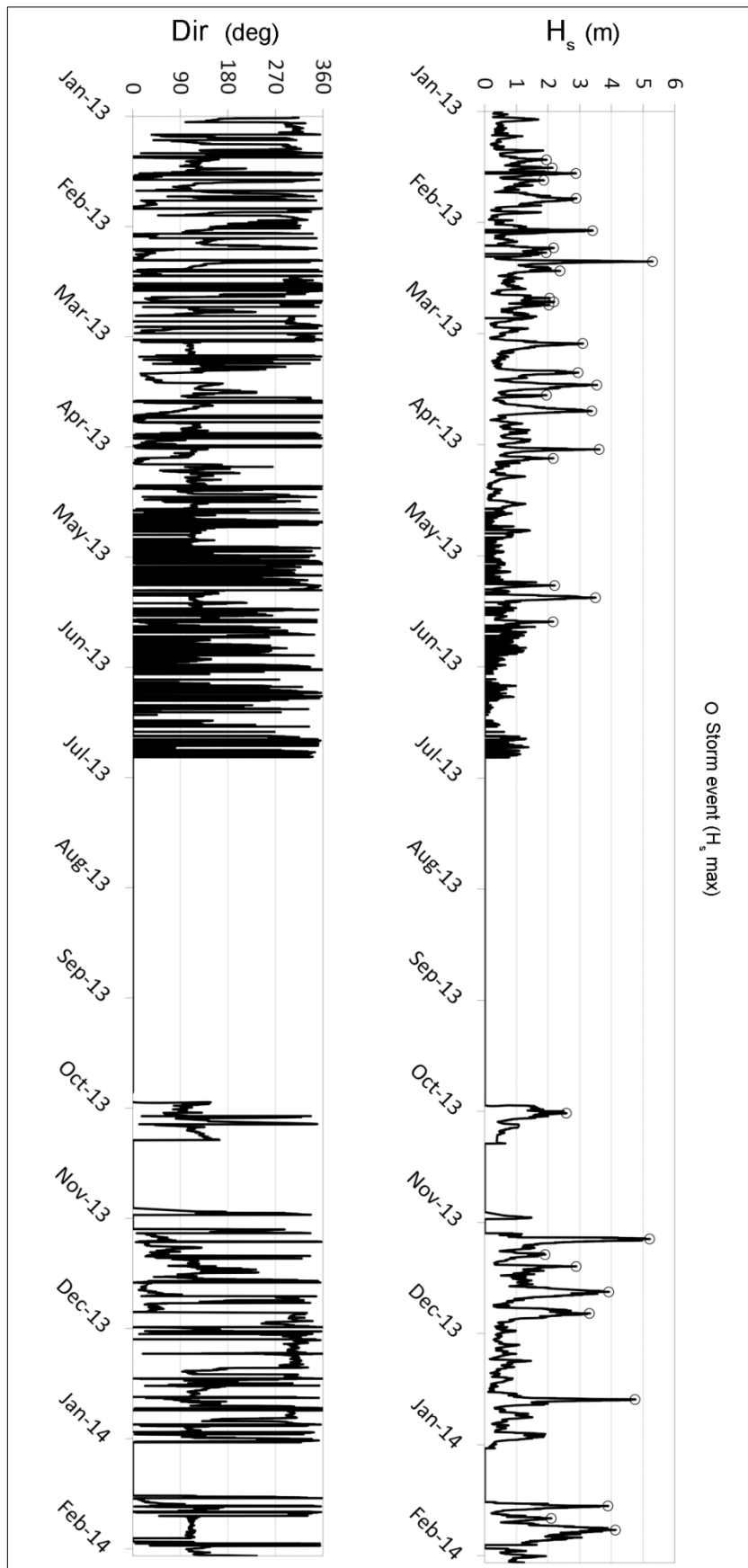
Summary time-table of fieldwork in Portonovo beach

# *Appendix B - Offshore wave data*



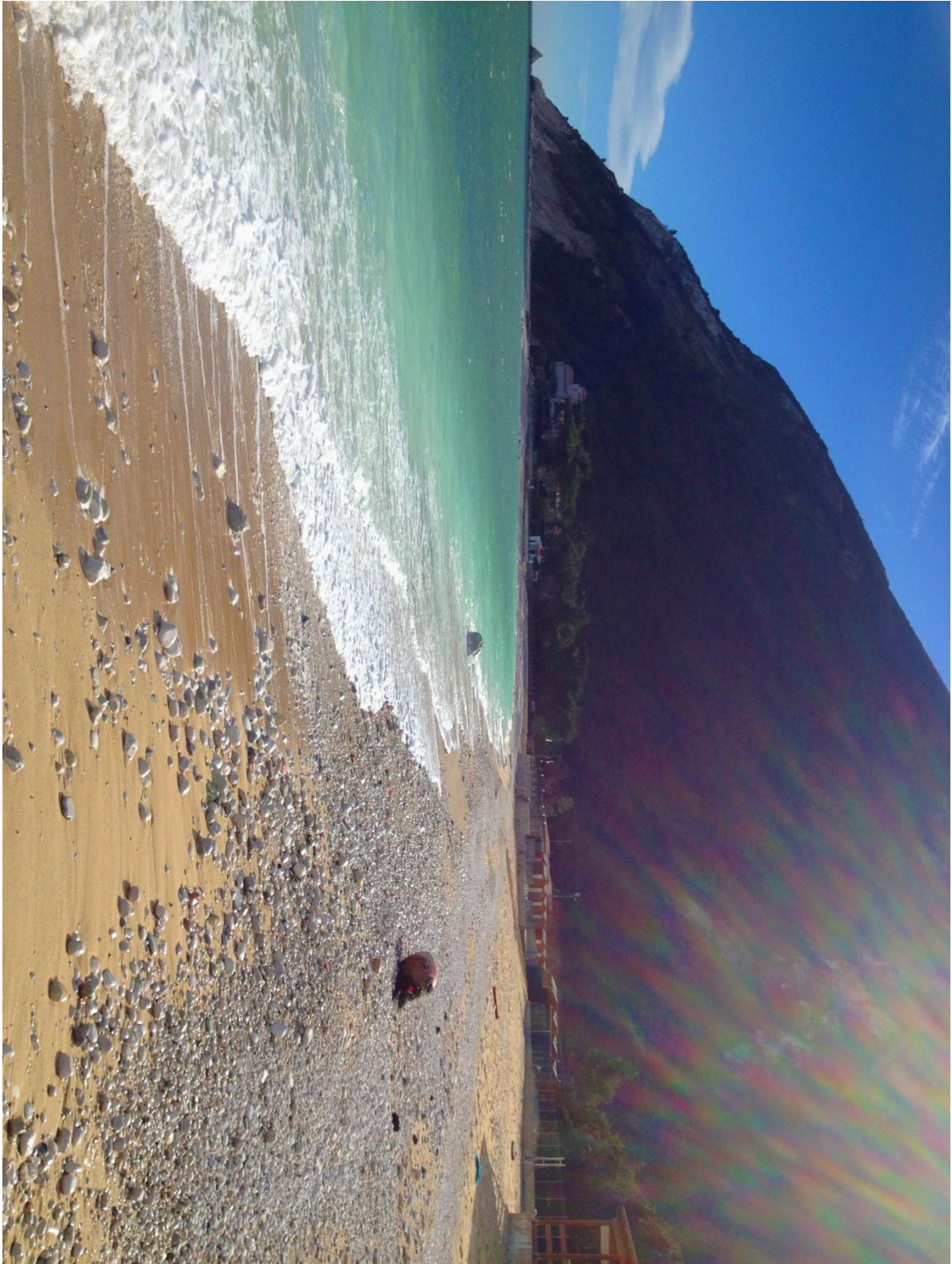
Offshore wave data for the year 2012 (Ancona Buoy, ISPRA - Servizio Mareografico "Rete Ondametrica Nazionale")



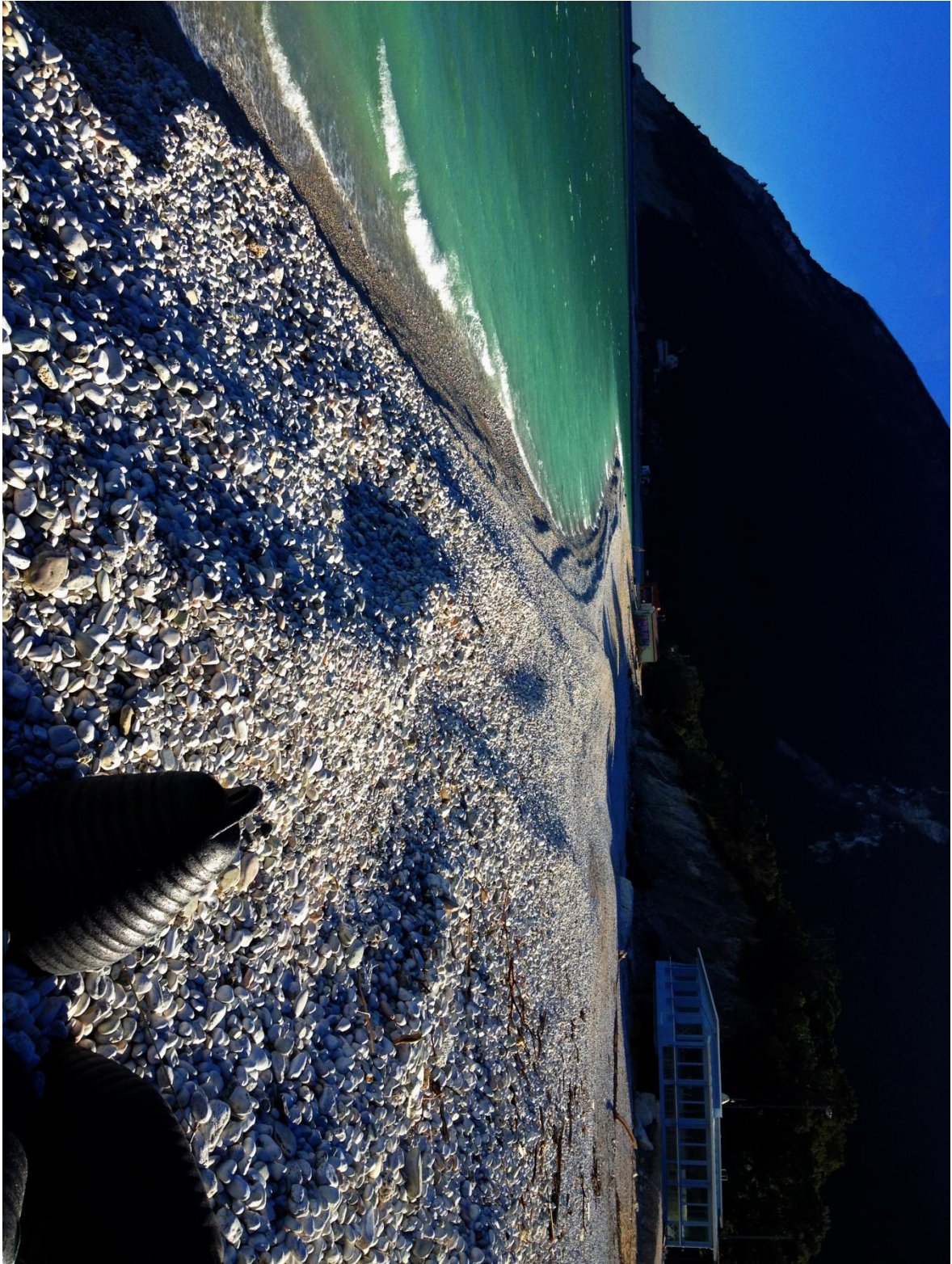


Offshore wave data for the year 2013 and part of the year 2014 (Ancona Buoy, ISPRA - Servizio Mareografico "Rete Ondametrica Nazionale")

# *Appendix C - Beach pictures*



Portonovo beach, looking south (February 2014).



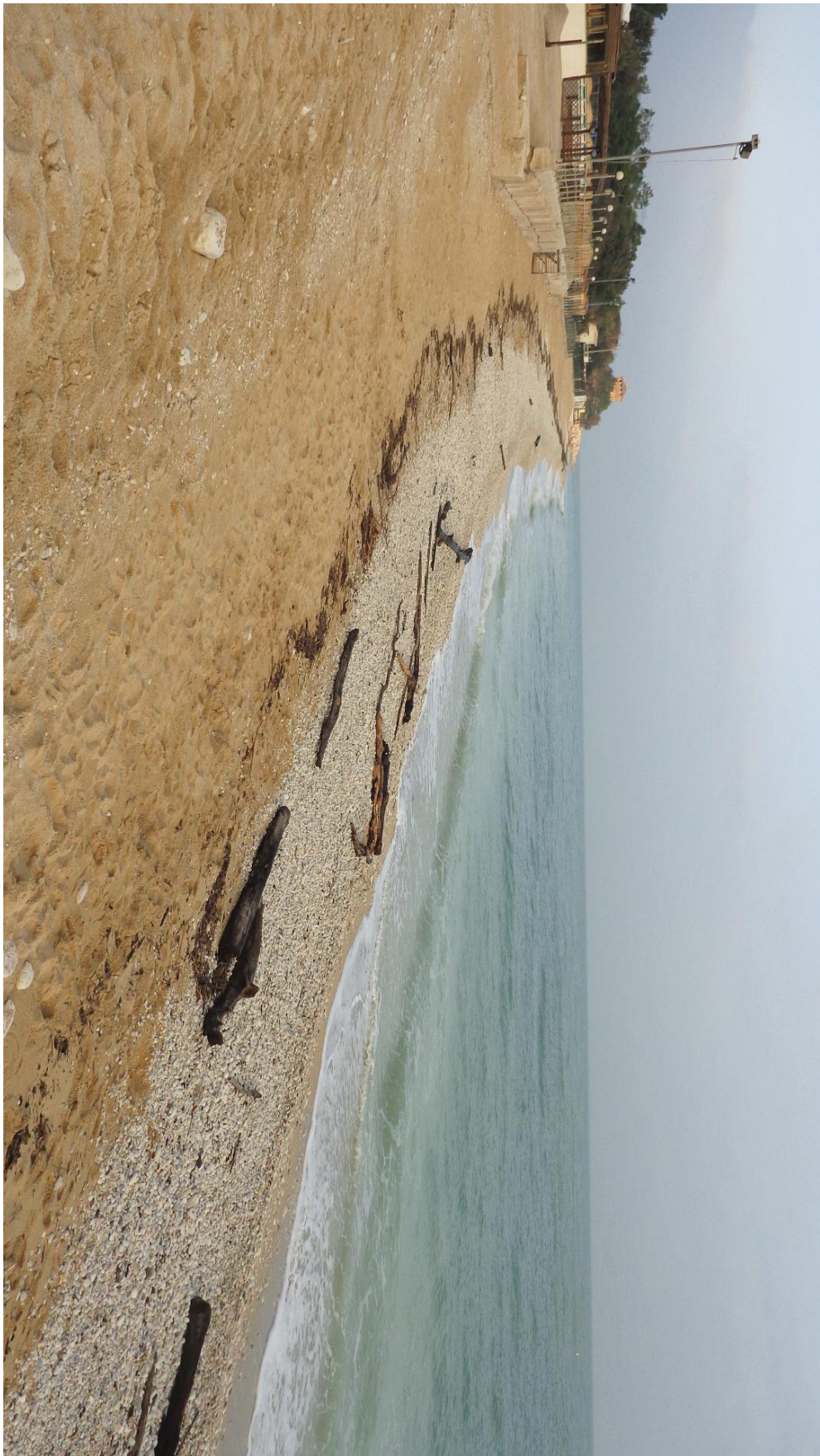
Storm berms in the northern area of Portonovo after a storm from ESE direction.



Throwing pebbles in Portonovo.



Cliff erosion (after “Halloween 2012 storm”).

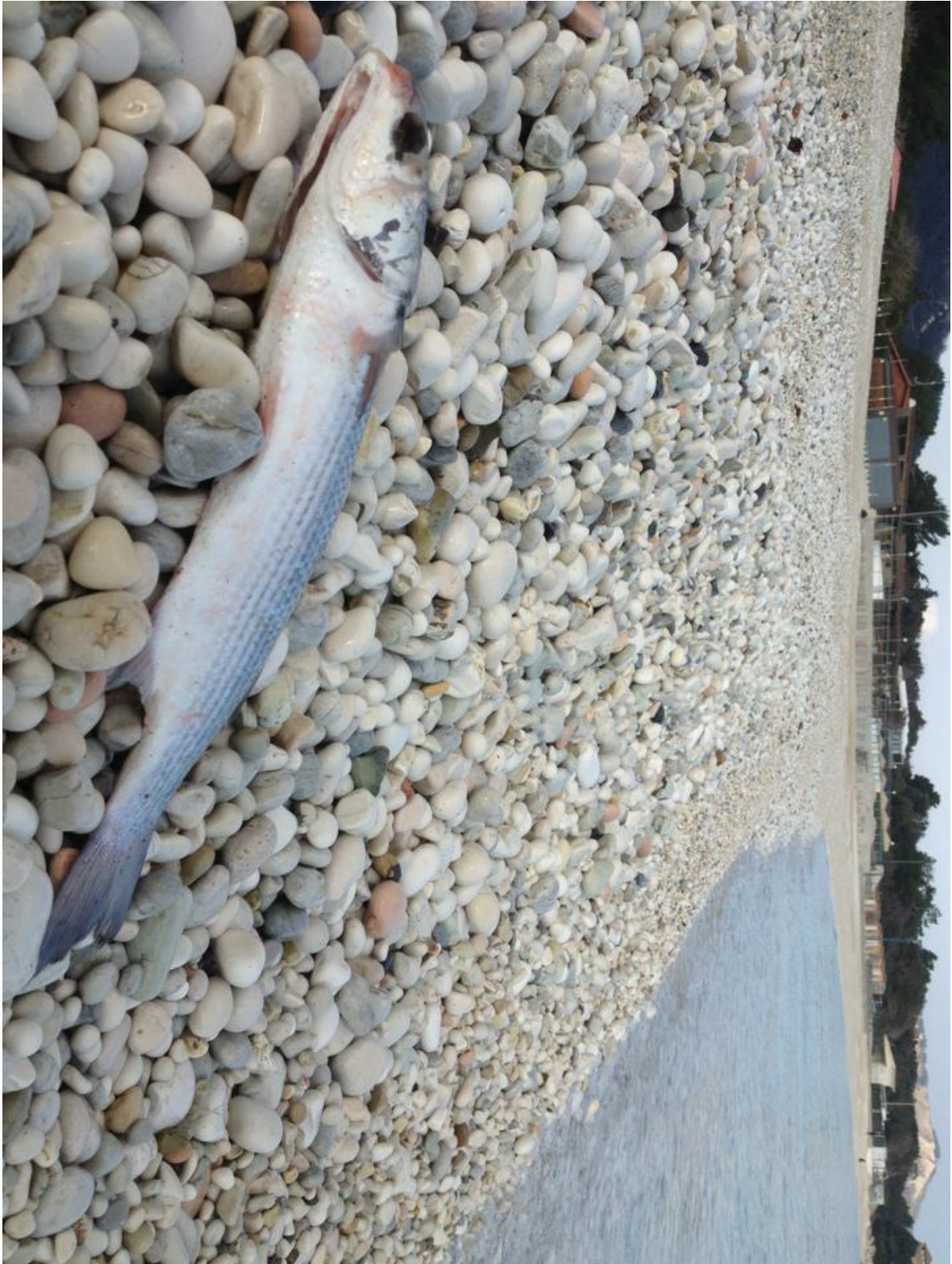


Sediment stripes.



The northern beach end in Portonovo (December 2012).





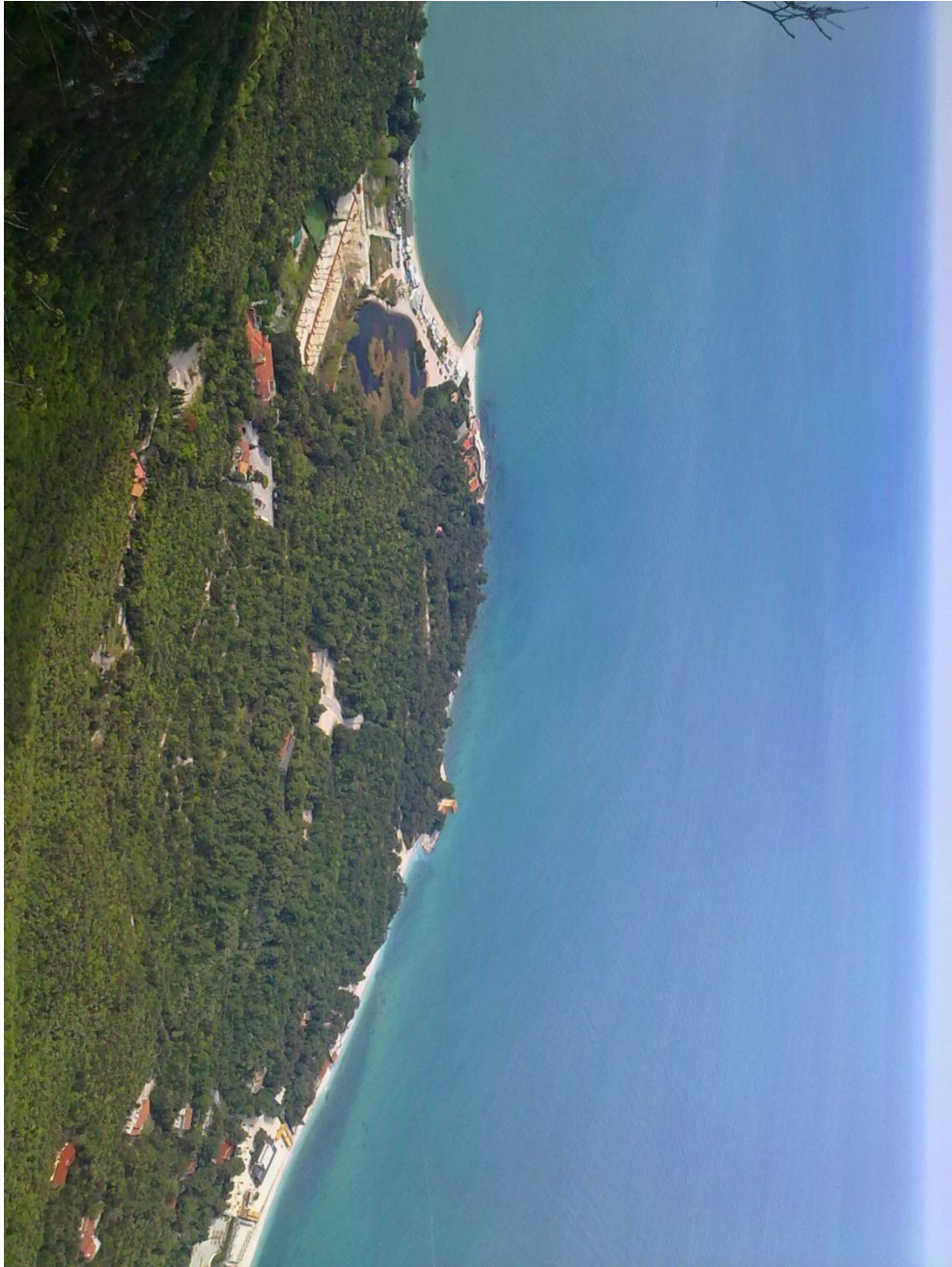
The southern embayment in Portonovo.



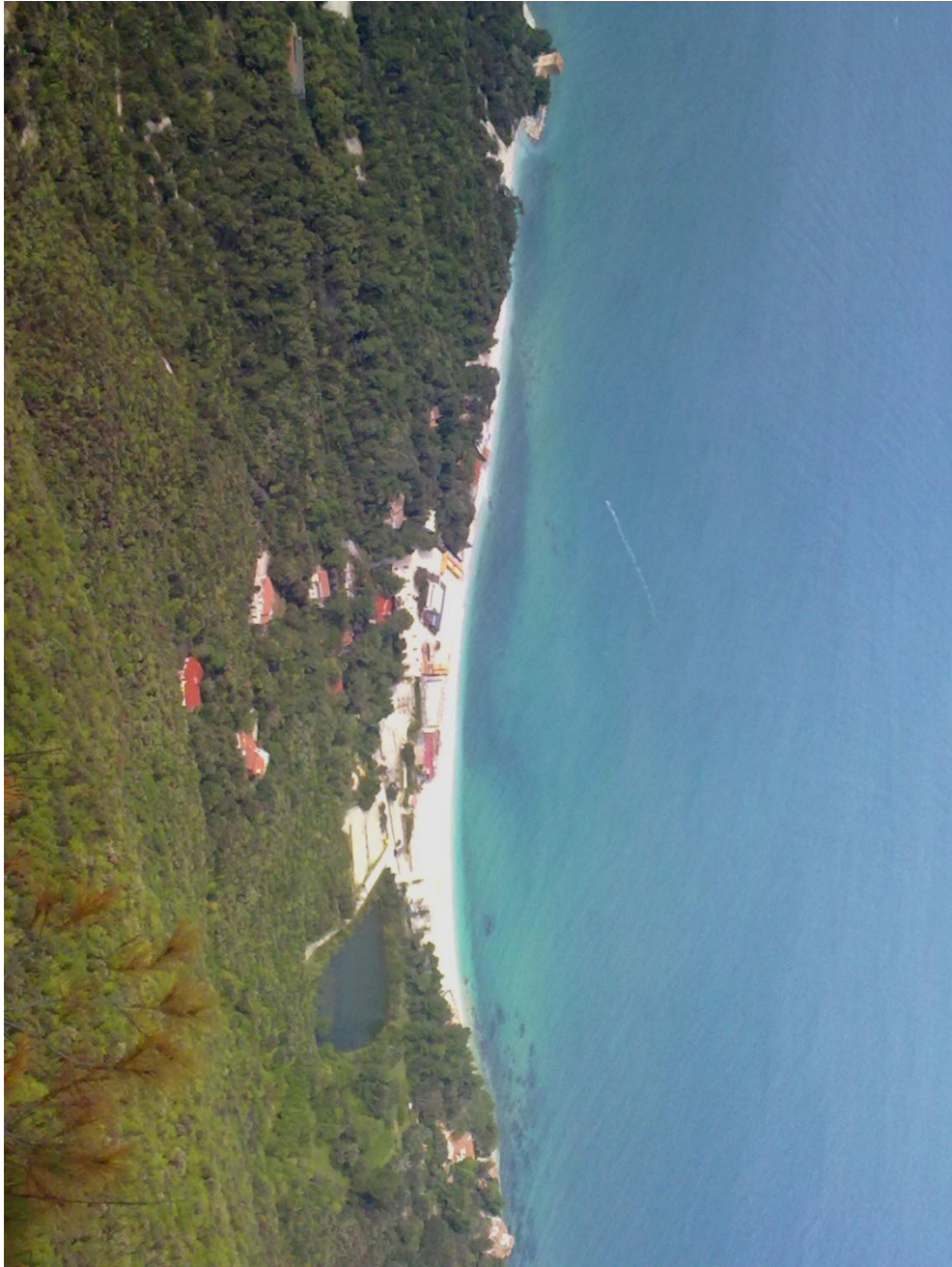
Lonely tracer.



Our mascot (...and the RFID reader).



Landslide body of Portonovo lied on the sea (April 2012).



The beach (April 2012).



The beach (March 2012).

# *Acknowledgements*

Desidero ringraziare in primo luogo il prof. **Paolo Ciavola** che ha reso possibile il completamento del presente lavoro dandomi sempre preziosi consigli ed insegnamenti lungo questo percorso durato tre anni. E' stato anche grazie a lui che ho avuto la possibilità di completare un periodo di studio e di crescita formativa fondamentale presso il New Jersey Institute of Technology di Newark (NJ, USA). A tal proposito, di grande importanza è stato l'apporto della prof. **Nancy Jackson** del NJIT per i consigli relativi alle prime fasi di stesura del mio primo articolo; suggerimenti che hanno anche notevolmente migliorato la revisione bibliografica del presente lavoro.

Ringrazio la Regione Marche, principalmente l'ufficio "Difesa della Costa" nelle figure del geol. **Stefano Parlani** e dell'ing. **Giorgio Filomena** per avermi dato accesso a tutti i dati relativi alla spiagge del Conero. Allo stesso modo ringrazio **ISPRA** (Istituto Superiore per la Protezione e la Ricerca Ambientale) e in particolare il Servizio Mareografico "Rete Ondametrica Nazionale" nella figura di **Gabriele Nardone** per avermi costantemente inviato i dati della boa ondametrica di Ancona.

Contestualmente al presente lavoro è indispensabile menzionare tra i ringraziamenti tutti i colleghi che sono passati in questi tre anni nel nostro gruppo di ricerca quali: **Mitch, Clara, Elisa, Quentin, Bruna, Karl, Enrico, Munna, Marta** e **Art**. Una menzione speciale la meritano sicuramente **Duccio** e **Alessandro**: il primo è ormai diventato come un fratello maggiore, è stato praticamente il correlatore mascherato di questa tesi ed è sempre stato disponibile a qualsiasi chiarimento o consiglio di carattere lavorativo e molto spesso anche di altro genere; il secondo è stato importante durante ogni esperimento sia per il grande apporto sul campo che per le immense grigliate portate a termine ogni sera con qualsiasi condizione meteo e anche per aver sempre tenuto alto il morale del gruppo. La grande mole di dati presi sul campo ha inevitabilmente richiesto la presenza di una grande forza lavoro composta da tesisti, amici, colleghi e curiosi tra i quali devo sicuramente menzionare: **Giovanni, Gino, Stefano, Silvia, Matteo, Enrico, Javito, Laura, Leonardo, Domenico** e **Rolfo**. Per la raccolta dei dati sul campo e la loro analisi in laboratorio, fondamentale è stato anche l'apporto dei tecnici "Bombers" **Paolo, Francesco** e **Umberto**. La grande mole di dati ha poi richiesto momenti di svago quotidiani per i quali devo ringraziare i membri non ancora citati del "Kazzengeo" come **Elisa, Ambra** e **Roberta**.

Riguardo alla sfera personale desidero ringraziare innanzitutto i miei genitori **Anna** e **Gianni**, che mi hanno dato l'opportunità di completare gli studi prima a Bologna, con



supporti economici, poi a Ferrara con sostegni morali, sperando che almeno in piccola parte questa mia fatica li risollevi moralmente da un anno abbastanza pessimo per la nostra famiglia. Ringrazio inoltre la mia ragazza **Silvia** (e la sua famiglia) che mi è sempre stata vicina in questo cammino, dandomi forza nei momenti più bui e convincendomi a credere in me stesso nonostante la distanza fisica che ci ha separato per gran parte del tempo. Ringrazio infine il resto della mia famiglia: zia **Luciana**, zio **Attilio**, **Valentina**, **Giacomo**, **Tiziana** e **Surf**.